KINETIC PROCESSES IN ALKALINE PEROXIDE BLEACHING

Philip James Wright, B.Sc. (Hons.), (Tas.)

Submitted in fulfilment of the requirements

for the degree of

Doctor of Philosophy.

Chemistry Department,

University of Tasmania,

October, 1993.

DECLARATION

To the best of my knowledge, this thesis contains no material previously published or written by another person, except where due reference is made in the text of the thesis.

P.J. Wright

12th October, 1993

THE STUDENT'S PRAYER

Now I lay me down to rest,
a pile of books upon my chest.
If I should die before dawn's first light,
that's one less page I'll have to write.

P.J.W.

TABLE OF CONTENTS

ACKNOWLEDGMENTS

I would like to acknowledge with gratitude the guidance provided by my supervisor, Dr. John Abbot, over the last three and a half years. My thanks go to Interox Chemicals and Australian Newsprint Mills for partly funding this project and to the Australian Government for providing the remaining funding through a post-graduate research scholarship. My appreciation is extended to Australian Newsprint Mills for the use of their excellent library and technical resources, and special thanks go to Mr. Stuart Maughn and Mr. Tony Parsons for providing the *E. regnans* mechanical pulp and for use of the Elrepho 2000 spectrometer.

I would like to thank Mr. Evan Peacock in the Central Science Laboratory for running ESR and NMR spectra, and the assistance of Mr. Noel Davies in running GC-MS samples was greatly appreciated. Many thanks are extended to Mr. Felix Guerzoni and Mr. Ashley Townsend for their help in acquainting me with the finer points of GC analysis. Special gratitude goes to Mr. Yos Ginting for the countless hours spent modifying the SIMPLEX algorithms which were so essential in carrying out the kinetic modelling studies. I am also grateful to Mr. Simon Vanderaa for his proof reading of sections of this thesis.

I would like to extend my appreciation to the members of the Paper Group at the University of Tasmania for their input and support during the course of the project. My thanks also go to the staff and fellow post-graduate students in the Chemistry Department at the University of Tasmania for making the last three and a half years an extremely enjoyable and rewarding experience.

Finally, I would like to thank my wife, Sue, for her constant love, care and support throughout the entire course of this degree.

ABSTRACT

The response of a commercial hardwood mechanical pulp, *E. regnans* stone groundwood, to alkaline peroxide bleaching has been studied by examining the kinetics of the bleaching process under conditions of constant reagent concentrations. Several kinetic models have been tested for their ability to describe the observed kinetic behaviour in terms of a minimum number of chemically meaningful parameters. A previously reported kinetic model, developed to describe the peroxide bleaching of softwoods, was found to be inadequate. As a consequence, two new kinetic models have been proposed, both of which are defined in terms of first order processes. The first model type assumes two distinct categories of chromophores which are eliminated to give colourless products. The chromophoric groups are divided into peroxide susceptible or peroxide resistant groups on the basis of their kinetic behaviour. The second model type assumes a single class of chromophores which are eliminated to give colourless products and potential chromophores. In this 'equilibrium' model, chromophore elimination is opposed by a chromophore creation route arising from conversion of potential chromophores to chromophores. An understanding of the main chemical processes occurring in peroxide bleaching has been achieved by analysing the behaviour of pseudo-first order rate constants for each model. Both of the proposed models are able to describe a number of kinetic features observed under constant reagent concentrations, such as a maximum in the rate of bleaching in the *p*H 11-12 range. However, only the model containing a reversible step can describe the full range of experimental behaviour observed when reagent concentrations are altered during bleaching, suggesting that colour formation is an important process during alkaline peroxide bleaching.

The kinetics of reactions between alkaline peroxide and model lignin chromophores have been examined to lend further interpretation to the kinetic models developed for the bleaching of pulp. Cinnamaldehyde has been studied as a model for α,β-unsaturated aldehyde chromophores while the reactions of *ortho* quinone

chromophores have been investigated using 4-*tert*-butylorthoquinone as a model. Reactions with cinnamaldehyde have shown that α,β-unsaturated aldehydes are readily attacked by perhydroxyl anions (HO_2^-) to give colourless epoxide intermediates. The epoxides are further degraded to benzaldehyde derivatives leading to an irreversible removal of colour. Reactions between alkaline peroxide and 4-*tert*-butylorthoquinone indicate that *ortho* quinones undergo competing colour removing and colour creation reactions with perhydroxyl anions and hydroxide ions respectively. The colour creation processes result in the formation of peroxide resistant hydroxy *para* quinones which lead to incomplete removal of colour during bleaching.

The kinetic behaviour of model α,β-unsaturated aldehydes and *ortho* quinones can be related to the reaction steps in the two chromophore kinetic model described previously, and can explain certain kinetic features observed during the bleaching of pulp. However, the process of chromophore formation contained in the equilibrium kinetic model was not observed in studies on model α,β-unsaturated aldehydes and *ortho* quinones, and further work is required to identify possible colour causing reactions under peroxide bleaching conditions.

CHAPTER 1

INTRODUCTION

During the last century, the production of wood pulp for paper and board manufacture has been dominated by chemical pulping processes such as kraft and sulphite pulping. These processes produce high value, high quality pulps which are suitable for a wide variety of applications ranging from packaging material to fine writing paper. However, associated with the production of chemical pulps are several inherent disadvantages which are summarised below.

(1) High capital costs are required to construct chemical pulp mills.

(2) Kraft chemical pulps are relatively dark and, for most applications, require bleaching with harmful chlorine based chemicals, resulting in water pollution problems caused by bleach plant effluents.

(3) Wood fibre is inefficiently used in chemical pulping. For example, in kraft pulping only 45-50% of the original weight of wood is recovered as pulp. The remainder is dissolved in pulping chemicals and is eventually burnt to generate energy for the operation of the pulp mill.

Increasing environmental awareness over the last decade has led to growing demands for the more efficient use of wood fibre from both plantation and native forest resources. In addition, stricter pollution control regulations have made reduction of pollution a priority in the pulp and paper industry. This has led to renewed interest in mechanical pulping methods. Mechanical pulping is the most efficient process for the utilisation of wood fibre and typically yields between 93-99% of the original weight of wood as pulp. Mechanical pulp mills can be built with comparatively low capital investment and without the pollution problems associated with the manufacture of chemical pulps. The use of hydrogen peroxide to bleach mechanical pulps has made

the achievement of moderate to high brightness gains possible without losses in yield or significant impact on the environment. These factors have contributed to a growing demand for peroxide bleached mechanical pulps over the last 10-15 years, particularly as partial substitutes for chemical pulps in higher quality paper grades.

Despite the prospects of an expanding market for peroxide bleached pulps, the underlying chemistry of peroxide bleaching is incompletely understood. A greater knowledge of peroxide bleaching chemistry is essential if the brightness response and stability of peroxide bleached pulps are to be improved in the future. With these points in mind, the overall aim of this study has been to gain a better understanding of the main kinetic processes taking place during the peroxide bleaching of *Eucalyptus regnans* mechanical pulp. To achieve this objective, the study has been divided into two stages. The first stage, comprising Chapters 2 and 3, describes the development and testing of several kinetic models for the peroxide bleaching of mechanical pulp. The second stage, comprising Chapters 4 and 5, details complementary kinetic investigations carried out with model lignin compounds to allow further refinement and interpretation of the kinetic models developed in the earlier chapters. In Chapter 6 the results of kinetic studies on model lignin compounds are discussed in terms of the kinetic models proposed for the bleaching of mechanical pulp.

1.1 General Overview

1.1.1 The Structure of Wood

In its simplest description, wood can be regarded as a matrix of fibres composed of cellulose, and the structurally related hemicelluloses, overlaid and saturated with a highly oxygenated aromatic polymer known as lignin and a mixture of lower molecular weight compounds called extractives[1].

Cellulose, the material required to make paper, is the main constituent of any woody plant and comprises approximately 40-45% of the dry substance in most wood species[2]. Cellulose is a linear homopolysaccharide with a degree of polymerisation of about 10,000 glucose units. In wood, individual cellulose molecules undergo intra and intermolecular hydrogen bonding to form bundles of cellulose molecules called microfibrils. In turn, microfibrils aggregate to form fibrils and finally cellulose fibres[2]. As a result of its fibrous structure, cellulose has a high tensile strength and is insoluble in most solvents.

Hemicelluloses are a group of heterogeneous polysaccharides which, like cellulose, provide physical support for the plant. In contrast with cellulose, hemicelluloses have a much smaller degree of polymerisation of about 200 units and may be branched. Hemicelluloses generally comprise between 20 and 30% of the dry weight of wood.

Lignin is another of the major components of wood and acts as a glue which binds the cellulose fibres together to give wood its inherent rigidity and strength[3]. Softwoods generally contain between 26-32% lignin while hardwoods have a slightly lower lignin content of 20-28%[2]. Lignins have been found to consist of polymers of phenylpropane (C_6 - C_3) which are divided into two classes according to their main structural elements. Softwood lignin is often referred to as 'guaiacyl lignin' since lignin of this type is largely a polymerisation product of guaiacyl monomers such as coniferyl alcohol (see Figure 1). Hardwood lignins are co-polymers of syringyl and guaiacyl units which vary in ratios from about 1 : 4 to 1 : 1[41]. Despite steady progress in lignin characterisation over the last fifty years, the exact nature of lignin still remains unclear as a result of its great structural complexity. This complexity is a result of the elaborate manner in which the phenylpropane units in lignin are linked, and is further complicated by the fact that the phenylpropane units are not structurally identical[4]. Nevertheless, detailed studies on isolated lignin preparations have clarified the main structural features of lignin, including the major functional groups and types of

linkages, and this work has been comprehensively reviewed in previous publications[2,4].

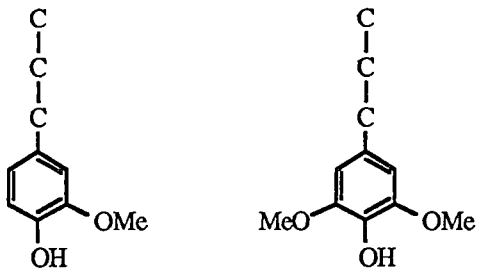

(a) (b)

FIGURE 1: The basic building blocks of lignin: (a) the guaiacyl monomer and (b) the syringyl monomer.

Extractives are the least abundant component of wood and may be divided into three sub-groups comprising aliphatic compounds (fats and waxes), terpenes and terpenoids, and phenolic compounds[2]. The content and composition of extractives varies considerably among wood species and also within different parts of the same tree[2]. Extractives are characterised by their ready extractability in organic solvents such as ethanol, acetone and dichloromethane, although a smaller proportion of extractives (eg. tannins) may be extracted with water.

1.1.2 The Sources of Colour in Wood

All wood possesses colour, however the degree of colouration differs markedly between trees of different species. For example *Pinus radiata* is a relatively bright species in comparison with a hardwood species such as *Eucalyptus regnans*. In addition, variations in the colour of wood removed from different sections of a single tree have also been reported[5]. In early studies on the sources of colour in some softwoods, a significant correlation was noted between the colour and lignin content

of both spruce (*Picea abies*)[5] and Douglas fir[6]. These results provided preliminary evidence that lignin was responsible for at least some of the colour in wood.

Further studies on the colour of the main wood components (cellulose, hemicellulose, extractives and lignin) confirmed that lignin was the major source of colour in softwoods[6-8] and, as a result, lignin is regarded as the component primarily responsible for imparting colour to softwood species. By contrast, the extractive components of eucalypt species are known to be highly coloured due to the presence of light absorbing polyphenolic compounds[42]. To produce a bright mechanical pulp from eucalypt species, it is therefore advantageous to remove as much of the extractives component as possible. Pale coloured eucalypt species such as *E. regnans*, *E. obliqua* and *E. delegatensis* possess an appreciable amount of water soluble extractives which can be removed by thoroughly soaking the wood prior to pulping[43]. The coloured polyphenolic extractives are more soluble in dilute alkali[43], and these extractives are removed to a large degree during the grinding of the wood, which is carried out in alkaline solution.

1.1.3 Measurement of Colour in Lignin Rich Pulps

The bleaching of lignin rich wood pulp is essentially the result of removal of light absorbing substances from the pulp[5], and in particular from the lignin where most of the colour originates. The colour of unbleached pulp is generally yellow or brown which results from absorption of visible light in the complementary part of the visible spectrum, the blue region. The absorption of light in this region has been shown to arise from the existence of a relatively intense, broad absorption band centred at about 280 nm and a pronounced shoulder which appears at around 350 nm, the tails of which both extend slightly into the blue region of the visible spectrum[9]. The chemical species responsible for these absorption bands will be discussed later.

In the paper making industry, the colour of pulp is usually quantified by the so called 'brightness' measurement. Brightness refers to the diffuse reflectance of a thick pile of paper handsheets made from the same pulp source and measured at a fixed wavelength. The brightness measurement is expressed as the percentage of light reflected from a sample relative to a standard white plate which is assigned a value of 100% reflectance. The absolute magnitude of measured brightness depends on the method of handsheet preparation, the optical geometry of the reflectance spectrometer, and the type of white standard used[5]. These variables have been standardised to a great extent by the formulation of the ISO brightness scale which has become the international industry standard. Most modern diffuse spectrometers (such as the Elrepho 2000 used in the present work) are manufactured to meet ISO specifications and report brightness measurements in % ISO units when the correct white standard is used.

The brightness quantity is wavelength dependent and values obtained for a single paper specimen generally differ markedly across the UV-visible wavelength range. For practical purposes, brightness is normally measured in the blue region of the UV-visible spectrum at a wavelength of 457 nm. This wavelength is a standard one in the paper industry and allows sensitive measurement of the extent to which the natural yellow-red colour of wood is removed during bleaching[10]. Brightnesses obtained at 457 nm also correlate closely with the human eye's perception of whiteness.

1.1.4 Kubelka - Munk Theory

Although brightness is a useful parameter for specifying the end use properties of paper, it is not a fundamental quantity but rather a complicated function of two more basic phenomena, light scattering and light absorption. Light scattering occurs when incident light strikes an internal or external fibre surface in paper while light absorption arises from the absorption of light by chromophoric substances.

When studying the chemistry of bleaching, the primary phenomenon of interest is light absorption because changes in this property are directly related to the removal of chromophoric structures[10-12]. For this reason, brightness is an unsuitable quantity for studying bleaching chemistry since it contains an additional component which describes the scattering properties of a paper sheet.

In 1931, Kubelka and Munk derived a cumbersome and incomplete set of equations to describe the relative contributions of light scattering and light absorption to brightness measurements. Kubelka[13] (1948) was later able to provide simplified and more practical forms of the so-called Kubelka-Munk equations, allowing light absorption and light scattering effects to be easily calculated from brightness measurements. Although initially employed in the textile industry, the Kubelka-Munk equations were recognised as particularly useful in studying the bleaching of pulp and paper, since they provided a direct method for monitoring absorption of light by chromophoric structures.

Derivation of the Kubelka-Munk equations is based on the scattering and absorption of light in successive thin layers of homogeneous material[10,13,14], (see Figure 2). The material is assumed to have a mass per unit area (or 'grammage') of W kg/m^2 and each thin layer has a grammage of dW kg/m^2. Two quantities, S and K, representing light scattering and light absorption phenomena respectively are defined so that if the surface layer of material is exposed to light of intensity I, a fraction of light I.S.dW is scattered while the amount I.K.dW is absorbed in the layer. The so-called light scattering (S) and light absorption (K) coefficients are both expressed in units of (grammage)$^{-1}$ ie. m^2/kg. The remaining light not absorbed or scattered in the surface layer continues through to the next layer where the absorption and scattering processes are repeated.

The complete derivation of the Kubelka-Munk equations from first principles is complex and results in many forms of equations, however only a few have practical applications. An excellent summary of the Kubelka-Munk equations as applied to the optical properties of paper has been presented by Robinson[15]. The most practical forms of the equations are presented in equations 1-3.

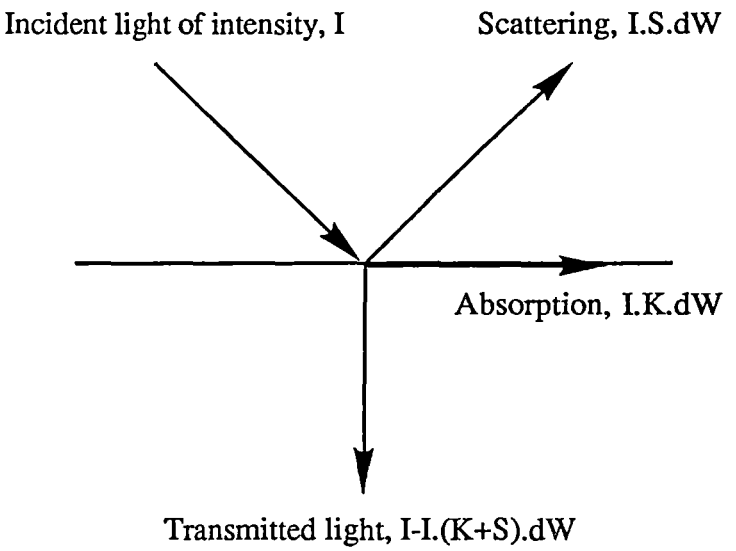

FIGURE 2: Diagram showing the physical basis for derivation of the Kubelka-Munk equations. K and S represent light absorption and scattering coefficients respectively (units m^2/kg) and W represents the mass/unit area of the surface (units kg/m^2).

1.1.5 Kubelka-Munk Equations

$$SW = \frac{R_{inf}}{1 - R_{inf}^2} \ln \left(\frac{1 - \Omega R_{inf}^2}{1 - \Omega} \right) \quad (1)$$

$$1 + \frac{K}{S} = \frac{1}{2}\left(\frac{1}{R_{inf}} + R_{inf} \right) = a \quad (2)$$

$$\frac{1}{2}\left(\frac{1}{R_{inf}} - R_{inf} \right) = \sqrt{a^2 - 1} \quad (3)$$

where R_{inf} = reflectance of an infinitely thick pile of sheets

R_0 = reflectance of a single sheet on a black background

Ω = opacity = R_0/R_{inf}

W = grammage = mass/unit area (kg/m^2)

K = absorption coefficient (m^2/kg)

S = scattering coefficient (m^2/kg)

When measuring the light absorption coefficients of paper sheets using the Kubelka-Munk equations, care must be taken to ensure that the sheets conform to three 'rules' arising from theoretical considerations during derivation of the equations[13,14]. The three rules are:

(a) that the optical density of the sheet must not be too low (eg. a thin specimen or poorly scattering material)

(b) that light must not be substantially absorbed before scattering (eg. a very dark material)

(c) that light scattering must not dominate over light absorption (eg. a very light material)

These three rules define the boundaries of an 'allowed region' in which all absorption coefficient measurements should fall[14]. When absorption coefficients fall outside these limits, the Kubelka-Munk equations cease to be exact and more approximate equations must be used[13]. The position of the different boundary limits are somewhat ill-defined and depend on factors such as instrument geometry and levels of acceptable error. Figure 3 shows limits of the Kubelka-Munk equations as proposed by Teder and Tormund[14].

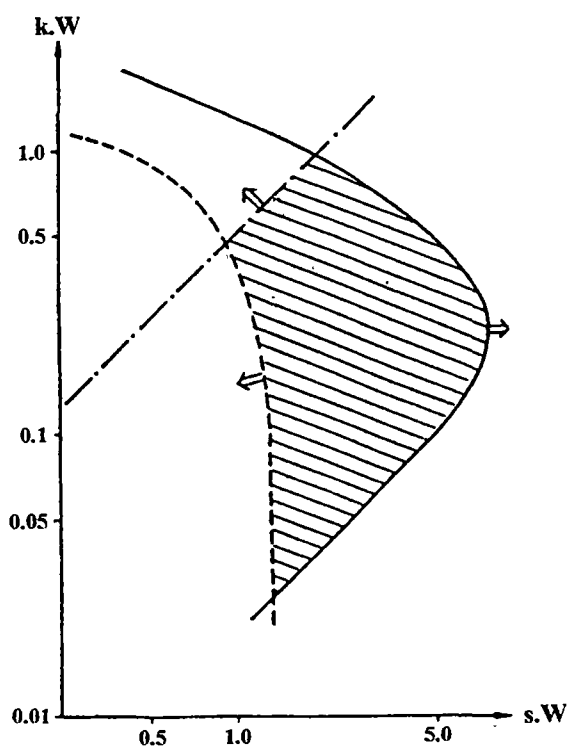

FIGURE 3: The limits of applicability of the Kubelka-Munk equations as calculated by Teder and Tormund[14]. The acceptable region is shaded.

1.1.6 Mechanical Pulping Processes

Despite recent trends towards thermomechanical and chemimechanical pulping methods, the stone groundwood process remains the oldest and most widely used process for converting wood to pulp by mechanical means. In stone groundwood pulping, debarked logs are pressed longitudinally against a rapidly rotating grindstone while water is sprayed onto the grinding zone. As a result of friction, temperatures in the grinding zone typically reach 150-190°C and cause the lignin component of the wood to plasticise, thus allowing physical separation of the wood fibres. The bundles of fibres torn from the wood are progressively refined to smaller units by further grinding before being deposited in a grinding pit[16]. The defibration of mechanical pulp by grinding is accompanied by an increase in colour which has been attributed to factors such as wood quality, wood storage and barking efficiency. Chemical reactions occurring during defibration, such as quinone formation, have also been reported to create colour during mechanical pulp production[17].

Mechanical pulping processes are characterised by very high fibre yields of 93-99% depending on the wood species, wood quality and grinding characteristics[16]. Softwoods are usually the preferred wood source for grinding due to their relatively low energy requirements, however lower density hardwoods such as *Eucalyptus regnans* are also suitable for groundwood production. Groundwood pulps are practically non-delignified and, as a consequence, are susceptible to yellowing with ageing. In the past, this has limited the application of groundwood pulps to temporary paper grades such as newsprint, catalogues, magazines, toilet tissues and paperboards[16]. As environmental awareness increases and efficient fibre utilisation become more important, it is forecast that bleached mechanical pulps will find further application as substitutes for bleached chemical pulps in the production of higher value paper grades such as writing papers and liquid-proof packaging.

1.1.7 The Bleaching of Mechanical Pulps with Alkaline Peroxide

The main purpose of bleaching pulp is to improve the optical properties of paper to a level sufficient for the forecast application. The most important optical property affected by bleaching is whiteness or brightness, however other intimately linked properties such as opacity and printability are also generally affected by bleaching[1]. In the bleaching of chemical pulps, the primary aim is to brighten the pulp by almost completely removing residual lignin. In contrast, the bleaching of mechanical pulps is achieved by selectively converting chromophores in the pulp lignin to colourless species without delignification, which would decrease the pulp yield.

The bleaching of mechanical pulps is most commonly carried out by reduction of chromophores using sodium dithionite ($Na_2S_2O_4$), or by oxidation of chromophores with hydrogen peroxide (H_2O_2). Although chromophores are effectively eliminated using dithionite, the reduced leucochromophores are easily re-oxidised to chromophores in the presence of oxygen and light to give a yellow coloured paper[2]. Dithionite solutions are corrosive and can attack paper machine wires and other equipment. They also suffer the disadvantage of reacting readily with oxygen, leading to loss of bleaching agent[5]. Hydrogen peroxide is able to more extensively degrade chromophores in lignin and produces a brighter, more stable pulp than dithionite bleaching. The corrosion problems associated with dithionite are also greatly reduced in peroxide bleaching. For these reasons, hydrogen peroxide has become increasingly popular as a lignin retaining bleaching agent for mechanical pulps, and more recently as a delignifying agent in the bleaching of chemical pulps[18,19].

The effectiveness of hydrogen peroxide as a bleaching agent for mechanical pulps is generally attributed to the action of the perhydroxyl anion (HO_2^-)[20] which exists in equilibrium with undissociated hydrogen peroxide under alkaline conditions, as shown in equation (1).

$$H_2O_2 + OH^- \rightleftharpoons HO_2^- + H_2O \qquad (1)$$

In conventional peroxide bleaching, sodium hydroxide is added to hydrogen peroxide solution to promote the formation of perhydroxyl anion, however excessive addition of alkali catalyses the decomposition of perhydroxyl anion to oxygen according to the overall reaction in equation (2).

$$2\,HO_2^- \longrightarrow O_2 + 2\,HO^- \qquad (2)$$

As a result of base catalysed decomposition at high *p*H, industrial peroxide bleaching is usually performed at an initial *p*H value of about 11 which falls during bleaching to a final value of about 9 as carboxylic acids are formed by oxidation reactions.

To gain a better understanding of peroxide bleaching in terms of the active bleaching agent (HO_2^-) the equilibrium constant for the equilibrium between hydrogen peroxide and the perhydroxyl anion in equation (1) must be accurately known. Teder and Tormund[21] have shown that the temperature dependence of the base dissociation constant for hydrogen peroxide, K_b, can be described by the equation:

$$pK_b = \frac{1330}{T} - 2.13 + 0.15\sqrt{[Na^+]} \qquad (3)$$

where

T = absolute temperature (K)

and

$$K_b = \frac{[OH^-]\,[H_2O_2]}{[HO_2^-]} \qquad (4)$$

From equations (3) and (4) it is evident that formation of perhydroxyl anion is favoured by increasing temperature, however industrial peroxide bleaching is generally carried out at 50°- 60°C since peroxide decomposition is accelerated at higher temperatures, leading to wastage of reagent.

The overall reaction for base catalysed decomposition of peroxide (equation 2) has been shown to occur through a variety of mechanisms involving hydroxyl and superoxide anion radicals[22-24] (Figure 4). The effects of these short lived radical intermediates on pulp brightness are still largely unknown, but recent work indicates that the highly reactive hydroxyl radical may assist in delignification by attacking electron rich sites in lignin, such as aromatic rings[25-27].

$$H_2O_2 + HO_2^- \longrightarrow HO^\cdot + O_2^{\cdot-} + H_2O$$

$$O_2^{\cdot-} + HO^\cdot \longrightarrow O_2 + HO^-$$

$$2\,O_2^{\cdot-} + H_2O \longrightarrow {}^1O_2 + HO_2^- + HO^-$$

$${}^1O_2 + O_2^{\cdot-} \longrightarrow O_2 + O_2^{\cdot-}$$

FIGURE 4: Example base catalysed peroxide decomposition mechanisms involving generation of radical species (after Gierer[24], Agnemo and Gellerstedt[23] and Roberts *et al*[22]).

The presence of transition metal ions such as iron, copper and manganese is also known to catalyse the decomposition of alkaline hydrogen peroxide. Several peroxide decomposition mechanisms involving transition metals are shown in Figure 5. These metals have been found to originate in the native wood, in the grinding water, in impurities in the bleaching reagents or through corrosion of equipment during pulp production[5]. Copper and iron show moderate catalytic activity towards decomposition, however manganese has the most serious effect on peroxide stability[30].

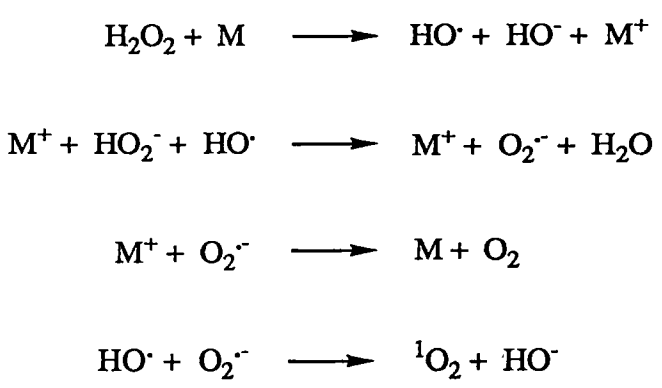

FIGURE 5: Example peroxide decomposition mechanisms involving transition metal ions (after Baral *et al*[28], Walling[29], Gierer[24] and Agnemo and Gellerstedt[23]). M = Fe^{2+}, Mn^{3+}, Cu^{+}.

To minimise peroxide decomposition during bleaching, two types of additives are normally employed during peroxide bleaching. The first type stabilises peroxide bleaching liquors by providing a buffering action in the normal bleaching *p*H range of 9-11. Sodium silicate is the most widely used additive of this type and has been found to give considerable improvements in the bleaching response of mechanical pulp[31]. In addition, sodium silicate appears to deactivate metal ions towards decomposition reactions[30], however the exact mechanism of deactivation is unknown. Magnesium ions, added as magnesium sulphate, have a similar deactivation effect on metal ions and produce a synergystic effect when added with sodium silicate, although the mechanism for this is also largely unknown[5].

The second type of additive reduces peroxide decomposition by removing trace levels of transition metal ions from pulp in a pre-bleaching treatment. Pre-treatment typically involves the application of a chelating agent such as ethylenediamine tetracetic acid (EDTA), pentasodium diethylenetriamine pentacetate (DTPA) or diethylenetriamine pentamonophosphonic acid (DTMPA). Manganese and copper are easily removed by pre-treatment with chelating agents, but a proportion of the iron remains firmly complexed to natural chelants in the lignin and cannot be completely removed[5].

The reaction of alkaline peroxide with lignin is non-selective[32] and it is believed that only a small proportion of peroxide is consumed in decolouration of chromophoric structures[5]. It is generally accepted that the main peroxide bleaching reactions involve elimination of *para* and *ortho* quinones[33,34], coniferaldehyde structures[35-37], and to a lesser degree, α-aryl carbonyls[36,38], although the actual reaction mechanisms are not known exactly in many cases. The reactions of these chromophoric compounds with alkaline peroxide are discussed in more detail in the following chapters.

The peroxide bleaching of mechanical pulp is usually carried out in a downflow tower, however processes such as refiner peroxide bleaching are also practised. In tower bleaching, thickened pulp of a consistency between 10% and 20% is fed into a bleaching tower. The bleaching chemicals are metered individually by pump and are mixed together just prior to their addition to the bleaching tower. The pulp is mixed thoroughly during the bleaching process which generally lasts between 1.5 to 3 hours[5]. The bleached pulp is diluted with water to about 4% consistency before being discharged from the bottom of the tower where it must be adjusted to a slightly acid *p*H to prevent alkali darkening reactions.

The addition of alkaline peroxide to pulp during refining has the advantage of avoiding costs associated with the construction and operation of a dedicated bleaching tower[39]. In addition, refiner bleaching offers the advantage of vigorous mixing at elevated temperatures (> 100°C) thus promoting rapid reaction. The high temperatures encountered during refiner bleaching increase the rate of thermal peroxide decomposition, therefore the optimum *p*H levels in refiner bleaching are somewhat lower than those in tower bleaching, to assist in peroxide stabilisation. Sodium silicate cannot be used to stabilise peroxide in refiner bleaching since it coats the refiner plates and quickly shortens their useful lifetime. Under optimised conditions, refiner bleaching is capable of producing comparable brightness gains to those obtained in tower bleaching[40], however it is still not a widely practised method for bleaching mechanical pulps.

REFERENCES

1. Barker, G.J. and Cullinan, H.T., The Production of Wood Pulp in Australia., *Search*, **20(6)**, 195-97, (1989).

2. Sjöstrom, E., Wood Chemistry, 1st Edition, Academic Press, New York, 1984.

3. Yan, J.F. and Johnson, D.C., Delignification and Degelation: Analogy in Chemical Kinetics., *J. Applied Polymer Sci.*, **26**, 1623-35, (1981).

4. Wardrop, A.B., in Lignins: Occurrence, Formation, Structure and Reactions., Chapter 2, 'Occurrence and Formation in Plants', K.V. Sarkanen and C.H. Ludwig (Eds.), 1st Edition, Wiley-Interscience, New York, 1971.

5. Lorås, V., In Pulp and Paper - Chemistry and Chemical Technology, Chapter 5, 'Bleaching', J.P. Casey.(Ed.), Chemistry and Chemical Technology, Volume 1: Pulp and Paper., 3rd Edition, Wiley-Interscience, New York, 1980.

6. Wilcox, M.D., Measuring the Brightness, Light Absorption Coefficient, and Light Scattering Coefficient of Wood., *Svensk Papperstidning*, **78(1)**, 22-26, (1975).

7. Norrstrom, H., Light Absorbing Properties of Pulp and Pulp Components. Part 1. Method., *Svensk Papperstidning*, **72(2)**, 25-31, (1969).

8. Barton, G.M., Significance of Western Hemlock Phenolic Extractives in Groundwood Pulping., *Tappi*, **56(5)**, 115-18, (1973).

9. Polcin, J. and Rapson, W.H., Effects of Bleaching Agents on the Absorption Spectra of Lignin in Groundwood Pulp: Part 1. Reductive Bleaching., *Pulp Paper Mag. Can.*, **72(3)**, 69-80, (1971).

10. Robertson, G.J., in Fundamentals Of Paper Performance, Chapter 9, 'General and Theoretical Concepts of the Optical Properties of Paper.', APPITA Technical Association, 1985.

11. Lundqvist, M., Kinetics of Hydrogen Peroxide Bleaching of Mechanical Pulp., *Svensk Papperstidning*, **82(1)**, 16-21, (1979).

12. Axegård, P., Moldenius, S. and Olm, L., Basic Chemical Kinetic Equations are Useful for an Understanding of Pulping Processes., *Svensk Papperstidning*, **82(5)**, 131-36, (1979).

13(a). Kubelka, P., New Contributions to the Optics of Intensely Light-Scattering Materials. Part 1. and references contained therein, *J. Opt. Soc. Amer.*, **38(5)**, 448-57, (1948).

13(b). Kubelka, P., Errata: New Contributions to the Optics of Intensely Light-Scattering Materials. Part 1., *J. Opt. Soc. Amer.*, **38(12)**, 1067, (1948).

14. Teder, A. and Tormund, D., Kinetics of Chlorine Dioxide Bleaching., *Trans. Tech. Assoc. CPPA*, **3(2)**, TR41-46, (1977).

15. Robinson, J.V., A Summary of Reflectance Equations for Application of the Kubelka-Munk Theory to Optical Properties of Paper., *Tappi*, **58(10)**, 152-53, (1975).

16. Fengel, D. and Wegener, G., Wood: Chemistry, Ultrastructure, Reactions., Chapter 16, 'Pulping Processes', 1st Edition, De Gruyter, Berlin, 1984.

17. Gellerstedt, G., Pettersson, I. and Sundin, S., Chemical Aspects of Hydrogen Peroxide Bleaching, *1st International Symposium of Wood and Pulping Chemistry*, Volume II, 120-124, (1981).

18. Lachenal, D. and Papadopoulos, J., Improvement of Hydrogen Peroxide Delignification., *4th Int. Symp. Wood and Pulping Chem.*, 295-299, (1987).

19. Lachenal, D., de Choudens, C. and Monzie, P., Hydrogen Peroxide as a Delignifying Agent., *Tappi*, **63(4)**, 119-122, (1980).

20. Andrews, D.H. and Singh, R.P., In The Bleaching of Pulp, Chapter 8, 'Peroxide Bleaching', R.P. Singh (Ed.), Tappi Press, Atlanta, 1979.

21. Teder, A. and Tormund, D., The Equilibrium Between Hydrogen Peroxide and the Peroxide Ion - A Matter of Importance in Peroxide Bleaching., *Svensk Papperstidning*, **83(4)**, 106-109, (1980).

22. Roberts, J.L., Morrison, M.M. and Sawyer, D.T., Base Induced Generation of Superoxide Ion and Hydroxyl Radical from Hydrogen Peroxide., *J. Am. Chem. Soc.*, **100(1)**, 329-30, (1978).

23. Agnemo, R. and Gellerstedt, G., The Reactions of Lignin with Alkaline Hydrogen Peroxide. Part II. Factors Influencing the Decomposition of Phenolic Structures., *Acta Chem. Scand.*, **B33(5)**, 337-42, (1979).

24. Gierer, J., Mechanisms of Bleaching with Oxygen-Containing Species., *4th Int. Symp. Wood and Pulp. Chem.*, 279-288, (1987).

25. Reitberger, T., Gierer, J., Jansbo, K., Yang, E. and Yoon, B-H., On the Participation of Hydroxyl Radicals in Oxygen and Hydrogen Peroxide Bleaching Processes., *6th Int. Symp. Wood and Pulp. Chem.,* Vol. 1, 93-97, (1991).

26. Sjögren, B., Reitberger, T. and Zachrison, H., The Importance of Radical Reactions for Brightness Increase in Hydrogen Peroxide Bleaching of Mechanical Pulps., *5th Int. Symp. Wood and Pulp. Chem.*, 161-166, (1989).

27. Gierer, J. and Yang, E., Model Studies of the Reactions Between Hydroxyl Radicals and Aromatic Lignin Structures., *6th Int. Symp. Wood and Pulp. Chem.,* 197-200, (1991).

28. Baral, S., Lume-Pereira, C., Janata, E. and Henglein, A., Chemistry of Colloidal Manganese Dioxide. Part 2. Reaction with O_2^- and H_2O_2 (Pulse Radiolysis and Stop Flow Studies)., *J. Phys. Chem.*, **89**, 5779-83, (1985).

29. Walling, C., Fenton's Reagent Revisited., *Acc. Chem. Res.*, **8**, 125-131, (1975).

30. Colodette, J., Fairbank, M.G. and Whiting, P., The Effect of pH Control on Peroxide Brightening of Stone Groundwood Pulp., *Tech. Sect. CPPA*, 75th Annual Meeting, B45-49, (1989).

31. Ali, T., McArthur, D., Stott, D., Fairbank, M. and Whiting, P., The Role of Silicate in Peroxide Brightening of Mechanical Pulp. Part 1. The Effects of Alkalinity, pH, Pre-treatment with Chelating Agent and Consistency., *Tech. Sect. CPPA*, 72nd Annual Meeting, B15-26, (1986).

32. Jones, G.W., The Effect of Sodium Peroxide Bleaching on the Components of Eastern Spruce Groundwood., *Tappi*, **33(3)**, 149-60, (1950).

33. Gellerstedt, G., Hardell, H-L. and Lindfors, E-L., The Reactions of Lignin with Alkaline Hydrogen Peroxide. Part IV. Products from the Oxidation of Quinone Model Compounds., *Acta Chem. Scand.*, **B34(9)**, 669-73, (1980).

34. Imsgard, F., Falkehag, S. and Kringstad, K., On Possible Chromophoric Structures in Spruce Wood., *Tappi*, **54(10)**, 1680-84, (1971).

35. Pew, J.C. and Connors, W.J., Colour of Coniferous Lignin., *Tappi*, **54(2)**, 245-51, (1971).

36. Gellerstedt, G. and Agnemo, R., The Reactions of Lignin With Alkaline Hydrogen Peroxide. Part III. The Oxidation of Conjugated Carbonyl Structures., *Acta Chem. Scand.*, **B34(4)**, 275-80, (1980).

37. Bailey, C.W. and Dence, C.W., Reactions of Alkaline Hydrogen Peroxide with Softwood Lignin Model Compounds, Spruce Milled Groundwood Lignin and Spruce Groundwood., *Tappi*, **52(3)**, 491-500, (1969).

38. Holah, D.G. and Heitner, C. and references contained therein, The Colour and UV-Visible Absorption Spectra of Mechanical and Ultra-High Yield Pulps Treated With Alkaline Hydrogen Peroxide., *J. Pulp Paper Sci.*, **18(5)**, J161-64, (1992).

39. Strunk, W.G. and Meng, T., Status Report: Pulp Bleaching with Hydrogen Peroxide During Refining., *Pulp and Paper*, **60(11)**, 111-15, (1986).

40. Sharpe, P.E. and Rothenberg, S., Refiner Hydrogen Peroxide Bleaching of Thermomechanical Pulps., *Tappi J.*, **71(5)**, 109-13, (1988).

41. Fengel, D. and Wegener, G., in Wood: Chemistry, Ultrastructure, Reactions., Chapter 6, 'Characterisation and Properties of Lignins and Lignin Derivatives', 1st Edition, De Gruyter, Berlin, 1984.

42. Hillis, W.E., The Contribution of Polyphenolic Wood Extractives to Pulp Colour., *Appita*, **23(2)**, 89-101, (1969).

43. Hillis, W.E. and Swain, T., in Wood Extractives., Chapter 12, 'Extractives in Groundwood and Newsprint', W.E. Hillis (Ed.), 1st Edition, Academic Press, London, 1962.

CHAPTER 2

KINETIC MODELS FOR PEROXIDE BLEACHING UNDER ALKALINE CONDITIONS. ONE AND TWO CHROMOPHORE MODELS.

2.1 Literature Review

2.1.1 Kinetic Models for Pulping and Bleaching

In the past, kinetic models for the peroxide bleaching of high yield pulps have been far outnumbered by models related to delignification processes, for example kraft[1,2] and alkaline pulping[3-6] and chlorine[7], chlorine dioxide[8] and oxygen bleaching[9]. As a consequence, the form of model most commonly applied to alkaline peroxide bleaching has been adapted from empirical kinetic equations originally devised to describe delignification processes. An example of such an equation is shown in (1) for alkaline pulping[3].

$$- dL / dt = k [L]^a [X]^b [Y]^c \qquad (1)$$

where L = lignin concentration, usually measured as Kappa number

X, Y = concentrations of pulping or bleaching reagents. eg. X = AQ and $Y = OH^-$ for soda-anthraquinone pulping

k = rate constant

a, b, c = orders of reaction

Empirical kinetic models suffer the drawback of providing little insight into basic chemical processes occurring during a reaction. Indeed, many authors have pointed out that the main purpose of empirical kinetic expressions is to facilitate control and

optimisation of industrial processes[1,4,5,7-11]. The orders of reaction in an empirical model such as (1) do not possess any chemical meaning but are considered to be variable parameters, the values of which are determined by fitting an empirical expression to experimental data.

The application of empirical equations to pulping and bleaching processes generally results in non-integral reaction orders, often with values in the range 3 - 5 [7,8,10-13]. In the past, many attempts have been made to interpret the chemical significance of such high orders of reaction even though these values possess no chemical meaning. Several authors have proposed that a number of parallel first order processes can behave as a single process of high, non-integral order[8,10-14]. Axegård *et al*[14] proposed that different kinds of chemical hindrance, such as chromophore formation, can result in apparent high orders for bleaching reactions. They also discussed the possibility that the rate determining step in pulping and bleaching reactions may involve heterogeneous processes such as diffusion which would produce high reaction orders.

A number of authors have rejected the application of empirical 'power law' models to delignification kinetics on the grounds that these models do not consider the molecular structure of lignin[3-5,15-17]. In attempting to establish the molecularity of delignification processes, these authors have treated delignification as the depolymerisation of an extensive three dimensional network according to the rules of the Flory - Stockmayer theory. This theory is a relatively simple one which assumes that polymeric branching in lignin occurs in a tree-like fashion. The branched polymer is characterised in terms of a statistical molecular weight distribution and equal reactivity is assumed among functional groups in the polymer. The major disadvantage of the Flory - Stockmayer theory is that complex expressions are required to describe the statistical distribution of molecular weights and reaction rates in lignin depolymerisation. Many assumptions and approximations must also be made before use of the theory becomes practical[18]. Nevertheless, several kinetic models

based on this macromolecular approach have been able to describe delignification in a chemically meaningful way[4,5]. For example, when applied to soda and kraft pulping, a 'two-gel' kinetic model suggested a first order delignification reaction with respect to lignin monomer[4]. This forward reaction was opposed by a reverse reaction which was found to be second order in lignin monomer. Kinetic evidence indicated that the opposing reaction could be associated with lignin recondensation while the forward reaction was associated with depolymerisation by pulping chemicals.

2.1.2 Kinetic Studies of Alkaline Peroxide Bleaching

Despite the growing importance of hydrogen peroxide as a bleaching agent for high yield pulps, very few investigations have been published dealing with the peroxide bleaching kinetics of mechanical and thermomechanical pulps under alkaline conditions. The first investigation of peroxide bleaching kinetics was carried out by Martin[19] who examined the bleaching of Eastern spruce groundwood. In this work, oxygen evolution due to decomposition of peroxide was subtracted from total peroxide consumption to determine the amount of peroxide consumed in reactions with the groundwood. The rate of total peroxide consumption was found to be a first order process at constant *p*H levels in the range 10.5 - 12.0. The rates of peroxide decomposition and reaction with groundwood were also found to be first order processes over the same *p*H range. As a result, equation (2) was proposed as a rate equation describing peroxide disappearance during the bleaching of Eastern spruce groundwood

$$- d[H_2O_2]_{total} / dt = \{k_d + k_r\}[H_2O_2]_{total} \quad \text{at constant } p\text{H.} \qquad (2)$$

where k_d, k_r = pseudo-first order rate constants for decomposition and reaction with pulp respectively

$[H_2O_2]_{total}$ = $[H_2O_2 + HO_2^-]$

Martin also noted that significant amounts of evolved oxygen were consumed during bleaching. The disappearance of this oxygen was found to occur at a rate independent of the peroxide concentration and was attributed to alkaline oxidation reactions which produced appreciable quantities of carbon dioxide.

A more detailed kinetic study of the peroxide bleaching kinetics of mechanical pulp was published in 1979 by Lundqvist[12]. In this work, isothermal bleaching experiments were conducted under constant concentrations of alkali and peroxide. These 'constant conditions' experiments were carried out by bleaching a spruce groundwood pulp at a consistency of 0.3%. At such low fibre concentrations, reagent consumption proceeded at a slow enough rate to allow peroxide and alkali levels to be replenished as they were consumed. The elimination of chromophores during bleaching was studied as a function of time by measuring the light absorption coefficients (K) of bleached pulp handsheets. The results of these bleaching experiments were fitted to an empirical mathematical model of the form:

$$- dC_K / dt = k [H_2O_2]^a [OH^-]^b C_K^n \qquad (3)$$

where C_K = the concentration of chromophores estimated by light absorption coefficient (K)

k = reaction rate constant

t = reaction time

a, b, n = orders of reaction.

The order of reaction with respect to peroxide concentration, *a*, was determined to be 1.0 in agreement with the earlier work of Martin[19]. The remaining orders of reaction, *b* and *n*, were found to have values of 0.3 and 5 respectively. From a mechanistic standpoint, Lundqvist recognised that a reaction order of 5 in chromophore concentration was highly improbable since, in strict kinetic terms, it would require the reaction of 5 chromophores with each other in a rate determining step. Instead it was proposed that a reaction involving three parallel first order reactions might imitate a single process of higher order.

The approach taken by Lundqvist was further extended by Moldenius and Sjögren[10,11] who examined the peroxide bleaching kinetics of a number of softwood mechanical and thermomechanical pulps. Bleaching experiments were conducted under constant conditions and also under 'differential conditions' which closer resemble the declining concentrations of peroxide and alkali encountered in industrial peroxide bleaching. Experimental results obtained under constant conditions at 0.3% consistency were fitted to the empirical model in equation (3) and resulted in reaction orders of $a = 1.0$, $b = 0.45$ and $C_K = 4.8$. Orders of reaction for experiments carried out under differential conditions at 15% consistency were approximately half the values obtained in constant conditions experiments. It was proposed that physical factors such as diffusion might influence the rate determining step at higher consistencies leading to the observed difference in reaction orders under differential and constant reagent conditions. Moldenius and Sjögren also reported a maximum in the rate of bleaching at *p*H 11.5 in constant conditions experiments, even though equation (3) predicted an indefinite increase in bleaching rate with alkali concentration. The maximum in bleaching rate was ascribed to a balance in the bleaching action of perhydroxyl anion (HO_2^-) and colour creation by alkali in condensation reactions.

More recently, the peroxide bleaching kinetics of *P. radiata* TMP pulp fractions have been examined in the context of the empirical model in equation (3)[13]. Constant conditions experiments were carried out at 60°C and at a pulp consistency of 1%. Reaction orders for the peroxide bleaching of whole TMP were reported to have values of $a = 1.2$, $b = 0.25$ and $n = 4.8$, while the fibre fraction yielded reaction orders of $a = 1.2$, $b = 0.21$ and $n = 5.0$. The reaction orders for the bleaching of pulp fines were only slightly different with values of $a = 1.0$, $b = 0.35$ and $n = 4.5$ being reported. From the similar kinetic response of fibre and fines, reflected in similar orders of reaction, it was concluded that fibre and fines lignin contains similar chromophoric structures.

2.2 Introduction

The present chapter examines the kinetics of chromophore elimination during peroxide bleaching of an *E. regnans* stone groundwood pulp. The effects of alkaline peroxide on the pulp have been followed by measuring changes in the concentration of chromophores as a function of time. The elimination of chromophores is conveniently followed by measuring light absorption coefficients (K) which are proportional to the chromophore concentration at a fixed wavelength[12,14]. Bleaching kinetics have been studied under constant reagent conditions at 50°C and 0.3% pulp consistency. These so called 'constant conditions' experiments are a well established technique for investigating peroxide bleaching kinetics and involve maintaining alkali and peroxide concentrations at constant levels during each experiment.

The constant conditions technique has several advantages[10,11,14]:

(1) The effects of each variable are easily isolated and mathematical treatment of data is straightforward.

(2) The reaction conditions resemble those used in the bleaching of model chromophore compounds, enabling simple comparison of the bleaching of pulp and model compounds.

(3) The influence of diffusion on kinetic behaviour is minimised since each fibre is effectively surrounded by bleaching solution under the low pulp consistencies employed.

When applied to peroxide bleaching, empirical kinetic models provide little or no mechanistic information. In the past, 'macromolecular' kinetic models have been developed to better reflect the chemistry of delignification[3-5,15-17], however these models are unsuitable for modelling peroxide bleaching kinetics since alkaline peroxide selectively removes chromophores from lignin without delignification. Therefore the aim of this kinetic study is to develop kinetic models which can better

assist in unravelling the underlying chemical phenomena involved in peroxide bleaching.

Several new kinetic models based on a simple network of parallel and/or consecutive first order processes are investigated in this chapter. The main advantage in assuming first order processes is that kinetic behaviour can be more readily interpreted with respect to individual reactions involved in peroxide bleaching. The new models have been formulated in terms of a minimum number of chemically meaningful parameters since it is often impossible to evaluate a large number of parameters in more complex models[18]. It is not expected that a completely correct kinetic model will result from such an approach, however, as stated above, it is hoped that the newer models will better reflect the underlying chemistry of peroxide bleaching.

2.3 Experimental

2.3.1 Chemicals

Hydrogen peroxide (30%) and sulphuric acid (98%) were supplied by Ajax Chemicals. Semi-conductor grade sodium hydroxide (Aldrich, 99.99%) was used as the alkali source to minimise the introduction of transition metal impurities.

2.3.2 Pulping and Bleaching Procedure

Stone groundwood (SGW) pulp was prepared from approximately 150 year old *E. regnans* blocks which were soaked in distilled, de-ionised water for three days prior to grinding. The wood was ground in a dilute solution of sodium hydroxide using a laboratory scale grindstone at Australian Newsprint Mills, Boyer. The resulting pulp was concentrated from 1.5% to 20% consistency by filtration and was refrigerated at 4°C until use.

Bleaching experiments were performed by adding sufficient *E. regnans* SGW pulp to 6 L of 18 MΩ de-ionised water such that a pulp slurry of 0.3% consistency was achieved. The slurry was vigorously stirred in a polyethylene reaction vessel which was immersed in a water bath to maintain a constant temperature of 50°C. Before each bleaching run, an aliquot of pulp was removed to make blank handsheets so that any changes in the pulp, due to storage, could be monitored.

Kinetic bleaching runs were initiated by simultaneously adding enough alkali (1M NaOH) and hydrogen peroxide to reach the target conditions. Subsequently, constant *p*H was maintained by adding alkali from a *p*H controller supplied by Cole-Parmer. The concentration of peroxide was maintained at constant levels by regular addition of the appropriate volumes of hydrogen peroxide, calculated from iodometric titration[20]. Following initiation of bleaching, aliquots of pulp slurry (400 mL) were removed at regular intervals to make pulp handsheets. The bleaching reaction was quenched by acidification of the slurry to *p*H 2.5 with sulphuric acid (2.5 M), followed by filtration to remove the bleaching liquor. Handsheets having conditioned basis weights of 35-45 g/m^2 were formed by filtering the required volume of re-dispersed pulp slurry onto Whatman No. 540 filter paper, as described in the Appita Standard[21]. Using this procedure, 3 handsheets were obtained from each aliquot. The sheets were fan dried for several hours at room temperature and were allowed to equilibrate at constant temperature (25°C) and humidity (50%) before measurement of conditioned basis weights.

After drying, black-backed and self-backed reflectance measurements were made on each sheet, at a wavelength of 457 nm, using an Elrepho 2000 reflectance spectrometer. Individual opacity (W), scattering coefficient (S) and light absorption coefficient (K) properties were calculated from Kubelka-Munk theory[22-24]. These properties were reported as the average per group of 3 handsheets (see Appendix 1.1). Absorbance difference spectra between unbleached and bleached handsheets were run on a Varian DMS 100 UV-visible spectrometer equipped with an integrating sphere.

2.4 Results

2.4.1 Influence of Peroxide Concentration on Bleaching Rates

An example of the influence of peroxide concentration on the rate of chromophore elimination, measured by the decrease in the light absorption coefficient (K), is illustrated in Figure 1 for bleaching at constant *p*H (*p*H 10). To enable comparison with other studies, light absorption coefficients were measured at a wavelength of 457 nm. All curves in Figure 1 are characterised by a rapid initial decrease in the light absorption coefficient which is favoured by increasing concentrations of peroxide. Following this initial phase of bleaching, the rates of chromophore elimination gradually decrease until a limiting rate is reached which appears to be independent of peroxide concentration. Since peroxide and alkali concentrations were maintained at constant levels during bleaching, the observed decrease in bleaching rate with time cannot be attributed to depletion of bleaching chemicals. Instead, the shapes of the bleaching profiles in Figure 1 reflect the differing susceptibilities of chromophoric groups in lignin to removal by alkaline peroxide. The same trends in the bleaching behaviour of *E. regnans* SGW were evident in similar bleaching experiments carried out at *p*H 9, 11 and 12.

At this point, it is worth noting that the peroxide bleaching chemistry of hardwood pulps such as *E. regnans* SGW will not be exactly the same as softwood species since hardwood lignins contain syringyl units not found in softwoods. Despite these differences, the general features of the bleaching profiles for *E. regnans* in Figure 1 are consistent with those reported in kinetic bleaching studies using northern hemisphere softwood pulps[11,13,25] (Figure 2). The similarity of these bleaching curves would seem to indicate that minor differences in the structure of hardwood and softwood lignins do not strongly influence trends in kinetic behaviour.

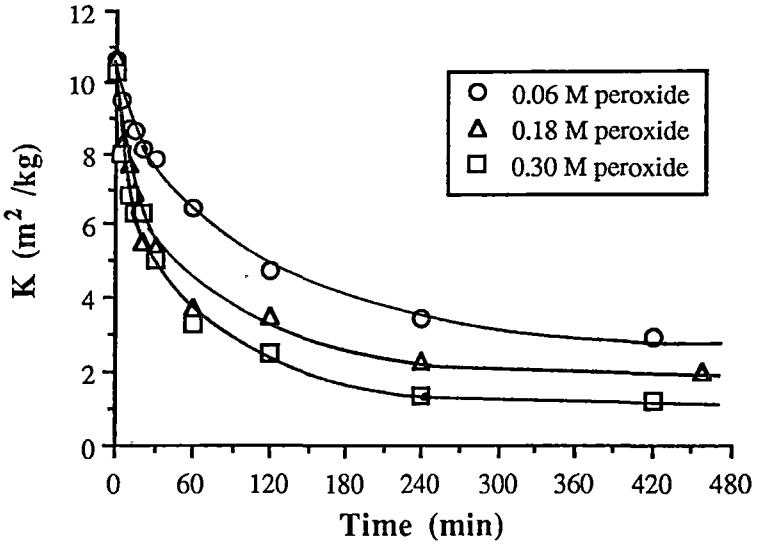

FIGURE 1: Bleaching profiles showing the effects of alkaline peroxide concentration on light absorption coefficients during bleaching of *E. regnans* SGW under constant reagent conditions. T = 50°C, *p*H 10, 0.3% consistency.

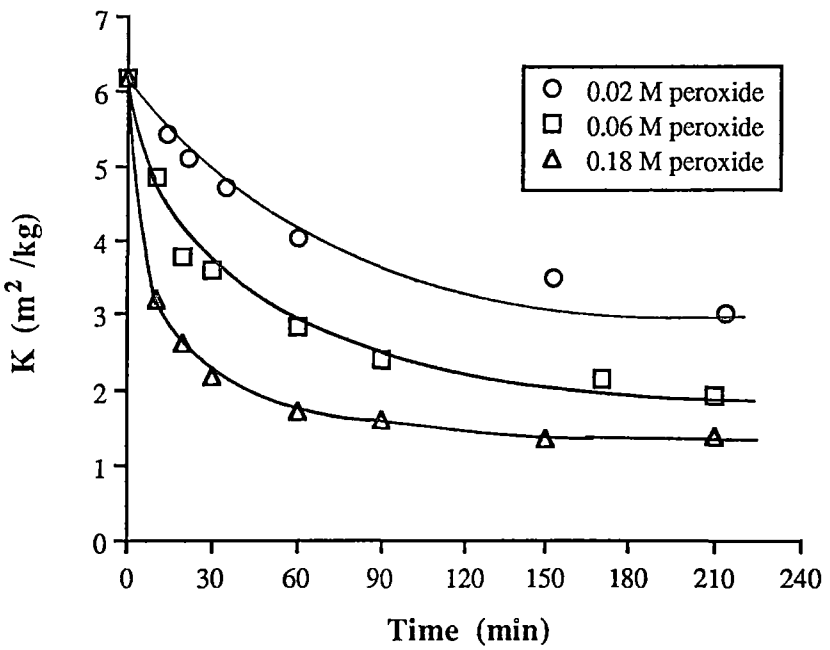

FIGURE 2: Bleaching profiles from the alkaline peroxide bleaching of *P. radiata* TMP under constant reagent conditions. T = 50°C, *p*H 11, 0.3% consistency. Results after Abbot and Ginting[25].

2.4.2 *Influence of Alkali Concentration on Bleaching Rates*

The influence of alkali concentration on the rate of peroxide bleaching was investigated by bleaching *E. regnans* SGW at a single peroxide concentration and various *p*H levels. Kinetic profiles from these experiments are illustrated in Figure 3. The same general features noted in Figure 1 are evident in Figure 3, with a rapid initial removal of colour being followed by a slower bleaching phase at each *p*H level examined. Further inspection of Figure 2 indicates that bleaching rates are favoured by increasing *p*H levels in the range 9-11, however the response at *p*H 12 is slightly poorer than that at *p*H 11 indicating a maximum bleaching effect in the *p*H 11-12 range. The same effect has previously been noted by Moldenius and Sjögren[11] who attributed the maximum in bleaching rate to a balance in the bleaching action of perhydroxyl anion (HO_2^-) and colour creation by alkali in condensation reactions.

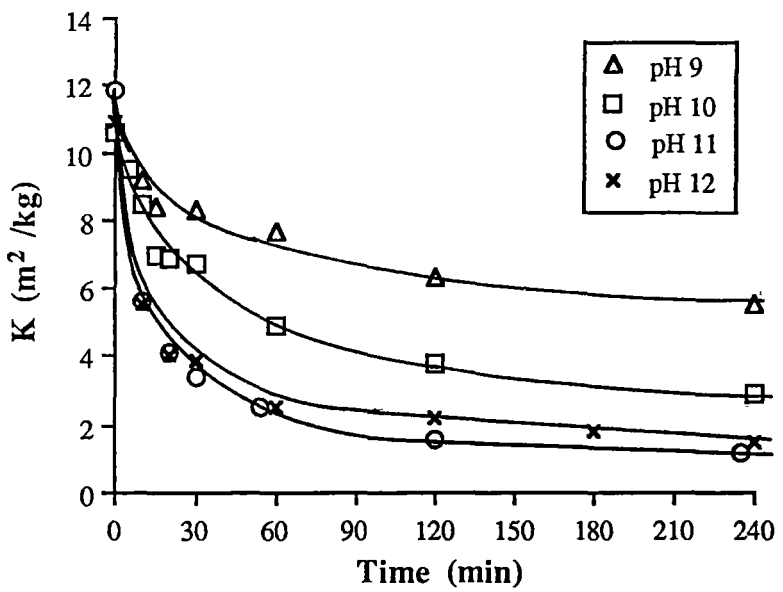

FIGURE 3: Bleaching profiles showing the effects of alkali measured as *p*H on light absorption coefficients during bleaching of *E. regnans* SGW under constant reagent conditions. T = 50°C, 0.12 M peroxide, 0.3% consistency.

2.4.3 UV-visible Difference Absorption Spectra

UV-visible difference absorption spectra of peroxide bleached *E. regnans* SGW were carried out by measuring the reflectance spectra of bleached pulps relative to an unbleached sample. Reflectance values obtained at 2 nm intervals were converted to absorbance units to produce the spectra shown in Figure 4. These spectra reveal a major decrease in absorption in the 360-380 nm range due to the removal of chromophores absorbing in this region. In addition, the specific absorption at wavelengths in the 420-520 nm range also progressively decreases with time. The main features of the difference spectra in Figure 4 are consistent with recently published difference spectra for alkaline peroxide bleached mechanical and thermo-mechanical softwood pulps[25]. In this work, the decrease in absorption at 360-380 nm was attributed to elimination of α,β-unsaturated aldehydes by reaction with perhydroxyl anions, while loss of absorption in the 420-520 nm range was associated with the oxidation of quinone groups.

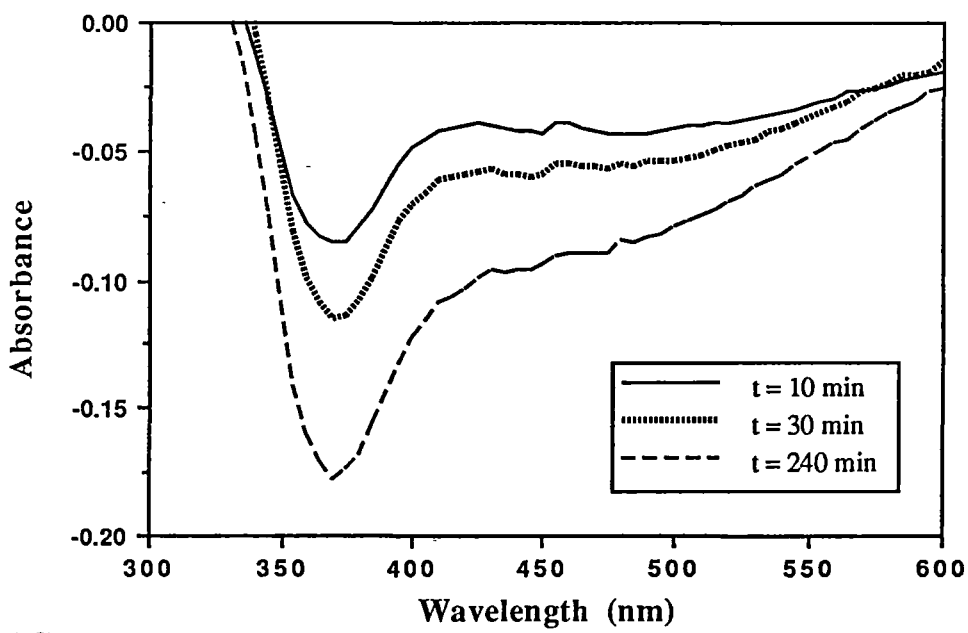

FIGURE 4: UV-visible difference spectra showing the progressive removal of chromophores absorbing in the 360-380 nm and 420-520 nm regions. *E. regnans* bleached under constant reagent conditions, T = 50°C, 0.2 M H_2O_2, *p*H 11.

It is evident from Figure 4 that loss of absorbance at 457 nm is due to removal of α,β-unsaturated aldehyde and quinone bands, which overlap at 457 nm. In other words, the decreases in light absorption coefficient (K) observed in Figures 1 and 3 result primarily from elimination of α,β-unsaturated aldehydes and quinones.

2.4.4 Kinetic Models for Peroxide Bleaching of Mechanical Pulp

Model I : Simple Empirical Models

Over the past decade there have been a number of attempts to formulate kinetic expressions which describe chromophore elimination during peroxide bleaching[10-14]. Using kinetic results from experiments at constant conditions, empirical expressions of the form of equation (3) have been formulated to describe the bleaching rate in terms of hydroxide, total peroxide and chromophore concentrations.

$$-\frac{d C_K}{dt} = k [OH^-]^a [H_2O_2]^b [C_K]^c \qquad (3)$$

where C_K = chromophore concentration as measured by light absorption coefficient (K).

Orders of reaction *a*, *b*, and *c* are determined experimentally and have been reported to have non-integer values. Equation 1 predicts that, at constant *p*H and peroxide concentration, the variation in chromophore concentration with time can be expressed as:

$$-\frac{d C_K}{dt} = k [C_K]^c \qquad (4)$$

where *k* is a pseudo *c*-order rate constant which is dependent on *p*H and total peroxide concentration.

Integration of equation (4) yields an expression of the form shown in equation (5).

$$C_K^{1-c} = (c-1)\,kt \qquad (5)$$

The reaction order, *c*, can be found from the slope of a plot of ln C_K vs. ln t, if a linear relationship is observed. These types of plots are depicted in Figure 5 for results from the bleaching of *E. regnans* SGW in the present work, and also for the results of Moldenius *et al*[10,11] and Allison *et al*[13] (Figure 6). Figure 5 clearly indicates that a linear fit of the experimental data for *E. regnans* is not satisfactory when an empirical single chromophore kinetic model is used. It is also clear that the data of Allison *et al* and Moldenius *et al* deviates slightly from the expected linear behaviour, particularly at longer bleaching times. This implies that the empirical model in equation (1) is only successful over a short range of time, with experimental behaviour at longer durations being poorly described.

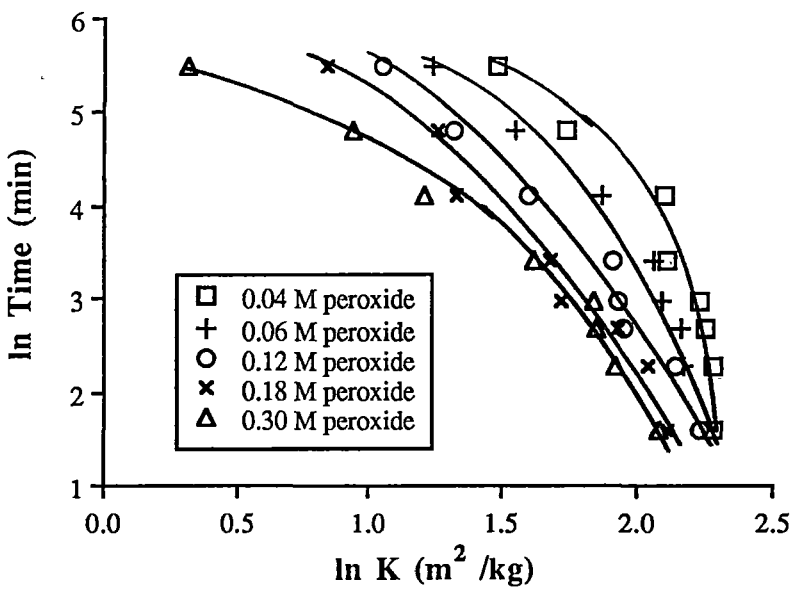

FIGURE 5: Plots of the natural log of absorption coefficient (K) against the natural log of time for the bleaching of *E. regnans* under constant reagent conditions at *p*H 10, 50°C.

(a)

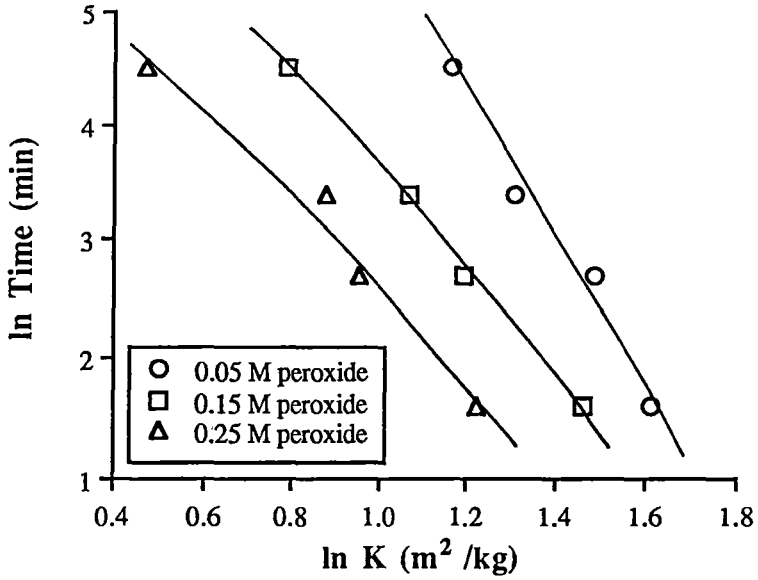

(b)

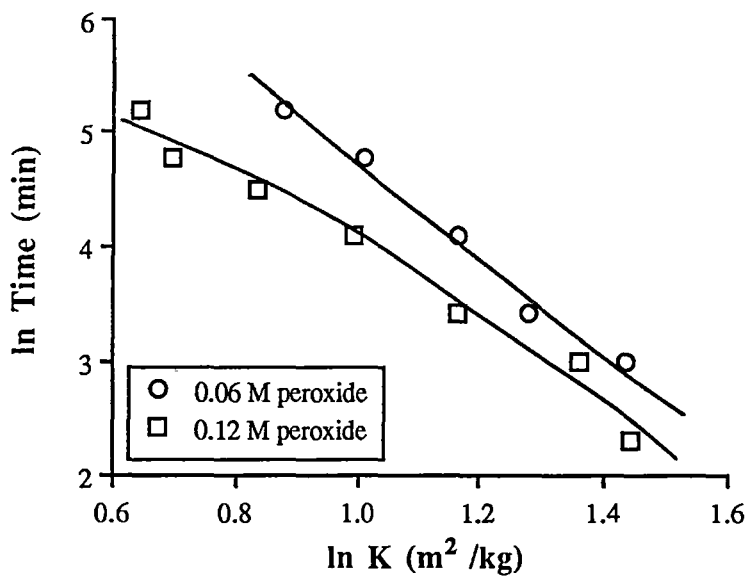

FIGURE 6: Plots of the natural log of absorption coefficient (K) against the natural log of time for (a) the bleaching of *P. radiata* TMP after Allison *et al*[13] and (b) the bleaching of spruce groundwood after Moldenius *et al*[11].

To achieve a better correlation between experimental results for the bleaching of *E. regnans* and a theoretical expression, two alternative types of model were investigated.

2.4.5 Model II : The Two Chromophore Model

Inspection of the experimental bleaching profiles in Figure 1 suggests the existence of at least two categories of chromophores which are responsible for light absorption at 457 nm. The first type (C_1) can be considered to be present during the initial stages of bleaching and is easily removed with alkaline peroxide. The rate of removal of C_1 is also strongly dependent on the concentration of peroxide present. This is clear from a comparison of initial rates of chromophore elimination when peroxide concentration is increased by a factor of approximately 5 (Figure 1).

The influence of the second chromophoric type (C_2) becomes dominant during the latter stages of bleaching when C_1 has largely been removed. Figure 1 indicates that C_2 is removed at a much slower rate than C_1. The rate of removal of C_2 does not depend strongly on peroxide concentration since the rate of chromophore removal becomes almost independent of peroxide concentration at long bleaching times. Similar conclusions regarding the existence of two distinct chromophore types can be drawn by inspection of similar plots for bleaching of softwood species under constant conditions[10-13] (eg. Figure 2).

At this stage C_1 and C_2 are better regarded as multi-component, lumped constituents which are defined entirely on the basis of their kinetic behaviour, however it is conceivable that C_1 and C_2 might eventually be identified with individual chromophoric structures in lignin. It is recognised that the assumption of two chromophoric categories is a major simplification since chromophores such as α,β-unsaturated aldehydes, *o*-quinones and α-aryl carbonyls have been shown to exist in lignin, each reacting via different routes[27-32]. Consideration of every individual chromophore in the lignin polymer and its subsequent reaction would result in a model

of considerable complexity and so the two chromophore model has been formulated in an attempt to describe the bleaching process using a minimum number of kinetically meaningful parameters.

The model chromophore types were assumed to be present in fixed initial concentrations of C_1^0 and C_2^0. C_1^0 is best thought of as representing the quantity of easily bleached chromophores originally present in unbleached pulp while C_2^0 represents the quantity of harder to remove chromophores. The sum of C_1^0 and C_2^0 corresponds to the light absorption coefficient of unbleached pulp. Upon reaction with peroxide, each type gives rise to a group of colourless products, C_P, via two parallel first order processes, as shown in Scheme 1. C_1 is assumed to react at a much faster rate than C_2 , hence C_2 can be identified with the latter part of the bleaching curves in Figure 1, while C_1 is largely responsible for the rapid initial loss of colour.

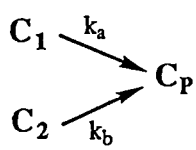

Scheme 1: The two chromophore kinetic model

2.4.6 Procedure for Calculation of Rate Constants

To further investigate the two chromophore model, estimates of values for the first order rate constants (k_a and k_b) and initial chromophore concentrations (C_1^0 and C_2^0) were required to allow simulation of experimental data.

Chromophore category C_2 was associated with the latter stages of bleaching, and was assumed to follow first order kinetics. Estimates of the corresponding rate constant (k_b) and initial chromophore concentration (C_2^0) were calculated by simultaneously

solving the equation for first order decay of C_2 (equation 6) using the final two light absorption coefficient values at each peroxide concentration.

$$C_2 = C_2^0 e^{-k_b t} \qquad (6)$$

The initial concentration of chromophore type C_1 (C_1^0) was easily calculated since

$$C_1^0 = C_{total}^0 - C_2^0 \qquad (7)$$

where C_{total}^0 is the light absorption coefficient of an unbleached pulp handsheet.

After 10 minutes bleaching, the amount of C_2 present was calculated from equation (6) allowing the corresponding amount of C_1 at 10 minutes to be calculated from equation (8).

$$C_1 = C_{total} - C_2 \qquad (8)$$

where C_{total} is the light absorption coefficient of a pulp handsheet after 10 minutes bleaching.

The rate constant associated with the removal of C_1 (k_a) was then estimated in the same way as k_b using data points at 0 and 10 minutes to define an initial rate through equation (9).

$$C_1 = C_1^0 e^{-k_a t} \qquad (9)$$

The validity of the model scheme in Scheme 1 was tested by performing kinetic simulations using TUTSIM, a commercially available program for the simulation of continuous dynamic systems. A description of TUTSIM in relation to soda-additive delignification has been given previously[6]. Substitution of C_1^0, C_2^0, k_a and k_b into TUTSIM allowed plots of light absorption coefficient as a function of time to be

generated for comparison with experimental data (see Appendix 1.2). Values of the estimated rate constants were adjusted slightly until minimisation of a least squares fit between experimental and theoretical points had been achieved. Typical comparisons of experimental and theoretical data at 0.06 M and 0.18 M peroxide are shown in Figure 7 at *p*H 10. It is evident from this Figure that Model II is successful in duplicating the experimental data, however to achieve a reasonable fitting of experimental points at different peroxide concentrations, it was necessary to adjust the values of initial chromophore concentrations (C_1^0 and C_2^0) as shown in Table 1. Such a variation of C_1^0 and C_2^0 contradicts the original idea that C_1^0 and C_2^0 should be present in a fixed ratio in unbleached *E. regnans* pulp.

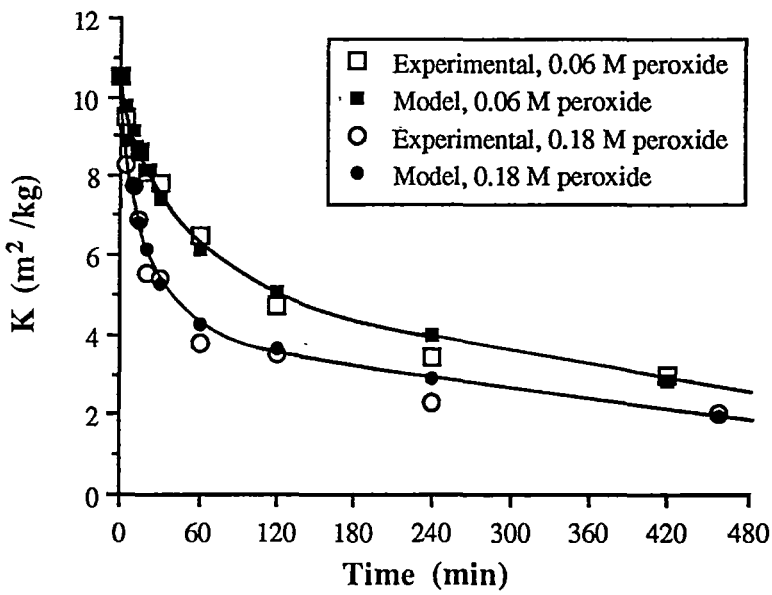

FIGURE 7: Comparison of experimental and model bleaching profiles from the peroxide bleaching of *E. regnans* SGW. Simulated points generated using the two chromophore kinetic model, T = 50°C, *p*H 10.

TABLE 1: Values of C_1^0 and C_2^0 required to provide optimum fitting of experimental data from the bleaching of *E. regnans* SGW at various peroxide concentrations. *p*H = 10, 0.3% pulp consistency, T = 50°C.

Peroxide Concentration (M)	C_1^0 (m^2/kg)	C_2^0 (m^2/kg)
0.038	4.47	6.02
0.062	6.30	4.19
0.11	6.62	3.87
0.18	7.83	2.66
0.29	8.94	1.55

2.4.7 Model III : The Two Chromophore Consecutive Reaction Model

To overcome the limitations of the two chromophore model, a newer model was formulated. While continuing with the idea of two chromophore types, the possibility of colourless products, C_P, being formed from C_1 via a consecutive reaction was considered (Scheme 2). In this model there are two parallel competing pathways for reaction of C_1; it can react directly to form colourless products, C_P, or it may react to give the more peroxide resistant chromophore, C_2. The faster C_1 reacts to produce C_P (eg. at higher peroxide concentrations) the smaller will be the opportunity for C_2 to accumulate.

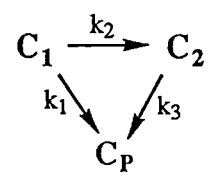

Scheme 2: The two chromophore consecutive reaction model

By inspection of Figures 1 and 3, the final sections of the bleaching profiles appeared to approach a common limiting slope at higher alkali and peroxide concentrations. As a result, the first order rate constant controlling this section of each kinetic curve (k_3)

was assigned a common value which was independent of peroxide and alkali concentration. Values of k_3 and C_2^0 were calculated from the final two light absorption coefficients at 0.29 M peroxide, *p*H 10 since the final section of this curve appeared to best define a limiting slope common to all the bleaching profiles. Assuming first order decay, values of $C_2^0 = 1.55$ and $k_3 = 0.001$ min^{-1} were obtained. For each bleaching curve, the rate constant responsible for the rapid initial rate (k_1) was estimated from the initial slope defined by light absorption coefficients at 0 and 10 minutes bleaching, as in Model II (section 2.4.6). The remaining parameter (k_2) was adjusted to minimise a least squares fit of model and experimental data at each concentration of peroxide. Simulated curves for model III were generated using TUTSIM. In some cases a simplex algorithm was also used to solve the rate constants k_1 - k_3. This algorithm is detailed more fully in Chapter 3. An example of the comparison between experimental and simulated values is shown in Figure 8 for results at *p*H 10. Figure 9 shows a typical concentration - time profile for the model species C_1, C_2 and C_P.

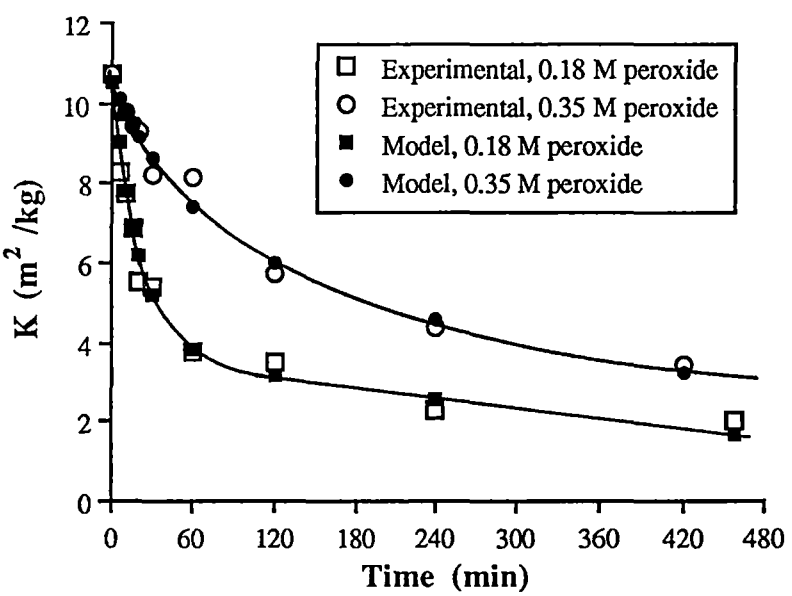

FIGURE 8: Comparison of experimental and model bleaching profiles from the peroxide bleaching of *E. regnans* SGW. Simulated points generated using the two chromophore consecutive reaction model, T = 50°C, *p*H 10.

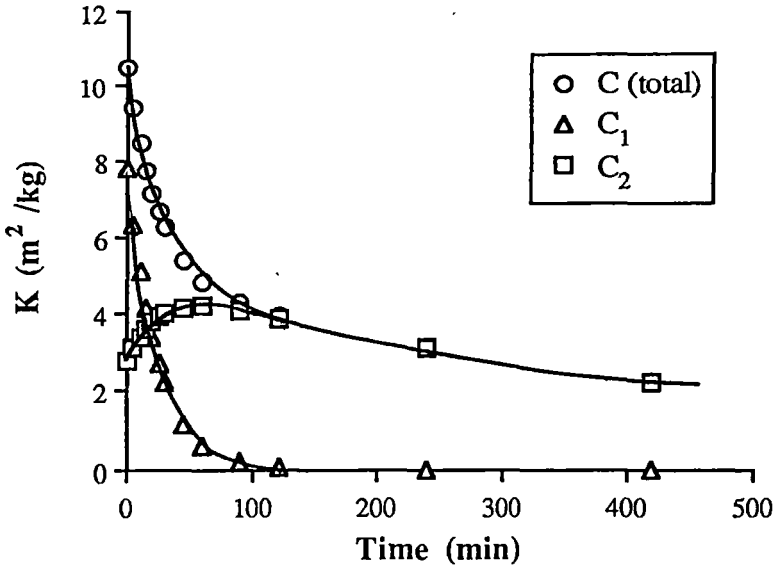

FIGURE 9: Typical example of the way in which model chromophores C_1 and C_2 contribute to the overall light absorption coefficient, C (total) during bleaching. *E. regnans* bleached under constant conditions, T = 50°C, 0.12 M H_2O_2, *p*H 10.

It is evident from Figure 8 that Model III is effective at simulating the experimental results for bleaching of *E. regnans* SGW without the need to alter $C_1^0 : C_2^0$ ratios, which was the main drawback of Model II. A comparison of the standard errors for fitting of experimental data to Model II and Model III is shown in Table 2. Such a comparison suggests that Model III is able to provide better fitting of experimental points than Model II across a range of peroxide concentrations.

TABLE 2: Comparison of model fits of experimental data at various peroxide levels, *p*H 10.

Peroxide Concentration (M)	MODEL II Std. Error (m^2/kg)[a]	MODEL III Std. Error (m^2/kg)[a]
0.038	0.34	0.33
0.062	0.78	0.42
0.11	0.39	0.45
0.18	0.52	0.45
0.29	1.0	0.59

[a] Standard Error = [(sum of squares of residuals) / (N-1)]$^{1/2}$, N = no. of data points.

Figure 10 indicates that Model III can also be applied to kinetic results for the bleaching of various softwood pulps[11,13].

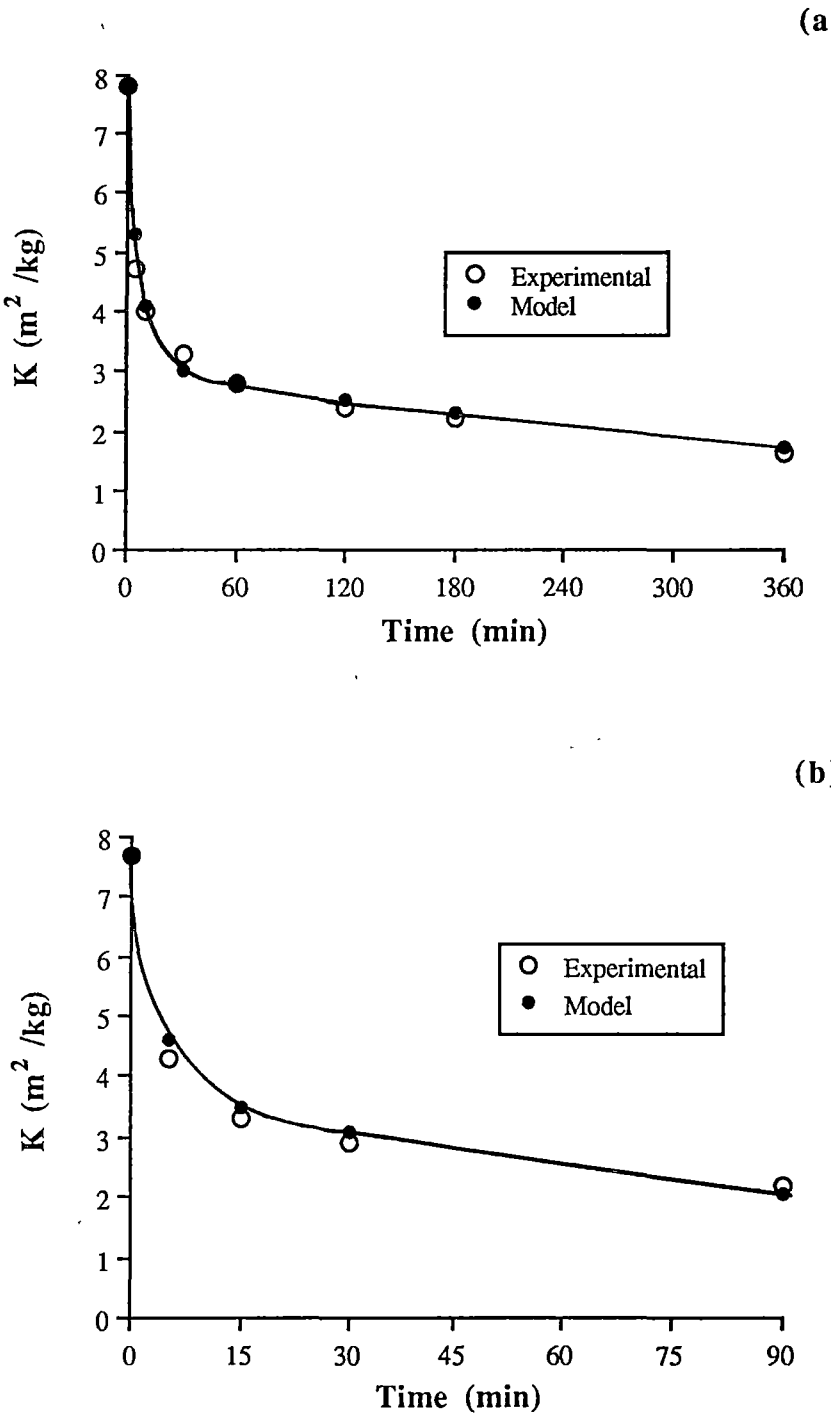

FIGURE 10: Comparison of experimental and model bleaching profiles from the peroxide bleaching of (a) spruce groundwood (after Moldenius *et al*[11]) and (b) *P. radiata* TMP (after Allison *et al*[13]). Simulated points generated using the two chromophore consecutive reaction model.

2.5 Discussion

2.5.1 Behaviour of Rate Constant k_1

The influence of total peroxide concentration on the rate constant associated with initial chromophore removal (k_1) is shown in Figure 11 at each *p*H level examined.

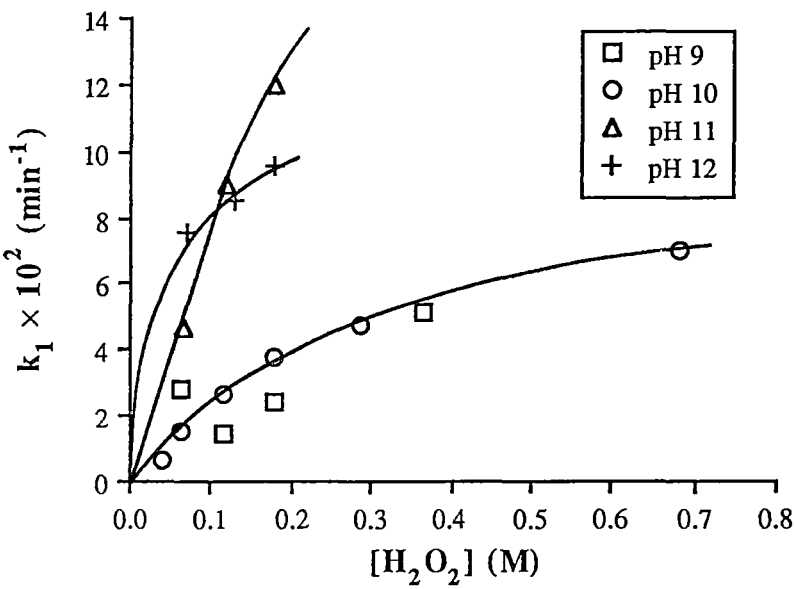

FIGURE 11: Dependence of first order rate constant k_1 on total peroxide concentration at various *p*H levels.

It is evident that the process of converting the chromophore type C_1 to colourless products, C_P, is not a simple first order process with respect to peroxide since the expected linear relationship between k_1 and peroxide concentration is not observed. Figure 11 also demonstrates that there is a 'falling off' in the response of k_1 to increasing peroxide concentration at higher levels of addition. This behaviour implies that conversion of C_1 to C_P does not take place in a single elementary step as depicted in the model scheme, but occurs through a more complex sequence of processes.

From Figure 12, a plot of k_1 vs. $[H_2O_2]^{0.5}$ at *p*H 10 produces a close to linear relationship, suggesting an expression of the form $k_1 \propto [H_2O_2]^a$ can suitably describe the dependence of k_1 on peroxide concentration.

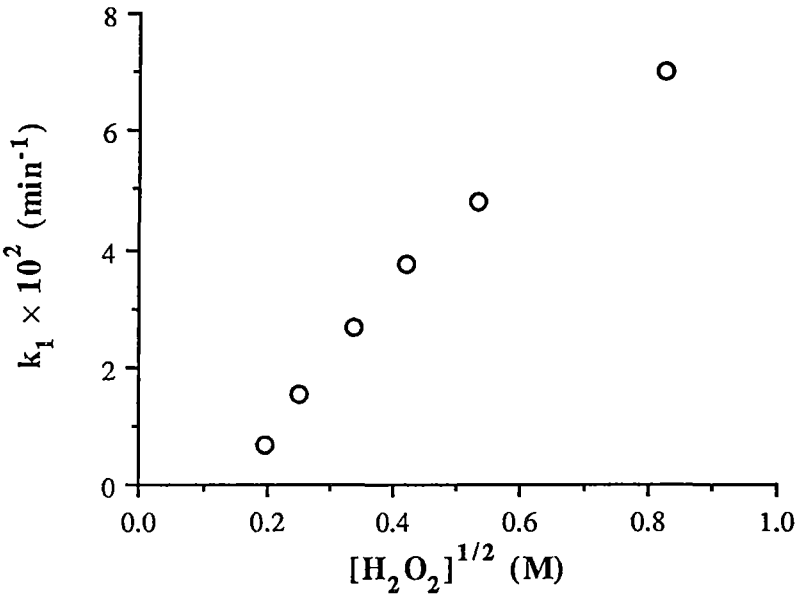

FIGURE 12: Dependence of first order rate constant k_1 on the square root of total peroxide concentration at *p*H 10, 50°C.

This type of kinetic expression may be explained by assuming a consecutive mechanism involving an intermediate, as illustrated in Scheme 3. Rate constants k_{1a} and k_{1b} represent respective formation and removal of an intermediate species C_1^*, while k_1 represents the overall observed rate constant. Reaction processes of this type leading to apparent non-integer orders of reaction have been discussed for soda-additive delignification[6], and can explain features such as 'square root' relationships.

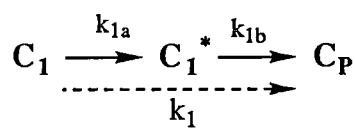

Scheme 3: Proposed mechanism to explain the observed relationship between k_1 and H_2O_2 concentration in Figure 12.

The peroxide anion (HO_2^-) is generally believed to be the active species during peroxide bleaching[33], therefore kinetic expressions for chromophore elimination should preferably be expressed in terms of HO_2^- concentration rather than total peroxide concentration, as shown in Figure 13. The perhydroxyl anion concentrations in Figure 13 were evaluated from the base dissociation constant (K_b) for the hydrogen peroxide/perhydroxyl anion equilibrium at 50°C (equation 10).

$$HO_2^- + H_2O \rightleftharpoons H_2O_2 + OH^- \qquad (10)$$

The hydrogen peroxide base dissociation constant was calculated from the equation of Teder and Tormund[34], shown in equation (11). At 50°C, the pK_b for equation (10) was found to be 1.99 M.

$$pK_b = 1330/T - 2.13 + 0.15\,[Na^+]^{0.5}, \quad T = \text{absolute temperature (K)} \qquad (11)$$

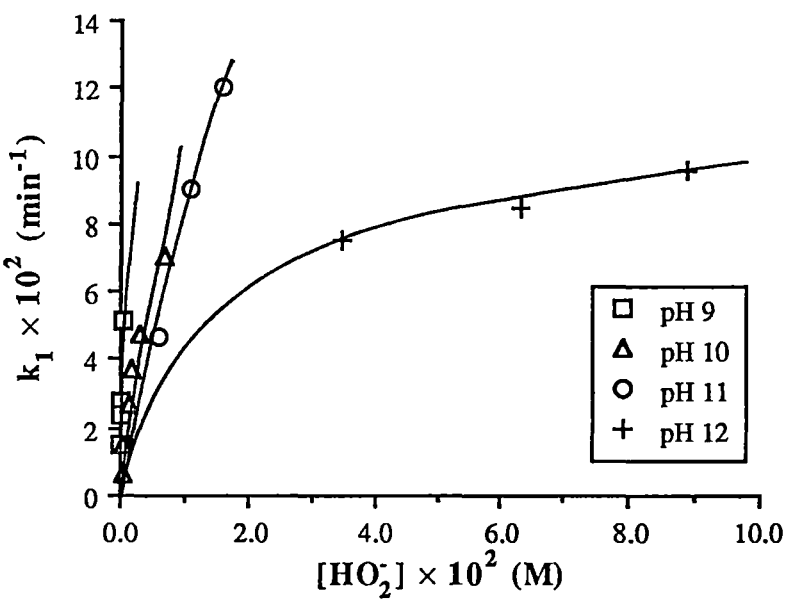

FIGURE 13: Dependence of first order rate constant k_1 on the perhydroxyl anion concentration at 50°C.

A progression in bleaching response over the *p*H range studied is apparent in Figure 13, with the action of the HO_2^- anion having greatest effect at the lowest *p*H level. If the exclusive role of alkali was to generate perhydroxyl anions, then the rate constants at each *p*H would be expected to lie on a common curve when plotted against HO_2^- concentration. Figure 13 clearly indicates that this is not the case, and alkali appears to exert a retarding effect on the initial bleaching rate in addition to its role of inducing perhydroxyl ion formation. This observation is consistent with the results of other experiments[10,11,19,33] which show that excess alkali can inhibit peroxide bleaching, although the cause of this phenomenon has frequently been associated with increased peroxide decomposition[19,33,35-38] rather than actual inhibition of bleaching reactions. Studies of peroxide bleaching of softwoods under constant reagent conditions have also shown[10,11] that the bleaching process is retarded at high *p*H (>11.5), and this effect was attributed to chromophore creation as a result of alkaline condensation reactions.

2.5.2 Behaviour of Rate Constant k_2

The rate constant k_2 represents the ease with which chromophore type C_1 is converted into C_2. This rate constant was evaluated using the least squares fitting procedure described in section 2.4.6. In order to maximise the rate of chromophore elimination, it is desirable to reduce conversion of C_1 to C_2, however Figure 14 shows that k_2 does not depend strongly on either *p*H or peroxide concentration. In practical terms, Model III predicts that it is impossible to exert significant control over the rate of C_1 to C_2 conversion by varying *p*H or peroxide anion concentration.

2.5.3 Behaviour of Limiting Rate Constant k_3

The rate constant k_3 controls the rate at which chromophore type C_2 is converted to C_P. From bleaching experiments over a range of peroxide and alkali concentrations, k_3 was assumed to be first order and independent of peroxide and alkali concentration.

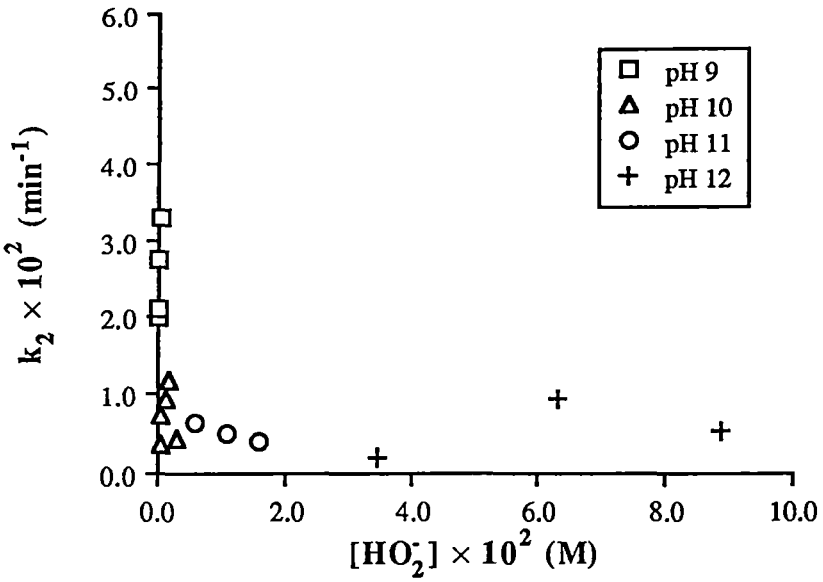

FIGURE 14: Dependence of first order rate constant k_2 on the perhydroxyl anion concentration.

A common limiting value of $k_3 = 0.001$ min^{-1} was found to apply across the entire range of reagent concentrations examined. The overall magnitude of k_3 implies that the conversion of C_2 to C_P is the slowest of all the steps in Model III. Like k_2, the insensitivity of k_3 to both peroxide and alkali concentration means that little can be done to accelerate C_2 to C_P conversion by way of changing peroxide or alkali concentrations.

TABLE 3: Typical values of rate constants for Model III

Rate Constant (min^{-1})†	*p*H 9	*p*H 10	*p*H 11	*p*H 12
k_1	0.015 - 0.028	0.015 - 0.038	0.046 - 0.12	0.075 - 0.096
k_2	0.020 - 0.028	0.007 - 0.012	0.004 - 0.007	0.002 - 0.010
k_3	0.001	0.001	0.001	0.001

† Rate constants over 0.06 - 0.18 M peroxide concentration range.

Analysis of the kinetic bleaching behaviour of *E. regnans* in terms of Model III indicates that alkaline peroxide bleaching responses are favoured by high concentrations of perhydroxyl anion (HO_2^-) and low concentrations of alkali. These conditions would be difficult to achieve in practice since formation of perhydroxyl anion is promoted by alkali (equation 10). For example, at 50°C and *p*H 9, a 0.9 M peroxide concentration would be required to generate an equivalent amount of HO_2^- as that produced at 0.01 M peroxide, *p*H 11. Therefore, very high hydrogen peroxide concentrations would be required to produce an acceptable bleaching response at low *p*H levels. This would be uneconomic in terms of a single stage bleaching process due to wastage of reagent, however the relative stability of hydrogen peroxide at low alkalinities would provide some scope for recycling of reagent in a multi-stage process.

2.6 Conclusions

Kinetic phenomena during bleaching of a Eucalypt mechanical pulp have been studied under constant conditions of *p*H and peroxide. Analysis of the results has shown that a kinetic model based on the assumption of two distinct chromophore types can be used to obtain adequate agreement between theory and experiment. The model developed in this chapter gives a better fitting for results with *E. regnans* than previously proposed empirical models and the newer model also defines overall bleaching responses in terms of first order processes, rather than high reaction orders obtained with an empirical model. A maximum bleaching rate in the *p*H 11-12 region can be explained by a two chromophore consecutive reaction model whereas empirical models predict a continuous increase in bleaching rate without limit. A two chromophore model suggests that the dominant reaction during the initial stages of bleaching might occur through a sequential process involving an intermediate, the formation of which would be favoured by less alkaline conditions. It cannot be stated that the models investigated here provide a unique solution to the experimental data, and more supporting chemical information must be obtained to differentiate between other possible reaction networks.

REFERENCES

1. Olm, L. and Tistad, G., Kinetics of the Initial Stage of Kraft Pulping., *Svensk Papperstidning*, **82(15)**, 458-64, (1979).

2. Obst, J.R., Kinetics of Kraft Pulping of a Middle Lamella Enriched Fraction of Loblolly Pine., *Tappi J.*, **68(2)**, 100-104, (1985).

3. Yan, J.F., A Basic Question of Delignification Kinetics., *Tappi*, **63(11)**, 154, (1980).

4. Yan, J.F. and Johnson, D.C., Delignification and Degelation: Analogy in Chemical Kinetics., *J. Applied Polymer Sci.*, **26**, 1623-35, (1981).

5. Yan, J.F., Molecular Theory of Delignification., *Macromolecules*, **14**, 1438-45, (1981).

6. Abbot, J., Simulation and Interpretation of Kinetic Phenomena for Soda-Additive Delignification., *J. Wood Chem. Technol.*, **9(4)**, 467-89, (1989).

7. Axegård, P., Kinetics of Alkaline Bleaching for the Kraft CE Sequence., *Svensk Papperstidning*, **82(12)**, 361-67, (1979).

8. Germgård, U. and Teder, A., Kinetics of Chlorine Dioxide Prebleaching., *Trans. Tech. Sect. CPPA*, **6(2)**, TR31-36, (1980).

9. Olm, L. and Teder, A., The Kinetics of Oxygen Bleaching., *Tappi*, **62(12)**, 43-46, (1979).

10. Sjögren, B. and Moldenius, S., Effects of Bleaching Parameters on Kinetics and Stoichiometry of Peroxide Bleaching of Mechanical Pulp., *1st Int. Symp. Wood and Pulping Chem.*, Vol. 2, 125-131, (1981).

11. Moldenius, S. and Sjögren, B., Kinetic Models for Hydrogen Peroxide Bleaching of Mechanical Pulps., *J. Wood Chem. Technol.*, **2(4)**, 447-71, (1982).

12. Lundqvist, M., Kinetics of Hydrogen Peroxide Bleaching of Mechanical Pulp., *Svensk Papperstidning*, **82(1)**, 16-21, (1979).

13. Allison, R.W. and Graham, K.L., Peroxide Bleaching of Mechanical Pulp Fractions from Radiata Pine., *J. Pulp and Paper Sci.*, **15(4)**, J145-150, (1989).

14. Axegård, P., Moldenius, S. and Olm, L., Basic Chemical Kinetic Equations are Useful for an Understanding of Pulping Processes., *Svensk Papperstidning*, **82(5)**, 131-36, (1979).

15. Szabo, A. and Goring, D.A.I., Degradation of a Polymer Gel: Application to Delignification of Sprucewood., *Tappi*, **51(10)**, 440-44, (1968).

16. Bolker, H.I. and Brenner, H.S., Polymeric Structure of Spruce Lignin., *Science*, **170**, 173-76, (1970).

17. Bolker, H.I., Rhodes, H.E.W. and Lee, K.S., Degradation of Insoluble Lignin by Chlorine Monoxide., *J. Agric. Food Chem.*, **25(4)**, 708-16, (1977).

18. Schöön, N-H., Interpretation of Rate Equations from Kinetic Studies of Wood Pulping and Bleaching., *Svensk Papperstidning*, **85(15)**, R185-93, (1982).

19. Martin, D.M., The Bleaching of Eastern Spruce Groundwood with Alkaline Peroxide. I. Reaction Kinetics., *Tappi*, **40(2)**, 65-71, (1957).

20. Vogel, A.I., in Quantitative Inorganic Analysis, 1st Edition, p. 425, Longmans, Green and Co., London, 1947.

21. Appita Standard Method P446s-82

22. Kubelka, P., New Contributions to the Optics of Intensely Light Scattering Materials. Part 1., *J. Opt. Soc. Am.*, **38(5)**, 448-67, (1948).

23. Robinson, J.V., A Summary of Reflectance Equations for Application of the Kubelka-Munk Theory to Optical Properties of Paper., *Tappi*, **58(10**, 152-53, (1975).

24. ISO Draft Proposal, ISO/DP 9416, Determination of Light Scattering and Absorption Coefficients., (1986).

25. Abbot, J. and Ginting, Y.A., Development of Kinetic Models for Alkaline Peroxide Bleaching., *J. Pulp and Paper Sci.*, **18(3)**, J85-93, (1992).

26. Holah, D.G. and Heitner, C., The Colour and UV-Visible Absorption Spectra of Mechanical and Ultra-High Yield Pulps Treated with Alkaline Hydrogen Peroxide., *J. Pulp and Paper Sci.*, **18(5)**, J161-65, (1992).

27. Bailey, C.W. and Dence, C.W., Reactions of Alkaline Hydrogen Peroxide with Softwood Lignin Model Compounds, Spruce Milled Groundwood Lignin and Spruce Groundwood., *Tappi*, **52(3)**, 491-500, (1969).

28. Polcin, J. and Rapson, W.H., Effects of Bleaching Agents on the Absorption Spectra of Lignin in Groundwood Pulps. Part 1: Reductive Bleaching., *Pulp and Paper Mag. Can.*, 72(3), 69-80, (1971).

29. Lebo, S., Lonsky, W., McDonough, T., Medvecz, P. and Dimmel, D., The Occurrence and Light Induced Formation of *ortho*-Quinonoid Lignin Structures in White Spruce Mechanical Pulp., *J. Pulp Paper Sci.*, **16(5)**, J139-43, (1990).

30. Gellerstedt, G. and Agnemo, R., The Reactions of Lignin with Alkaline Hydrogen Peroxide. Part III. The Oxidation of Conjugated Carbonyl Structures., *Acta Chem. Scand.*, **B34(4)**, 275-80, (1980).

31. Hocking, M.B. and Ong, J.H., Kinetic Studies of Dakin Oxidation of *o*- and *p*- Hydroxyacetophenones., *Can. J. Chem.*, **55**, 102-10, (1977).

32. Gellerstedt, G., Hardell, H-L. and Lindfors, E-L., The Reactions of Lignin with Alkaline Hydrogen Peroxide. Part IV. Products from the Oxidation of Quinone Model Compounds., *Acta Chem. Scand.*, **B34(9)**, 669-73, (1980).

33. Andrews, D.H. and Singh, R.P., In The Bleaching of Pulp, Chapter 8, ' Peroxide Bleaching', R.P. Singh (Ed.), Tappi Press, Atlanta, 1979.

34. Teder, A. and Tormund, D., The Equilibrium Between Hydrogen Peroxide and the Peroxide Ion - A Matter of Importance in Peroxide Bleaching., *Svensk Papperstidning*, **83(4)**, 106-109, (1980).

35. Spittler, T.D. and Dence, C.W., Destruction and Creation of Chromophores in Softwood Lignin by Alkaline Hydrogen Peroxide., *Svensk Papperstidning*, **80(9)**, 275-84, (1977).

36. Gierer, J. and Imsgard, F., The Reactions of Lignins With Oxygen and Hydrogen Peroxide in Alkaline Media., *Svensk Papperstidning*, **80(16)**, 510-18, (1977).

37. Kutney, G.W. and Evans, T.D., Peroxide Bleaching of Mechanical Pulps. Part 2. Alkali Darkening - Hydrogen Peroxide Decomposition., *Svensk Papperstidning*, **88(9)**, R84-89, 1985).

38. Agnemo, R., Gellerstedt, G. and Lindfors, E-L., Reactions of 1,2-Dimethyl-Cyclohexene with Alkaline Hydrogen Peroxide., *Acta Chem. Scand.*, **B33(2)**, 154-56, (1979).

CHAPTER 3

KINETIC MODELS FOR PEROXIDE BLEACHING UNDER ALKALINE CONDITIONS. EQUILIBRIUM MODELS.

3.1 Introduction

In the previous chapter, the kinetic behaviour associated with the bleaching of *E. regnans* mechanical pulp was examined under constant reagent conditions by following the decrease in light absorption coefficient (K) with time. Analysis of this behaviour led to the formulation of a peroxide bleaching model based on two distinct categories of chromophore, C_1 and C_2. Both categories were considered to be initially present in the pulp and, under bleaching conditions, were assumed to react via first order processes to yield colourless products (C_P) via the mechanism outlined in Figure 1(a) (the other mechanisms in Figure 1 will be discussed later). Chromophore type C_1 was assumed to react quickly, producing a rapid decrease in light absorption coefficient, while the chromophoric group C_2 was assumed to be more resistant to bleaching, and was identified as being responsible for a much slower removal of colour.

The two chromophore consecutive reaction model was initially favoured for several reasons. Firstly, a good fitting between experimental and theoretical data was obtained, and secondly, the reaction steps could be defined in terms of chemically meaningful first order processes. Finally, a maximum bleaching rate in the *p*H range 11-12 was predicted, in agreement with experimental observations[1-3], whereas previously published empirical models[2-6] predicted a continuous increase in bleaching rate with *p*H.

(a)

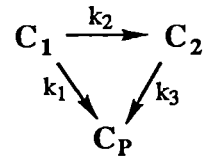

(b)

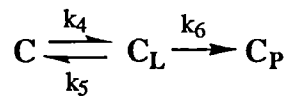

(c)

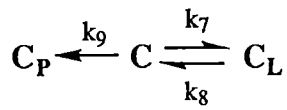

(d)

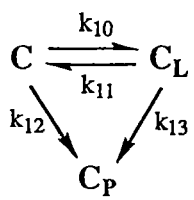

(e)

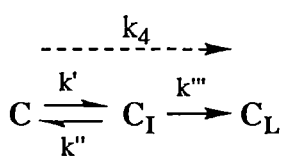

FIGURE 1: Kinetic models for the bleaching of *E. regnans* SGW with alkaline peroxide. (a) Two Chromophore Consecutive Reaction Model, (b) Equilibrium Model I, (c) Equilibrium Model II, (d) Equilibrium Model III, (e) Postulated mechanism for C to C_L conversion.

Although the fitting of experimental kinetic data by the consecutive reaction model was a significant improvement on existing empirical kinetic models[2-6], an apparent adequate fitting of data points should not be used as the sole criterion of model validity. With any multi-parameter kinetic model, it is important to formulate tests to

compare experimental behaviour with model predictions as a means to establishing model validity.

In this chapter, the study of kinetic models has been extended to include new models incorporating a reversible step in which chromophores are created as well as eliminated. The analysis of peroxide bleaching kinetics in terms of a reversible reaction has also been considered in the context of identifying possible contributions from ionic and radical induced processes in the overall reaction scheme.

3.2 Experimental

The chemicals and procedure for the bleaching of *E. regnans* SGW under conditions of constant reagent concentrations were identical to those described in the Experimental section of the previous chapter (section 2.3). The kinetics of peroxide bleaching were studied by monitoring the elimination of chromophores measured as light absorption coefficients at 457 nm. During kinetic runs, peroxide or alkali concentrations were adjusted to new constant levels to examine the response of the SGW pulp to increases and decreases in reagent concentration. The light absorption coefficient - time data for these kinetic runs are detailed in Appendix 2.1.

3.3 Results

3.3.1 Two Chromophore Consecutive Reaction Model Tests

The experiments undertaken to test the consecutive reaction model were essentially two stage bleaching sequences carried out under constant conditions at 50°C and 0.3% consistency. The aim of these experiments was to check the ability of the present model to predict the effects of sudden changes in reagent conditions.

(i) Increase in Peroxide Concentration at Constant pH

E. regnans SGW pulp was bleached under constant conditions (0.12 M peroxide, *p*H 11) for 3 hours at 50°C. Bleaching progress was followed by monitoring the decrease in light absorption coefficient (K) with time. After 3 hours bleaching, enough hydrogen peroxide was added to increase the peroxide concentration to 0.18 M while maintaining the *p*H at 11. Light absorption coefficients were followed for a further 1 hour. The results of this bleaching procedure, depicted in Figure 2, show that when the total peroxide concentration was increased at constant *p*H, the absorption coefficients slowly shifted from the 0.12 M bleaching profile to the 0.18 M profile. In other words, increasing the peroxide concentration increased the rate of bleaching.

This effect cannot be explained in terms of the two chromophore consecutive reaction model. At the stage of bleaching when the peroxide concentration was increased (ie. after 180 min) the consecutive reaction model predicts that the remaining chromophores would exist entirely in the difficult to remove C_2 state (see Figure 3).

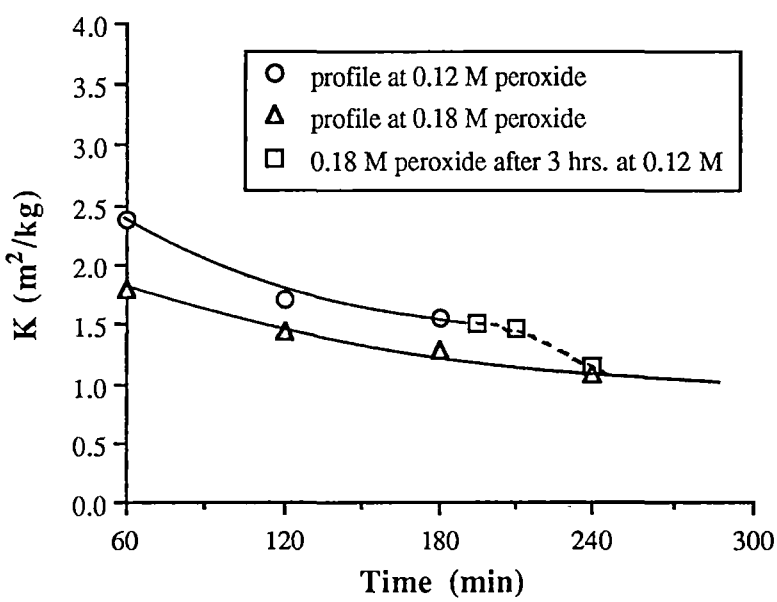

FIGURE 2: Effect on light absorption coefficient (K) when peroxide levels are increased at *p*H 11, 50°C.

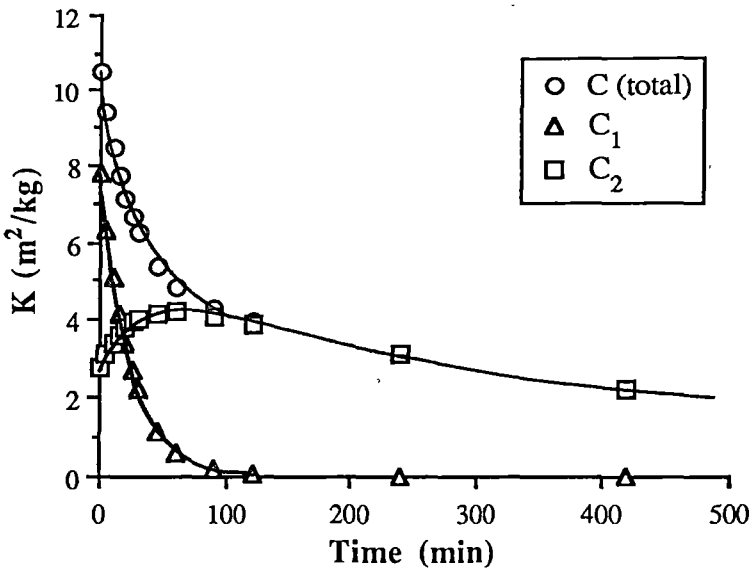

FIGURE 3: Example of the variation in two chromophore consecutive reaction model parameters, C_1 and C_2, (see Figure 1a) with time. Points calculated from rate constants obtained at *p*H 10, 0.12 M peroxide, 50°C.

Thus, in terms of the two chromophore consecutive reaction model, the decrease in absorption coefficient after 180 minutes is a result of C_2 being converted to the colourless C_P type. The associated first order rate constant for this process is represented by k_3 in Figure 1(a). In the previous chapter k_3 was found to be small and independent of peroxide concentration, which is clearly in conflict with the experimental observations here.

(ii) Decrease in Peroxide Concentration at Constant pH

An *E. regnans* SGW pulp was bleached at *p*H 11 and 0.12 M peroxide concentration for 3 hours following an identical procedure to that in (i). After 3 hours, the reaction was stopped by cooling and acidifying the slurry to *p*H 3, followed by filtration of the pulp. The pulp was then re-bleached at *p*H 11, but at a lower peroxide level (0.03 M peroxide) for a further hour while light absorption coefficients were followed.

Figure 4 shows that when peroxide levels were decreased at constant *p*H, light absorption coefficients continued to follow the original bleaching path, rather than shifting towards a profile corresponding to a lower amount of peroxide. In other words, no darkening of the pulp was observed. The experiment was repeated by reducing peroxide concentration from 0.12 M to 0.01 M after 3 hours bleaching, however an increase in light absorption coefficient was still not apparent. This implies that reduction of the peroxide concentration by a factor of 10 does not significantly impede bleaching rate. Similar observations have been noted before in the context of industrial peroxide bleaching[7]; as long as there is some residual peroxide present at the end of a bleaching stage the pulp will not darken. Figure 4 is consistent with the predictions of the two chromophore consecutive reaction model since the rate constant controlling the removal of C_2 (k_3) would not be greatly influenced by a decrease in peroxide concentration.

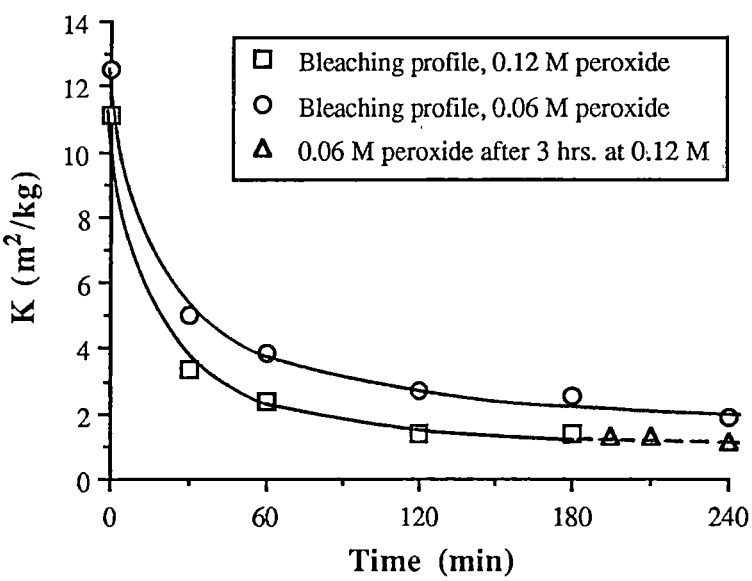

FIGURE 4: Effect on light absorption coefficient (K) when peroxide levels are decreased at *p*H 11, 50°C.

(iii) Increase in pH at Constant Peroxide Concentration

An *E. regnans* SGW pulp was bleached for 3 hours under identical conditions to those in (i). After 3 hours, the *p*H was increased from 11 to 12 by addition of sodium hydroxide (2 M) and the reaction was allowed to proceed for a further hour. The change in light absorption coefficient with time is shown in Figure 5. Inspection of this figure indicates that absorption coefficients slowly shifted from the *p*H 11 bleaching profile to the profile at *p*H 12 after the *p*H was increased. As a result, the pulp was observed to darken slightly. Such a darkening is surprising considering that formation of the active bleaching species, the perhydroxyl anion (HO_2^-)[1], is favoured by increasing *p*H (see Table 1). This information implies that the bleaching action of (HO_2^-) is impeded at high *p*H, in agreement with the results of the previous chapter where a maximum bleaching rate was observed in the *p*H 11-12 range.

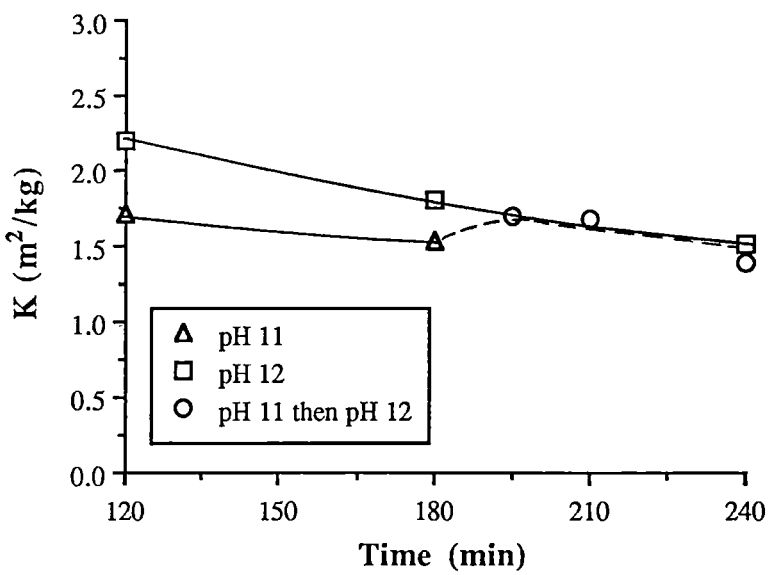

FIGURE 5: Effect on light absorption coefficient (K) when *p*H is increased at constant peroxide levels (0.12 M). T = 50°C.

TABLE 1 : The influence of increasing *p*H on the formation of perhydroxyl ions from hydrogen peroxide at 50°C (calculated from the equation of Teder & Tormund[8]).

$[H_2O_2]$ (M)	*p*H	$[HO_2^-]$ (M)
0.06	9.0	5.7×10^{-5}
0.12	9.0	1.1×10^{-4}
0.18	9.0	1.7×10^{-4}
0.06	10.0	5.7×10^{-4}
0.12	10.0	1.1×10^{-3}
0.18	10.0	1.7×10^{-3}
0.06	11.0	5.2×10^{-3}
0.12	11.0	1.0×10^{-2}
0.18	11.0	1.6×10^{-2}
0.06	12.0	2.9×10^{-2}
0.12	12.0	5.8×10^{-2}
0.18	12.0	8.7×10^{-2}

The darkening observed in Figure 5 also provides evidence of a degree of reversibility which cannot be explained in terms of the two chromophore consecutive reaction model. The model predicts that, after 180 minutes, chromophore type C_1 would have been fully converted to C_2 and C_P (see Figure 3). The darkening which occurred on increasing the *p*H suggests that chromophores were being created from C_2 in some way, a possibility which is not taken into account by the consecutive reaction model.

3.3.2 Equilibrium Models

The preceding model tests highlight several deficiencies in the two chromophore consecutive reaction model. Although this model can adequately describe the kinetics of chromophore removal under conditions of constant peroxide concentration and *p*H, it cannot explain the observed effects when reagent concentrations are changed during bleaching. If peroxide bleaching behaviour under mill conditions is to be described, a

valid kinetic model must ultimately account for bleaching responses when reagent concentrations are not held at constant levels.

In particular, the consecutive reaction model is unable to explain the darkening which occurs when *p*H is increased from 11 to 12 at constant peroxide levels. This observation suggests that a reversible step should be incorporated in a new kinetic model. Several plausible models containing a reversible step are presented in Figures 1(b), 1(c) and 1(d). Experimentally, light absorption coefficients also appear to reach approximately limiting values after long bleaching times (Figure 6), and these values are dependent on the amount of peroxide present. This type of behaviour may be explained by the concept of attainment of equilibrium. Based on this reasoning, two models involving an equilibrium between chromophores (C) and colourless chromophoric precursors (C_L) were investigated as better descriptions of experimental data. Each model contains a step representing irreversible formation of colourless products (C_P) from chromophores (Figure 1c) or leuco-chromophores (Figure 1b).

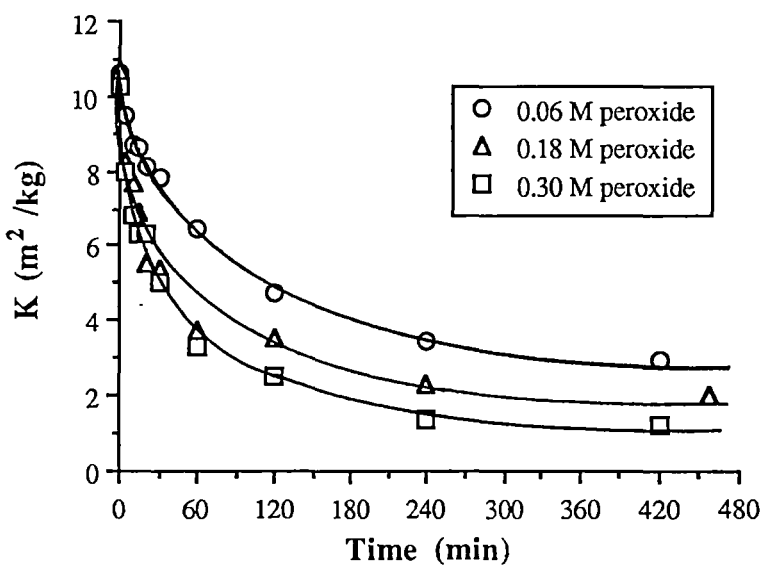

FIGURE 6: Typical light absorption coefficient (K) - time plots for *E. regnans* SGW bleached under constant conditions (*p*H 10, 50°C, 0.3% pulp consistency).

The fundamental chemical meanings of C, C_L and C_P remain the same as the consecutive reaction model parameters, C_1, C_2 and C_P, discussed in Chapter 2. That is, each group represents a category of compounds in lignin classified on the basis of their kinetic behaviour, measured by light absorption properties at 457 nm. At this stage, the model parameters are not linked with any single structural entity in the lignin polymer. For example, the chromophoric group, C, might be best regarded as representing a range of chromophores in lignin including α,β-unsaturated carbonyls, quinones and α-aryl carbonyls. In the same way, C_P might represent a group of colourless mono and dicarboxylic acids produced on oxidation of α,β-unsaturated carbonyls[9], quinones[10,11] and α-aryl carbonyls[9,12] by alkaline peroxide (see Figure 7).

3.3.3 Fitting of Equilibrium Models to Experimental Data

The equilibrium models outlined in Figure 1(b) and 1(c) were fitted to existing kinetic data from Chapter 2 for the bleaching of *E. regnans* pulps under constant reagent conditions at 50°C and 0.3% consistency (Appendix 1.1). The concentration of chromophores present before bleaching (C^0) was considered to correspond to the light absorption coefficient of handsheets made from unbleached pulp, while the initial concentrations of leuco-chromophores ($C_L{}^0$) and colourless products ($C_P{}^0$) were originally set to zero.

Assuming first-order processes, differential equations describing the changes in C, C_L and C_P with time were solved by Laplace transformation to give explicit equations for the variation in each model species with time. Rate constants were computed using a program containing an iterative simplex algorithm* (see Appendix 2.2 for listing). This algorithm allowed various combinations of the rate constants, k_4, k_5 and k_6 (Figure 1b) or k_7, k_8 and k_9 (Figure 1c), to be substituted into the explicit equations to generate theoretical bleaching curves. The simplex algorithm calculated least squares

* Program written by Dr. Mike Whitbeck, Desert Research Institute, Reno, Nevada, USA as part of the REACT chemical analysis software system.

fits between theoretical and experimental points and iterations were ceased once minimisation of the fits had occurred.

α,β-unsaturated carbonyls

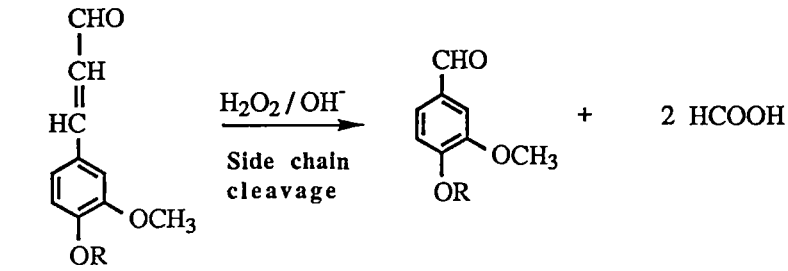

(R = H, Lignin)

***o*-quinones**

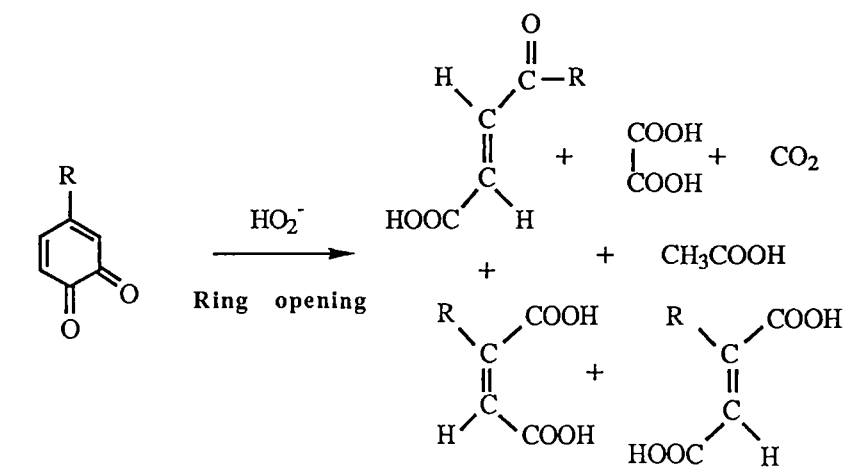

α-aryl carbonyls

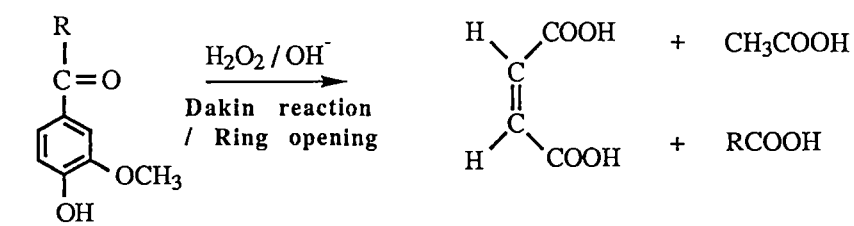

FIGURE 7: Previously reported schemes for the reaction of α,β-unsaturated carbonyls[9], *o*-quinones[10,11] and α-aryl carbonyl chromophores[12] with alkaline peroxide.

The rate constants corresponding to the minimum standard deviation were regarded as the optimum solutions. Figure 8 illustrates some model fits of experimental data using the equilibrium model in Figure 1(b) and from Table 2 it is evident that these fits are generally very good. Table 2 also demonstrates that the equilibrium models shown in Figure 1(b) and 1(c) fit the experimental data equally well, making selection of a preferred equilibrium model impossible on the basis fitting alone.

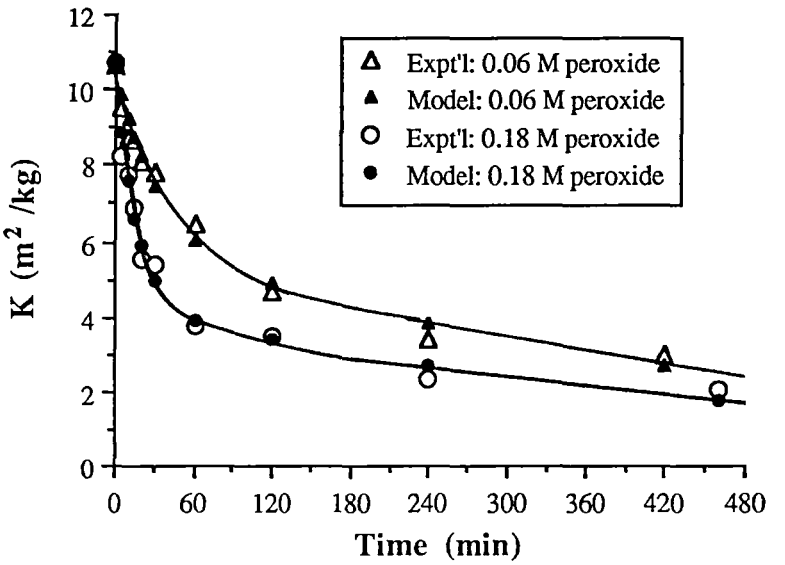

FIGURE 8: Examples of model fits of experimental bleaching curves using the equilibrium model depicted in Figure 1(b). *E. regnans* pulp bleached under constant conditions (*p*H 10, 50°C, 0.3% pulp consistency).

TABLE 2 : Standard deviations in the fitting of the equilibrium models in Figures 1(b) and 1(c) to experimental data from the bleaching of *E. regnans* at 50°C. Initial concentration of species C_L set to $C_L^0 = 0$.

	Standard Deviation in K (m^2/kg)			
$[H_2O_2]$ (M)	*p*H 9	*p*H 10	*p*H 11	*p*H 12
Model - Fig. 1(b)				
0.06	0.181	0.378	0.368	0.205
0.12	0.280	0.370	0.240	0.267
0.18	0.300	0.384	0.328	0.189
Model - Fig. 1(c)				
0.06	0.181	0.378	0.368	0.205
0.12	0.280	0.370	0.240	0.267
0.18	0.300	0.384	0.328	0.189

The equilibrium models in Figures 1(b) and 1(c) were found to tolerate a wide range of values for the initial concentration of chromophoric precursors, C_L^0, without seriously reducing each model's ability to fit experimental data. In Table 3, standard errors are shown for the fitting of the equilibrium model in Figure 1(c) to experimental data, using an arbitrary large value of $C_L^0 = 400$. By comparison with Table 2, where C_L^0 was set to 0, it is evident that only slightly greater standard errors resulted from the setting of C_L^0 to 400. In chemical terms, the setting of C_L^0 to a much larger value than C^0 would correspond to the generation of chromophores from a large pool of chromophoric precursors embedded in the lignin polymer. A simple interpretation of this situation might even be to associate C_L with the lignin polymer itself. The profile of C_L in Figure 9(a) indicates that the concentration of potential chromophores decreases slowly with time when $C_L^0 >> C^0$, in contrast with the behaviour of C_L when set to zero. Under these circumstances, an increase in the concentration of C_L is required for adequate fitting of an equilibrium model to experimental data (Figure 9b).

TABLE 3 : Standard deviations in the fitting of the equilibrium model in Figures 1(c) to experimental data from the bleaching of *E. regnans* at 50°C. Initial concentration of species C_L set to $C_L^0 = 400$.

	Standard Deviation in K (m^2/kg)			
$[H_2O_2]$ (M)	*p*H 9	*p*H 10	*p*H 11	*p*H 12
Model - Fig. 1(c)				
0.06	0.181	0.588	0.693	0.580
0.12	0.280	0.570	0.661	0.552
0.18	0.315	0.546	0.602	0.316

case by considering trends in the rate constants, k_4-k_6, for the equilibrium model shown in Figure 1(b).

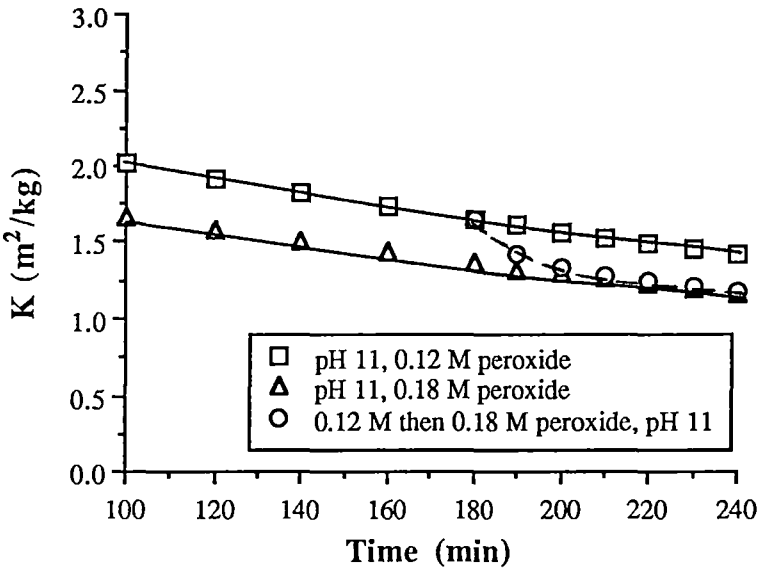

FIGURE 10: Equilibrium model prediction of the change in light absorption coefficient (K) when peroxide levels are increased at constant *p*H.

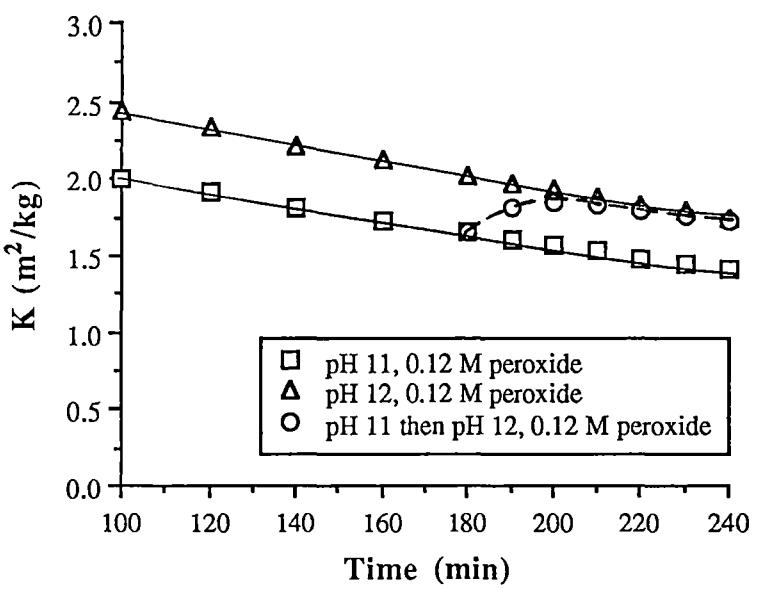

FIGURE 11: Equilibrium model prediction of the change in light absorption coefficient (K) when *p*H is increased at constant peroxide concentration.

3.3.4 Features of the Equilibrium Model

An advantage of the equilibrium model over the two chromophore consecutive reaction model is that the behaviour observed in Figures 2 and 5, when reagent conditions were changed part way through a bleach, can now be described in terms of a kinetic model. Figures 10 and 11 show the behaviour predicted by an equilibrium model when peroxide concentration is increased at constant *p*H, or *p*H is increased at constant peroxide concentration. The theoretical lines in Figures 10 and 11 were generated by substituting the first order rate constants, k_4 - k_6, into equations describing the kinetic behaviour of the equilibrium model in Figure 1(b). Values for the first order rate constants, k_4 - k_6, in Figure 1(b) were obtained by computer optimisation of experimental bleaching curves under constant conditions. The third line in each graph shows the predicted behaviour when reagent concentration is suddenly altered. These lines were generated by setting the rate constants to new values, corresponding to the new reagent concentrations, after 180 minutes bleaching time. By comparison of Figures 2 and 5, it can be seen that the predicted response is close to that observed experimentally in terms of changes in light absorption coefficients. As a matter of interest, the model also predicts that darkening should occur when peroxide levels are reduced at constant *p*H (Figure 12), although Figure 4 shows that such an effect was not observed experimentally.

3.3.5 Behaviour of Equilibrium Model Rate Constants

The respective rate constants for each of the equilibrium models depicted in Figures 1(b) and 1(c) were determined by computer optimisation of experimental bleaching curves as detailed in section 3.3.3, using a value of $C_L^0 = 0$ for the initial concentration of potential chromophores. Due to the similarity of the equilibrium models, analogous trends in their respective first order rate constants, k_4-k_6 and k_7-k_9, were observed. The general behaviour of these rate constants is illustrated in this

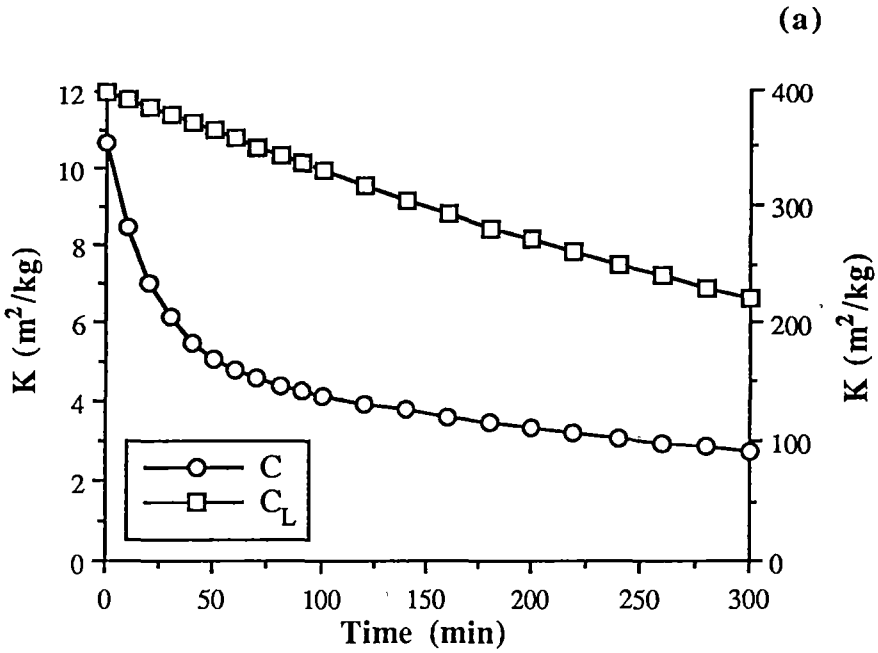

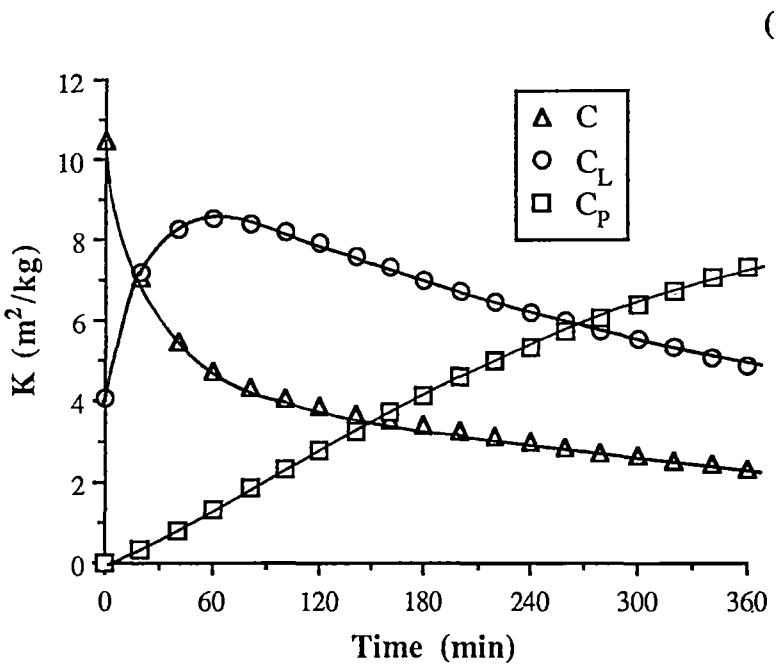

FIGURE 9: Typical concentration - time profiles of equilibrium model species C, C_L, C_P at *p*H 10, 0.12 M peroxide, 50°C, 0.3% pulp consistency. (a) equilibrium model in Figure 1(b) with $C_L^0 = 400$. (b) equilibrium model in Figure 1(b) with $C_L^0 = 0$.

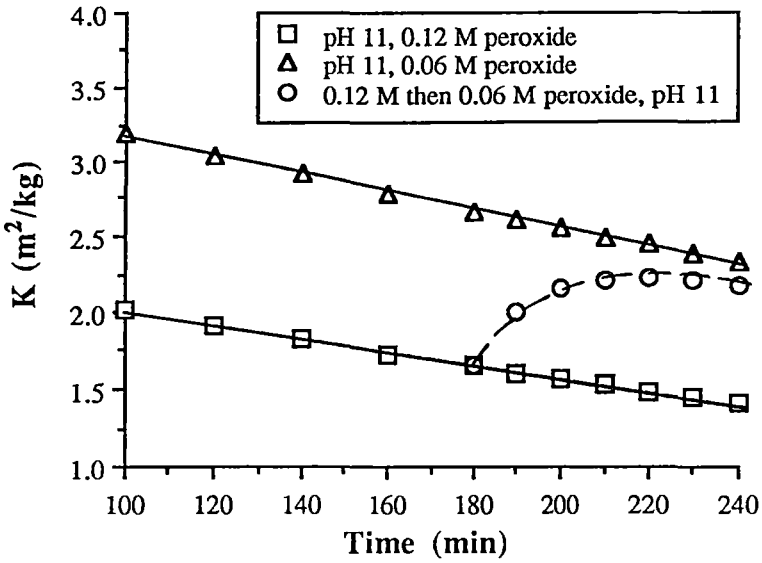

FIGURE 12: Equilibrium model prediction of the change in light absorption coefficient (K) when peroxide levels are decreased at constant *p*H.

(i) Behaviour of Rate Constant, k_4

Figure 13 demonstrates the dependence of k_4, the dominant rate constant controlling removal of colour, on the concentration of perhydroxyl ion (HO_2^-) which is generally considered to be the primary active bleaching species[1].

It is apparent that the magnitude of k_4 increases with the concentration of HO_2^- at a given *p*H, but the relationship is non-linear and falls off at higher concentrations of the anion. At very high concentrations of HO_2^-, the rate constant appears to reach a limiting value, as shown at *p*H 12 in Figure 13. This behaviour suggests that the chemical process described by the conversion of C to C_L does not take place in either a single step (ie. an elementary process in which HO_2^- reacts with C) or through a sequential mechanism in which only C and HO_2^- participate in a rate determining step.

It is also clear that the results at different *p*H levels in Figure 13 do not fall on a common curve. This implies that the dominant process for chromophore removal is

strongly influenced by the hydroxide ion (OH^-) as well as the perhydroxyl anion (HO_2^-). The trend shown in Figure 13 implies that the forward reaction of C to C_L is promoted by the presence of HO_2^- and inhibited by the presence of OH^-.

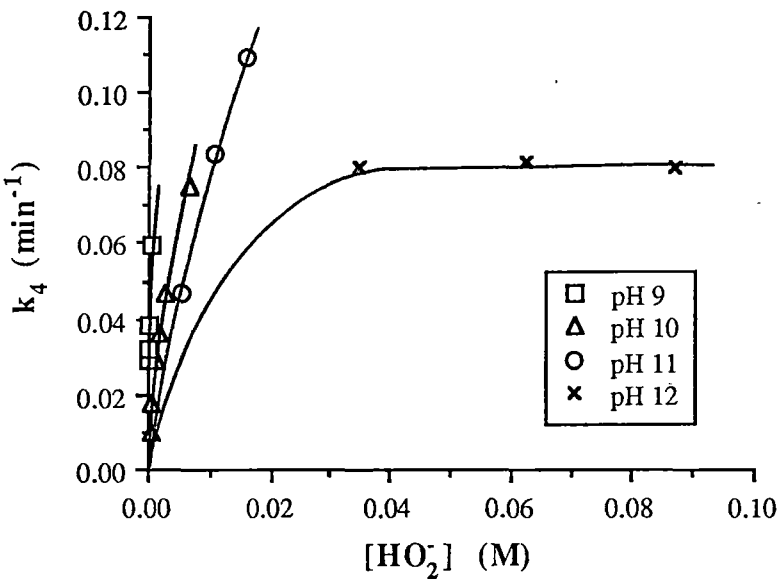

FIGURE 13: Variation in equilibrium model rate constant, k_4, with perhydroxyl anion concentration.

A plausible mechanism to account for the kinetic behaviour of k_4 is shown in Figure 1(e). In this mechanism the formation of an intermediate species (C_I) is postulated. The rate of formation of C_I is directly proportional to the concentration of HO_2^- (rate constant k') while the reverse process is proportional to the concentration of OH^- (rate constant k''). Formation of the leuco-chromophoric product (C_L) takes place in a single irreversible step (rate constant k''') which is assumed to be independent of HO_2^- and OH^-. Assuming this type of mechanism, it is possible to generate a family of curves, as in Figure 14, which resemble the experimental curves in Figure 13. Such a mechanism would explain the non-linear dependence of k_4 on HO_2^-, the

limiting value of k_4 at very high HO_2^- concentrations and the inhibiting influence of the hydroxide ion.

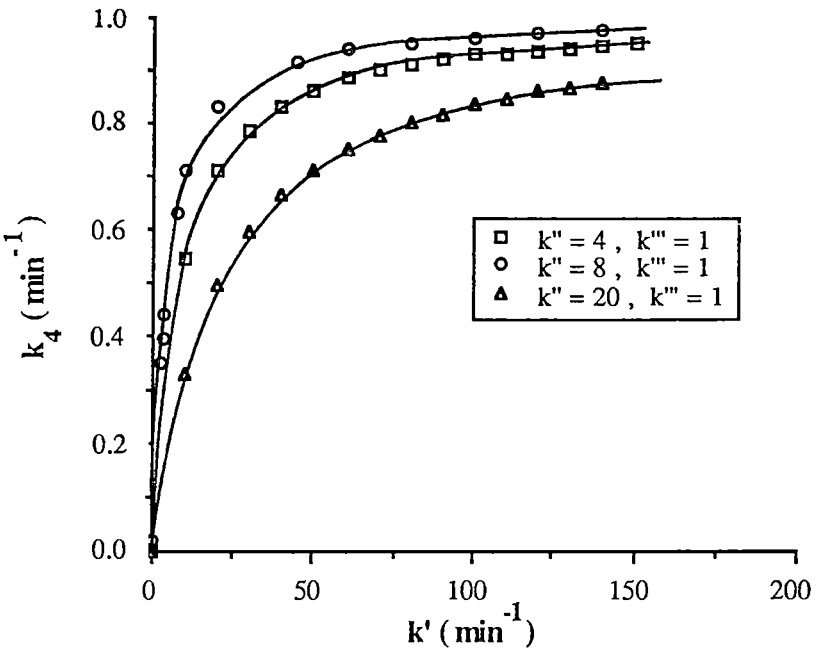

FIGURE 14: Computer simulation of the behaviour of first order rate constant, k_4. Curves were calculated using the proposed mechanism in Figure 1(e).

(ii) Behaviour of Rate Constants k_5 and k_6

The dependence of rate constant k_5 on perhydroxyl ion concentration is depicted in Figure 15 over the *p*H range 9-12. At constant *p*H, k_5 appears to be almost independent of perhydroxyl ion concentration. Despite the perhydroxyl ion and alkali concentrations varying by a factor of approximately 1000, Figure 15 shows that k_5 changes by a factor of about 3 over the *p*H range 9-12. From this observation it can be concluded that k_5 is much less sensitive to alkali and peroxide concentrations than k_4.

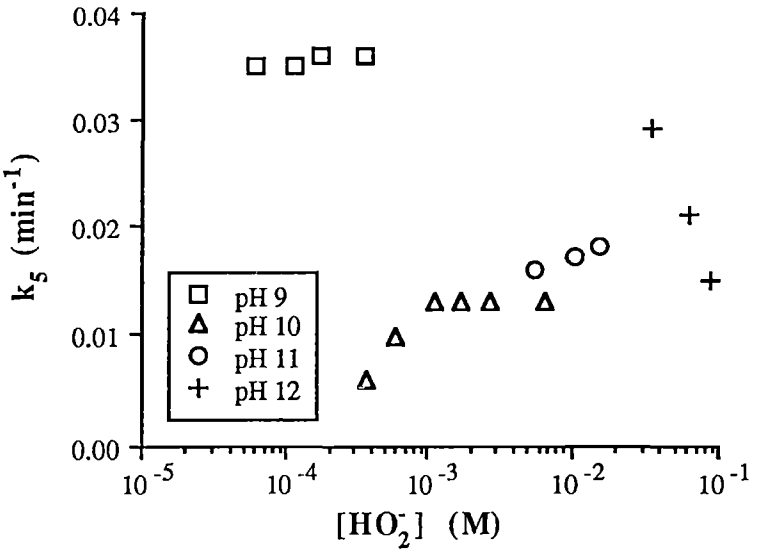

FIGURE 15: Variation in equilibrium model rate constant, k_5, with perhydroxyl anion concentration.

The rate at which the model leuco-chromophoric group (C_L) is irreversibly converted to a colourless product (C_P) is described by the rate constant k_6. This rate constant represents the slow residual rate of reaction after equilibrium has been achieved. As was the case for the two chromophore consecutive reaction model in Chapter 2, k_6 was found to be considerably smaller in magnitude than both k_4 and k_5 indicating that conversion of C_L to C_P is the slowest step of all. The rate constant also appears to be insensitive to both alkali and peroxide levels (Figure 16) suggesting that little can be done to accelerate this reaction step by way of changing reagent concentrations. Over the entire range of conditions examined, k_6 was invariably found to have a value between 0.0025 - 0.0030 min^{-1}.

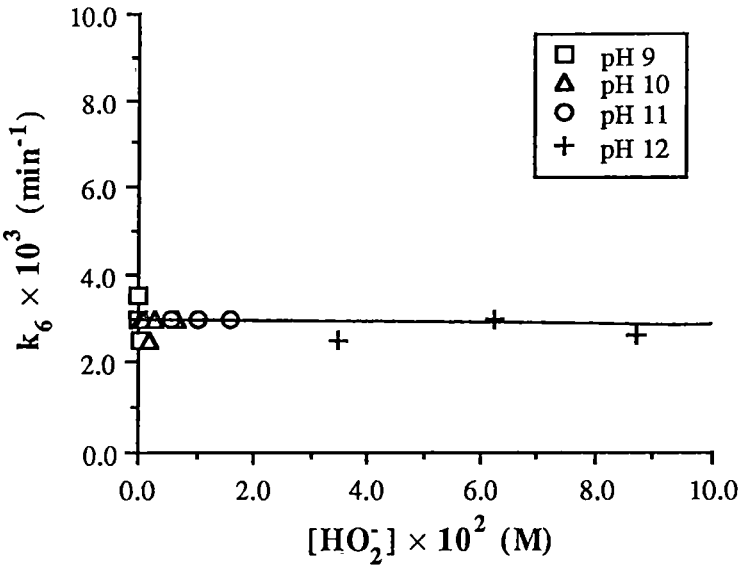

FIGURE 16: Variation in limiting rate constant, k_6, with perhydroxyl anion concentration.

3.4 Discussion

3.4.1 Peroxide Bleaching Mechanisms

Table 4 shows that the adequacy of fitting is identical for the consecutive reaction model (Figure 1a), two 3 parameter equilibrium models (Figures 1b and 1c) and a 4 parameter equilibrium model (Figure 1d). It is therefore impossible to distinguish between these models solely on the basis of fitting between experimental and theoretical points. However, as already demonstrated; the favoured equilibrium models (Figures 1b and 1c) can predict the response of pulp under constant reagent conditions or when the concentrations of either peroxide or hydroxide are increased to new, constant levels. This model can apparently also explain behaviour when a pulp is repeatedly bleached in a series of consecutive stages with the same initial conditions[13].

TABLE 4 : Pseudo-1st order rate constants and standard deviations for the fitting of 4 different models to a single peroxide bleaching curve (*p*H 10, 0.12 M peroxide).

	Model Type			
	Figure 1(a)	*Figure 1(b)*	*Figure 1(c)*	*Figure 1(d)*
Rate Constants (min^{-1})	$k_1 = 0.025$ $k_2 = 0.021$ $k_3 = 0.002$	$k_4 = 0.030$ $k_5 = 0.014$ $k_6 = 0.003$	$k_7 = 0.025$ $k_8 = 0.016$ $k_9 = 0.006$	$k_{10} = 0.027$ $k_{11} = 0.014$ $k_{12} = 0.003$ $k_{13} = 0.002$
Std. Deviation (m^2/kg)	0.370	0.370	0.370	0.370

Application of the equilibrium model under constant reagent conditions leads to the conclusion that the principle reaction leading to elimination of chromophores is controlled by ionic species, as demonstrated by the behaviour of k_4. This reaction possibly proceeds through an intermediate species, the formation of which depends directly on the perhydroxyl anion and is retarded by the hydroxide ion. However, without detailed kinetic information regarding the reactions of individual chromophores with alkaline peroxide, it is difficult to verify the validity of such a proposal or to associate the scheme in Figure 1(e) with any known bleaching reaction.

Analysis of experimental bleaching behaviour in terms of the equilibrium model in Figure 1(b) reveals that the rate constants, k_5 and k_6, are more or less insensitive to the concentrations of OH^- and HO_2^- ions. A plausible explanation for this phenomenon might be to assign these reactions to radical dependent processes. There has been considerable interest in the possible participation of radical species in peroxide bleaching and delignification reactions over the past decade[14-24]. Although it appears that superoxide ($O_2^{-\bullet}$) and hydroxyl radicals ($OH^\bullet$) may play a significant role, there is evidence that radical species may participate in both chromophore elimination and chromophore creation processes[15,16,24]. This is an interesting observation since application of the equilibrium model may imply the participation of

radical induced reactions in both brightening processes (k_6) and darkening processes (k_5).

The equilibrium model can apparently explain the behaviour of pulps under constant reagent conditions and when the concentrations of ionic reagents (HO_2^- and OH^-) are increased, however the response to decreasing concentrations of these species is not predicted (refer to Figure 12). For example, a strict application of the model would predict that washing the pulp with water after prolonged bleaching should result in darkening ($k_4 \rightarrow 0$, k_5 is relatively independent of ion concentrations). This is not observed in practice, but can be rationalised if radical processes requiring peroxide decomposition are responsible for conversion of C_L to C.

Improvements in kinetic models for alkaline peroxide bleaching have resulted from testing the ability of existing models to explain a wide range of experimental bleaching behaviour. Despite the success of this approach, it is doubtful whether significant improvements on the current equilibrium models can be made by undertaking additional bleaching tests with pulp. To further refine the equilibrium kinetic models for peroxide bleaching, more detailed information on the kinetic behaviour of chromophoric groups in lignin is required. Such information might allow modification of the equilibrium models to better reflect the underlying chemical kinetic processes associated with chromophore elimination during alkaline peroxide bleaching. For this reason, parallel studies with model lignin chromophores are required to provide supporting evidence for the current equilibrium kinetic scheme. Confirmation is also required regarding the participation of ionic species and radicals as suggested by the present kinetic analysis.

3.5 Conclusions

The two chromophore consecutive reaction model for peroxide bleaching has been tested by carrying out a series of two stage bleaching experiments under constant reagent conditions. When peroxide levels or *p*H are suddenly increased during bleaching, the consecutive reaction model is unable to describe the resulting experimental behaviour. Two equilibrium models were investigated and were found to adequately duplicate experimental observations while retaining the benefits of the consecutive reaction model in terms of satisfactory fitting between theoretical and experimental results.

The behaviour of equilibrium model rate constants suggests that initial chromophoric species, C, may be converted to stable leuco-chromophores, C_L, through a series of steps which are dependent on ionic species. Furthermore, these leuco-chromophores can be eliminated to form colourless products (C_P) or they may be reconverted to coloured species (C). These processes can possibly be assigned to reactions involving radicals, such as the hydroxyl or superoxide radical.

The present model based on an equilibrium concept can adequately describe the kinetic behaviour of the chromophores in alkaline hydrogen peroxide under constant reagent conditions. It can also describe transient and final behaviour when increasing reagent concentrations to a new set of constant reagent conditions.

REFERENCES

1. Andrews, D.H. and Singh, R.P., In The Bleaching of Pulp, Chapter 8, ' Peroxide Bleaching', R.P. Singh (Ed.), Tappi Press, Atlanta, 1979.

2. Sjögren, B. and Moldenius, S., Effects of Bleaching Parameters on Kinetics and Stoichiometry of Peroxide Bleaching of Mechanical Pulp., *Ist Int. Symp. Wood and Pulp. Chem.*, Vol. 2, p. 125-31, (1981).

3. Moldenius, S. and Sjögren, B., Kinetic Models for Hydrogen Peroxide Bleaching of Mechanical Pulps., *J. Wood Chem. Technol.*, **2(4)**, 447-71, (1982).

4. Lundqvist, M., Kinetics of Hydrogen Peroxide Bleaching of Mechanical Pulp., *Svensk Papperstidning,* **82(1)**, 16-21, (1979).

5. Axegård, P, Moldenius, S. and Olm, L., Basic Chemical Kinetic Equations are Useful for an Understanding of Pulping Processes., *Svensk Papperstidning*, **82(5)**, 131-36, (1979).

6. Allison, R.W. and Graham, K.L., Peroxide Bleaching of Mechanical Pulp Fractions from Radiata Pine., *J. Pulp and Paper Sci.*, **15(4)**, J145-150, (1989).

7. Lorås, V. , In Pulp and Paper - Chemistry and Chemical Technology, Chapter 5, 'Bleaching', J.P. Casey.(Ed.) , Chemistry and Chemical Technology, Volume 1: Pulp and Paper., 3rd Edition, Wiley-Interscience, New York, 1980.

8. Teder, A. and Tormund, D., The Equilibrium Between Hydrogen Peroxide and the Peroxide Ion - A Matter of Importance in Peroxide Bleaching., *Svensk Papperstidning*, **83(4)**, 106-109, (1980).

9. Gellerstedt, G. and Agnemo, R., The Reactions of Lignin with Alkaline Hydrogen Peroxide. Part III. The Oxidation of Conjugated Carbonyl Structures., *Acta Chem. Scand.*, **B34(4)**, 275-80, (1980).

10. Bailey, C.W. and Dence, C.W., Reactions of Alkaline Hydrogen Peroxide with Softwood Lignin Model Compounds, Spruce Milled Groundwood Lignin and Spruce Groundwood., *Tappi*, **52(3)**, 491-500, (1969).

11. Gellerstedt, G., Hardell, H-L. and Lindfors, E-L., The Reactions of Lignin with Alkaline Hydrogen Peroxide. Part IV. Products from the Oxidation of Quinone Model Compounds., *Acta Chem. Scand.*, **B34(9)**, 669-73, (1980).

12. Hocking, M.B. and Ong, J.H., Kinetic Studies of Dakin Oxidation of *o*- and *p*- Hydroxyacetophenones., *Can. J. Chem.*, **55**, 102-10, (1977).

13. Abbot, J. and Ginting, Y.A., Development of Kinetic Models for Alkaline Peroxide Bleaching., *J. Pulp and Paper Sci.*, **18(3)**, J85-93, (1992).

14. Gierer, J. and Jansbo, K., Mechanisms of Hydroxyl Radical Reactions with Lignin Studied with a Simple Model System., *6th Int. Symp. Wood and Pulp. Chem.*, 157-160, (1991).

15. Sjögren, B., Reitberger, T. and Zachrison, H., The Importance of Radical Reactions for Brightness Increase in Hydrogen Peroxide Bleaching of Mechanical Pulps., *5th Int. Symp. Wood and Pulp. Chem.*, 161-166, (1989).

16. Gierer, J. and Yang, E., Model Studies of the Reactions Between Hydroxyl Radicals and Aromatic Lignin Structures., *6th Int. Symp. Wood and Pulp. Chem.*, 197-200, (1991).

17. Gellerstedt, G., Pettersson, I. and Sundin, S., Chemical Aspects of Hydrogen Peroxide Bleaching, *1st International Symposium of Wood and Pulping Chemistry*, Volume II, 120-124, (1981).

18. Omori, S. and Dence, C.W., The Reactions of Stabilised and Unstabilised Alkaline Hydrogen Peroxide With Lignin Model Dimers., *1st International Symposium of Wood and Pulping Chemistry*, Volume 2, 112-19, (1981).

19. Agnemo, R., Gellerstedt, G. and Lindfors, E-L., Reactions of 1,2-Dimethyl-Cyclohexene with Alkaline Hydrogen Peroxide., *Acta Chem. Scand.*, **B33(2)**, 154-56, (1979).

20. Agnemo, R. and Gellerstedt, G., The Reactions of Lignin with Alkaline Hydrogen Peroxide. Part II. Factors Influencing the Decomposition of Phenolic Structures., *Acta Chem. Scand.*, **B33(5)**, 337-42, (1979).

21. Gierer, J., Mechanisms of Bleaching with Oxygen-Containing Species., *4th Int. Symp. Wood and Pulp. Chem.*, 279-288, (1987).

22. Barkhau. R., Bastian, J. and Thompson, N.S., The Reaction of Model Lignins with Oxygen Radicals., *Tappi J.*, 110, (1985).

23. Reitberger, T., Chemiluminescence as a Means to Study the Role of Hydroxyl Radicals in Oxidative Processes., *Holzforschung*, **42(6)**, 351-56, (1988).

24. Reitberger, T., Gierer, J., Jansbo, K., Yang, E. and Yoon, B-H., On the Participation of Hydroxyl Radicals in Oxygen and Hydrogen Peroxide Bleaching Processes., *6th Int. Symp. Wood and Pulp. Chem.*, Vol. 1, 93-97, (1991).

CHAPTER 4

KINETIC STUDIES OF REACTIONS BETWEEN MODEL LIGNIN α,β - UNSATURATED ALDEHYDES AND ALKALINE PEROXIDE

In the preceding chapters, several kinetic models for the alkaline peroxide bleaching of *E. regnans* mechanical pulp were investigated. Further understanding of these models required more information regarding the individual chemical processes taking place during peroxide bleaching. As a result, kinetic studies on model lignin chromophores have been undertaken in the following two chapters, with the aim of unravelling some of the kinetic processes responsible for the bleaching behaviour of mechanical pulps.

The colour of mechanical pulps, measured by light absorption coefficient at 457 nm, is generally attributed to the presence of three main chromophoric groups in the lignin polymer[1]. These three groups consist of conjugated structures based on α,β-unsaturated aldehydes of which coniferaldehyde is an example, *ortho* and *para* benzoquinones and less chromophoric α-aryl carbonyls such as acetovanillone (Figure 1).

MODEL LIGNIN CHROMOPHORES

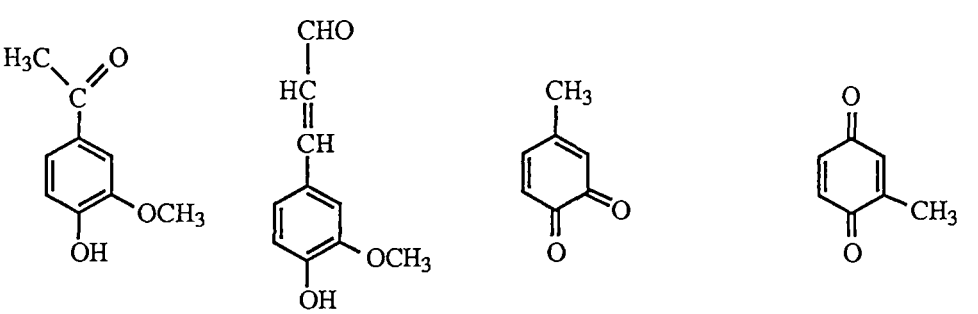

acetovanillone coniferaldehyde 4-methyl-*o*-quinone 2-methyl-*p*-quinone

FIGURE 1: Examples of model compounds representing chromophores in lignin.

Although the proportions of these chromophores in lignin will vary slightly depending on wood species and pulp type, it should be possible to explain the kinetic bleaching responses of mechanical pulps in terms of reactions involving the three main chromophore types. The kinetics of reactions between alkaline peroxide and α,β-unsaturated aldehydes have been incompletely studied, and little information exists regarding the kinetics of quinone structures exposed to alkaline peroxide. This chapter describes kinetic investigations performed on a model α,β-unsaturated aldehyde, cinnamaldehyde, in alkaline peroxide solution. In the following chapter, a kinetic study of similar reactions involving a model lignin *ortho* quinone is presented.

4.1 Literature Review

A vast body of literature exists on the topic of α,β-unsaturated aldehydes in native wood lignins and mechanical pulps. The importance of these structures is a result of their considerable chromophoric activity which is thought to account for a significant proportion of the colour of lignin. In particular, much attention has been focussed on mechanisms leading to the formation of α,β-unsaturated aldehydes in lignin, the reactions of these structures with various pulping and bleaching chemicals, assessment of their numbers and types, and their spectroscopic and other physical properties. Several excellent reviews of these topics have appeared in the past[2-5] and no attempt has been made here to provide an exhaustive review of the available literature dealing with various aspects of α,β-unsaturated aldehydes. Rather, the current review is confined to relatively recent studies in which the roles of α,β-unsaturated aldehydes during peroxide bleaching are examined.

4.1.1 Detection of α,β-Unsaturated Aldehyde Structures in Lignin

Information regarding α,β-unsaturated carbonyl groups in lignin has been drawn from a wide range of sources, however there is broad agreement that α,β-unsaturated carbonyls

are naturally occurring constituents in native lignin. Preliminary evidence pointing to the presence of α,β-unsaturated aldehydes in wood originated from chemical degradation studies on assorted soft and hardwood lignins[2]. For instance, degradation of native lignins by hydrolysis[6], acidolysis[7], acetolysis[8] and solvolysis[9] has resulted in the isolation of the α,β-unsaturated aldehyde, coniferaldehyde (3-methoxy-4-hydroxy-cinnamaldehyde), and its hardwood analogue, 5-methoxy-coniferaldehyde (Figure 2).

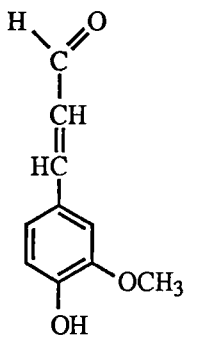

coniferaldehyde

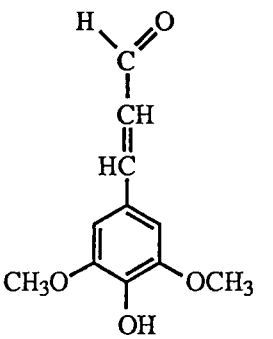

5-methoxy-coniferaldehyde

FIGURE 2: α,β-unsaturated aldehyde structures isolated from lignin after chemical degradation.

In addition to chemical degradation studies, more direct evidence for the presence of α,β-unsaturated aldehydes in wood has been obtained using methods such as UV-visible spectroscopy, infra-red spectroscopy and ^{13}C-nmr spectroscopy.

The UV-visible spectra of mechanical pulps exhibit features consistent with the presence of α,β-unsaturated aldehydes in lignin[10]. The spectra are relatively simple and display a peak at about 300 nm with a pronounced shoulder occurring closer to 400 nm[11-13]. Complementary studies on model lignin compounds and derivatised lignins have greatly assisted in the interpretation of UV-visible spectra of mechanical pulps. Based on the behaviour of model lignin compounds, Adler and Marton[14] proposed that α,β-unsaturated aldehydes such as coniferaldehyde were partly responsible for the absorption of light by spruce lignin in the region above 300 nm.

The work of Adler and Marton was later extended by Pew and Connors[15] who studied the absorption spectra of monomeric and dimeric α,β-unsaturated aldehydes. The effects of aromatic substituents (auxochromes) on light absorption characteristics were also investigated. Pew and Connors found that suitable auxochromes were able to extend α,β-unsaturated aldehyde absorption bands well into the visible region, giving rise to increases in colour. In particular, α,β-unsaturated aldehydes present in hardwoods were shown to absorb more visible light than the corresponding softwood compounds. Absorption bands of dimeric model α,β-unsaturated aldehydes extended further into the visible region than the corresponding monomers, and this red shift in absorption was enhanced by impregnation of model compounds into a cellulose matrix. It was proposed that removal of α,β-unsaturated aldehydes from mechanical pulp resulted in a net reduction in absorption at about 350 nm.

Infra-red spectra of mechanical pulp samples reveal a number of characteristic bands, including a relatively strong band in the 1650-1670 cm^{-1} region which has been attributed to carbonyl stretch[11-13,16,17]. Polcin and Rapson[11] have demonstrated that α,β-unsaturated carbonyls are partly responsible for the signal at 1670 cm^{-1} by observing a loss in its intensity when these chromophores were selectively removed with sodium dithionite. It was further proposed that spruce groundwood pulp contained more carbonyls of α,β-unsaturated aldehyde type than western hemlock groundwood. Infra-red studies employing second derivative spectra have demonstrated the presence of α,β-unsaturated aldehyde groups in Eucalyptus regnans cold soda pulps[13]. Carbonyls of the α,β-unsaturated aldehyde type have also been observed in photoacoustic infra-red studies of black spruce refiner mechanical pulp[17]. These structures and other conjugated carbonyls were reported to produce a small, broad peak centred at 1650 cm^{-1}.

Recently, pyrolysis-gas chromatography-photo ionisation-mass spectrometry (Py-GC-MS) has been employed in the analysis of beech milled wood lignin[18]. Small but significant amounts of guaiacyl and syringyl α,β-unsaturated carbonyls were detected among more than 40 other monomers in the pyrolysed lignin. In ^{13}C-nmr studies of spruce milled wood lignin, coniferaldehyde units in the lignin have been observed to produce a small signal with a chemical shift of about 196 ppm[19]. Signals ascribed to coniferaldehyde units have also been detected in ^{13}C-nmr studies of birch, spruce and aspen milled wood lignins[20].

Despite widespread evidence of α,β-unsaturated aldehydes in native lignin, the origin of these structures is not well understood. It is generally believed that several processes may be responsible for the formation of coniferaldehyde structures in wood lignin. For example, hydroxycinnamic acids produced during lignification have been shown to undergo enzymatic reduction to produce the corresponding α,β-unsaturated aldehydes and alcohols[21]. Enzymatic dehydrogenation of coniferyl alcohol structures in lignin has also been reported to produce coniferaldehyde structures[22], while the biological attack of wood by fungal species such as white and brown rot may produce α,β-unsaturated aldehydes in wood lignin[23].

4.1.2 Determination of α,β-Unsaturated Aldehyde Content in Lignin

The importance of α,β-unsaturated carbonyls in wood chemistry is reflected in the many publications dealing with the assessment of their numbers in softwoods and hardwoods. The most common techniques for quantifying α,β-unsaturated carbonyls in lignin typically involve chemical derivatisation and/or reaction with selective colouring agents followed by spectrophotometric measurement. Studies such as these have been comprehensively reviewed by Lai and Sarkanen[24]; only a short summary of some of the more important literature is presented here.

In 1948, Adler and Ellmer[6] first developed reactions in which phloroglucinol or *p*-aminobenzoic acid was reacted selectively with α,β-unsaturated carbonyls to produce

distinctively coloured pulps. Spectrophotometry was used to measure the extent of these colour reactions, and spruce wood lignin was estimated to contain 2 to 2.5 coniferaldehyde structures per 100 phenylpropane units using this technique. Later, Adler and Marton[14] examined the UV-visible difference spectra of spruce milled wood lignin subjected to catalytic hydrogenation. Hydrogenation rapidly and selectively reduced ethylenic and carbonyl functionalities, including coniferaldehyde structures, leading to a decrease in UV-visible absorbance above 300 nm. Based on the similar behaviour of model substances, spruce milled wood lignin was estimated to contain approximately 3 etherified coniferaldehyde structures and less than 1 phenolic coniferaldehyde unit per 100 phenylpropane units. Colour reactions coupled with spectrophotometric detection have also been used to quantify α,β-unsaturated carbonyls in hardwood Brauns lignins[25], while extractive procedures were used to determine the α,β-unsaturated carbonyl content of hardwood milled wood lignins[26]. From these studies, α,β-unsaturated carbonyls in hardwoods were reported to exist in approximately half the numbers quoted for equivalent softwood preparations (eg. 1-2 coniferaldehyde units/100 phenylpropane units in birch milled wood lignin[26]).

In more recent work, Hirashima and Sumimoto[27] devised a direct method for the determination of α,β-unsaturated carbonyl content in Japanese red pine milled groundwood. The absorbance of the groundwood sheets was measured after application of the phloroglucinol - HCl colour reagent developed by Adler and co-workers. The absorbance of coloured sheets was related to α,β-unsaturated carbonyl content through calibration curves prepared by impregnating lignin free sheets with coniferaldehyde and coniferaldehyde methyl ether. The impregnated sheets were subsequently treated with the colour reagent and their absorbance measured. Hirashima and Sumimoto reported that, for every 100 phenylpropane units, Japanese red pine contained 1.1 to 1.5 coniferaldehyde units and 1.4 to 3.0 etherified coniferaldehyde units. Peroxide bleaching of the pulp reportedly oxidised more than 80% of the α,β-unsaturated aldehyde groups in the lignin.

4.1.3 Effects of Alkaline Peroxide on α,β-Unsaturated Aldehydes

Bleaching studies on mechanical pulps and lignin preparations have revealed that α,β-unsaturated aldehydes are among the most reactive functional groups towards alkaline peroxide. The effects of alkaline peroxide bleaching on α,β-unsaturated aldehydes have been studied using an assortment of techniques including UV-visible and infra-red spectroscopy, colour reactions and ^{13}C-nmr. The vast majority of these studies report that α,β-unsaturated carbonyls are rapidly destroyed during peroxide bleaching resulting in a brightening of the pulp.

In studies conducted with black spruce and balsam fir mechanical pulps, a specific colour test for α,β-unsaturated aldehydes was developed through selective reaction with resorcinol and phloroglucinol[28]. The mechanical pulps examined were found to contain small amounts of α,β-unsaturated carbonyls which were responsible for a large part of the visible light absorbed. When the pulp samples were bleached with alkaline peroxide and treated with the colour reagents, no development of colour was observed, indicating that peroxide bleaching completely removed α,β-unsaturated aldehyde groups from black spruce and balsam fir lignins.

Experiments employing ^{13}C-nmr also support the comprehensive elimination of α,β-unsaturated aldehyde groups from mechanical pulp lignins during alkaline peroxide bleaching. In ^{13}C-nmr studies on spruce milled wood lignin, Holmbolm and co-workers[19] observed a small signal at 196 ppm corresponding to the aldehyde carbon in α,β-unsaturated carbonyls. This peak was almost completely removed when the milled wood lignin was treated with alkaline peroxide. Peroxide bleaching was also shown to increase the carboxyl content of the lignin.

The technique of photoacoustic Fourier transform infra-red spectroscopy (FTIR-PAS) has recently been applied to the study of mechanical pulp brightening by St. Germain and Gray[17]. When black spruce mechanical pulp was treated with alkaline peroxide, a loss in

peak intensity at 1650 cm^{-1} was observed. This was ascribed to the removal of conjugated carbonyl structures including α,β-unsaturated aldehydes. Oxidative-reductive studies of softwood mechanical pulps using UV-visible and infra-red spectroscopy have also confirmed extensive attack on α,β-unsaturated aldehydes during alkaline peroxide bleaching[12]. *In situ* infra-red spectra of bleached pulp samples revealed a significant decrease in the 1670 cm^{-1} band characterising α,β-unsaturated carbonyls. A reduction in chromophoric species absorbing light above 300 nm was also observed, supporting the loss of α,β-unsaturated aldehydes[12].

In more recent work, removal of α,β-unsaturated aldehydes has been described during peroxide bleaching of stone groundwood, TMP and CTMP pulps[1]. Elimination of these chromophores was detected by following changes in UV-visible absorption spectra, ISO brightness and the tristimulus L*, a*, b* values during bleaching.

4.1.4 Reactions of α,β-Unsaturated Aldehydes with Alkaline Peroxide

The relatively minor occurrence of chromophores in lignin and the complex nature of lignin itself has made direct study of peroxide bleaching chemistry very difficult. Although removal of α,β-unsaturated aldehydes from lignin and mechanical pulps has been observed spectroscopically[11-13,16,17,19,27], the most detailed information regarding reaction mechanisms during peroxide bleaching has resulted from studies of model lignin chromophores, including model α,β-unsaturated aldehydes.

Several studies dealing with the reaction of α,β-unsaturated aldehydes and alkaline peroxide have appeared in the literature during the last 40 years. Although there is general agreement that α,β-unsaturated aldehydes react readily with alkaline peroxide, contradictory information exists concerning reaction products and the reaction mechanisms involved. It is likely that most of these discrepancies result from the wide variety of reaction conditions used in the different studies.

The first study into the effects of hydrogen peroxide on α,β-unsaturated aldehydes was made by Payne[29] who isolated epoxides of unsaturated aldehydes under mild alkaline conditions. It was concluded that the ethylene bond of α,β-unsaturated aldehydes underwent nucleophilic attack by perhydroxyl anion (HO_2^-) at the β-carbon in a Michael addition similar to that reported for other α,β-unsaturated systems.

In a later study of the reactions of lignin-related model compounds, Reeves and Pearl[30] reported rapid conversion of an α,β-unsaturated aldehyde, cinnamaldehyde, to benzaldehyde upon oxidation with alkaline peroxide at 25°C. Cleavage of the side chain to form benzaldehyde was proposed to occur by two possible mechanisms involving either epoxide intermediates or direct loss of the side chain.

The work of Reeves and Pearl was extended by Gellerstedt and Agnemo[31] who investigated the oxidation of coniferaldehyde and coniferaldehyde methyl ether structures with alkaline peroxide. Reactions were carried out in aqueous dioxane solution over a 0-30°C temperature range. It was found that the rate of loss of coniferaldehyde methyl ether obeyed second order kinetics and that removal of α,β-unsaturated aldehydes was initiated by nucleophilic attack of perhydroxyl anions on the β-carbon of the ethylene bond, in agreement with Payne[29]. Gellerstedt and Agnemo also monitored the rate of formation of the product aldehyde, 3,4-dimethoxy-benzaldehyde, and reported that product formation occurred at a slower rate than consumption of the starting material, thus indicating the presence of an undetected intermediate. This intermediate was identified as a cyclic 1,2-dioxolane structure which was proposed to arise from rearrangement of a hydroperoxide intermediate at *p*H 8.5.

In a later study of the epoxidation kinetics of α,β-unsaturated aldehydes and esters, cinnamaldehyde in methanol solution was observed to undergo epoxidation at a rate dependent on perhydroxyl anion and cinnamaldehyde concentrations[32]. The proposed epoxidation mechanism was the same as in previous studies[29,31] and involved nucleophilic attack of perhydroxyl anion at the β-carbon, followed by ring closure and

elimination of hydroxide ion. The electron donating effects of a methyl group at the β-carbon were found to lower the rate of epoxidation. Under the reaction conditions employed (*p*H 12, 30°C), the epoxide ring was observed to undergo further cleavage to yield benzaldehyde, however no kinetic information was reported regarding this reaction.

Tishchenko and co-workers[33] have also examined the reaction of cinnamaldehyde with alkaline peroxide. Oxidations were performed in dioxane solution under very mild conditions (*p*H 10-11, -5°C). A cyclic 1,2-dioxolane structure analogous to that reported by Gellerstedt and Agnemo[31] was isolated as the major reaction product, although some cinnamaldehyde epoxide was detected when the reaction was carried out at *p*H 8.

Recently, epoxidation of cinnamaldehyde with peroxide at room temperature has been reported at high alkalinities in water/methanol solvent[34]. Under such conditions, the epoxide of cinnamaldehyde was oxidised to the corresponding carboxylic acid which subsequently formed a polymer. Oxidation of the cinnamaldehyde epoxide most probably resulted from reactions with oxygen which would be readily generated by the base induced decomposition of hydrogen peroxide at such high alkalinities[35]. Upon acidification with sulphuric acid, the polymeric species underwent decarboxylation to yield phenyl-acetaldehyde.

4.2 Introduction

In this chapter, kinetic and mechanistic information is presented for reactions taking place when cinnamaldehyde, a model α,β-unsaturated aldehyde, is oxidised by alkaline peroxide. Kinetic studies on cinnamaldehyde have been performed under constant reagent concentrations to allow easy comparison with kinetic studies on mechanical pulp. The influence of solvents and aromatic substituents on reaction rates are examined, as are factors affecting stereochemistry. The contribution of α,β-unsaturated aldehydes to the kinetic behaviour of peroxide bleached *E. regnans* mechanical pulp is also discussed.

4.3 Experimental

4.3.1 Equipment

Gas chromatograms of reaction product mixtures were obtained using a Hewlett-Packard 5890 Series II gas chromatograph fitted with a 25 m × 0.22 mm i.d. BP 20 fused silica, polar phase capillary column supplied by SGE. Eluting compounds were detected with a flame ionisation detector. Mass spectra were recorded on a Hewlett-Packard 5970 Mass Selective Detector. *p*H measurements were made using an Orion Research Model 960 *p*H meter and glass electrode calibrated against commercial buffer solutions of *p*H 7.00, 10.00 and 11.00 (Mallinkrodt BuffAR). Infra-red spectra were recorded on an Hitachi 270-30 spectrophotometer while proton nmr spectra were recorded on a Bruker AM 300 MHz spectrometer at 25°C. UV-visible spectra were recorded on a Shimadzu UV-160 spectrometer.

4.3.2 Materials

Model compounds and other reagents were obtained from commercial sources. Commercial supplies of cinnamaldehyde (Fluka) were purified by vacuum distillation (b.p. 77-78°C, 1 mm Hg; *lit.* b.p. 127°C, 15 mm Hg) as were samples of benzaldehyde (Aldrich, b.p. 60-61°C, 10 mm Hg; *lit.* b.p. 62°C, 10 mm Hg). Analysis of the purified cinnamaldehyde indicated > 99.5% abundance of the *trans* isomer based on GC peak areas. Aqueous hydrogen peroxide (Ajax, 30% w/v, 10.5 M by iodometric titration) was used without further purification and transition metal decomposition of peroxide was minimised by using semiconductor grade sodium hydroxide (Aldrich, > 99.99%). Solvent methanol was distilled and dried over molecular sieves and deionised, doubly distilled 18 MΩ water was employed.

4.3.3 Synthesis of Cinnamaldehyde Epoxide

Cinnamaldehyde epoxide (3-phenyl-2,3-epoxy-propanal) was synthesised by the oxidation of cinnamaldehyde with alkaline *tert*-butyl hydroperoxide (Aldrich, 70%) using the method described by Payne[36]. Low yields of product (~10%) were recovered using the described method however better yields (~55%) were produced when the oxidation was performed at higher *p*H (*p*H 10.5) and temperature (50°C) than reported. The cinnamaldehyde epoxide was purified by vacuum distillation and was recovered as a colourless, viscous liquid (b.p. 83-84°C, 1 mm Hg; *lit.* b.p. 66-68°C, 0.2 mm Hg[36]). The IR spectrum of the product was identical to that previously reported[36] and exhibited characteristic epoxide stretching bands at 870 cm^{-1} and 1230 cm^{-1}. Analysis of the product by GC-MS and ^{1}H-nmr indicated that 2 epoxide diastereomers had been formed in a *ca.* 1:8 ratio based on GC peak areas. From ^{1}H-nmr spectra, the more abundant diastereomer was assigned a *trans* configuration. Comparison of the GC elution order of the epoxide isomers with the structurally related *cis* and *trans* isomers of cinnamaldehyde supported the assignment of the trans epoxide isomer as the major product. MS [M^+ 148(12), 147(20), 131(5), 119(25), 105(12), 92(13), 91(100), 90(28)]. ^{1}H-nmr ($CDCl_3$): *cis* isomer; δ 3.50, dd, J 4.6 Hz, 6.1 Hz; 4.34, d, J 4.6 Hz; 9.05, d, 5.9 Hz. *trans* isomer, δ 3.40, dd, J 1.8 Hz, 6.0 Hz; 4.12, d, J 1.8 Hz; 9.14, d, J 6.0 Hz (see Appendix 3.1).

4.3.4 Identification of Cinnamaldehyde Oxidation Products

Cinnamaldehyde (2.5 mmol) was reacted with alkaline peroxide (0.2 M, *p*H 11) in 1:1 methanol/water solution (200 mL) at 25°C. A mixed methanol/water solvent was employed since cinnamaldehyde was only sparingly soluble in aqueous solution. After 1 hour, the reaction solution was quenched by acidification with phosphate buffer (20 mL, 2 M NaH_2PO_4, *p*H 6.5) and 3 × 30 mL dichloromethane extracts were taken. The dichloromethane solution was concentrated under vacuum and analysed by GC-MS. Benzaldehyde and cinnamaldehyde epoxide were detected as major reaction products in

these trial oxidations of cinnamaldehyde with alkaline peroxide. Small quantities of phenyl-acetaldehyde, acetophenone and benzoic acid were detected as minor products. When the reaction solution was bubbled with a slow stream of nitrogen in a similar trial, the minor products were not observed, suggesting that reactions involving dissolved oxygen were responsible for their formation.

4.3.5 Method for Kinetic Runs

Kinetic experiments were carried out in a stoppered polyethylene reaction vessel immersed in a constant temperature water bath. A 1:1 water/methanol solution (200.0 mL) containing cinnamaldehyde (2.8 mmol) and an unreactive standard (3,4-dimethoxy-acetophenone, 1.3 mmol) was thermally equilibrated for several minutes and dissolved oxygen was purged with a slow stream of nitrogen. Kinetic runs were initiated by adding the required amounts of sodium hydroxide and hydrogen peroxide to reach the desired conditions. Samples for analysis (10 mL) were periodically withdrawn and iodometric titrations were carried out to determine total peroxide levels. Constant sodium hydroxide and hydrogen peroxide concentrations were maintained by adding the necessary amounts of each compound based on *p*H measurements and iodometric titration respectively. In blank runs, carried out in the absence of peroxide, alkali consumption was followed by titration against standardised hydrochloric acid (0.01 M) using a phenolphthalein indicator.

Several kinetic runs were performed in aqueous solution to investigate the effects of solvent polarity on reaction rates. In these experiments, cinnamaldehyde (0.2 mmol) was dissolved in distilled, deionised water (500 mL) and was reacted with 20-50 times molar excesses of alkaline peroxide at constant *p*H and temperature. Due to the large excesses of reagent, maintenance of constant concentrations was not required. Aliquots of solution (10.00 mL) were removed at various times during reaction for analysis by UV-visible spectroscopy.

4.3.6 Analysis of Samples

Samples withdrawn during kinetic runs were quenched by acidification with phosphate buffer (5 mL, 2 M NaH_2PO_4, *p*H 6.5). The quenched sample was saturated with sodium chloride and extracted with dichloromethane (3 × 5 mL portions). A second standard (*p*-dichlorobenzene, 0.014 M, 5.00 mL) was added to each extracted portion and the total volume was made up to 25.00 mL.

Extracted samples were analysed by gas chromatography. Baseline resolution of extracted components was achieved using a simple temperature gradient program (60°C isothermal 5 min., 140°C at 10°C/min, 200°C at 5°C/min.). A head pressure of 15 psi was used. Cinnamaldehyde, benzaldehyde and cinnamaldehyde epoxide peak areas were referenced to the peak areas of the 3,4-dimethoxy-acetophenone and *p*-dichlorobenzene standards. Concentrations were determined from standard curves relating peak area ratios to concentration over the experimental working range (Appendix 3.2).

Samples removed during kinetic runs in aqueous solution were quenched by acidification with phosphate buffer (5 mL, 2 M NaH_2PO_4, *p*H 6.5) and made up to a volume of 25.00 mL. Disappearance of cinnamaldehyde was followed by monitoring the decrease in absorbance at 315 nm. A calibration curve relating absorbance at 315 nm to concentrations of cinnamaldehyde was established by measuring the absorbances of standard cinnamaldehyde solutions. Adherence of these solutions to Beer's Law was excellent for absorbances less than 1.5 (correlation coefficient, $r^2 = 1.000$) (Appendix 3.3).

4.4 Results

4.4.1 Reaction of Cinnamaldehyde with Alkaline Peroxide

Results obtained in the absence of dissolved oxygen indicated that cinnamaldehyde behaved in a similar manner to α,β-unsaturated ketones[37] when exposed to solutions of alkaline hydrogen peroxide. Kinetic profiles showing typical concentration-time dependencies of the starting material and reaction products are presented in Figure 3. Inspection of this Figure indicates that cinnamaldehyde reacted quickly with alkaline peroxide to form cinnamaldehyde epoxide (3-phenyl-2,3-epoxy-propanal), the side chain being cleaved more slowly to yield benzaldehyde. Gas chromatograms of reaction solutions always exhibited peaks due to the presence of *cis* and *trans* epoxide isomers in ratios of *ca.* 1:8 by peak area (Figure 4). Although other oxidation products such as benzoic and cinnamic acids would have been easily detected by GC, no evidence for their formation was observed when solutions were purged with nitrogen.

Kinetic and stoichiometric information (discussed below) indicated that reactions (1) and (2) were the major reactions occurring in the presence of alkaline hydrogen peroxide.

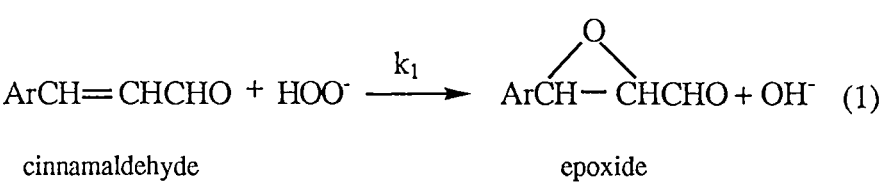

(1)

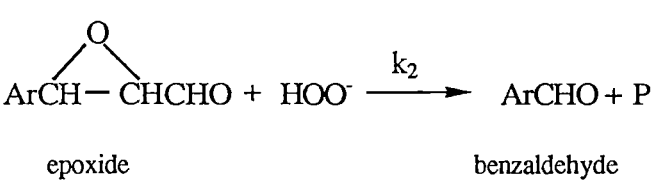

(2)

where P represents side chain cleavage products containing 2 carbon atoms.

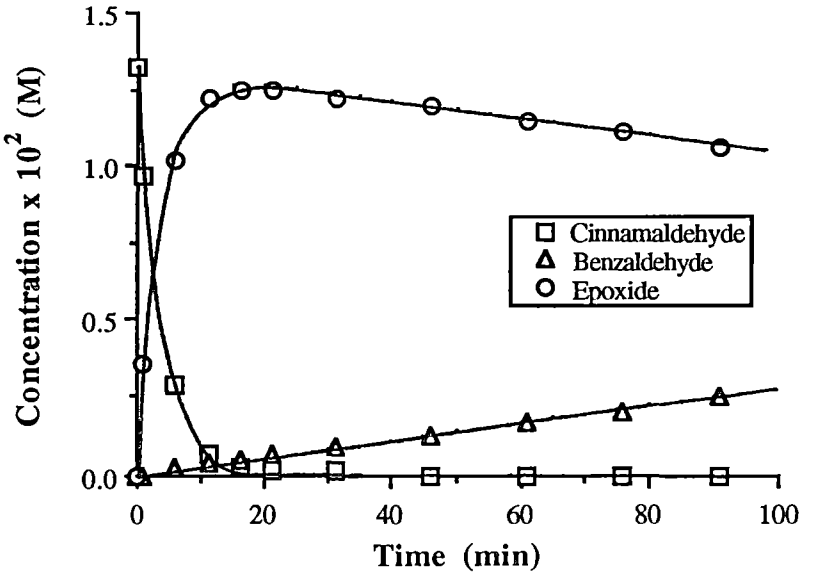

FIGURE 3 : Concentration-time profiles showing formation of cinnamaldehyde epoxide and benzaldehyde during reaction of cinnamaldehyde with alkaline peroxide. 0.187 M peroxide, *p*H 10.1, 25°C. Illustrated curves are mathematical fits of experimental data.

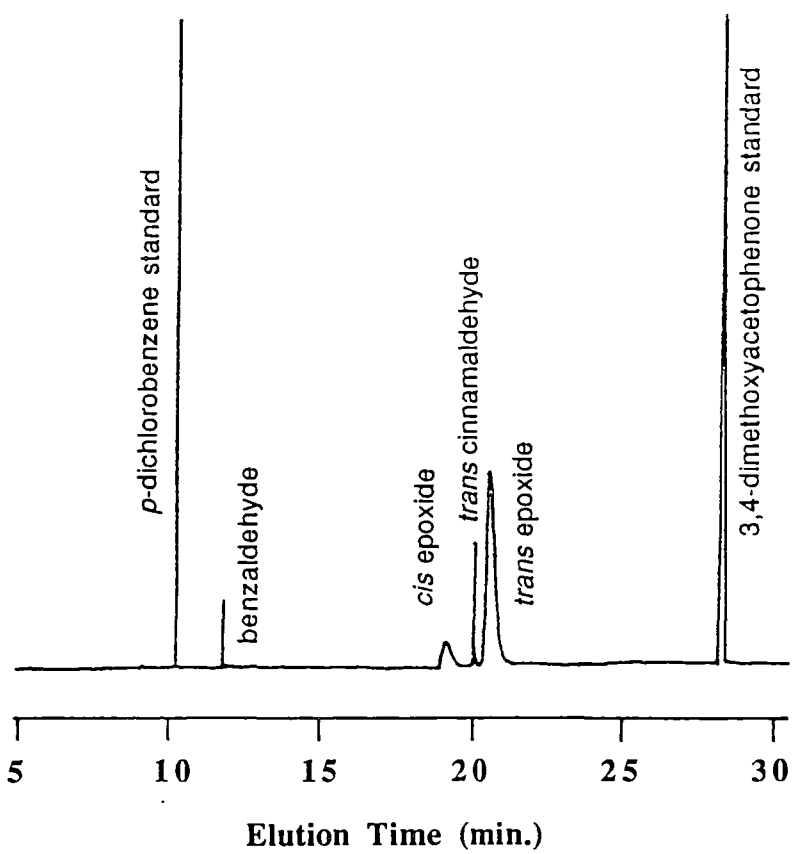

FIGURE 4 : Gas chromatogram of extracted sample from the reaction of cinnamaldehyde with alkaline hydrogen peroxide. Reaction time = 10 min., 0.179 M peroxide, *p*H 10.1, 25°C.

Peroxide stoichiometries in reactions (1) and (2) were evaluated during the first 20 minutes of reaction. After this time, slow base catalysed decomposition of peroxide and consumption by side chain fragments became the dominant modes of peroxide depletion and resulted in elevated peroxide stoichiometries for reactions (1) and (2). Stoichiometries calculated during the first 20 minutes of kinetic runs were consistent with the consumption of about 1 mole of peroxide per mole of cinnamaldehyde and epoxide reacted (Table 1). The fate of the side chain fragment, P, in reaction (2) was not studied further, but previous work with other α,β-unsaturated aldehydes[31] suggests that P underwent further oxidation by perhydroxyl anion to yield 2 equivalents of formic acid.

TABLE 1 : Initial peroxide stoichiometries in reactions (1) and (2).
0.179 M H_2O_2, *p*H 10.1, 25°C.

Time (min.)	Δ Cinnamaldehyde ($\times 10^3$ moles)	Δ Benzaldehyde ($\times 10^3$ moles)	Δ H_2O_2 ($\times 10^3$ moles)	Δ H_2O_2 / Δ (Cinnamaldehyde + Benzaldehyde)
5	6.80	0.25	7.6	1.08
10	8.99	0.39	11.3	1.20
15	9.41	0.55	12.0	1.20
20	9.53	0.68	15.3	1.50
			Average	1.24

4.4.2 Reaction of Cinnamaldehyde with Alkali

In the absence of peroxide, the reactions of cinnamaldehyde and cinnamaldehyde epoxide with alkali suggested the participation of a further two reaction pathways where cinnamaldehyde and the epoxide were degraded to benzaldehyde. Kinetic information (discussed later) and reaction stoichiometries monitored by alkali consumption (Table 2) indicated that reactions (3) and (4) took place in the presence of alkali, but at much slower

rates than (1) and (2) in alkaline peroxide solutions. Both reactions were observed to follow 1st order kinetics with respect to the alkali and substrate, and 2nd order kinetics overall.

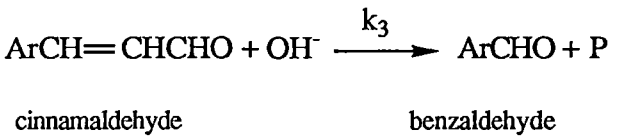

(3)

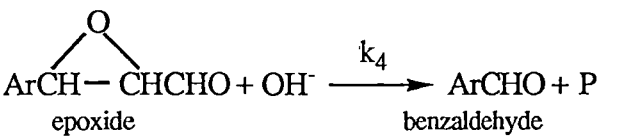

(4)

TABLE 2 : Stoichiometries for the reaction of base with cinnamaldehyde (3) and cinnamaldehyde epoxide (4) at 25°C.

Time (min.)	Δ Cinnamaldehyde ($\times 10^3$ M)	Δ NaOH ($\times 10^3$ M)	$\frac{\Delta \text{NaOH}}{\Delta \text{Cinnamaldehyde}}$	Δ Epoxide ($\times 10^3$ M)	Δ NaOH ($\times 10^3$ M)	$\frac{\Delta \text{NaOH}}{\Delta \text{Epoxide}}$
30	0.14	0.32	2.3	0.72	0.53	0.74
60	0.16	0.48	2.8	1.57	1.75	1.11
90	0.18	0.43	2.3	2.29	2.32	1.01
120	0.20	0.36	1.8	2.56	2.67	1.04
150	0.26	0.63	2.4	3.17	3.01	0.95
180	-	-	-	3.44	3.54	1.03
210	-	-	-	3.93	3.98	1.01
			Average = 2.3		Average	= 0.98

In Table 2, the average stoichiometric ratio of 2.3 for the reaction of alkali with cinnamaldehyde (3) suggests that, after initial cleavage of the cinnamaldehyde side chain, further quantities of alkali were consumed in reactions with the side chain fragment, P. In contrast, only one equivalent of alkali was used in the reaction with epoxide (4)

indicating that the side chain fragment from this reaction was stable towards further reaction with base.

4.4.3 Evaluation of Hydrogen Peroxide Dissociation Constant in 1:1 Methanol/Water Solvent

To investigate the role of perhydroxyl ion in the reaction of alkaline peroxide with cinnamaldehyde, the equilibrium constant for the dissociation of hydrogen peroxide to form perhydroxyl anions and water in reaction (5) was obtained using the method of Teder and Tormund[38]. The equilibrium constant, K_5, in 1:1 methanol/water solvent was determined by adding known amounts of standardised NaOH solution (~0.001 M) to a solution of H_2O_2 (~0.1 M) and measuring the resultant hydroxide ion concentration as *p*H. The difference in the amount of alkali added and the amount measured by *p*H was equal to the amount of HO_2^- formed.

$$H_2O_2 + OH^- \rightleftharpoons HO_2^- + H_2O \qquad (5)$$

The total amount of peroxide present ($H_2O_2 + HO_2^-$) was determined by iodometric titration of an aliquot of solution withdrawn after each addition of NaOH. In this way, the concentrations of all the species in equation (5) were determined so that values for K_5 could be calculated from equation (6). Values of log (K_5) across the temperature range 17-35°C are presented in Table 3. From Table 3, the equilibrium constant for reaction (5) in the 1:1 methanol/water solvent employed was determined to be log (K_5) = 2.26 ± 0.09 M^{-1}. Any temperature dependence of K_5 was negligible across the temperature range studied (17.5 - 35.0°C).

$$K_5 = \frac{[HO_2^-]}{[H_2O_2][OH^-]} = \frac{1}{K_b} \qquad (6)$$

TABLE 3 : Dissociation constants for alkaline hydrogen peroxide in 1:1 methanol/water solvent over the temperature range 17.5 - 35.0°C.

T = 17.5°C

$[H_2O_2 + HO_2^-]$ (M)	$[OH^-]$ added ($\times 10^4$ M)	$[OH^-]$ measured ($\times 10^5$ M)	$[HO_2^-]$ ($\times 10^5$ M)	$[H_2O_2]$ (M)	log K_5
0.1036	0.995	0.351	9.60	0.103	2.42
0.0935	1.89	1.52	17.4	0.0934	2.09
0.0846	2.70	2.19	24.8	0.0844	2.13
0.0759	3.42	2.53	31.7	0.0756	2.22
0.0646	4.07	3.01	37.7	0.0642	2.29
0.0615	4.66	3.18	43.4	0.0611	2.35
0.0555	5.19	4.01	47.9	0.0551	2.34
				Average =	2.26 ± 0.12

T = 25.0°C

$[H_2O_2 + HO_2^-]$ (M)	$[OH^-]$ added ($\times 10^4$ M)	$[OH^-]$ measured ($\times 10^5$ M)	$[HO_2^-]$ ($\times 10^4$ M)	$[H_2O_2]$ (M)	log K_5
0.0910	2.17	1.11	2.06	0.0908	2.31
0.0828	4.12	2.69	3.85	0.0825	2.24
0.0736	5.88	4.56	5.42	0.0731	2.21
0.0663	7.46	6.61	6.80	0.0656	2.20
0.0593	8.88	7.80	8.10	0.0585	2.25
0.0531	10.2	9.10	9.25	0.0521	2.29
				Average =	2.25 ± 0.05

T = 35.0°C

$[H_2O_2 + HO_2^-]$ (M)	$[OH^-]$ added ($\times 10^4$ M)	$[OH^-]$ measured ($\times 10^5$ M)	$[HO_2^-]$ ($\times 10^4$ M)	$[H_2O_2]$ (M)	log K_5
0.105	1.00	0.530	0.946	0.104	2.24
0.0948	1.90	1.23	1.78	0.0933	2.19
0.0842	2.71	1.82	2.53	0.0843	2.22
0.0768	3.44	2.37	3.20	0.0756	2.25
0.0685	4.09	3.23	3.77	0.0642	2.26
0.0606	4.68	3.50	4.33	0.0611	2.31
0.0545	5.21	4.13	4.80	0.0551	2.32
				Average =	2.26 ± 0.05

4.4.4 Calculation of Rate Constants for Reactions in 1:1 Methanol/Water Solvent

Estimates of pseudo-rate constants, k_1' and k_2', for reactions (1) and (2) with peroxide were obtained from linear pseudo-first order plots of cinnamaldehyde and epoxide disappearance (Figure 5). Pseudo 1st order plots for disappearance of the epoxide (Figure 5b) were constructed using data obtained after the complete reaction of cinnamaldehyde (eg. after 20 min. in Figure 3). Maintenance of constant alkali and peroxide concentrations meant that any peroxide loss due to base catalysed decomposition could be ignored in the reaction system.

Pseudo first order rate constants for the major reactions (1) and (2) were calculated using a reaction simulation program in which the proposed reaction schemes for (1) and (2) and estimates of the corresponding rate constants (k_1', k_2') were entered as input (see Appendix 3.4). Reaction rates for schemes (3) and (4) were too small in comparison with (1) and (2) to allow accurate calculation of the pseudo-first order rate constants (k_3', k_4') using the simulation program.

Refined pseudo rate constants (k_1' and k_2') were calculated from initial estimates by an iterative simplex algorithm contained in the simulation program*. Combinations of k_1' and k_2' were substituted into differential rate equations describing reactions (1) and (2) until theoretical responses of the reacting species were judged to best match experimental kinetic data by minimisation of a least squares fit. Calculated pseudo first order rate constants for reactions (1) and (2) are presented in Table 4.

Second order rate constants for reactions 1 and 2 (k_1 and k_2) were determined from linear plots of k_1' and k_2' against perhydroxyl anion (HO_2^-) concentration. Perhydroxyl anion concentrations at each concentration of H_2O_2 and alkali were calculated using the mean peroxide dissociation constant, K_5, obtained in section 4.4.3. The degree of linearity in Figure 4 illustrates the adherence of reactions (1) and (2) to 2nd order kinetics.

---

* Program written by Dr. Mike Whitbeck, Desert Research Institute, Reno, Nevada, USA.

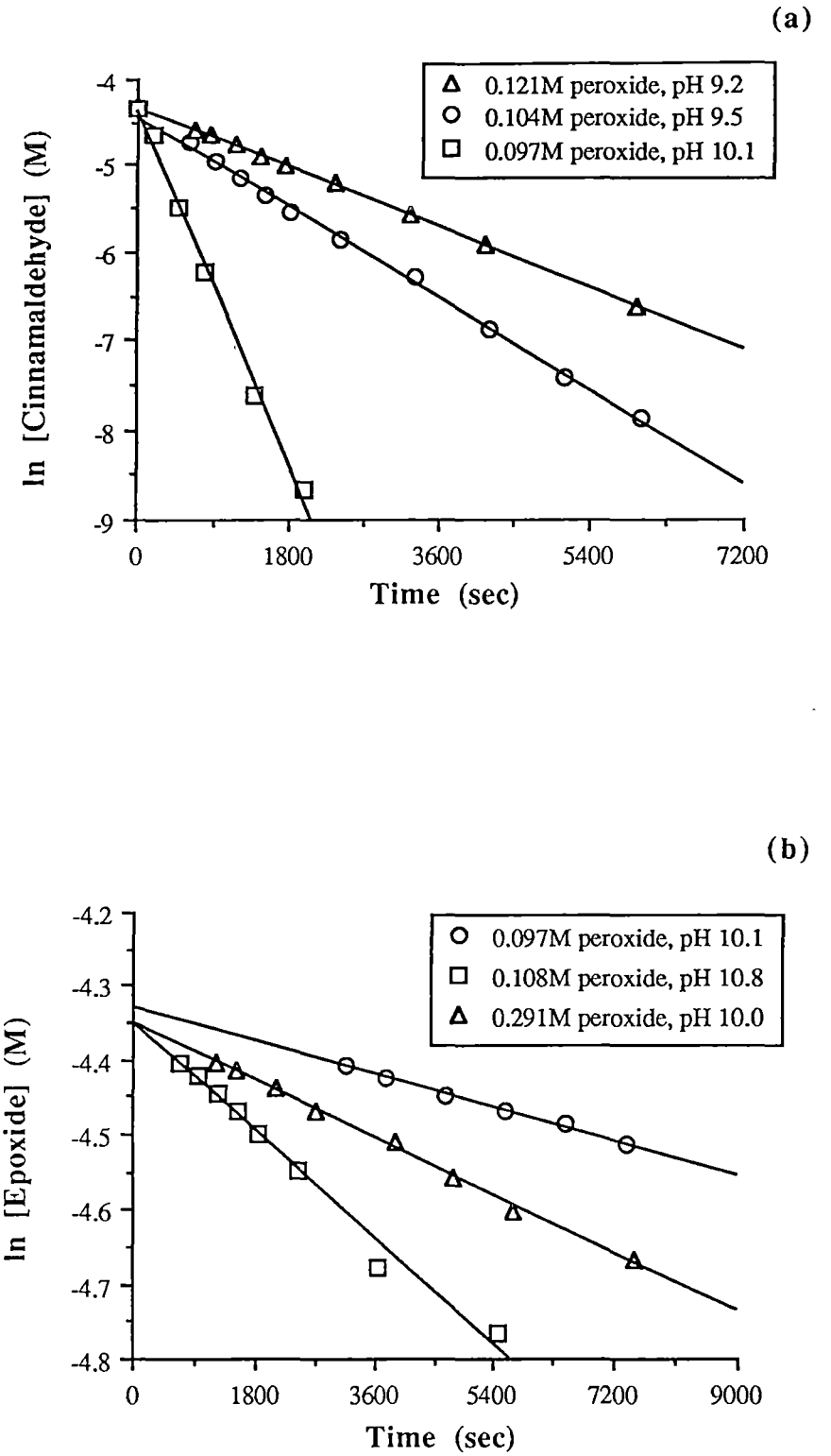

FIGURE 5 : Typical pseudo-first order plots showing disappearance of (a) cinnamaldehyde and (b) cinnamaldehyde epoxide during reaction with alkaline peroxide at 25°C.

TABLE 4 : Refined pseudo-first order rate constants for reactions (1) and (2).

Temperature (°C)	*p*H	$[H_2O_2]$ (M)	$[HO_2^-]$ ($\times 10^4$ M)	k_1' ($\times 10^4$ s^{-1})	k_2' ($\times 10^6$ s^{-1})
25.0	9.2	0.121	3.4	3.9	9.3
25.0	9.5	0.104	5.8	6.6	13.8
25.0	10.1	0.097	21	23.5	17.3
25.0	10.1	0.179	40	44.7	41.2
25.0	10.0	0.291	52	53.7	41.5
25.0	10.8	0.108	120	124	95.7
35.0	9.5	0.097	5.5	15.6	26.3
17.6	9.5	0.107	6.0	4.1	9.9

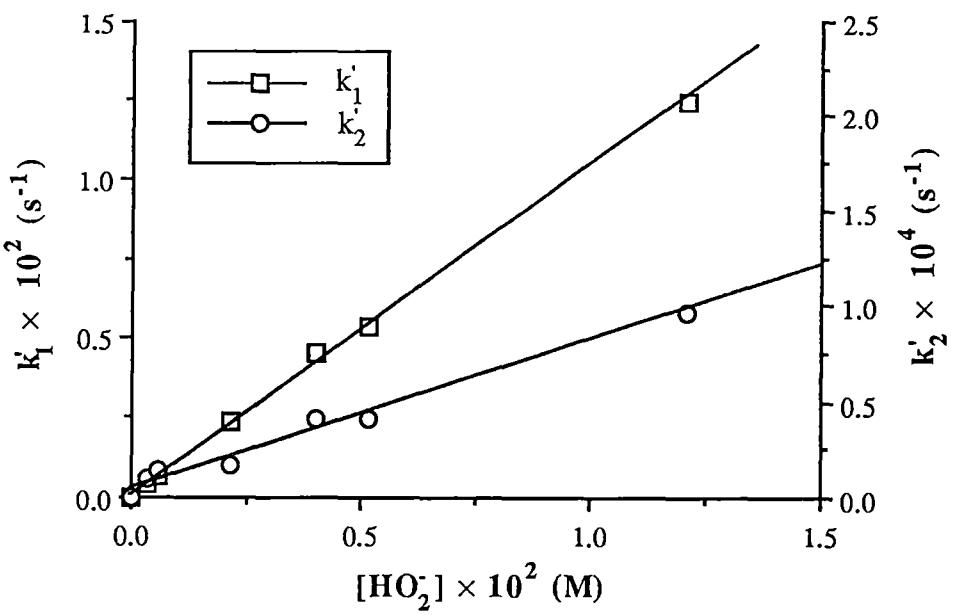

FIGURE 6 : Plots showing linear dependence of pseudo-first order rate constants, k_1' and k_2', on perhydroxyl anion concentration. Regression coefficients: $r^2 = 1.00$ (k_1'), $r^2 = 0.99$ (k_2').

The rate equations for reaction of cinnamaldehyde and cinnamaldehyde epoxide with perhydroxyl anion can be expressed as:

$$- d[\text{Cinnamaldehyde}]/dt = k_1[\text{Cinnamaldehyde}][HO_2^-] \quad (6)$$

$$- d[\text{Epoxide}]/dt = k_2[\text{Epoxide}][HO_2^-] \quad (7)$$

In kinetic runs performed in alkaline solution, linear pseudo-first order plots for cinnamaldehyde and cinnamaldehyde epoxide removal were obtained (Figure 7). Cinnamaldehyde removal was extremely slow under the conditions employed and could only be monitored by following benzaldehyde formation, since the amounts of cinnamaldehyde consumed were less than the detection limits of the analytical GC procedure. Benzaldehyde concentrations were subtracted from the initial concentrations of cinnamaldehyde to yield cinnamaldehyde-time plots for reactions with alkali. Epoxide removal was also slow, however the reaction with alkali proceeded rapidly enough for epoxide consumption to be monitored by GC analysis. Pseudo-first order rate constants for reactions (3) and (4) (k_3' and k_4') were obtained from the slopes of pseudo-first order plots. These values are presented in Table 5. The difficulties in studying the rates of reactions (3) and (4) are reflected in the relatively large errors in the second order rate constants, k_3 and k_4, in Table 5. These rate constants were determined from linear plots of k_3' and k_4' against hydroxide ion (OH^-) concentration (Figure 8). While the linearity of these plots is not excellent, Figure 8 does suggest that reactions (3) and (4) obey second order kinetics. The rate equations for these reactions may be written as:

$$- d[\text{Cinnamaldehyde}]/dt = k_3[\text{Cinnamaldehyde}][OH^-] \quad (8)$$

$$- d[\text{Epoxide}]/dt = k_4[\text{Epoxide}][OH^-] \quad (9)$$

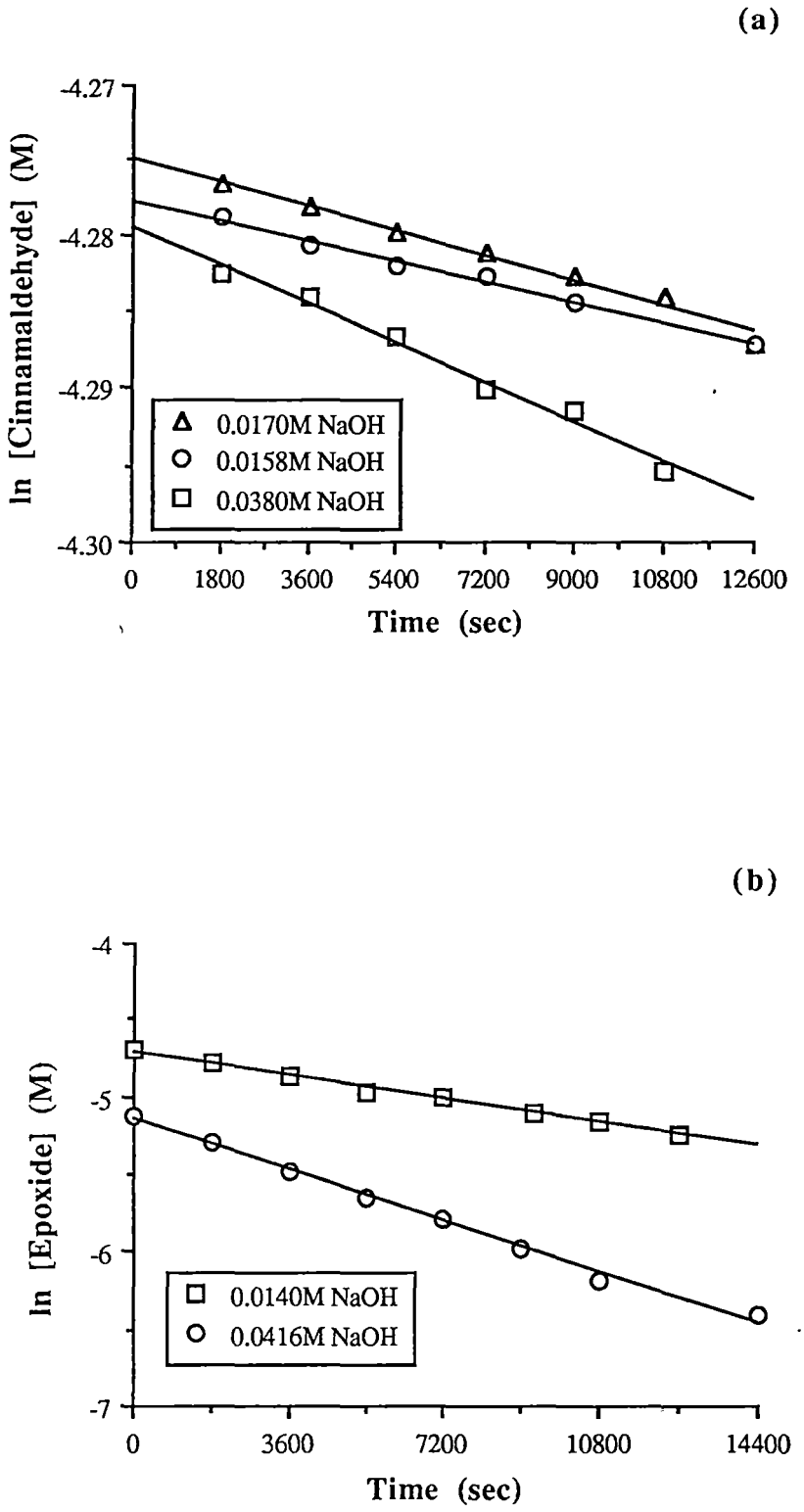

FIGURE 7 : Typical pseudo-first order plots showing disappearance of (a) cinnamaldehyde and (b) cinnamaldehyde epoxide during reaction with alkali at 25°C.

TABLE 5 : Pseudo-first order rate constants, k_3' and k_4', for the reactions of cinnamaldehyde and cinnamaldehyde epoxide respectively with alkali at 25°C.

[NaOH] (M)	k_3' ($\times 10^7\ s^{-1}$)	k_3'/[NaOH] ($\times 10^5\ Lmol^{-1}s^{-1}$)	[NaOH] (M)	k_4' ($\times 10^5\ s^{-1}$)	k_4'/[NaOH] ($\times 10^3\ Lmol^{-1}s^{-1}$)
0.0158	7.43	4.70	0.0137	4.24	3.09
0.0170	9.12	5.36	0.0298	7.27	2.44
0.0380	15.2	4.00	0.0416	9.08	2.18
	Mean k_3 =	4.7 ± 0.7		Mean k_4 =	2.6 ± 0.5

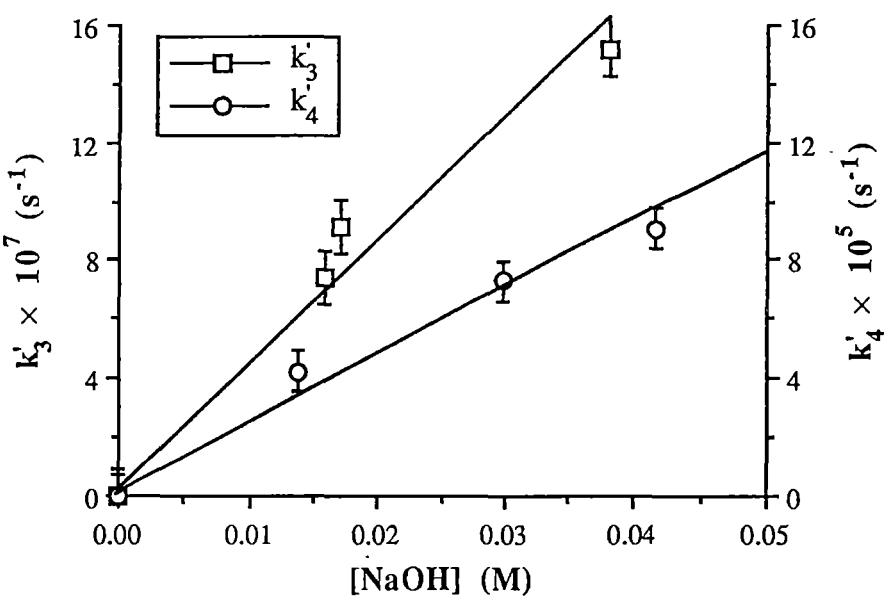

FIGURE 8 : Plots showing linear dependence of pseudo-first order rate constants, k_3' and k_4', on alkali concentration. Regression coefficients: $r^2 = 0.97$ (k_3'), $r^2 = 0.98$ (k_4').

The complete set of 2nd order rate constants for reactions (1)-(4) at 25°C are presented in Table 6. Arrhenius plots of the rate constants, k_1 and k_2, obtained at *p*H 9.5 (Table 4) resulted in activation energies of 62 ± 3 kJ/mol and 46 ± 3 kJ/mol for reactions (1) and (2) respectively and suggested that temperature does not exert a strong influence on the epoxidation and ring cleavage reactions over the temperature range studied.

TABLE 6 : Observed second order rate constants for reactions (1)-(4) with cinnamaldehyde in 1:1 methanol/water solvent at 25°C. Previously reported[37] second order rate constants for equivalent reactions with the analogous ketone, benzalacetone, are provided for comparison.

Second Order Rate Constants ($L\ mol^{-1}s^{-1}$)	Cinnamaldehyde (1:1 $MeOH/H_2O$ solvent)	Benzalacetone (Aqueous solvent)
k_1	1.03 ± 0.01	0.22
k_2	0.0076 ± 0.0004	0.05
k_3	0.000047 ± 0.000007	0.00016
k_4	0.0026 ± 0.0005	0.0032

4.4.5 Calculation of Rate Constant, k_1, for Reactions in Aqueous Solution

The rate constant for the reaction of cinnamaldehyde with perhydroxyl anion in aqueous solution (k_1) was determined by studying the decrease in absorbance due to cinnamaldehyde at 315 nm. Destruction of the chromophoric system in cinnamaldehyde was accompanied by a decrease in absorbance at around 280 nm (Figure 9) and a corresponding absorbance increase at 200 nm as the less conjugated cinnamaldehyde epoxide and benzaldehyde were formed. First order plots for removal of cinnamaldehyde were linear (Figure 10) allowing pseudo-first order rate constants, k_1', to be obtained from the slope of such plots. The dependence of k_1' on perhydroxyl anion concentration is shown in Table 7.

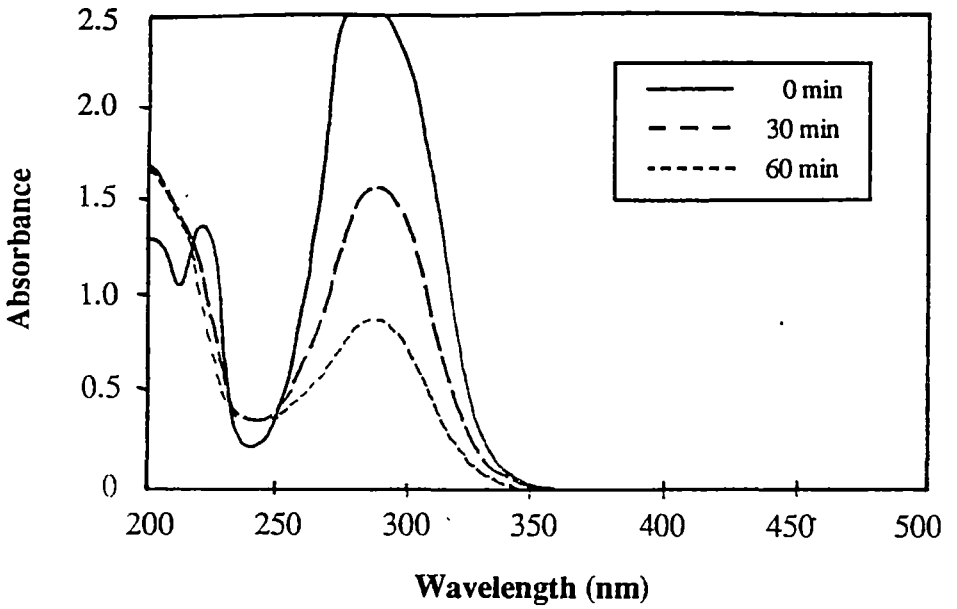

FIGURE 9 : UV-visible absorption spectra showing the disappearance of the cinnamaldehyde band at 280 nm and formation of cinnamaldehyde epoxide and benzaldehyde bands at 200 nm during kinetic runs with cinnamaldehyde and alkaline peroxide in aqueous solution. 0.01 M H_2O_2, *p*H 9.5, T = 25°C.

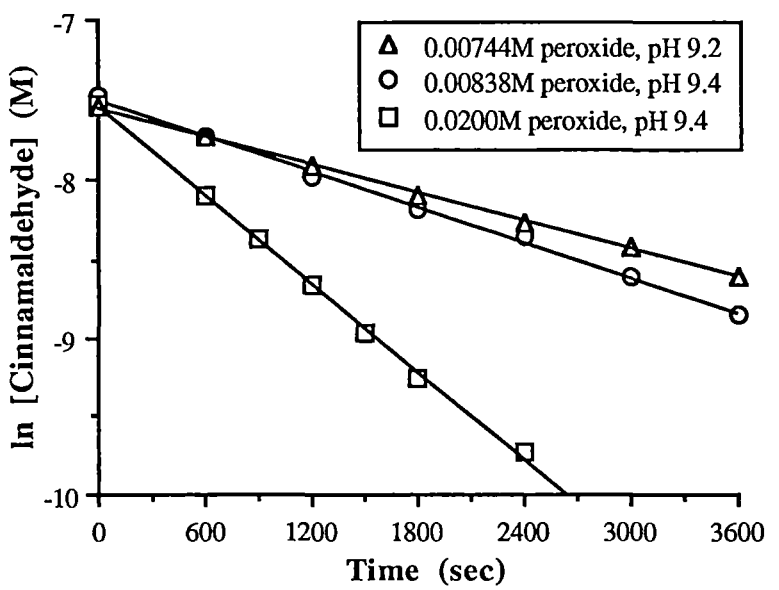

FIGURE 10 : Pseudo-first order plots showing rates of disappearance of cinnamaldehyde in aqueous alkaline peroxide solution at 25°C.

TABLE 7 : Dependence of pseudo-first order rate constant, k_1', on perhydroxyl anion (HO_2^-) concentration for the reaction of cinnamaldehyde with alkaline peroxide in aqueous solution. T = 25°C.

$[H_2O_2]$ (M)	*p*H	$[HO_2^-]$ ($\times 10^5$ M)	k_1' ($\times 10^4$ s^{-1})	$k_1'/[HO_2^-]$ (L $mol^{-1}s^{-1}$)
0.00744	9.3	3.2	2.92	9.1
0.00838	9.4	4.5	3.72	8.2
0.0200	9.4	11	9.30	8.6
			Mean k_1 =	8.6 ± 0.4

The perhydroxyl anion concentration at 25°C in Table 7 was calculated using the equation of Teder and Tormund[38] (10) which describes the temperature dependence of the hydrogen peroxide base dissociation constant (pK_b) in aqueous solution over a 20-80°C temperature range.

$$pK_b = 1330/T - 2.13 + [Na^+]^{0.5} \qquad (10)$$

where T is the absolute temperature in degrees Kelvin.

A linear plot resulted when k_1' was plotted against perhydroxyl anion concentration (Figure 11), indicating a second order reaction with respect to cinnamaldehyde and perhydroxyl anion. From the slope of Figure 11, the second order rate constant for reaction of cinnamaldehyde with perhydroxyl anion was found to be $k_1 = 8.6 \pm 0.4$ L $mol^{-1}s^{-1}$.

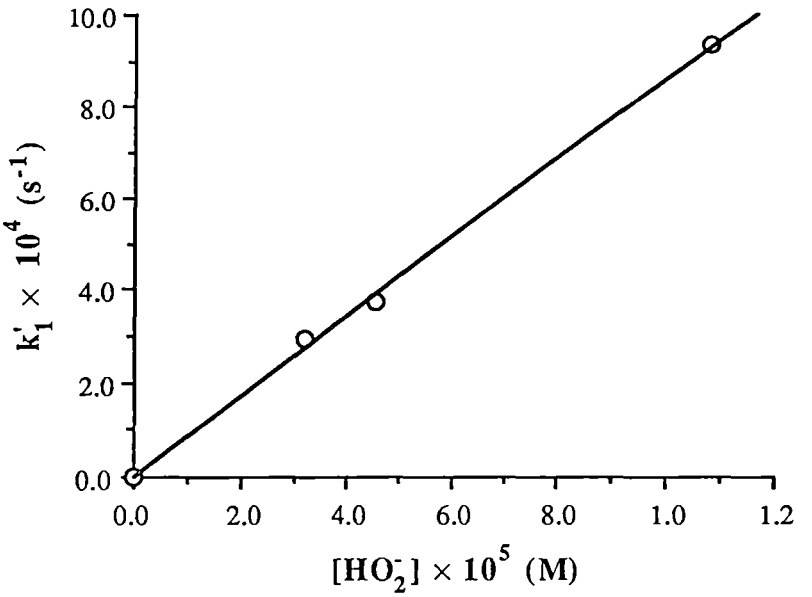

FIGURE 11: Plot showing linear dependence of pseudo-first order rate constant, k_1', on perhydroxyl anion concentration. Regression coefficient: $r^2 = 1.00$.

4.5 Discussion

4.5.1 Reaction Mechanisms

The reaction stoichiometries, kinetic behaviour and relative magnitudes of rate constants in Table 6 are in good agreement with analogous results reported for α,β -unsaturated ketones[37] . The similarity of these sets of results strongly suggests that α,β-unsaturated aldehydes and α,β-unsaturated ketones undergo common mechanisms of reaction. The rate constant representing nucleophilic addition of the perhydroxyl anion to cinnamaldehyde (k_1) is significantly higher than the corresponding value for the analogous ketone, benzalacetone, which is in accordance with the general observation that aldehydes are more reactive than ketones toward nucleophilic addition[39]. An exception to this rule apparently exists in the case of nucleophilic addition of hydroxide ion to cinnamaldehyde. The rate constant for this reaction (k_3) is slightly less than the equivalent value for benzalacetone (Table 6), however this unexpected result is probably

due to differences in the solvents employed and does not represent a genuine exception to the rule regarding aldehyde and ketone reactivity.

Experimental evidence from the work in this chapter is consistent with the widely accepted idea that epoxidation of unsaturated carbon to carbon bonds involves nucleophilic attack by perhydroxyl anions at the β-position of the α,β-unsaturated aldehyde in a Michael type reaction[29,32,33,37,40-42].

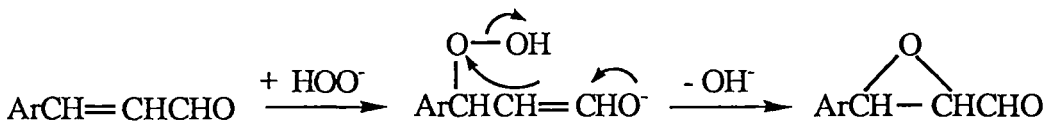

Cinnamaldehyde Epoxide (11)

Kinetic results also support the supposition that the rate-determining step in the cleavage of the epoxide in reaction (12) is initiated by the attack of perhydroxyl anion at the sterically less hindered α-position, as reported for α,β-epoxy ketones[37], esters[32] and 1,2-epoxy-1-methylethylbenzene[43].

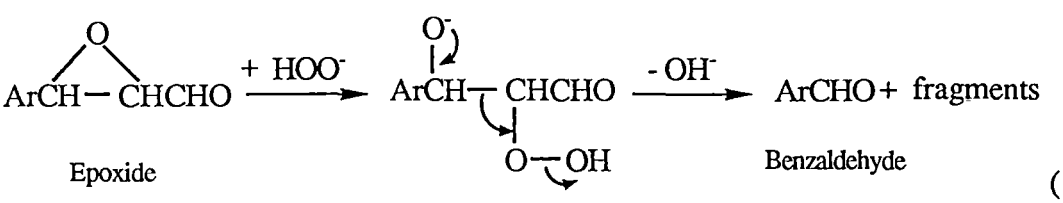

Epoxide Benzaldehyde (12)

The observed second order kinetics and stoichiometric evidence suggest that the alkaline cleavages of cinnamaldehyde and cinnamaldehyde epoxide side chains are initiated by nucleophilic attack of the hydroxide ion at the β- and α- carbons respectively in a similar manner to mechanisms (11) and (12).

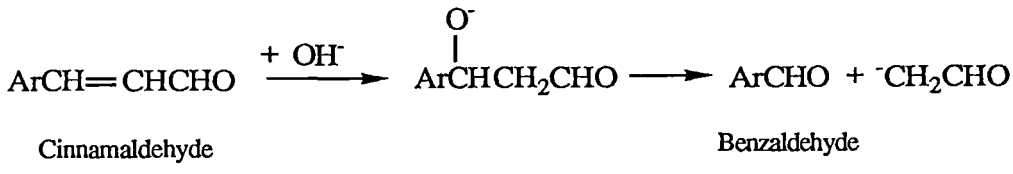

(13)

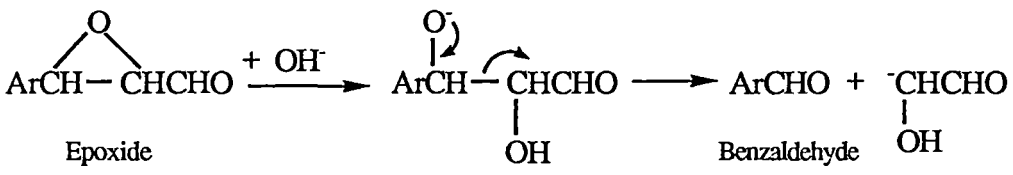

(14)

4.5.2 Solvent Effects

The effects of solvent on the rate of epoxidation (11) can be conveniently considered by comparing the second order rate constants for reaction of cinnamaldehyde with perhydroxyl anion in different solvents. The epoxidation of cinnamaldehyde at 30°C in a methanol solvent has been reported[32] to follow second order kinetics with a rate constant of 0.0774 L $mol^{-1}s^{-1}$. This rate constant is more than an order of magnitude lower than the corresponding value in the current study (k_1 = 1.03 L $mol^{-1}s^{-1}$) using 1:1 methanol/water solvent. In aqueous solution, k_1 was observed to increase further to 8.6 L $mol^{-1}s^{-1}$. These results strongly suggest that the epoxidation reaction (11) is favoured by increasing solvent polarity, probably as a result of increased stabilisation of the proposed anionic intermediate species.

Although increasing solvent polarity accelerates the rate of α,β-unsaturated carbonyl removal in solution, a reversal in this trend has been observed during the bleaching of Japanese red pine mechanical pulp in aqueous and ethanol solvents[27]. The rate of removal of coniferaldehyde structures from pulp was found to increase when bleaching was carried out in ethanol and this was ascribed to the greater capacity of a less polar solvent to impregnate the hydrophobic lignin polymer with bleaching chemicals.

4.5.3 Epoxidation Stereochemistry

The alkaline epoxidation of several unsaturated ketones has been observed to be a highly stereo-selective process[42]. It has been proposed that maximum overlap of electronic orbitals in the transition state molecule by co-planar alignment is more important than steric considerations in accounting for such high stereoselectivity. For α,β-unsaturated ketones, maximum orbital overlap is seriously compromised by repulsions involving the acyl group. For this reason, epoxidation of the ketone analogue of cinnamaldehyde, benzalacetone, has been shown to yield the corresponding *trans* epoxide isomer exclusively[44]. In the case of cinnamaldehyde, the acyl substituent has been replaced by a smaller hydrogen atom which would reduce stereoselectivity by lessening the repulsions which diminish orbital overlap in the transition state anion. By this reasoning, the detection of appreciable amounts of *cis* cinnamaldehyde epoxide in the current work (*ca.* 1:8 *cis*:*trans* ratio) can be adequately rationalised.

In the absence of unfavourable electronic interactions, steric factors in the transition state anion leading to cinnamaldehyde epoxide would also support the detection of a mainly *trans* product (Figure 12). Nucleophilic attack by perhydroxyl anions at the β-position results in sp^3 hybridisation of the α–β carbon-carbon bond thereby allowing rotation of the side chain about the bond axis. In this situation, rotation to favour the *cis* epoxide is severely limited due to steric hindrance from the aromatic ring.

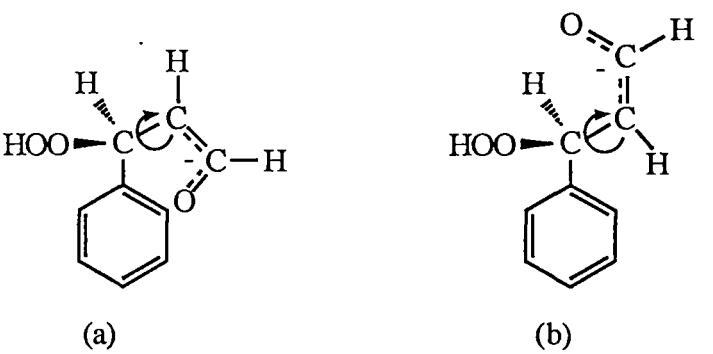

FIGURE 12 : Conformations of transition state molecule leading to formation of *cis* (a) and *trans* (b) cinnamaldehyde epoxide.

4.5.4 Effects of Aromatic Substituents on Rates of Epoxidation

The influence of aromatic substituents on the epoxidation rates of α,β-unsaturated aldehydes is reflected in the relative magnitudes of pseudo-first order rate constants for the epoxidation step (11). In studies on coniferaldehyde (3-methoxy-4-hydroxy-cinnamaldehyde) and coniferaldehyde methyl ether (3,4-dimethoxy-cinnamaldehyde)[31], pseudo-first order rate constants of 8.7×10^{-4} s^{-1} and 4.7×10^{-2} s^{-1} have been reported for the respective epoxidation steps at *p*H 10.5 and 30°C. In the present study, an equivalent value of 1.2×10^{-2} s^{-1} was obtained for the epoxidation of cinnamaldehyde at 25°C and a similar *p*H (*p*H 10.8) (Table 4). These results suggest that the aromatic methoxy and hydroxy substituents found in coniferaldehyde structures significantly reduce the rate of epoxidation. The electron releasing effects of aromatic methoxy and hydroxy substituents are well known and a decrease in rate is most probably due to increased electron density at the β-carbon which would hinder a nucleophilic addition such as (11). The rate of epoxidation is particularly affected by hydroxy substitution as reflected in the low pseudo-first order rate constant of 8.7×10^{-4} s^{-1} for coniferaldehyde. Unlike cinnamaldehyde and coniferaldehyde methyl ether, partial ionisation of the phenolic group in coniferaldehyde would occur under alkaline conditions, producing a formal negative charge at the *para* position. Delocalisation of this electron density in the phenolate anion would substantially decrease the rate of nucleophilic attack at the β-carbon compared to the undissociated coniferaldehyde and probably accounts for the low rate of epoxidation observed.

4.5.5 Reactions of α,β-Unsaturated Aldehydes During Peroxide Bleaching of Pulp

The kinetic studies carried out with cinnamaldehyde indicate that α,β-unsaturated aldehydes react readily with alkaline peroxide to form epoxide structures which yield α-aryl carbonyls such as benzaldehyde on further reaction. The reaction products absorb at lower wavelengths than the α,β-unsaturated carbonyl so that a bleaching effect would be observed if the same reactions were to occur in pulp.

Due to the inherent complexity of lignin, it is difficult to determine whether the reactions observed for cinnamaldehyde accurately represent the behaviour of α,β-unsaturated aldehydes in pulp during peroxide bleaching. Spectroscopic studies on lignin preparations and mechanical pulps indicate that α,β-unsaturated aldehydes are readily removed during peroxide bleaching[1,12,13,17,19,27] in agreement with the results of the current work. The formation of epoxide and α-aryl carbonyl structures during peroxide bleaching of pulp is harder to verify.

The most useful information regarding possible epoxide and α-aryl carbonyl production is found in previously reported ^{13}C-nmr spectra of unbleached and peroxide bleached spruce milled wood lignin[19] (Figure 13). The spectrum of the unbleached lignin (Figure 13a) shows a signal at 196 ppm (signal 1) attributed to the aldehydic carbon in α,β-unsaturated aldehydes. A second signal (signal 2) slightly upfield from 1 is attributed to the carbonyl carbon in α-aryl carbonyls such as benzaldehyde. Inspection of Figure 13b indicates that α,β-unsaturated aldehydes are comprehensively degraded by alkaline peroxide in agreement with the model studies. Aldehydic carbons in cinnamaldehyde epoxide structures would produce a signal at 196 ppm, so disappearance of this signal implies that any intermediate cinnamaldehyde epoxide structures in lignin are also effectively removed. Epoxide structures would be expected to produce a small signal around 60 ppm due to the carbons in the epoxide ring, however any changes in this region are masked by larger peaks. The appearance of 2 new peaks in the range 170-180 ppm was ascribed to the formation of carboxyl groups.

The kinetic studies on cinnamaldehyde suggest a small increase in signal 2 would be expected on bleaching due to the formation of benzaldehyde, however Figure 13 does not support such a prediction. Benzaldehyde was observed as a stable product in reactions carried out under nitrogen, however, in the presence of dissolved oxygen, benzaldehyde underwent further oxidation to form benzoic acid. Since no attempt was made to exclude oxygen during the bleaching of the milled wood lignin in Figure 11, it is possible that any α-aryl carbonyl groups produced by oxidation of α,β-unsaturated aldehydes might have

been converted to carboxylic acids. Formation of these carboxyl groups would partly account for the appearance of the 2 signals in the 170-180 ppm range in Figure 13b.

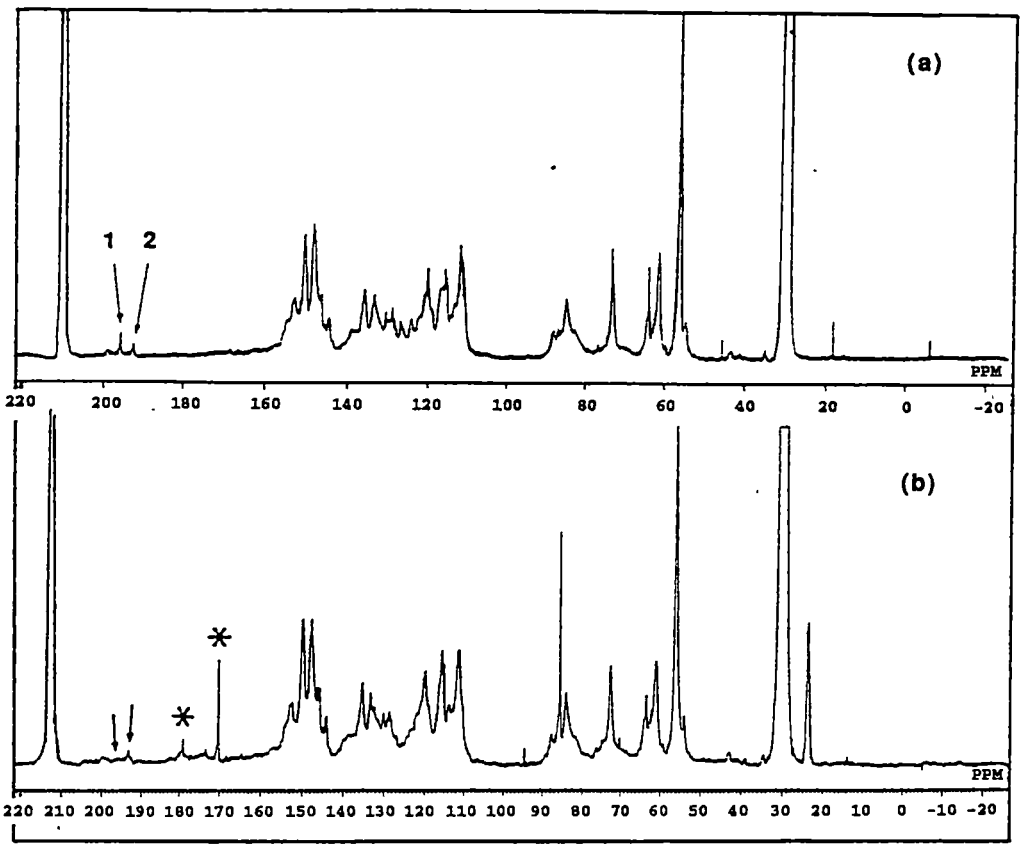

FIGURE 13 : ^{13}C-nmr spectra of (a) unbleached and (b) alkaline peroxide bleached spruce milled wood lignin after Holmbolm *et al*[19].

In comparing the peroxide bleaching behaviour of cinnamaldehyde and spruce milled wood lignin, the limitations of cinnamaldehyde as a model lignin compound must also be considered. In spruce lignin, α,β-unsaturated aldehydes are better represented by coniferaldehyde and coniferaldehyde methyl ether structures which possess hydroxy and methoxy aromatic substituents not present in cinnamaldehyde. Although the coniferaldehyde groups would be expected to react in the same way as cinnamaldehyde to form α-aryl carbonyls, additional reactions are possible due to *para* hydroxy substitution in coniferaldehyde[31]. Inspection of Scheme 1 shows that reaction of coniferaldehyde

with alkaline peroxide would produce a phenolic α-aryl carbonyl, vanillin, which is capable of further reaction via a Dakin mechanism to form a *para* quinone[31,45]. The *para* quinone is a highly reactive species which undergoes rapid oxidation to produce colourless dicarboxylic acids[46]. Carboxylic acid production by this route provides a further explanation for the appearance of carboxyl signals in Figure 13b.

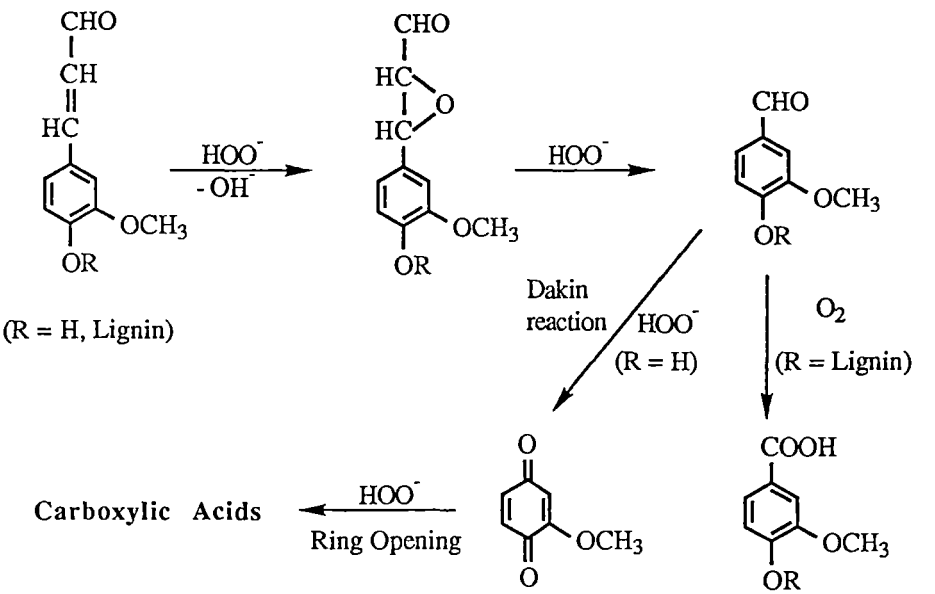

SCHEME 1 : Proposed reactions of coniferaldehyde structures in spruce milled wood lignin during alkaline peroxide bleaching.

4.5.6 Effects of α,β-Unsaturated Aldehyde Removal on Kinetic Behaviour of Mechanical Pulps

By reference to Scheme 1, removal of α,β-unsaturated carbonyls from mechanical pulp lignin produces less conjugated aromatic and aliphatic carboxylic acids. Based on the UV-visible absorption spectra of similar compounds, these species would be incapable of light absorption much above 350 nm. Destruction of α,β-unsaturated carbonyls during peroxide bleaching would therefore be expected to produce a loss in colour as measured by light absorption at 457 nm.

Although the relative rates of α,β-unsaturated aldehyde removal are decreased by electron releasing aromatic substituents (refer section 4.5.4), the literature indicates that α,β-unsaturated aldehydes are essentially completely removed during the initial stages of bleaching[1,19,27,28]. Based on previously reported reaction rates for coniferaldehyde structures in alkaline peroxide solution[31], theoretical concentration - time curves have been generated which model the overall removal of coniferaldehyde and etherified coniferaldehyde structures from lignin during peroxide bleaching (Figure 14). The curves in Figure 14 were produced assuming a 3:1 etherified coniferaldehyde: coniferaldehyde ratio as reported by Adler and Marton[14] for spruce milled wood lignin. More recently, Pan and Lachenal have reported the same 3:1 ratio for *in-situ* spruce lignin[47]. By comparison of Figure 14 with the bleaching profiles of *E. regnans* stone groundwood (Figure 15), it seems probable that extensive elimination of ether linked α,β-unsaturated aldehydes can be at least partially associated with the rapid initial bleaching phase observed for *E. regnans* stone groundwood in Figure 15. The removal of phenolic α,β-unsaturated aldehydes occurs more slowly and may be partly responsible for the levelling in bleaching response observed in Figure 15.

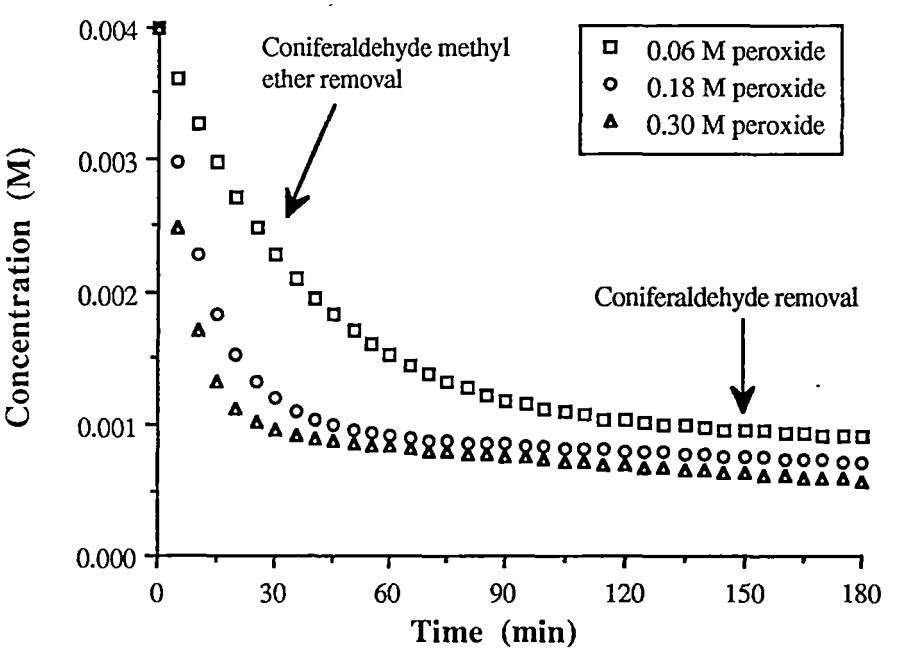

FIGURE 14 : Kinetic simulations of combined coniferaldehyde and coniferaldehyde removal during alkaline peroxide bleaching at *p*H 9.5. Simulations based on rate equations of Gellerstedt and Agnemo[31] at 30°C and a 3:1 coniferaldehyde : coniferaldehyde methyl ether ratio[14].

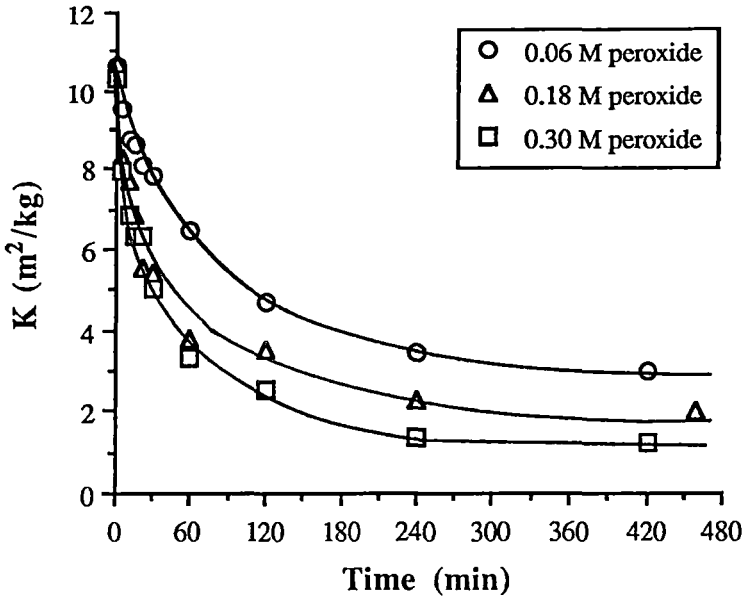

FIGURE 15 : Light absorption coefficient (K) - time profiles for the peroxide bleaching of *E. regnans* SGW at 50°C, *p*H 10. Pulp bleached under conditions of constant reagent concentration.

Further evidence for the relative resistance of phenolic α,β-unsaturated aldehydes to alkaline peroxide can be found in the work of Hirashima *et al*[27] and Pan and Lachenal[47]. Hirashima reported that about 80% of all α,β-unsaturated aldehydes could be easily removed in the bleaching of Japanese red pine. Similarly, Pan and Lachenal found that about 70% of the α,β-unsaturated aldehydes in spruce lignin were quantitatively converted to the corresponding α-carbonyls upon bleaching, as indicated in Scheme 1. It is likely that the remaining 20-30% of unreacted α,β-unsaturated carbonyls can be associated with phenolic structures given the 3:1 etherified coniferaldehyde : coniferaldehyde ratio often reported for spruce lignin. Further discussion of the effects of α,β-unsaturated aldehydes on the kinetic bleaching behaviour of mechanical pulps is presented in Chapter 6.

4.6 Conclusions

The oxidation of cinnamaldehyde (3-phenyl-2-propenal) by alkaline peroxide results in epoxidation of the double bond to form cinnamaldehyde epoxide (3-phenyl-2,3-epoxy-propanal) followed by ring opening and side chain cleavage to yield benzaldehyde and acidic fragments. The reactions are first order in the organic substrates and perhydroxyl anion and second order overall. In the absence of peroxide, two further reactions take place where cinnamaldehyde and cinnamaldehyde epoxide side chains are cleaved in reactions with hydroxide ion to form benzaldehyde and side chain fragments. These reactions are first order in the organic substrates and hydroxide ion and second order overall. The observed kinetic behaviour and the stereoselectivity of the epoxidation reaction are best explained by reaction mechanisms involving bimolecular nucleophilic attack. Increasing solvent polarity accelerates the rates of epoxidation in solution, although a reversal in this trend is observed in the bleaching of pulp due to the hydrophobic nature of lignin[27]. The removal of α,β-unsaturated aldehydes during peroxide bleaching results in formation of less conjugated products leading to an overall decrease in light absorption at 457 nm. The elimination rates of phenolic and non-phenolic α,β-unsaturated aldehydes follow the order: non-phenolic α,β-unsaturated aldehydes >> phenolic α,β-unsaturated aldehydes. Comparison of the bleaching kinetics of α,β-unsaturated aldehydes and *E. regnans* mechanical pulp indicates that removal of non-phenolic α,β-unsaturated aldehydes can partly account for the rapid loss in colour during the initial stages of alkaline peroxide treatment of mechanical pulp. The levelling off in bleaching response at longer times can be attributed to slower reacting phenolic α,β-unsaturated aldehydes.

REFERENCES

1. Holah, D.G. and Heitner, C. and references contained therein, The Colour and UV-Visible Absorption Spectra of Mechanical and Ultra-High Yield Pulps Treated With Alkaline Hydrogen Peroxide., *J. Pulp Paper Sci.*, **18(5)**, J161-64, (1992).

2. Sarkanen, K.V. and Ludwig, C.H. (Eds.), Lignins: Occurrence, Formation, Structure and Reactions., 1st Edition, Wiley-Interscience, New York, 1971.

3. Fengel, D. and Wegener, G., Wood: Chemistry, Ultrastructure, Reactions., 1st Edition, De Gruyter, Berlin, 1984.

4. Casey, J.P.(Ed.) , Chemistry and Chemical Technology, Volume 1: Pulp and Paper., 3rd Edition, Wiley-Interscience, New York, 1980.

5. Sjostrom, E., Wood Chemistry., 1st Edition, Academic Press, New York, 1984.

6. Adler, E., and Ellmer, L., Coniferyl Aldehyde Groups in Wood and In Isolated Lignin Preparations., *Acta Chem. Scand.*, **2**, 839-40, (1948).

7. Lundquist, K., On the Separation of Lignin Degradation Products., *Acta Chem. Scand.*, **18(5)**, 1316-17, (1964).

8. Fukuzumi, T., and Terasawa, M., Acetolysis Products of Lignin. I. Paper Chromatographic Separation of Acetolysis Products., *Mokuzai Gakkaishi*, **8**, 77-80, (1962).

9. Wallis, A.F.A., in Lignins: Occurrence, Formation, Structure and Reactions., K.V. Sarkanen and C.H. Ludwig (Eds.), Chapter 9, 'Solvolysis by Acids and Bases', 1st Edition, Wiley-Interscience, New York, 1971.

10. Goldschmid, O., in Lignins: Occurrence, Formation, Structure and Reactions., K.V. Sarkanen and C.H. Ludwig (Eds.), Chapter 6, 'Ultraviolet Spectra', 1st Edition, Wiley-Interscience, New York, 1971.

11. Polcin, J. and Rapson, W.H., Effects of Bleaching Agents on the Absorption Spectra of Lignin in Groundwood Pulps. Part 1: Reductive Bleaching., *Pulp and Paper Mag. Can.*, **72(3)**, 69-80, (1971).

12. Polcin, J. and Rapson, W.H., Effects of Bleaching Agents on the Absorption Spectra of Lignin in Groundwood Pulps. Part 2: Oxidative-Reductive Bleaching., *Pulp and Paper Mag. Can.*, **72(3)**, 80-91, (1971).

13. Michell, A.J., Nelson, P.J. and Chin, C.W.J., Diffuse Reflectance Spectroscopic Studies of the Bleaching and Yellowing of *Eucalyptus regnans* Cold Soda Pulp., *Appita*, **42(6)**, 443-48, (1989).

14. Marton, J. and Adler, E., Carbonyl Groups in Lignin III. Mild Catalytic Hydrogenation of Bjorkman Lignin., *Acta Chem. Scand.*, **15(2)**, 370-83, (1961).

15. Pew, J.C. and Connors, W.J., Colour of Coniferous Lignin., *Tappi*, **54(2)**, 245-51, (1971).

16. Hergert, H.L., in Lignins: Occurrence, Formation, Structure and Reactions., K.V. Sarkanen and C.H. Ludwig (Eds.), Chapter 7, 'Infra-red Spectra', 1st Edition, Wiley-Interscience, New York, 1971.

17. St. Germain, F. and Gray, D., Photoacoustic Fourier Transform Infra-red Spectroscopic Study of Mechanical Pulp Brightening., *J. Wood Chem. Technol.*, **7(1)**, 33-50, (1987).

18. Genuit, W. and Boon, J., Characterisation of Beech Milled Wood Lignin by Pyrolysis-Gas-Chromatography-Photoionisation Mass Spectrometry., *Anal. Chem.*, **59**, 508-13, (1987).

19. Holmbolm, B., Ekman, R., Sjoholm, R. and Thornton, J., Chemical Changes in Peroxide Bleaching of Mechanical Pulps., *Das Papier*, **45(10A)**, 16-22, (1992).

20. Robert, D.R., Bardet, M. and Gagnaire, D., Recent Progress in Liquid and Solid State NMR of Lignins from Exploded Wood., *4th International Symposium on Wood and Pulping Chemistry.*, p. 189-91, (1987).

21. Higuchi, T. and Brown, S.A., Lignin Biosynthesis Using Isotopic Carbon. XII. The Biosynthesis and Metabolism of Sinapic Acid., *Can. J. Biochem. and Physiol.*, **41**, 613-20, (1963).

22. Freudenberg, K. and Schluter, H., Intermediates in the Formation of Lignin., *Chem. Ber.*, **88**, 617-25, (1955).

23. Higuchi, T., Kawamura, I. and Kawamura, H., Properties of the Lignin in Decayed Wood., *J. Japan Forestry Soc.*, **37**, 298-302, (1955).

24. Lai, Y.Z., and Sarkanen, K.V., in Lignins: Occurrence, Formation, Structure and Reactions., K.V. Sarkanen and C.H. Ludwig (Eds.), Chapter 5, 'Isolation and Structural Studies', 1st Edition, Wiley-Interscience, New York, 1971.

25. DeBaun, R.M., and Nord, F.F., A Quantitative Phloroglucinol-Hydrochloric Acid Test in the Evaluation of Lignin Preparations., *Tappi*, **34**, 71-3, (1951).

26. Klemola, A., Investigations of Birchwood Lignin Degraded by Steam Hydrolysis., *Suom. Kemistilehti, A*, **41(7-8)**, 166-80, (1968).

27. Hirashima, H. and Sumimoto, M., Fundamental Properties of Mechanical Pulp Lignins II. Behaviour of Coniferyl Aldehyde Type Structures in Pulp Lignin., *Mokuzai Gakkaishi*, **33(1)**, 31-41, (1987).

28. Gupta, V.N., Carbonyl Chromophores in Eastern Canadian Groundwood., *Pulp and Paper Mag. Can.*, **73(6)**, 57-61, (1972).

29. Payne, G.B., Alkaline Epoxidation of α,β-Unsaturated Aldehydes., *J. Am. Chem. Soc.*, **26**, 250-52, (1961).

30. Reeves, R.H., and Pearl, I.A., Reaction Products Formed Upon the Alkaline Peroxide Oxidation of Lignin-Related Model Compounds., *Tappi*, **48(2)**, 121-125, (1965).

31. Gellerstedt, G. and Agnemo, R., The Reactions of Lignin With Alkaline Hydrogen Peroxide. Part III. The Oxidation of Conjugated Carbonyl Structures., *Acta Chem. Scand.*, **B34(4)**, 275-80, (1980).

32. Sri Rama Rao, D., Epoxidation of α,β-Unsaturated Aldehydes and Esters., *J. Indian Chem. Soc.*, **60**, 300-302, (1983).

33. Tishchenko, I.G., Burd, V.N. and Revinskii, I.F., Formation of a Peroxy Compound in the Epoxidation of Cinnamaldehyde., *Zh. Org. Khim.*, **22(3)**, 669, (1986).

34. Sugiyama, S., Kubo, S. and Hayashi, H., The Intermediate in the Formation of Phenylacetaldehyde from Cinnamic Aldehyde., *Chem. Express*, **4(7)**, 433-34, (1989).

35. Andrews, D.H. and Singh, R.P., In The Bleaching of Pulp, Chapter 8, ' Peroxide Bleaching', R.P. Singh (Ed.), Tappi Press, Atlanta, 1979.

36. Payne, G.B., Epoxidation of Cinnamaldehyde by Alkaline *tert*-Butyl Hydroperoxide., *J. Org. Chem.*, **25(1)**, 275-76, (1960).

37. Temple, R.D., The Epoxidation and Cleavage of α,β-Unsaturated Ketones with Alkaline Hydrogen Peroxide., *J. Org. Chem.*, **35(5)**, 1275-80, (1970).

38. Teder, A. and Tormund, D., The Equilibrium Between Hydrogen Peroxide and the Peroxide Ion - A Matter of Importance in Peroxide Bleaching., *Svensk Papperstidning*, **83(4)**, 106-09, (1980).

39. Morrison, R.T. and Boyd, R.N., in Organic Chemistry, Chapter 18, 'Aldehydes and Ketones', p. 733, Allyn and Bacon, Boston, 1983.

40. March, J., in Advanced Organic Chemistry, Chapter 5, 'Additon to Carbon-Carbon Multiple Bonds', p. 735, Wiley-Interscience, New York, 1985.

41. Bunton, C.A. and Minkoff, G.J., The Oxidation of α,β-Unsaturated Ketones with Alkaline Hydrogen Peroxide., *J. Chem. Soc.*, 665-68, (1949).

42. Zimmerman, H.E., Singer, L. and Thyagarajan, B.S., Overlap Control of Carbanionoid Reactions. I. Stereoselectivity in Alkaline Epoxidation., *J. Amer. Chem. Soc.*, **81**, 108-16, (1959).

43. Hoffman, J., A Cleavage Reaction Involving α-Methyl Styrene Oxide., *J. Amer. Chem. Soc.*, **79**, 503-04, (1957).

44. Kwart, H. and Kirk, L.G., Steric Considerations in Base Catalysed Condensation: The Darzens Reaction., *J. Org. Chem.*, **22(1)**, 116-20, (1957).

45. Hocking, M.B. and Ong, J.H., Kinetic Studies of Dakin Oxidation of *o*- and *p*- Hydroxyacetophenones., *Can. J. Chem.*, **55**, 102-10, (1977).

46. Gellerstedt, G., Hardell, H-L. and Lindfors, E-L., The Reactions of Lignin with Alkaline Hydrogen Peroxide. Part IV. Products from the Oxidation of Quinone Model Compounds., *Acta Chem. Scand.*, **B34(9)**, 669-73, (1980).

47. Pan, X. and Lachenal, D., Structure and Reactivity of Spruce Mechanical Pulp Lignins. Part I. Bleaching and Photo-Yellowing of *In-Situ* Lignins., *J. Wood Chem. Technol.*, **12(2)**, 135-47, (1992).

CHAPTER 5

KINETIC STUDIES OF REACTIONS BETWEEN MODEL LIGNIN *ORTHO* QUINONES AND ALKALINE PEROXIDE

5.1 Literature Review

Together with α,β-unsaturated aldehydes, quinoid structures are believed to constitute the major chromophoric systems in mechanical pulp lignins. The removal of quinoid structures is therefore essential if mechanical pulps are to be bleached to high brightness with alkaline hydrogen peroxide. As a result, many bleaching studies have been undertaken using an array of mechanical pulps, lignin preparations and lignin model compounds. Their aim has been to gain a greater understanding of the way quinone structures respond to bleaching treatments such as alkaline peroxide. Also of interest are the mechanisms of quinone formation, their number and type in lignin, and their overall contribution to the light absorption properties of mechanical pulp.

5.1.1 Evidence for Quinoid Structures in Lignin

Studies of lignin preparations and mechanical pulps indicate that the number and variety of quinones present in lignin may differ significantly between species, and that pulping procedures may further influence the number and type of quinones present in mechanical pulp lignins. The relatively high reactivity of quinones and their apparent scarcity in lignin has made verification of their existence in mechanical pulps difficult. As a consequence, several authors remain unconvinced of the presence of quinoid structures in some mechanical pulps and native lignins.

The detection of quinoid structures in lignin is largely dependent on the method of analysis. Destructive analytical methods such as pyrolysis mass spectroscopy (Py-MS)[1] and chemical degradation[2,3,4] have not been successful in detecting *o*- or *p*-quinones. Indeed, quinone monomers have not been included in proposed softwood lignin[3,4] or hardwood lignin[2,5] model structures based on chemical degradation studies. However, the liberation of small amounts of methanol on acidolysis of spruce lignin has been proposed to arise from demethoxylation of *p*- and *o*-quinones[6,7] present in the lignin.

More conclusive evidence for quinone structures in lignin has been achieved using a variety of non-destructive methods such as UV-visible and IR spectroscopy, and NMR techniques. These methods are often supplemented by the treatment of quinoid groups with selective derivatising agents to increase the specificity of analysis. Imsgard and co-workers[8] employed a colorimetric technique involving reduction of *o*-quinones to catechols followed by complexation with ferric ions to analyse the *o*-quinoid content of spruce milled-wood lignin. Colorimetric analysis of the red catechol complex led to an estimate of 0.7 *o*-quinones and 1 catechol structure per 100 phenylpropane units in lignin. It was proposed that this amount of quinone could account for between 35-60% of the light absorbed by spruce milled wood lignin at 457 nm. The existence of quinoid structures in spruce milled groundwood lignin has also been reported by Spittler and Dence[10] using UV-visible spectroscopy in conjunction with quinone reducing agents such as sodium borohydride ($NaBH_4$) and sodium dithionite ($Na_2S_2O_4$). In another UV-visible spectroscopic study of groundwood pulps, Polcin and Rapson[11,12] reacted spruce and western hemlock pulp with hydrogen peroxide, sodium borohydride, sodium dithionite and uranium (III). They concluded that spruce lignin contained simple quinoid structures while the darker western hemlock possessed more condensed quinoid structures. Polcin and Rapson partly attributed the residual yellow hue of peroxide bleached groundwood pulp to unreacted quinoid structures. The most recent evidence for the existence of quinones in mechanical pulp was reported by Lebo *et al*[13]. In this work, 5-6 *o*-quinone

structures were detected per 100 phenylpropane units in spruce TMP. Selectivity for quinones was achieved by tagging *o*-quinones with trimethyl phosphite and using ^{31}P-nmr as the method of detection.

Despite widespread evidence of quinones in native lignins and mechanical pulps, not all experimental evidence supports this idea. Fourier transform infra-red photoacoustic spectroscopic (FTIR-PAS) studies of black spruce mechanical pulp brightening have been unable to confirm the existence of quinones[14], however their presence was not completely excluded since IR spectroscopy of pulp does not facilitate specific analysis of quinones. Similarly, Holmbolm *et al*[15] were unable to detect any *o*- or *p*- quinone structures in native and peroxide bleached spruce milled-wood lignin using ^{13}C-nmr, even though their technique was capable of detecting as few as 0.2-1 quinoid groups per 100 phenylpropane units. As a result, Holmbolm and co-workers expressed scepticism about the presence of quinoid structures in spruce milled wood lignin.

5.1.2 Quinone Formation During Lignification

In contrast with α,β-unsaturated carbonyl chromophores, which are thought to be produced exclusively during lignification, *ortho* and *para* quinones can be introduced to the lignin of native wood and mechanical pulps during lignification, pulping, bleaching and storage.

Work undertaken using wood lignin preparations and lignin model compounds has led to the suggestion that small amounts of *o*- and *p*- benzoquinones may become incorporated in the lignin matrix during lignification, however the mechanistic pathways leading to quinone formation are unclear. Demethylation of phenoxy radicals has been proposed as a mechanism for the formation of *o*-quinones in spruce lignin[8]. Pew and Connors[16] have also reported that coloured *p*-benzoquinoid structures are readily generated from model lignin monomers by enzymatic

dehydrogenation, followed by hydrolysis under the slightly acidic conditions which prevail during wood lignification.

5.1.3 Quinone Formation During Mechanical Pulping

A significant proportion of the quinones in mechanical pulps are believed to be formed during the wood defibration process. The possibility of quinone formation during manufacture of mechanical pulps was demonstrated by Gellerstedt and Pettersson[17], who reported the creation of new chromophoric structures upon defibration of native spruce wood. Chromophore creation was ascribed to the autoxidation of hydroquinone and catechol structures in native lignin to form *para* and *ortho* quinones respectively. These quinoid structures were observed to undergo further autoxidation to form stable hydroxyquinones. Autoxidation was accelerated by the presence of transition metals such as Mn^{2+}, Cu^{2+} and Fe^{3+} which promoted generation of phenoxy-radical intermediates, however the influence of these metals was completely negated by the addition of chelating agents. Reactions between *para* quinones and phenols liberated from bark constituents during defibration of wood were also proposed to take place in the presence of oxygen to yield condensed *ortho* quinone structures.

5.1.4 Quinone Formation During Oxidation of Model Lignin Compounds

Many authors have reported the formation of quinoid structures during the bleaching of mechanical pulps and lignin model compounds with reagents such as oxygen[9,17-22], hydrogen peroxide[22-32], ozone, hypochlorite, chlorine dioxide[33], peracetic acid, nitrobenzene and potassium nitrosodisulphonate[32].

Through studies on lignin model compounds, alkaline oxygen and hydrogen peroxide solutions have been found to react with phenolic structures to produce similar *para* and *ortho* quinones. Formation of *p*-quinones is known to occur via Dakin and Dakin-like reactions which take place when appropriately substituted phenols react with perhydroxyl anions in alkaline peroxide solution[22-28]. Reactions between β-linked model lignin dimers and stabilised alkaline peroxide have confirmed that Dakin and Dakin-like processes also produce *p*-quinones when the requisite substituents are present in dimeric phenols[29-30]. In the presence of unstabilised peroxide, formation of *p*-quinones from model lignin dimers was still evident, however the overall product distribution suggested that additional, but less important mechanisms for quinone formation were also operating. It was proposed that these mechanisms involve peroxide decomposition products such as oxygen and oxygen radical species[29-30].

Dakin and Dakin-like reactions probably represent the main route in *p*-quinone formation in lignin, however generation of *p*-quinones through non-Dakin reactions has also been reported[22]. It is unlikely that such mechanisms operate to any great degree in lignin since the mechanism requires substituent migration which would be severely hindered in a polymeric system such as lignin.

Although *p*-quinones can be readily generated in lignin, the extent to which they remain in pulp after peroxide bleaching is uncertain. Kempf and Dence[26] have suggested that most of the *p*-quinones produced by Dakin and Dakin-like reactions would be split off from the lignin network to undergo further transformations in the bleaching liquor. A permanent effect on pulp brightness due to *p*-quinones would therefore not be anticipated unless the detached fragments were re-adsorbed onto the pulp fibres.

Unlike *p*-quinones, *o*-quinones remain connected to the lignin matrix during bleaching and probably constitute the main quinoid species in lignin after oxidative chemical treatment. Creation of intermediate *o*-quinone structures has been widely reported[18-

[21,25,26] during reaction of lignin model compounds with alkaline peroxide and alkaline oxygen solutions. The mechanism of *o*-quinone formation has been shown to take place through oxidation of catechols and/or demethylation of methoxyphenol structures which make up ~30% of phenylpropane units in lignin[3]. ESR studies have shown that free-radical mechanisms involving phenoxy radical intermediates are involved in the oxidation of catechols to the corresponding *o*-quinone intermediates in alkaline oxygen solution[18]. Demethylation of methoxyphenols to form *o*-quinones has also been reported to take place in both alkaline oxygen and alkaline peroxide solution[21,22,25,26] and is a probable route by which quinoid structures are formed during peroxide bleaching and alkali darkening reactions. Indeed, Bailey and Dence[25] have reported that the initial reaction of a model phenol, creosol, with alkaline peroxide consists almost exclusively of demethylation to form 4-methylorthoquinone. Dence and co-workers have also shown that quinone structures are more readily produced from syringyl (hardwood) model phenols than from guaiacyl (softwood) model phenols as measured by the degree of demethylation to form corresponding *o*-quinones[25,26].

5.1.5 Quinone Formation During Oxidation of Mechanical Pulps

The generation of *o*-quinones during alkaline oxygen and alkaline peroxide treatment of mechanical pulps has been reported by several authors. After treating high yield sulphite (HYS) and stoneground wood (SGW) pulp with alkaline oxygen, Guist *et al*[9] observed an increase in UV-visible absorption bands at 430 nm and 525 nm. These bands were subsequently attributed to *o*-quinones. The formation of intermediate quinone structures during the peroxide bleaching of milled-wood lignin and various mechanical pulps has also been proposed by Bailey and Dence[25] and Polcin and Rapson[12]. Bailey and Dence detected significant amounts of methanol when spruce milled-wood lignin and mechanical pulps were treated with unstabilised alkaline peroxide. This was ascribed to the formation of *o*-quinones by demethylation of methoxyphenolic units in the lignin. The formation of quinones during peroxide

bleaching of pulp was later confirmed by Polcin and Rapson[12] in spectroscopic studies on bleached spruce and western hemlock mechanical pulps.

A final possibility for quinone formation in mechanical pulps arises through exposure to light (light induced yellowing) and, to a much lesser degree, heat (thermal reversion). It has long been suspected that quinoid structures are formed on exposure of mechanical pulps to visible and UV light[34,35], but strong evidence for the formation of *o*-quinones in yellowed pulp has only recently emerged[13]. By tagging light yellowed pulps with trimethyl phosphite, ^{31}P-nmr was used to demonstrate that 5-6 *o*-quinones per 100 phenylpropane units are generated by irradiation of spruce TMP. This number of *o*-quinones reportedly accounted for the majority of colour produced in light-yellowed spruce mechanical pulp.

5.1.6 Reactions of Quinoid Structures with Alkaline Peroxide

The importance of quinoid chromophores in lignin has led to extensive study of their reactions with conventional lignin retaining bleaching agents, particularly alkaline hydrogen peroxide and sodium dithionite. The reactions of *o*-quinones with alkaline peroxide are discussed in more detail within the chapter, however a brief overview is given below.

Available evidence indicates that *ortho* and *para* quinones are capable of reaction with ionic and radical species present in alkaline peroxide to yield a wide assortment of reaction products. Several workers have reported that *o*-quinone structures are readily degraded to aliphatic carboxylic acids by nucleophilic attack of perhydroxyl anions at the carbonyl groups of the quinone[22,25,26]. Alternatively, nucleophilic attack by perhydroxyl anions can occur at other electron deficient sites in *o*-quinones, leading to epoxidation of ethylene bonds. Further rearrangements ultimately yield lactones and various short chain fragments[21-23]. Like *o*-quinones, *p*-quinones also react readily with perhydroxyl anions to form carboxylic acid fragments. These fragments arise via

the nucleophilic attack of perhydroxyl anions to form epoxide intermediates (in an analogous manner to *o*-quinones) or by direct cleavage of the quinoid ring[25,36]. Several studies have shown that *o*- and *p*-quinones may react with oxygen and superoxide radicals to generate intensely coloured hydroxyquinones which resist further reaction[17,19,20,23]. It has been suggested that these hydroxyquinones are partly responsible for the incomplete discharge of colour in peroxide bleached mechanical pulps, leading to a limit in brightness gains[37].

5.2 Introduction

In this chapter a simple model *ortho* quinone, 4-*tert*-butylorthoquinone, has been oxidised with alkaline hydrogen peroxide and the major reaction products investigated. Parallel kinetic experiments to those carried out in Chapters 2-4 have been carried out to investigate the relative reactivity of *o*-quinones in comparison with α,β-unsaturated aldehydes, and to establish the role *o*-quinone structures play in the bleaching behaviour of mechanical pulps.

Due to the difficulty of studying quinone structures *in-situ*, most information regarding their reaction with alkaline peroxide has resulted from studies involving model quinone structures. In order to draw meaningful conclusions about the behaviour of *o*-quinones in lignin, it is essential that the correct model compound is chosen for study. The model *o*-quinone studied in this chapter was selected for several reasons:

(1) Recent experimental evidence[13] suggests that *o*-quinone structures are more likely to exist in high yield pulps than *p*-quinones. As a result, an *ortho* quinone such as 4-*tert*-butylorthoquinone is more likely to represent typical quinoid structures in lignin.

(2) The bulky, electron donating 4-*tert*-butyl substituent provides the *o*-quinone with relative stability against oxidation in air resulting in easier handling. Some protection is also provided against self condensation and polymerisation reactions which may occur during synthesis and in reactions with alkaline peroxide.

(3) Reactions involving alkaline peroxide and compounds similar or identical to 4-*tert*-butylorthoquinone have previously been described[21-23,25,26], and the reaction products and mechanisms involved have been characterised. This information greatly simplifies the kinetic study of reactions between 4-*tert*-butylorthoquinone and alkaline peroxide.

5.3 Experimental

5.3.1 Equipment

UV-visible spectra were recorded on a Shimadzu UV-160 spectrometer. In some cases, spectra were also run on a Varian DMS 100 spectrometer. Gas chromatograms of reaction product mixtures were obtained using a Hewlett-Packard 5890 Series II gas chromatograph fitted with a BP 20 fused silica polar phase capillary column (25 m × 0.22 mm i.d.) or a BP 1 non-polar phase capillary column (25 m × 0.32 mm i.d.). Both columns were supplied by SGE. Eluting compounds were detected with a flame ionisation detector. *p*H measurements were made using a glass electrode and meter supplied by Cole-Parmer. Proton nmr spectra were recorded on a Bruker AM 300 MHz spectrometer at 25°C and mass spectra were recorded on a Hewlett-Packard 5970 mass selective detector. ESR spectra were recorded at 25°C on a Jeol JES series spectrometer operating at a modulation frequency of approximately 9 MHz. All ESR measurements were made in a flat quartz cell.

5.3.2 *Materials*

Model compounds and other reagents were obtained from various commercial sources. Samples of 4-*tert*-butylcatechol (> 98%) and 2-methoxy-4-methylphenol (> 98%) were obtained from Aldrich Chemicals and were used without further purification. Benzyltriethylammonium chloride phase transfer catalyst ($PhCH_2NEt_3^+Cl^-$, > 98%) was obtained from Fluka Chemicals. Sodium periodate ($NaIO_4$, > 99.8%) and aqueous hydrogen peroxide (30% w/v, 10.5 M by iodometric titration) were supplied by Ajax Chemicals. Transition metal catalysed peroxide decomposition was minimised by using semiconductor grade (> 99.99%) sodium hydroxide (Aldrich) as an alkali source. The glass *p*H electrode was calibrated against commercial buffers of *p*H 7.0, 10.0, and 11.0 (Mallinkrodt BuffAR) depending on the alkalinity of interest. A borax solution of *p*H 9.2 (0.01 molal) was employed for work in the lower *p*H range while a Na_2HPO_4/NaOH buffer solution of *p*H 12.0 for work at higher alkalinity was prepared[47]. Doubly distilled 18 MΩ water was employed in all kinetic runs.

5.3.3 *Synthesis of 4-tert-butylorthoquinone*

The model *ortho* quinone for kinetic studies, 4-*tert*-butylorthoquinone, was synthesised from the corresponding catechol, 4-*tert*-butylcatechol, using a method based on procedures described by Takata *et al*[38] and Durst *et al*[39]. To 1.2 g (7 mmol) of 4-*tert*-butylcatechol dissolved in dichloromethane was added a slight molar excess of sodium periodate (1.66 g, 8 mmol) dissolved in a minimum volume of water (10-15 mL). A small amount of benzyltriethylammonium chloride phase transfer catalyst ($PhCH_2NEt_3^+Cl^-$, 50 mg) was added to the mixture to accelerate the rate of oxidation of the catechol to *o*-quinone. Sterically unhindered *o*-quinones such as 4-*tert*-butylorthoquinone are known to undergo polymerisation[24] and Diels-Alder dimerisation[39] so a relatively short reaction time (3 min) and low temperature (0°C) was employed to minimise the formation of such undesirable by-products. After

reaction, the organic layer was separated, dried over calcium chloride, and evaporated to leave a deep red oil. The oily residue was dissolved in hot *n*-hexane (100 mL), and the hexane layer containing dissolved 4-*tert*-butylorthoquinone was decanted and evaporated to a volume of 10-20 mL. On cooling, deep red needles recrystallised from the hexane layer. These needles were filtered under vacuum and washed with ice cold hexane to yield 4-*tert*-butylorthoquinone in 50% yield, m.p. 64-65°C (*lit.* m.p. 66°C [40]). MS [M^+ 164(20), 136(18), 121(46), 108(46), 93(100), 91(52), 77(42)]. ^{1}H-nmr ($CDCl_3$): δ 1.24, s, 6.28, s, 6.40, d, J 11 Hz, 7.20, d, J 11 Hz (see Appendix 4.1). Thin layer chromatography of the final product on silica plates revealed a single yellow spot with an R_f value of 0.4 (4:1 light petroleum : acetone).

5.3.4 Semi-Preparative Oxidation of 4-tert-butylorthoquinone with Alkaline Peroxide and Analysis of Reaction Products

The oxidation of 4-*tert*-butylorthoquinone was carried out by reacting an aqueous solution of 4-*tert*-butylorthoquinone (6×10^{-3} M, 100 mL) with alkaline hydrogen peroxide (0.01 M, *p*H 10) under nitrogen at 0°C. A nitrogen purge was employed to minimise reactions involving oxygen[22,23] and to facilitate comparison with other kinetic studies[23,25,26]. Constant reagent concentrations were maintained by adding peroxide and alkali as they were consumed. After 15 min. reaction time, the reaction solution was adjusted to *p*H 7 with dilute acid (H_2SO_4) and extracted with 3×30 mL portions of dichloromethane to yield a neutral extract which was red in colour. Acidification of the aqueous layer to *p*H 2 resulted in a red to yellow colour change at *p*H 3-3.5, and the extraction procedure was repeated to yield an acidic extract which was yellow in colour. After completion of the extraction procedure, the aqueous layer was completely discharged of colour. The identities of products existing in the aqueous layer were not further pursued. The neutral and acidic extracts were evaporated to dryness and weighed. Oxidation at *p*H 10 afforded approximately 20 mg of neutral material and 30 mg of acidic material. The neutral and acidic residues were redissolved in a small volume of ethyl acetate (1-2 mL) for analysis by TLC and GC. TLC plates were analysed under UV light at a wavelength of 254 nm.

5.3.5 *Semi-Preparative Reaction of 4-tert-butylorthoquinone with Alkaline Solution and Analysis of Reaction Products*

The reaction of 4-*tert*-butylorthoquinone with alkali was performed by addition of NaOH (1 M) to a solution of 4-*tert*-butylorthoquinone (6×10^{-3} M) to give a *p*H of 12. The reaction was carried out under nitrogen in a glass reaction vessel thermostatted to 25°C in a constant temperature water bath. On basification, the initial yellow colour was rapidly lost to yield a colourless solution, however the colourless solution slowly turned to brown and then red on standing for a further 30-60 minutes in the absence of bubbled nitrogen. After 60 min. reaction, the solution *p*H was adjusted to 7 with dilute acid (H_2SO_4) and 3×30 mL dichloromethane extracts were taken to yield a neutral extract, which was red in colour. The red solution became pale yellow in colour during acidification to *p*H 2 and 3×30 mL dichloromethane extracts also yielded a yellow solution. Both extracts were evaporated to dryness and the residues were redissolved in ethyl acetate for analysis by TLC and GC-MS.

5.3.6 *Method for Kinetic Runs*

Kinetics experiments were performed in a glass reaction vessel immersed in a constant temperature water bath. A buffered aqueous solution of the starting *o*-quinone was prepared by dissolving a small amount of 4-*tert*-butylorthoquinone (40 mg, 0.2 mmol) in 200 mL boric acid solution (0.1 M). Complete dissolution of the starting material was promoted by immersion of the aqueous solution in an ultrasonic bath for 2-3 min. The exposure to ultrasound also served to remove potentially reactive dissolved oxygen from solution. The reaction solution was thermally equilibrated for several minutes and purged with a steady stream of oxygen free nitrogen to prevent re-absorption of oxygen.

Kinetic runs were initiated by adding the required amounts of sodium hydroxide (1 M) and hydrogen peroxide to reach the desired reaction conditions. On addition of peroxide, the solutions turned deep red in colour and the *p*H of the buffered solutions

slowly decreased indicating consumption of alkali and/or formation of acidic products. A trial reaction of the *o*-quinone with alkaline peroxide at 25°C was too rapid to allow kinetic study, so all subsequent oxidations were performed at 0°C. Trial kinetic runs at *p*H values greater than 8.5 also proceeded too rapidly to be studied and later runs were carried out at lower *p*H values. Constant *p*H levels were maintained by the addition of dilute sodium hydroxide (0.1 M) as the reactions progressed. Aliquots for analysis (10.00 mL) were periodically withdrawn and iodometric titrations were carried out at the beginning and end of kinetic runs to determine peroxide levels. For kinetic runs in the presence of alkali alone, base concentrations were determined by titration with standardised HCl (0.1 M) diluted to 0.001 M (methyl red end point).

5.3.7 Analysis of Samples

Samples removed during kinetic runs were quenched by acidification with phosphate buffer (5 mL, 1 M Na_2HPO_4, *p*H 2). Upon quenching, the reaction samples turned from red to straw yellow in colour at *p*H 3-3.5. The quenched samples were transferred to a volumetric flask and accurately diluted to 25.00 mL. The disappearance of 4-*tert*-butylorthoquinone was monitored by following the decrease in UV-visible absorbance at 400 nm. A calibration curve relating absorbance to concentration for 4-*tert*-butylorthoquinone at 400 nm was established by measuring the absorbances of standard 4-*tert*-butylorthoquinone solutions. Adherence of the calibration solutions to Beer's Law was excellent for absorbances less than 1.5 units in magnitude (correlation coefficient, $r^2 = 1.00$) (see Appendix 4.2).

Neutral and acidic extracts from the preparative oxidation of 4-*tert*-butylorthoquinone were analysed by gas chromatography (GC) and thin layer chromatography (TLC). Separation of sample components by GC was achieved using a simple temperature gradient program (*BP 20 column:* 2 µL splitless injections, 30 p.s.i. head pressure, 60°C isothermal, 5 min., 10°C /min. ramp to 200°C, 200°C isothermal, 20 min. *BP 1 column:* 2 µL splitless injections, 15 p.s.i. head pressure, 60°C, 10°C /min. ramp to

290°C, 290°C isothermal, 12 min.). Thin layer chromatography was carried out on silica plates using 4:1 petroleum ether : acetone as eluent. ESR experiments to confirm the participation of aryloxy-radicals in colour producing reactions were carried out by reacting 4-*tert*-butylcatechol (10^{-3} M, 10 mL) with alkali (NaOH, 0.1 M) at *p*H 11 in 4:1 dimethylformamide : water. The colourless catechol solution was thoroughly shaken to produce a fleeting yellow colour attributed to formation of 4-*tert*-butylorthoquinone[18]. The yellow colour was rapidly lost to yield a red solution which was examined for the presence of aryloxy-radical species.

5.4 Results

5.4.1 Reaction of 4-tert-butylorthoquinone with Aqueous Alkaline Peroxide

The addition of alkaline peroxide to a solution of 4-*tert*-butylorthoquinone (I) (Figure 1), caused the original yellow colour to be rapidly replaced by a red solution, which persisted for the remainder of the reaction. Analysis of the reacted solution by GC and TLC revealed the absence of starting material.

A neutral dichloromethane extract of the reacted solution contained two major components which were observed as colourless and red spots on TLC plates (R_f 0.28 and R_f 0.18 respectively). GC-MS analysis and comparison with authentic samples identified the colourless compound as 4-*tert*-butylcatechol (II), and the red spot as 2-*tert*-butyl-5-hydroxybenzoquinone (III) (Figure 1). GC-MS analysis of the neutral extract with a polar column revealed *ca.* 25 smaller peaks exhibiting molecular ions in the range *m/e* 60-194. The majority of these peaks displayed MS fragmentation patterns consistent with *tert*-butyl substituted lactones of acids such as muconic acid, maleic acid and fumaric acid. Major GC-MS peaks and their tentative structural assignments are listed in Table 1 and Figure 2 respectively.

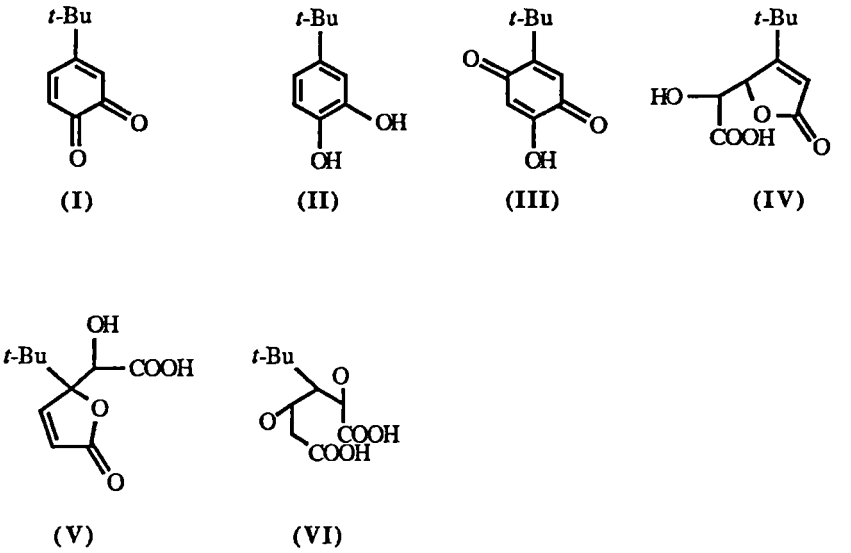

FIGURE 1: Compounds formed during the reaction between alkaline peroxide and 4-*tert*-butylorthoquinone (I), (after Gellerstedt *et al*[23]).

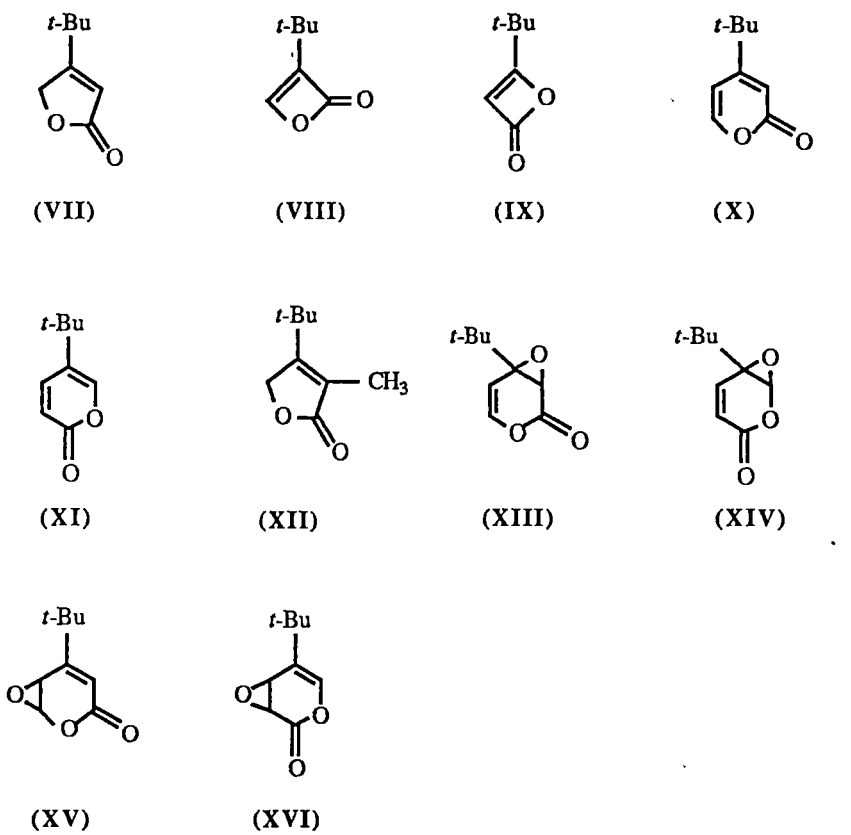

FIGURE 2: Lactone compounds identified by GC-MS analysis of peroxide reacted 4-*tert*-butylorthoquinone solutions.

Comparison of MS fragmentation patterns in Table 1 revealed that some of the proposed lactones existed as diastereomers and other geometric isomers. Several minor peaks exhibiting mass fragments in the range *m/e* 350-500 were also detected; their existence was ascribed to polymerisation of the starting material which has previously been noted by Bailey and Dence[25] and Durst *et al*[39]. The only other compound positively identified by its mass spectrum was acetic acid.

TABLE 1: Retention times and structural assignments of compounds detected by GC-MS of neutral and acidic dichloromethane extracts of 4-*tert*-butylorthoquinone oxidation products.

GC Column Type	Retention Time (min.)	Major MS peaks	Structural Assignment
BP 20 polar phase	9.2	60, 45	Acetic Acid
"	10.3	140, 125, 97, 83	VIII*
"	12.6	126, 111, 95, 83	IX*
"	13.1	152, 137, 124, 109	X
"	13.5	192, 177, 149	?
"	13.8	126, 97, 84	XI*
"	14.7	152, 137, 124, 109	XII*
"	15.7	166, 151, 123	?
"	16.3	166, 151, 123	?
"	16.7	152, 137, 109	XIII*
"	17.1	192, 177, 152	?
"	17.3	168, 153, 125, 109	XIV*
"	18.6	168, 153, 125, 97	XV*
"	18.9	166, 152, 124, 109	?
"	20.8	194, 179, 151, 123	?
"	21.4	168, 153, 125	XVI*
"	24.8	168, 153, 125	XVII*
"	25.2	>300	Condens'n Prods
BP 1 non-polar phase	5.7	180, 165, 152, 138	III
"	8.4	166, 151, 136, 123	II
"	14.0	304, 289, 247	Condens'n Prods
"	14.2	304, 289, 247	Condens'n Prods
"	18.0	342, 327, 312	Condens'n Prods

* Refer to Figure 2. Denotes tentative assignment only.
? No structural assignment was possible

An acidified dichloromethane extract of the reacted 4-*tert*-butylorthoquinone solution revealed the presence of (II) and (III) together with minor purple, brown and orange spots on silica plates (R_f 0.03, 0.10 and 0.38 respectively). The identities of the three coloured spots were not further pursued as a result of difficulties encountered during isolation. GC-MS analysis of the acidic extract exhibited a large peak due to acetic acid and a distribution of oxygenated fragments similar to those listed in Table 1.

5.4.2 Reaction of 4-tert-butylorthoquinone with Aqueous Alkaline Solution

Compounds (II) and (III) were detected in neutral and acidic dichloromethane extracts of 4-*tert*-butylorthoquinone reacted with alkali . Additional yellow and colourless spots were observed in chromatograms of neutral and acidic extracts (R_f 0.50 and R_f 0.55 respectively), while a further immobile orange spot was noted in the acidic extract. Further evidence (see below) suggested that the compounds responsible for the additional spots were condensation products of the starting material.

GC-MS analysis of the acidic dichloromethane extract with a non-polar capillary column resulted in two major peaks due to (II) and (III) together with 3 other minor components of molecular weight > 300 g/mol (Table 1). Experimental evidence indicated that two of these higher molecular weight components were diastereomers present in a *ca.* 1:1 ratio based on GC peak area. Both peaks exhibited identical mass spectra with molecular ions of *m/e* 304. The remaining higher molecular weight component produced a molecular ion of *m/e* 342. Polymerisation of the starting material was the most likely cause of such higher molecular weight material. GC-MS analysis of the neutral extract revealed the presence of (II) only.

The generation of (III) from 4-*tert*-butylorthoquinone in alkaline solution has been reported to occur via aryloxy-radical species which are formed when dissolved oxygen is present in solution[18]. Confirmation of the existence of these radicals in the present work was obtained by ESR analysis of a solution of 4-*tert*-butylorthoquinone reacted

with alkali at *p*H 10. The resultant ESR spectrum was similar to that previously reported[18,42] and exhibited a broad doublet in which no fine structure was visible (Figure 3). The lack of fine structure was possibly a result of the free electron coupling with methylene groups of the *t*-butyl substituent. It was observed that generation of the aryloxy-radical was accompanied by the characteristic yellow to red colour change indicative of conversion of 4-*tert*-butylorthoquinone to (III).

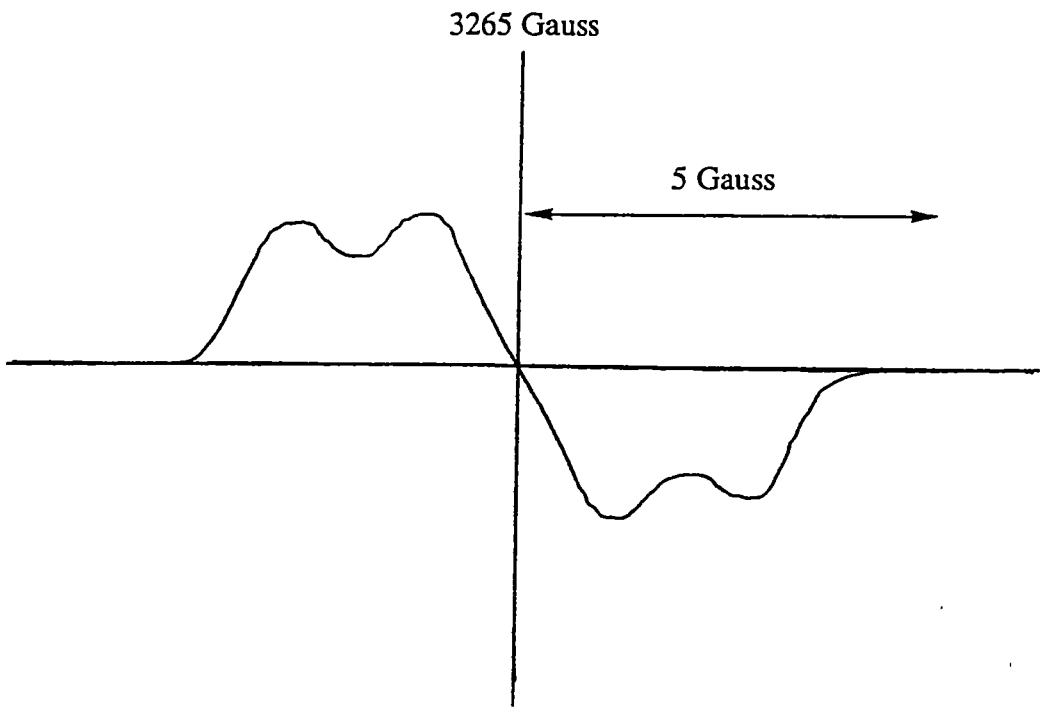

FIGURE 3: ESR spectrum of aryloxy-radical intermediate in the formation of 2-*tert*-butyl-5-hydroxybenzoquinone from 4-*tert*-butylorthoquinone.

5.4.3 Light Absorption Properties of 4-tert-butylorthoquinone Solutions Reacted with Alkaline Peroxide

A preliminary investigation of the light absorption properties of oxidised 4-*tert*-butylorthoquinone solutions was undertaken using UV-visible spectroscopy. At 0°C the reaction of 4-*tert*-butylorthoquinone (10^{-3} M) with alkaline peroxide (0.01 M, *p*H

8-12) resulted in a discharge of the original yellow solution to yield the red solution attributed to the formation of (III). Acidification of the solution resulted in the same appearance of a pale yellow solution which possessed much less colour than the original quinone solution. The loss in colour of 4-*tert*-butylorthoquinone solutions was followed with time by monitoring the decrease in the molar extinction coefficient of the *o*-quinone band centred at 400 nm (Figure 4) under conditions of constant alkali and peroxide concentration.

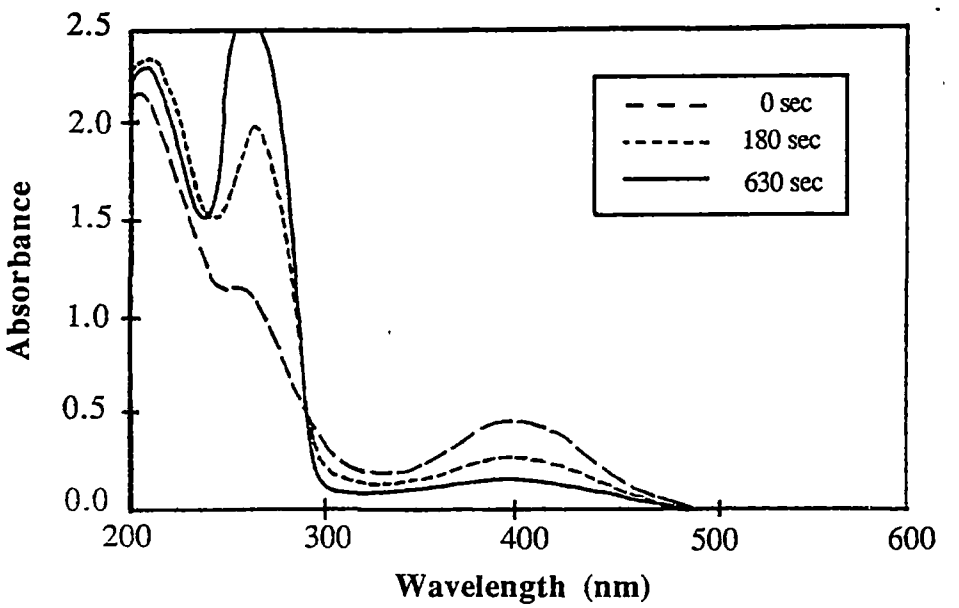

FIGURE 4: UV-visible spectra showing disappearance of the *o*-quinone band centred at 400 nm during the reaction with alkaline peroxide. Reaction conditions: 0.01 M peroxide, 0.001 M 4-*tert*-butylorthoquinone, *p*H 10, T = 0°C .

In Figure 5 the decrease in extinction coefficient with time is shown for a series of solutions of 4-*tert*-butylorthoquinone reacted with constant concentrations of peroxide at various *p*H levels. The set of curves is characterised by a loss in colour which is accelerated by increasing alkali concentration, followed by a flat region caused by the incomplete discharge of coloured species. It is evident that removal of colour is

favoured by increasing alkali levels in the *p*H range 8 to 10. The most effective removal of colour was observed in the *p*H 10-11 range, however raising the *p*H further gave no improvement with more coloured solutions resulting when *p*H was increased to 12.

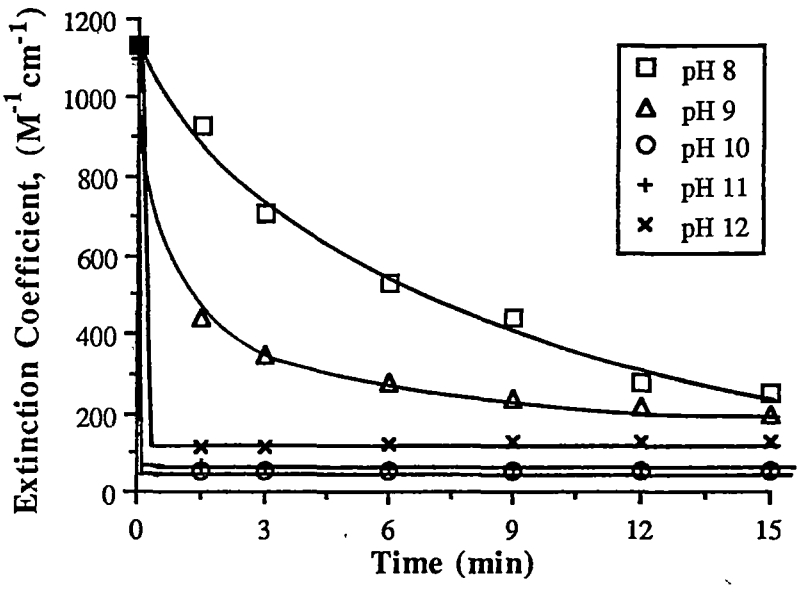

FIGURE 5: Extinction coefficient-time plots of 4-*tert*-butylorthoquinone solutions reacted with constant concentrations of peroxide at various *p*H levels. T = 0°C, 0.01 M peroxide .

The maintenance of constant reagent concentrations in Figure 5 implies that incomplete removal of colour can be attributed to alkaline peroxide resistant chromophores such as (III) formed in the reacted solutions. TLC analysis of products at the conclusion of each reaction in Figure 5 confirmed the presence of (II) and (III) and several minor unassigned spots, however no starting material was detected. It seems likely that the residual colour levels in Figure 5 are the result of different distributions of peroxide resistant chromophores, the concentrations of which are predominantly influenced by *p*H levels.

Figure 6 illustrates how molar extinction coefficient values are affected by increasing levels of peroxide at constant *p*H. Increasing peroxide levels appear to influence the initial rate of colour removal only, with residual levels of colour remaining virtually constant despite the different concentrations of peroxide applied. Comparison of Figures 5 and 6 demonstrates that solution *p*H has the greatest influence on the amount of residual colour remaining in peroxide reacted solutions of 4-*tert*-butylorthoquinone.

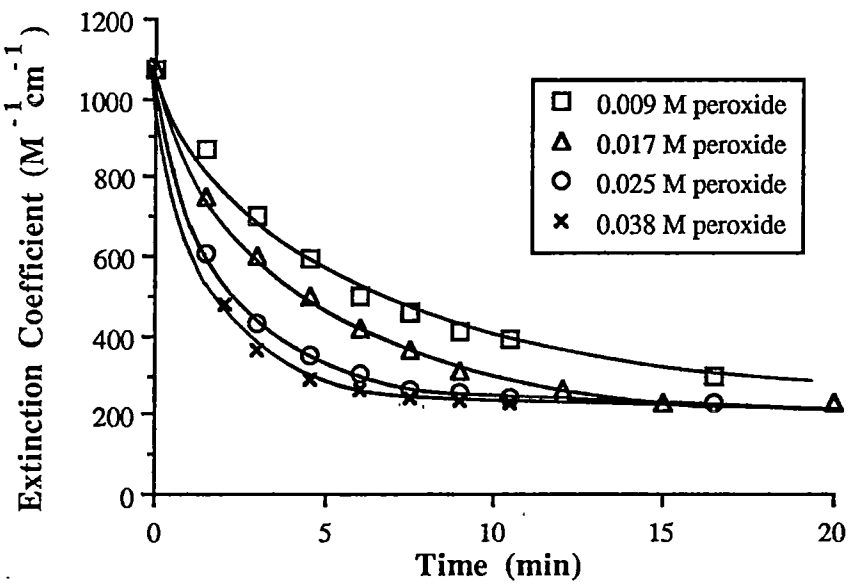

FIGURE 6: Extinction coefficient-time plots of 4-*tert*-butylorthoquinone solutions reacted with alkaline hydrogen peroxide at constant *p*H. T = 0°C, *p*H = 8.2.

The unresponsive nature of the residual chromophores formed by the reaction of 4-*tert*-butylorthoquinone with alkaline peroxide was demonstrated by altering the reagent concentrations of oxidised *o*-quinone solutions to afford conditions which would promote further chromophore removal. The results of these experiments, presented in Figure 7, show that a ten-fold change in alkali concentration at constant peroxide levels or a three-fold increase in peroxide concentration at constant *p*H were insufficient to alter the distribution of residual chromophores as reflected by the extinction coefficients of the oxidised solutions.

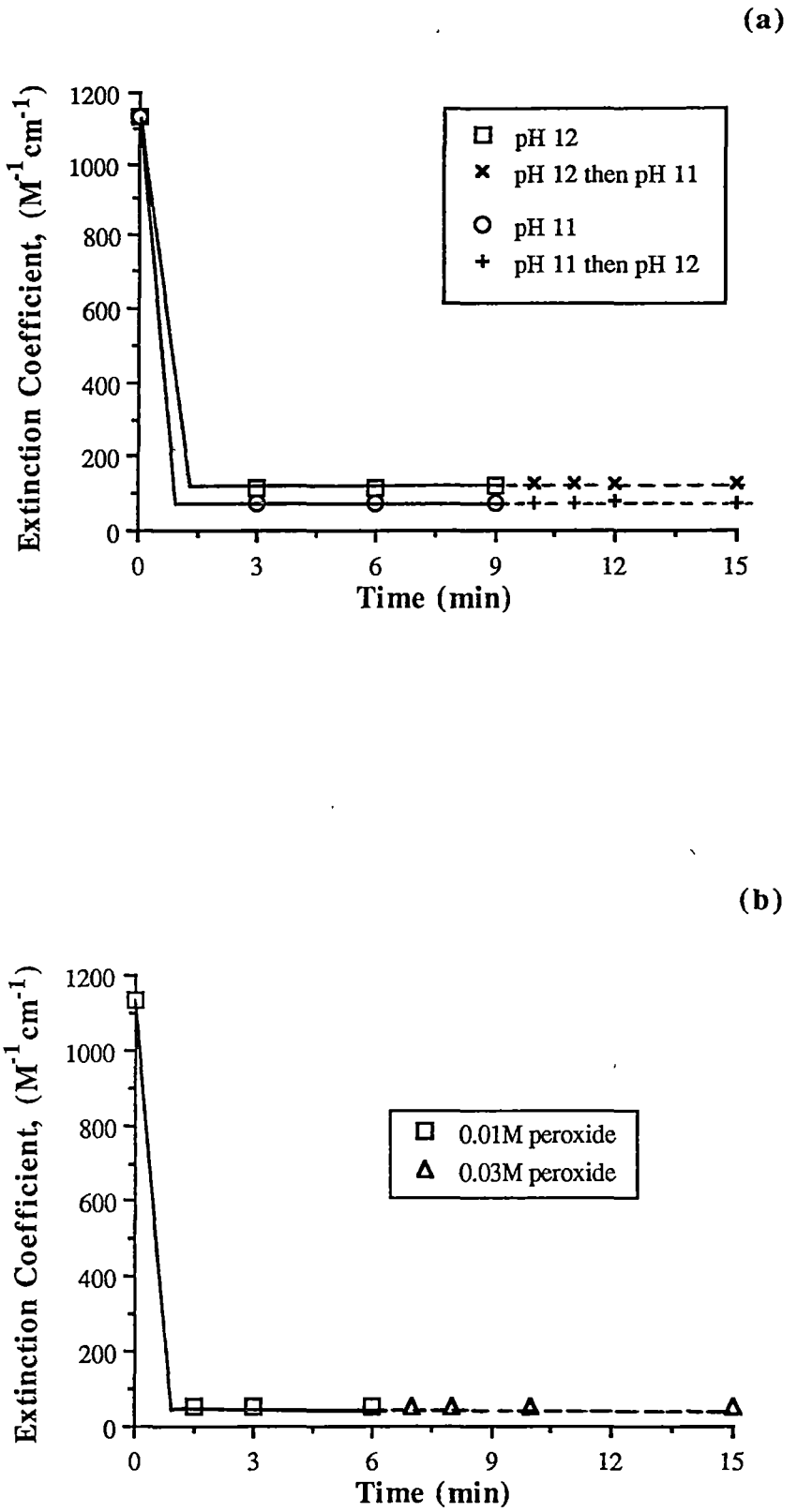

FIGURE 7: The effect on molar extinction coefficients of altering reagent concentrations during reaction of 4-*tert*-butylorthoquinone with alkaline peroxide. (a) solution *p*H altered at constant peroxide concentration of 0.01 M. (b) peroxide concentration increased at constant *p*H of 10.

5.4.4 Kinetic Studies of the Reaction Between 4-tert-butylorthoquinone and Alkali

The loss of colour in 4-*tert*-butylorthoquinone solutions reacted with alkali was parallelled by a decrease in the UV-visible absorption band of the *o*-quinone centred at 400 nm (Figure 8). The kinetics of the decolourisation process were studied in more detail by following the disappearance of the 400 nm band at 25°C over a two-fold alkali concentration range (0.001-0.002 M). In contrast with observations for the reaction at *p*H 12 (section 5.4.2), the yellow colour of the original solution was not completely discharged at these lower alkali levels before the very gradual onset of a brown/red colour change. Potential interference from this colourising reaction were avoided by studying the kinetics of decolourisation before the effects of the second reaction became noticeable. Such interference was generally observed to commence at reaction times in the 40-50 minute range.

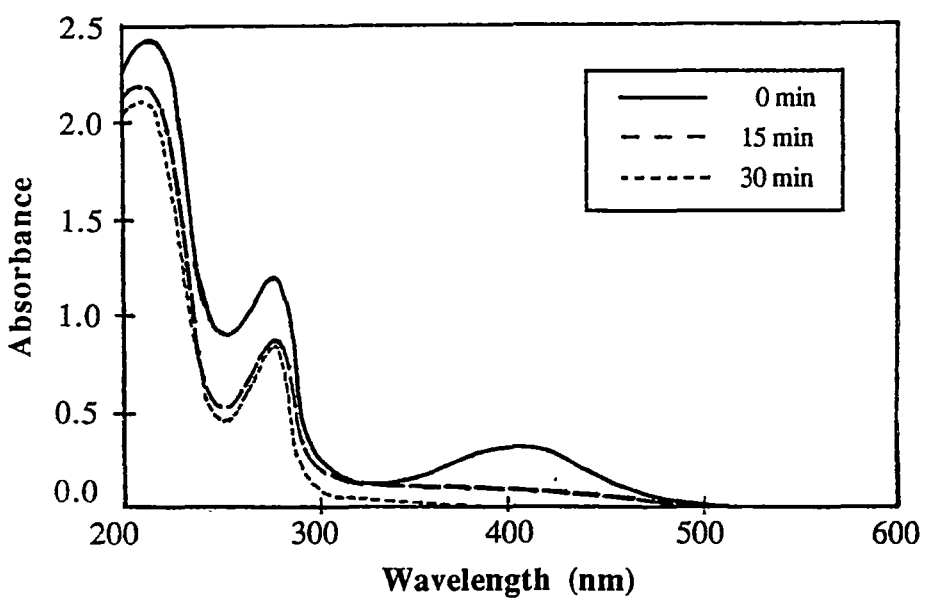

FIGURE 8: UV-visible spectra showing disappearance of the *o*-quinone band centred at 400 nm at various times during the reaction of 4-*tert*-butylorthoquinone with alkali. Reaction conditions: 0.001 M 4-*tert*-butylorthoquinone, 0.002 M NaOH, T = 25°C.

Figure 9 depicts pseudo-first order concentration-time profiles for the removal of 4-*tert*-butylorthoquinone in alkaline solution, as measured by the decrease in absorbance at 400 nm. The degree of linearity in the pseudo-first order plots of quinone removal indicates that the reaction in alkaline solution was a first order process with respect to 4-*tert*-butylorthoquinone.

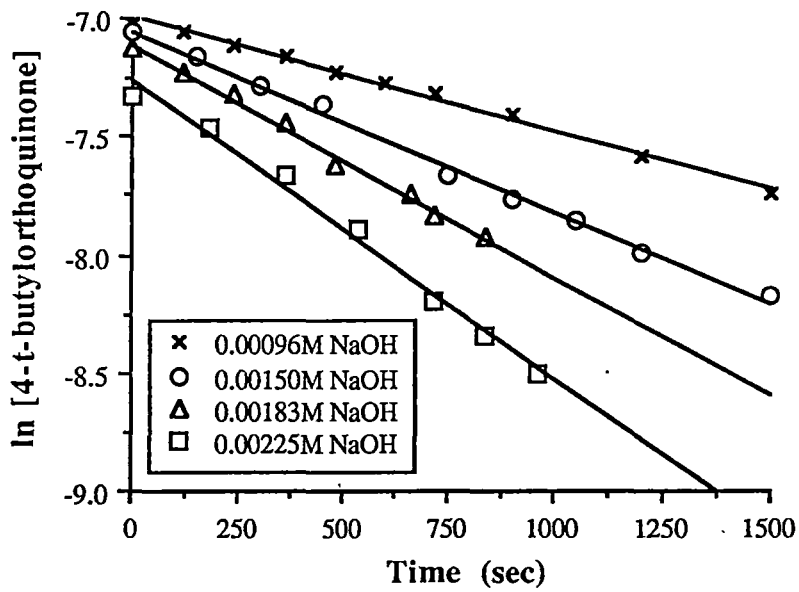

FIGURE 9: Pseudo-first order concentration-time profiles for the removal of 4-*tert*-butylorthoquinone in alkaline solution as measured by the decrease in absorbance at 400 nm. T = 0°C.

Pseudo-first order rate constants are presented in Table 2 for the loss of quinone over the investigated alkali concentration range. A plot of the data in Table 2 (Figure 10) was linear and confirmed that the reaction of 4-*tert*-butylorthoquinone with alkali was a first order process with respect to both quinone and alkali, and second order overall.

TABLE 2: Values of pseudo-first order rate constants, k_1', for the reaction of 4-*tert*-butylorthoquinone with various concentrations of alkali. T = 25°C .

[NaOH] (M) × 10^4	k_1' (s^{-1}) × 10^4	k_1'/[NaOH] (L $mol^{-1}s^{-1}$)
9.55	4.88	0.511
15.0	7.70	0.513
18.3	9.88	0.540
22.5	12.7	0.564

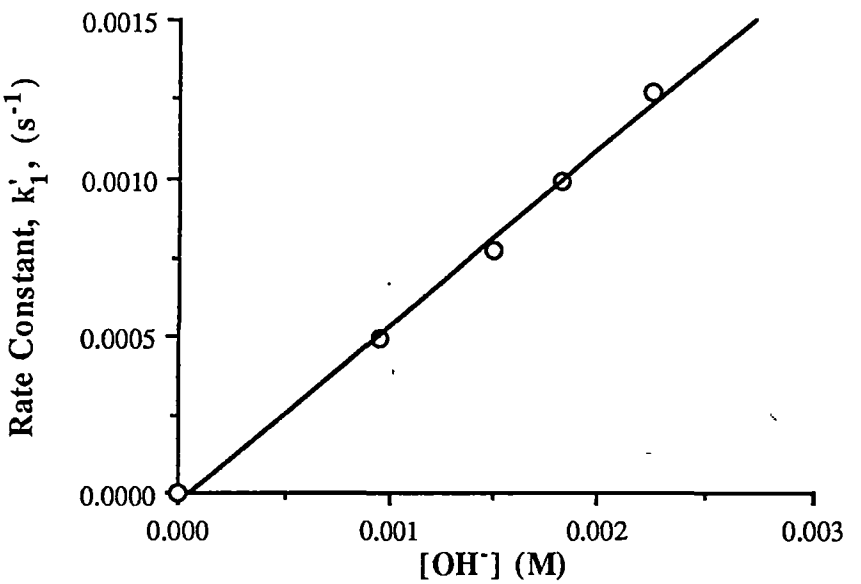

FIGURE 10: Linear plot of pseudo first order rate constant for 4-*tert*-butylorthoquinone removal in alkali, k_1', against hydroxide ion concentration at 25°C . Correlation coefficient, $r^2 = 0.995$.

The rate equation for the decolourising reaction between 4-*tert*-butylorthoquinone and alkali can therefore be written as:

$$- d[\text{Quinone}]/dt = k_1[\text{Quinone}][OH^-] \qquad (1)$$

where k_1 is the second order rate constant for the reaction. From the slope of Figure 10, this rate constant was calculated to have a value of $k_1 = 0.56 \pm 0.02$ L mol^{-1}s^{-1} at 25°C. Activation energy studies of the same reaction over the temperature range 0-40°C (Table 3) resulted in a linear Arrhenius plot with a slope corresponding to an activation energy of 65 ± 3 kJ/mole ($r^2 = 0.994$).

TABLE 3: Activation energy data for the reaction of 4-*tert*-butylorthoquinone with alkali over the temperature range 0-40°C.

Temperature (°C)	k_1 (L mol^{-1}s^{-1})	1/T (K^{-1} × 10^3)	ln k_1 (L mol^{-1}s^{-1})
0.3	0.04	3.658	-3.2
25.0	0.56	3.355	-0.58
30.2	0.70	3.297	-0.36
39.0	1.39	3.204	0.33

5.4.5 Kinetic Studies of the Reaction Between 4-tert-butylorthoquinone and Alkaline Peroxide

The kinetics of the reaction between 4-*tert*-butylorthoquinone and alkaline peroxide were also studied spectrophotometrically by following the decrease in the quinone absorbance band centred at 400 nm. The removal of *o*-quinone was not accompanied by a proportional decrease in absorbance, and significant colour remained even after complete consumption of *o*-quinone. This was attributed to the formation of peroxide resistant species such as (III) which absorb in the same spectral region as the starting material.

The detection of a complex mixture of reaction products (section 5.4.1) indicates that 4-*tert*-butylorthoquinone reacts with alkaline peroxide by a number of different routes, however the kinetic behaviour of 4-*tert*-butylorthoquinone degradation (Figure 6)

resembles that of a process involving simple quinone → product (Q → P) conversion. This implies that the reaction products observed in section 5.4.1 behave kinetically as a single product species, B, under the conditions employed and can be treated as a single species in a kinetic analysis of 4-*tert*-butylorthoquinone removal.

Assumption of a simple Q → P kinetic scheme allowed the effective molar extinction coefficients of the product solutions to be calculated by dividing the final absorbances by product concentration, based on total conversion of starting material to products. This enabled the absorbance of product species at 400 nm to be subtracted from the total absorbance so that quinone removal could be followed spectrometrically. By reference to Figure 6, the effective molar extinction coefficients of the reacted solutions were found to be essentially independent of peroxide concentration at constant *p*H. Over the relatively narrow *p*H range employed for kinetic runs (*p*H 8.2-8.3), reacted solutions of 4-*tert*-butylorthoquinone were observed to reach a common residual extinction coefficient of 228 ± 5 $M^{-1}cm^{-1}$ (average of 6 kinetic runs). This value, representing the total molar extinction coefficient of products absorbing at 400 nm, was subtracted from the measured absorbance at 400 nm to yield the concentration of *o*-quinone at any time. The expression relating measured absorbance and *o*-quinone concentration is shown below.

At any time, t ,

$$ABS_{total} = ABS_{quinone} + ABS_{products}$$

$$= \varepsilon_1[Q_t] + \varepsilon_2[P_t] \quad \text{by Beer's Law at fixed optical path length}$$

$$= \varepsilon_1[Q_t] + \varepsilon_2\{[Q_0] - [Q_t]\}$$

$$= (\varepsilon_1 - \varepsilon_2)[Q_t] + \varepsilon_2[Q_0]$$

$$\therefore \quad [Q_t] = \frac{ABS_{total} - \varepsilon_2 [Q_0]}{(\varepsilon_1 - \varepsilon_2)} \qquad (2)$$

where

ABS_{total} = measured absorbance at 400 nm.

ε_1 = 1071 $M^{-1}cm^{-1}$, the molar extinction coefficient of 4-*tert*-butylorthoquinone at 400 nm.

ε_2 = 228 $M^{-1}cm^{-1}$, the effective residual molar extinction coefficient of reaction products at 400 nm.

$[Q_0]$ = initial concentration of 4-*tert*-butylorthoquinone.

$[Q_t]$ = concentration of 4-*tert*-butylorthoquinone at time t, calculated assuming a simple, monomolecular Q → P conversion.

$[P_t]$ = concentration of products at time t, also based on simple Q → P kinetics.

A typical plot illustrating removal of 4-*tert*-butylorthoquinone as a function of time is presented in Figure 11. The concentrations of *o*-quinone and reaction products in Figure 11 were calculated by the subtractive absorbance method in equation (2).

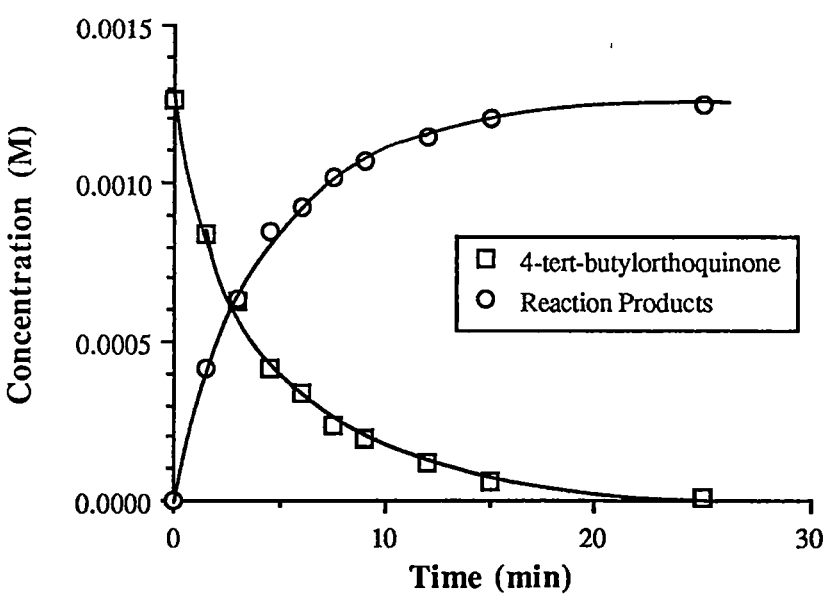

FIGURE 11: Concentration - time plot showing disappearance of 4-*tert*-butylorthoquinone and formation of products during reaction with alkaline peroxide. 0.0101 M peroxide, *p*H 8.3, T = 0°C.

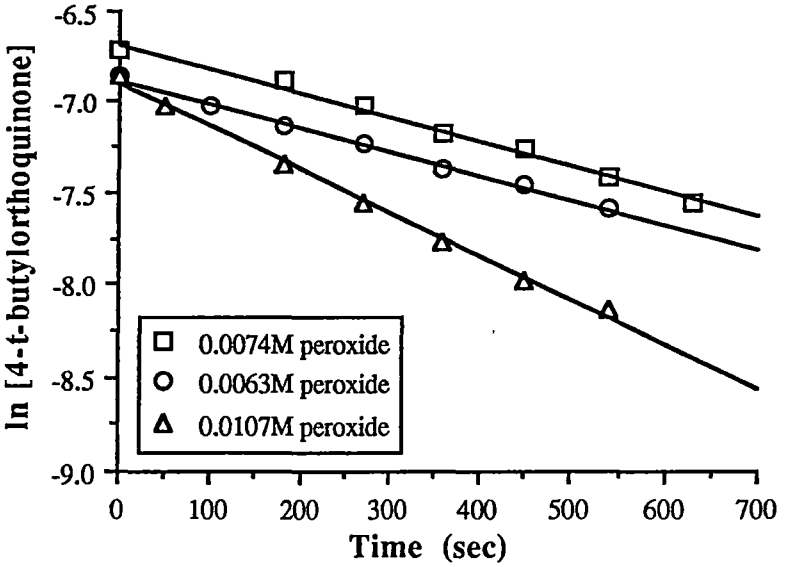

FIGURE 12: Typical pseudo-first order plots for the disappearance of 4-*tert*-butylorthoquinone reacted with alkaline hydrogen peroxide at 0°C, *p*H 8.2.

Pseudo-first order plots for quinone disappearance (Figure 12) were linear and indicated that removal of 4-*tert*-butylorthoquinone in alkaline peroxide solution was a first order process with respect to quinone concentration. On the basis of these results, the rate equation describing 4-*tert*-butylorthoquinone removal in alkaline peroxide can be written as:

$$- d[\text{Quinone}]/dt = k'[\text{Quinone}] \qquad (3)$$

The constant k' denotes pseudo-first order rate constants, which were obtained from the slope of plots such as those in Figure 12. Kinetic analysis of the reaction of 4-*tert*-butylorthoquinone in alkali (Section 5.4.4) indicates that equation (3) represents the sum of two components which describe the effects of alkali and alkaline peroxide respectively on the *o*-quinone:

$$- d[\text{Quinone}]/dt = \{k_1[OH^-] + k_2'\}[\text{Quinone}] \qquad (4)$$

where k_2' is the pseudo-first order rate constant for quinone removal by alkaline peroxide and k_1 is the second order rate constant for quinone removal by alkali. Comparison of equations (3) and (4) shows that the rate constant representing reaction with alkaline peroxide, k_2', can be obtained directly by subtraction:

$$k_2' = k' - k_1[OH^-] \qquad (5)$$

From the studies of *o*-quinone removal in alkali at 0°C (Table 3), substitution of k_1 = 0.04 L $mol^{-1}s^{-1}$ into equation (5) shows the $k_1[OH^-]$ term to be insignificant with respect to k' so that $k_2' = k'$. The values of pseudo-first order rate constants, k_2', at various perhydroxyl anion concentrations are presented in Table 4. The perhydroxyl anion concentration at 0°C in Table 4 was calculated by extrapolation of the equation of Teder and Tormund[43] (6) which describes the temperature dependence of the hydrogen peroxide base dissociation constant (pK_b) over the range 20-80°C.

$$pK_b = 1330/T - 2.13 + [Na^+]^{0.5} \qquad (6)$$

where T is the absolute temperature in degrees Kelvin.

TABLE 4: Values of pseudo-first order rate constant, k_2', for the reaction of 4-*tert*-butylorthoquinone with various concentrations of perhydroxyl anion. Reactions carried out at 0°C. Perhydroxyl anion concentrations calculated from the extrapolated equation of Teder and Tormund[43].

$[H_2O_2]$ (M) × 10^3	*p*H	$[HO_2^-]$ (M) × 10^6	k_2' (s^{-1}) × 10^3
14.8	8.1	10.3	2.66
6.27	8.2	5.48	1.34
7.37	8.2	6.45	1.48
7.66	8.2	6.70	1.67
10.7	8.2	9.36	2.37
13.0	8.2	11.4	2.87

A plot of the pseudo-first order rate constant, k_2', against the concentration of perhydroxyl anion (HOO^-) was linear (Figure 13) and indicated that the rate of *o*-quinone removal was first order with respect to both quinone and perhydroxyl anion concentration, and second order overall. The adherence of the reaction to second order kinetics appears to support the validity of the initial assumption that 4-*tert*-butylorthoquinone degradation behaves kinetically as a simple 'quinone → product' conversion under the reaction conditions employed.

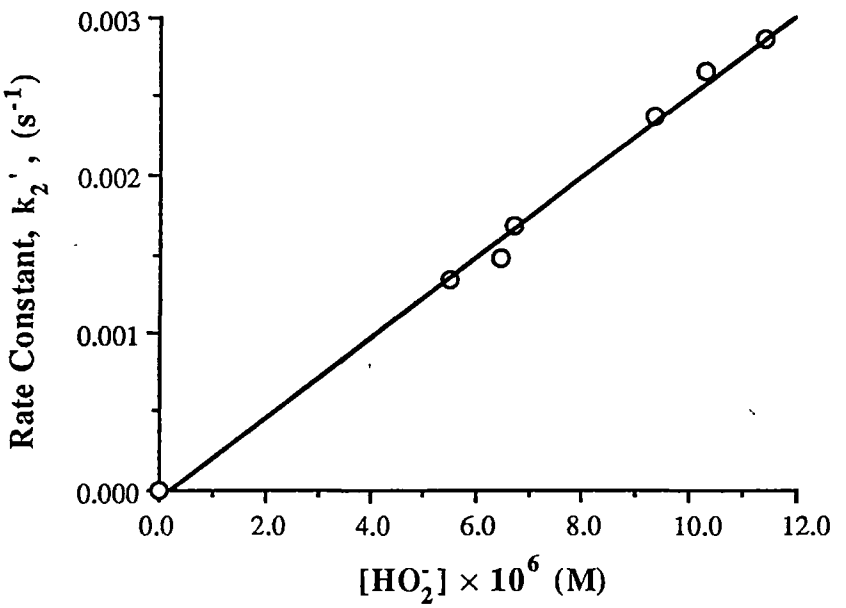

FIGURE 13: Linear plot of pseudo first order rate constant for 4-*tert*-butylorthoquinone removal in alkaline peroxide, k_2', against perhydroxyl anion concentration. Correlation coefficient, $r^2 = 0.996$.

The rate equation describing the removal of 4-*tert*-butylorthoquinone by perhydroxyl anion can therefore be written as:

$$- d[\text{Quinone}]/dt = k_2[\text{Quinone}][HOO^-] \qquad (7).$$

From the slope of the line in Figure 13, k_2 was found to have a value of $k_2 = 256 \pm 9$ L $mol^{-1}sec^{-1}$ at 0°C.

5.5 Discussion

5.5.1 Reaction Routes

The results of this chapter, together with previous studies[18,22,23,25,26] support the view that the reaction of alkaline peroxide with *ortho* quinone structures such as 4-*tert*-butylorthoquinone is a complex process which takes place via competing oxidative and reductive routes. These routes involve several reactive species, both ionic and radical, as depicted in Scheme 1. The kinetic results summarised by equations (1) and (7) indicate that the rate determining steps in the reaction of 4-*tert*-butylorthoquinone with alkali or alkaline peroxide involve bimolecular nucleophilic attack by perhydroxyl and/or hydroxide anions on the quinone substrate. It has been proposed that nucleophilic attack may take place at four possible sites in the two α,β-unsaturated ketone systems existing in *ortho* quinones[18-21,23,25,26,44]. The multiple sites for nucleophilic attack in 4-*tert*-butylorthoquinone results in the wide variety of reaction routes and products shown in Scheme 1, routes A-E.

5.5.2 Cleavage of the Quinoid Nucleus - Route A (Scheme 1)

Studies with model *ortho* quinones derived from guaiacyl (softwood) and syringyl (hardwood) model compounds have demonstrated that Route A involves oxidative fragmentation of quinoid nuclei to form colourless, low molecular weight dicarboxylic acids and simple aliphatic acids[22,25,26]. It has been proposed that Route A is initiated by oxidative cleavage between the adjacent carbonyl groups C-1 and C-2 causing rupture of the quinoid ring[25,26]. The kinetic results of this study are in agreement with previous work which suggests that nucleophilic attack by perhydroxyl anions initiates the oxidative cleavage[22]. The polar di-acidic products depicted in Route A were not observed in the current work. However the detection of various lactones (see Figure 2) suggests that unsaturated dicarboxylic acids such as those in Route A rearrange under the conditions of elevated temperature encountered in GC-MS analysis. A possible mechanism leading to formation of (VIII) and (IX) during GC-MS analysis is shown in Scheme 2.

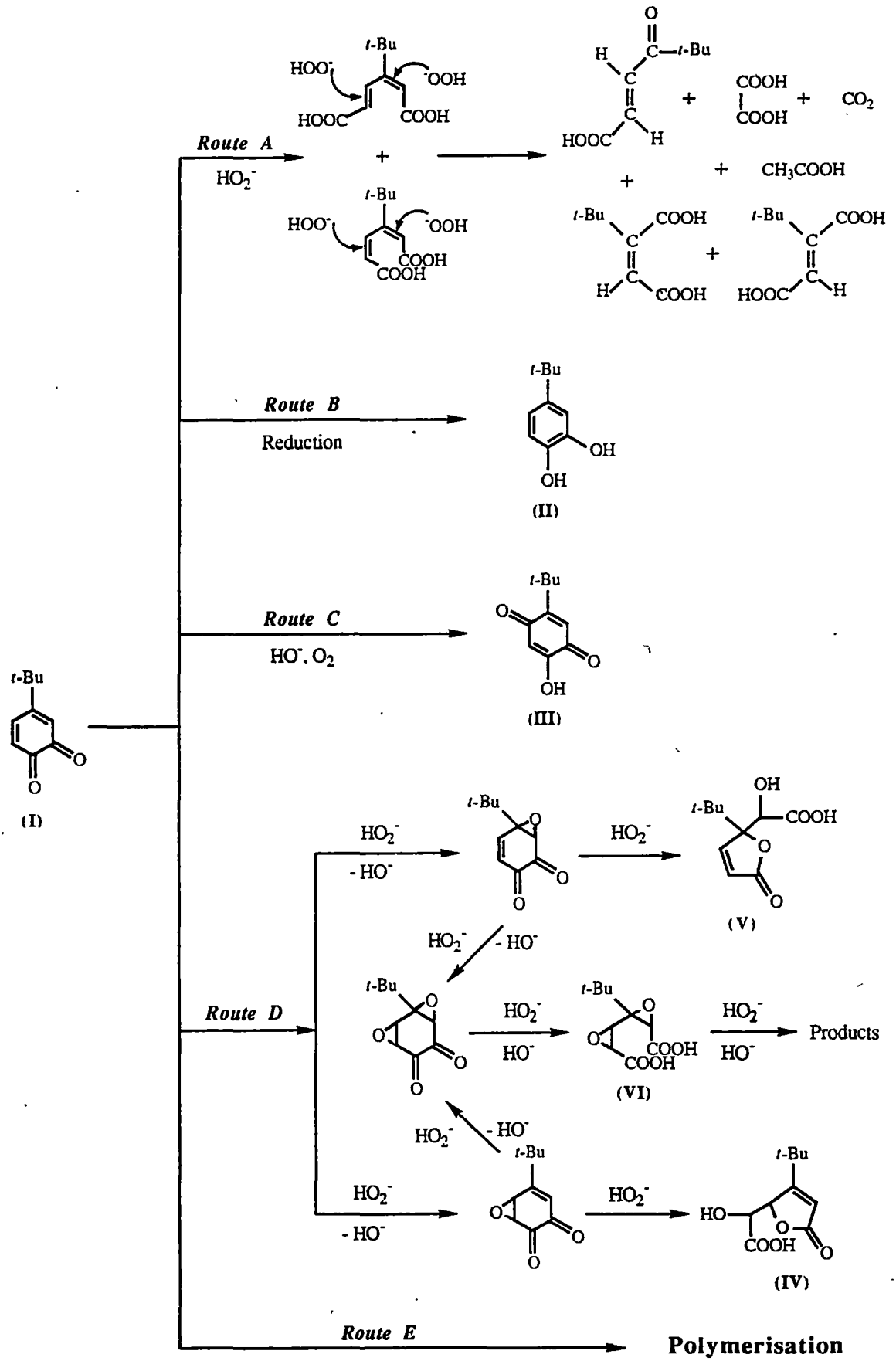

SCHEME 1: Different routes by which 4-*tert*-butylorthoquinone reacts with alkali and alkaline peroxide.

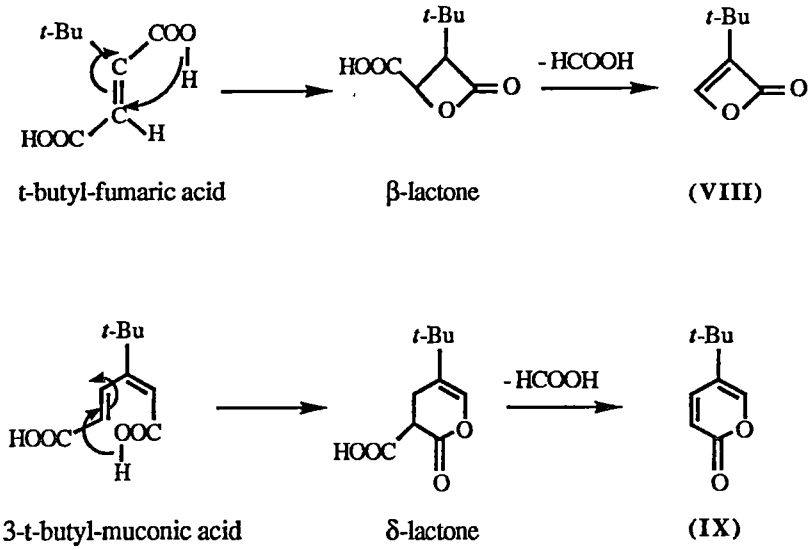

SCHEME 2: Proposed mechanism for lactone formation from *t*-butyl substituted dicarboxylic acids formed by reaction with alkaline peroxide with 4-*tert*-butylorthoquinone.

This mechanism involves ring closure to form lactones followed by decarboxylation. An alternative mechanism for the formation of lactones has been provided by Gierer and Imsgard[21]. It was suggested that lactones of di-carboxylic acids can be formed when alkaline solutions are acidified during work-up, since lactone formation is favoured by neutral to acidic conditions[45]. Because Route A does not involve the formation of coloured or potentially coloured material, it can be regarded as the primary route by which colour is irreversibly removed during the reaction of 4-*tert*-butylorthoquinone with alkaline peroxide.

5.5.3 Reduction of 4-tert-butylorthoquinone - Route B (Scheme 1)

In competition with the fragmentation pathway indicated by Route A is a parallel reductive route which results in the formation of a chromophoric precursor, 4-*tert*-butylcatechol, (II), (Route B). Formation of 4-*tert*-butylcatechol has previously been reported in the oxidation of 4-*tert*-butylorthoquinone with alkaline peroxide[23], however no mechanism for its formation was proposed. Cyclic voltammetric studies of *o*-quinones closely related to 4-*tert*-butylorthoquinone show that reversible

reduction to catechols such as 4-*tert*-butylcatechol takes place with the transfer of 2 electrons[46]. For 4-methylorthoquinone and 4-ethylorthoquinone, the standard reduction potentials were reported as 0.792 V and 0.806 V respectively. *O*-quinones possessing highly branched groups such as the *t*-butyl substituent in 4-*tert*-butylorthoquinone were predicted to exhibit even greater reduction potentials to form catechols. This information suggests that 4-*tert*-butylorthoquinone may spontaneously undergo reduction to form 4-*tert*-butylcatechol in the presence of suitable reducing species. An example redox reaction which may result in reduction of 4-*tert*-butylorthoquinone in peroxide solution is shown in equation (8).

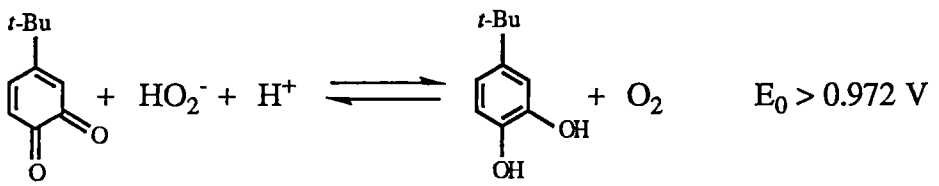

(I) (II) (8)

The calculation of $E_0 > 0.972$ V as the standard potential for equation (8) was based on standard reduction potentials of $E_0 = -0.076$ V for reduction of water and oxygen to perhydroxyl anions[47] and $E_0 > 0.806$ V for the reduction of 4-*tert*-butylorthoquinone to 4-*tert*-butylcatechol[46]. Under the prevailing experimental conditions (constant peroxide concentration, removal of O_2 by purging) the equilibrium in equation (8) might reasonably be expected to lie to the right. This would account for the absence of 4-*tert*-butylorthoquinone and the detection of significant amounts of 4-*tert*-butylcatechol in peroxide reaction mixtures.

5.5.4 Reaction of 4-tert-butylorthoquinone with Alkali - Route C (Scheme 1)

Route C represents the oxidative pathway by which the peroxide resistant chromophore, (III), is created. The results of Stone and Waters[18] and this chapter support the idea that conversion of 4-*tert*-butylorthoquinone to (III) occurs by

nucleophilic attack of hydroxide ions to give an anionic intermediate, which then rearranges to (XVII) (Scheme 3).

The aryloxy-radical (XVIII) is readily produced by the interaction of (XVII) with oxygen radical species such as hydroxyl ($OH^{\cdot}$) and superoxide ($O_2^{-\cdot}$) radicals which can be formed by dissolution of oxygen in alkaline solution or by base induced decomposition of alkaline peroxide[48]. The ESR signal observed in Figure 3 is ascribed to the formation of the intermediate (XVIII) in the reaction of 4-*tert*-butylorthoquinone with alkali. Rearrangement of radical (XVIII) takes place to form (III), which exists as the red coloured anion in alkaline solution. The characteristic red solutions resulting from formation of (III) were not observed in work conducted with nitrogen purging (Section 5.5.2), thus it would appear that (XVII) is stable in relatively oxygen free alkaline solutions where the generation of reactive oxygen radical species such as superoxide ion is restricted.

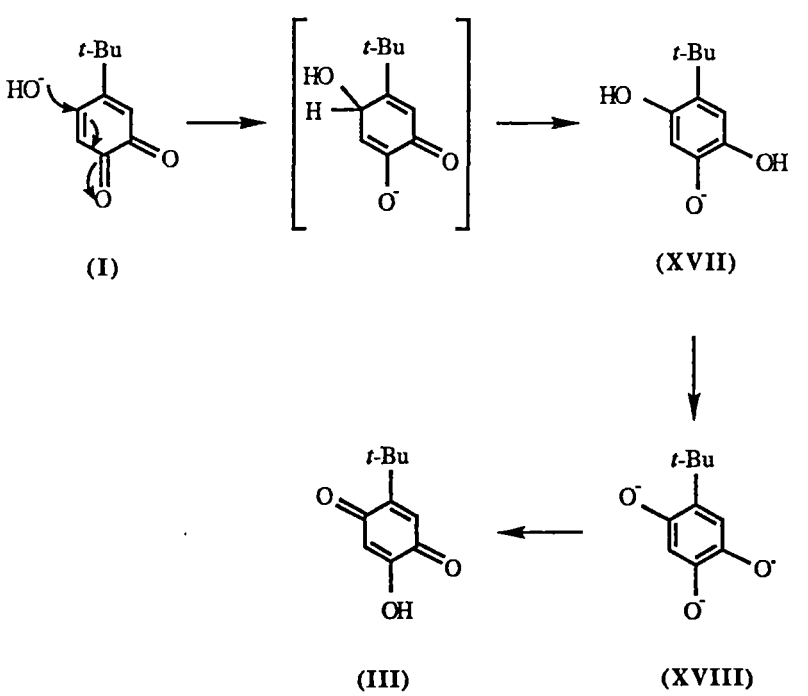

SCHEME 3: Proposed mechanism for formation of (III) from 4-*tert*-butylorthoquinone under alkaline conditions.

5.5.5 *Epoxidation of 4-tert-butylorthoquinone - Route D (Scheme 1)*

Oxidative route (Route D) is responsible for the formation of compounds (IV)-(VI) from 4-*tert*-butylorthoquinone[22,23]. Route D is similar to the scheme proposed for α,β-unsaturated carbonyls in the previous chapter with the reaction being initiated by nucleophilic attack of perhydroxyl anions to form epoxy intermediates. The *o*-quinone is thought to undergo nucleophilic attack by perhydroxyl ions at either C-4 or C-5 to form *o*-quinone mono-epoxides on elimination of hydroxide. Further nucleophilic attack results in formation of an *o*-quinone di-epoxide which is oxidatively cleaved to yield the dicarboxylic acid, (VI). Cleavage of the mono or di-epoxide rings then occurs in a manner analogous to that reported for α,β-unsaturated carbonyls to produce acidic fragments similar to those shown in Route A. Alternatively, oxidative cleavage between the carbonyl groups of the *o*-quinone mono-epoxides can take place to yield mono-epoxide dicarboxylic acids which are subsequently converted to the lactones, (IV) and (V), via intramolecular nucleophilic attack[21-23]. The detection of lactones such as (VII) in the present work (Figure 2) suggests that glyoxylic acid is readily eliminated from (IV) and (V), as shown in Scheme 4, in agreement with Gierer and Imsgard[22].

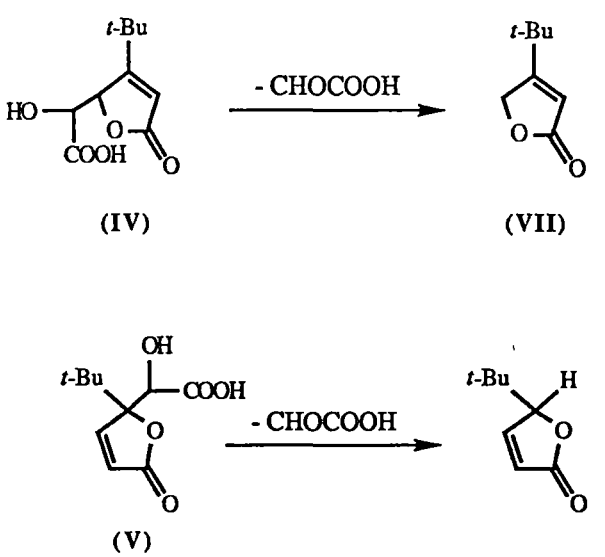

SCHEME 4: Elimination of glyoxylic acid from lactones (IV) and (V) to yield lactone (VII).

5.5.6 Polymerisation Reactions - Route E (Scheme 1)

Bailey and Dence[25] have shown that when sufficiently high concentrations of model guaiacyl *ortho* quinones are present in solution, a less important reaction route involving polymerisation of the *ortho* quinone may occur (Route E). This pathway was confirmed by the detection of small quantities of polymeric material in the current work. Polymerisation of this type has been demonstrated to occur to a much lesser degree for syringyl model compounds[26] and other compounds in which sterically bulky substituents are introduced at positions adjacent to the quinoid group[21,39,40]. This has been attributed to steric protection given by bulky substituents against nucleophilic attack, and resonant deactivation of the α,β-unsaturated ketone systems in *o*-quinones by electron donating substituents[21]. In softwood and hardwood lignins, it is unlikely that *ortho* quinone structures would be free to interact to undergo polymerisation during peroxide bleaching.

5.5.7 Light Absorption Properties of 4-tert-butylorthoquinone Solutions Bleached with Alkaline Peroxide

Compound (III) which is produced by Route C in Scheme 1 is much more resistant to further oxidation with alkaline peroxide than the starting material[23,26], and is most likely responsible for the different levels of residual colour observed in the current work (Figure 5). It is also likely that such peroxide resistant chromophores are at least partly responsible for the so-called brightness 'ceilings' which are observed when lignin rich pulps are bleached with even large excesses of alkaline peroxide[49,50]. The family of extinction coefficient-time curves depicted in Figure 5 are strikingly similar to the analogous light absorption coefficient-time curves obtained when *E. regnans* stone groundwood pulp is treated with alkaline peroxide under constant reagent conditions (Figure 14).

Increasing the alkali concentration can be seen to produce a similar response in the residual colour levels of the *E. regnans* mechanical pulp as measured by light

absorption coefficients (K). A maximum in pulp brightness is achieved at a slightly higher *p*H (*p*H~11.5) than that observed for the *o*-quinone solutions (*p*H ~10.5). The similarity of Figures 5 and 14 indicates that *ortho* quinone structures might contribute at least partly to the overall peroxide bleaching behaviour of *E. regnans* SGW.

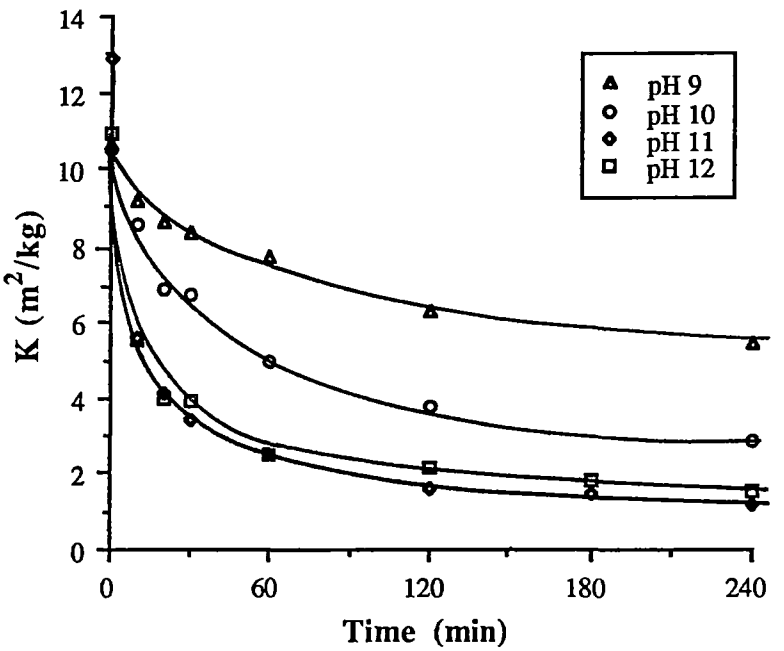

FIGURE 14: Evidence for maximum in the bleaching rate of *E. regnans* pulp in the *p*H range 11-12. Pulp bleached under constant peroxide concentrations (0.118 M peroxide, 50°C, 0.3% pulp consistency).

Equations (1) and (7) suggest that the rate of removal of 4-*tert*-butylorthoquinone is favoured by increasing perhydroxyl anion and alkali concentrations. Formation of the peroxide resistant chromophore (III) is also favoured by increasing alkali concentration (see Scheme 3) and possibly oxygen radical concentration, which is itself promoted by high alkalinities through base induced peroxide decomposition[48]. The maximum in colour removal observed in Figure 5 can be explained in terms of a competition between the degradation of 4-*tert*-butylorthoquinone by reaction with perhydroxyl anions (Routes A, B and D, Scheme 1), and the formation of (III) by

reaction with alkali and oxygen species (Route C). The rate of colour removal represented by Routes A, B and D would be favoured by increasing *p*H due to the positive effect of alkali on perhydroxyl anion concentration. It is conceivable that the colour removing reactions would be dominated by the colour creation reaction (Route C) at higher *p*H levels leading to the observed maximum in bleaching rate at *p*H~10.5.

5.5.8 Reaction Kinetics of 4-tert-butylorthoquinone in Alkaline Peroxide

Given the complexity of the reaction routes depicted in Scheme 1 and the variety of ionic and radical species taking part, it is surprising that the kinetic rate equations for removal of 4-*tert*-butylorthoquinone with alkaline peroxide (equations 1 and 7), are so simple and contain terms involving 4-*tert*-butylorthoquinone and perhydroxyl and hydroxide ions only. The complex reaction scheme and simple rate equations can be rationalised if the rate determining steps in Routes A, B and D (Scheme 1) are assumed to proceed via nucleophilic attack of the perhydroxyl anion on 4-*tert*-butylorthoquinone. The respective rate constants for these processes are k_a, k_b, k_{d1} and k_{d2} as shown in Scheme 5.

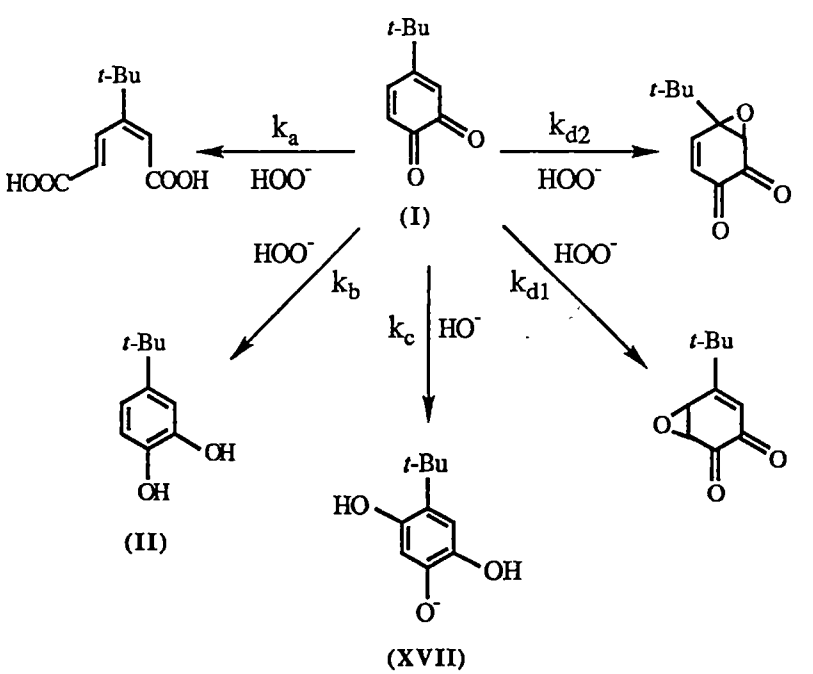

SCHEME 5: Proposed kinetic scheme involving initial attack by perhydroxyl (HOO^-) and hydroxide (OH^-) anions on 4-*tert*-butylorthoquinone.

This assumption of nucleophilic attack by perhydroxyl anions as a rate determining step appears to be a valid one based on the preceding discussion dealing with the reaction of perhydroxyl anions with 4-*tert*-butylorthoquinone (Sections 5.5.1 - 5.5.3). Work conducted in the absence of peroxide suggests that formation of (III) via Route C is initiated by the nucleophilic attack of hydroxide ion with an associated rate constant, k_c. With reference to Scheme 5 and the above assumptions, the rate of removal of 4-*tert*-butylorthoquinone can be written as:

$$-d[\text{Quinone}]/dt = k_a[\text{Quinone}][HOO^-] + k_b[\text{Quinone}][HOO^-] + k_c[\text{Quinone}][OH^-] + k_{d1}[\text{Quinone}][HOO^-] + k_{d2}[\text{Quinone}][HOO^-] \quad (8)$$

This rearranges to:

$$-d[\text{Quinone}]/dt = k_c[\text{Quinone}][OH^-] + \{k_a+k_b+k_{d1}+k_{d2}\}[\text{Quinone}][HOO^-] \quad (9)$$

which is the form of Equations (1) and (7). By direct comparison of Equation (9) with Equations (1) and (7), it can be seen that

$$k_1 = k_c \text{ and}$$

$$k_2 = \{k_a+k_b+k_{d1}+k_{d2}\}$$

The rapid rate at which 4-*tert*-butylorthoquinone reacted with alkaline peroxide at 0°C suggests that *ortho* quinones would be readily eliminated from the lignin matrix under conventional pulp bleaching conditions. The work in this chapter also suggests that *ortho* quinones react at a much faster rate than α,β-unsaturated aldehydes (see previous chapter). Indeed, previous work undertaken with model compounds indicates that *ortho* quinones may exist only as intermediates during alkaline peroxide bleaching[22,25,26]. However UV-visible reflectance spectra of mechanical pulps reacted with excess peroxide for extended durations still exhibit an absorbance peak in the 400-500 nm range attributed to quinone structures[11,12]. The results of this chapter

suggest that the formation of peroxide resistant structures such as (III), which absorb in the same spectral region as 4-*tert*-butylorthoquinone, could be partly responsible for the incomplete removal of the quinone absorbance band in peroxide treated mechanical pulps.

5.6 Conclusions

The reaction of 4-*tert*-butylorthoquinone with alkali and alkaline peroxide results in the formation of a number of products, some of which possess colour and are stable toward further reaction. The wide diversity of reaction products is a reflection of the different modes of nucleophilic attack by which 4-*tert*-butylorthoquinone is degraded in alkaline peroxide solution. Despite the apparent complexity of the modes of reaction, the rate equation for removal of 4-*tert*-butylorthoquinone is remarkably simple and involves terms indicative of bimolecular nucleophilic attack by perhydroxyl (HOO^-) or hydroxide (HO^-) ions as the rate determining step. Coloured, peroxide resistant hydroxyquinones are formed by reaction of 4-*tert*-butylorthoquinone with alkaline peroxide and may be partly responsible for the brightness ceiling observed when mechanical pulps are bleached with alkaline peroxide. The similarity of light absorption-time curves obtained when solutions of 4-*tert*-butylorthoquinone and mechanical pulps are reacted with alkaline peroxide suggests that *o*-quinones may play an important role in the peroxide bleaching of lignin rich pulps. Bleaching reactions resulting from attack by perhydroxyl ions occur at a much faster rate than colour formation reactions for 4-*tert*-butylorthoquinone.

REFERENCES

1. Genuit, W. and Boon, J., Characterisation of Beech Milled Wood Lignin by Pyrolysis-Gas-Chromatography-Photoionisation Mass Spectrometry., *Anal. Chem.*, **59**, 508-13, (1987).

2. Nimz, H., Beech Lignin-Proposal of a Constitutional Scheme., *Angew. Chem. (Int. Ed.)*, **13(5)**, 313-21, (1974).

3. Adler, E., Hernestrom, S. and Wallden, I., Estimation of Phenolic Hydroxyl Groups in Lignin., *Svensk Papperstidning*, **61(18B)**, 641-47, (1958).

4. Glasser, W.G. and Glasser, H.R., Evaluation of Lignin's Chemical Structure by Experimental and Computer Simulation Techniques., *Paperii Puu*, **63(2)**, 71-74, 77-80, 82-83, (1981).

5. Bland, D.E., Eucalypt Lignin., *Appita*, **38(1)**, 53-56, (1985).

6. Lundquist, K. and Ericsson, L., Acid Degradation of Lignin VI. Formation of Methanol., *Acta Chem. Scand.*, **25(2)**, 756-58, (1971).

7. Hemra, L. and Lundquist, K., Acidolytic Formation of Methanol from Quinones and Quinonoid Compounds Related to Lignin., *Acta Chem. Scand.*, **27(1)**, 365- 66, (1973).

8. Imsgard, F., Falkehag, S. and Kringstad, K., On Possible Chromophoric Structures in Spruce Wood., *Tappi*, **54(10)**, 1680-84, (1971).

9. Guist, W., McLellan, F. and Whiting, P., Alkali Darkening and its Similarities to Thermal Reversion, *Tech. Sect. CPPA, 76th Annual Meeting*, B51-60, (1990).

10. Spittler, T. and Dence, C.W., Destruction and Creation of Chromophores in Softwood Lignin by Alkaline Hydrogen Peroxide., *Svensk Papperstidning*, **80(9)**, 275-84, (1977).

11. Polcin, J. and Rapson, W.H., Effects of Bleaching Agents on the Absorption Spectra of Lignin in Groundwood Pulps. Part 1: Reductive Bleaching., *Pulp and Paper Mag. Can.*, **72(3)**, 69-80, (1971).

12. Polcin, J. and Rapson, W.H., Effects of Bleaching Agents on the Absorption Spectra of Lignin in Groundwood Pulps. Part 2: Oxidative-Reductive Bleaching., *Pulp and Paper Mag. Can.*, **72(3)**, 80-91, (1971).

13. Lebo, S., Lonsky, W., McDonough, T., Medvecz, P. and Dimmel, D., The Occurrence and Light Induced Formation of *ortho*-Quinonoid Lignin Structures in White Spruce Mechanical Pulp., *J. Pulp Paper Sci.*, **16(5)**, J139-43, (1990).

14. St. Germain, F. and Gray, D., Photoacoustic Fourier Transform Infra-red Spectroscopic Study of Mechanical Pulp Brightening., *J. Wood Chem. Technol.*, **7(1)**, 33-50, (1987).

15. Holmbolm, B., Ekman, R., Sjoholm, R. and Thornton, J., Chemical Changes in Peroxide Bleaching of Mechanical Pulps., *Das Papier*, **45(10A)**, 16-22, (1992).

16. Pew, J.C. and Connors, W.J., Colour of Coniferous Lignin., *Tappi*, **54(2)**, 245-51, (1971).

17. Gellerstedt, G. and Pettersson, B., Autoxidation of Lignin., *Svensk Papperstidning*, **83(11)**, 314-18, (1980).

18. Stone, T.J. and Waters, W.A., Aryloxyl-radicals. Part IV. Electron Spin Resonance Spectra of Some *ortho*-Monobenzosemiquinones and Secondary Radicals Derived Therefrom., *J. Chem. Soc.*, 1488-94, (1965).

19. Fitzpatrick, J.D. and Steelink, C., The Origin of the Paramagnetic Species in Lignin Solutions. Autoreduction of 2,6-Dimethoxybenzoquinone and Related Quinones to Radical Anions in Alkaline Solution., *J. Org. Chem.*, **37(5)**, 762-67, (1972).

20. Clare, S.I. and Steelink, C., Free Radical Intermediates in the Formation of Chromophores from Alkaline Solutions of Hardwood Lignin Model Compounds., *Tappi*, **56(5)**, 119-23, (1973).

21. Eckert, R.C., Chang, H-M. and Tucker, W.P., Oxidative Degradation of Phenolic Lignin Model Compounds with Oxygen and Alkali., *Tappi*, **56(6)**, 134-38, (1973).

22. Gierer, J. and Imsgard, F., The Reactions of Lignins With Oxygen and Hydrogen Peroxide in Alkaline Media., *Svensk Papperstidning*, **80(16)**, 510-18, (1977).

23. Gellerstedt, G., Hardell, H-L. and Lindfors, E-L., The Reactions of Lignin with Alkaline Hydrogen Peroxide. Part IV. Products from the Oxidation of Quinone Model Compounds., *Acta Chem. Scand.*, **B34(9)**, 669-73, (1980).

24. Reeves, R.H. and Pearl, I.A., Reaction Products Formed Upon the Alkaline Peroxide Oxidation of Lignin Related Model Compounds., *Tappi*, **48(2)**, 121-25, (1965).

25. Bailey, C.W. and Dence, C.W., Reactions of Alkaline Hydrogen Peroxide with Softwood Lignin Model Compounds, Spruce Milled Groundwood Lignin and Spruce Groundwood., *Tappi*, **52(3)**, 491-500, (1969).

26. Kempf, A.W. and Dence, C.W., The Reactions of Hardwood Lignin Model Compounds with Alkaline Hydrogen Peroxide., *Tappi*, **58(6)**, 104-08, (1975).

27. Gellerstedt, G. and Agnemo, R., The Reactions of Lignin With Alkaline Hydrogen Peroxide. Part III. The Oxidation of Conjugated Carbonyl Structures., *Acta Chem. Scand.*, **B34(4)**, 275-80, (1980).

28. Hocking, M.B. and Ong, J.H., Kinetic Studies of Dakin Oxidation of *o*- and *p*- Hydroxyacetophenones., *Can. J. Chem.*, **55**, 102-10, (1977).

29. Omori, S. and Dence, C.W., The Reactions of Stabilised and Unstabilised Alkaline Hydrogen Peroxide With Lignin Model Dimers., *International Symposium of Wood and Pulping Chemistry*, Volume 2, p.112-19, Stockholm, (1981).

30. Nonni, A.J. and Dence, C.W., The Reactions of Alkaline Hydrogen Peroxide With Lignin Model Dimers. Part III: 1,2-Diaryl-1,3-Propanediols., *Holzforschung*, **42**, 37-46, (1988).

31. Pero, R.W. and Dence, C.W., The Role of Transition Metals on the Formation of Colour From Methoxyhydroquinone, an Intermediate in the Peroxide Bleaching of TMP., *J. Pulp Paper Sci.*, **12(6)**, J192-97, (1986).

32. Wozniak, J.C., Dimmel, D.R. and Earl, W.M., The Generation of Quinones from Lignin and Lignin-Related Compounds., *J. Wood Chem. Technol.*, **9(4)**, 491-511, (1989).

33. Gierer, J., The Chemistry of Delignification. Part II., *Holzforschung*, **36**, 55-64, (1982).

34. Gellerstedt, G. and Pettersson, E-L., Light Induced Oxidation of Lignin. Part II. The Oxidative Degradation of Aromatic Rings., *Svensk Papperstidning*, **80(1)**, 15-21, (1977).

35. Leary, G., Photochemical Production of Quinoid Structures in Wood., *Nature*, **217**, 672-73, (1969).

36. Ishikawa, H. and Oki, T., Oxidative Decomposition of Lignin. II. The Degradation by Sodium Peroxide of Aromatic Compounds Structurally Related to Softwood Lignin., *Kami-pa Gikyoshi*, **18(11)**, 477-84, (1964).

37. Gellerstedt, G., Pettersson, I. and Sundin, S., Chemical Aspects of Hydrogen Peroxide Bleaching, *International Symposium of Wood and Pulping Chemistry*, Volume II, p. 120-124, Stockholm, (1981).

38. Takata, T., Tajima, R. and Ando, W., Oxidation of Dihydroxy Aromatics by Hypervalent Iodine Oxides: A Facile Quinone Synthesis., *J. Org. Chem.*, **48(24)**, 4764-66, (1983).

39. Durst, H.D., Mack, M.P. and Wudl, F., A Mild and Efficient Oxidising Agent for Dihydroxybenzenes., *J. Org. Chem.*, **40(2)**, 268-69, (1975).

40. Minisci, F., Citterio, A., Vismara, E., Fontana, F. and De Bernardinis, S., Facile and Convenient Syntheses of Quinones from Phenols., *J. Org. Chem.*, **54(3)**, 728-31, (1989).

41. Silverstein, R.M., Bassler, G.C. and Morrill, T.C., In Spectrometric Identification of Organic Compounds, 4th edition, Chapter 6, 'Ultraviolet Spectroscopy', p 305-331, Wiley and Sons, New York, 1981.

42. Hoskins, R., Paramagnetic Resonance in Semiquinone Ions of Substituted *o*-Benzoquinones., *J. Chem. Physics*, **23**, 1975-76, (1955).

43. Teder, A. and Tormund, D., The Equilibrium Between Hydrogen Peroxide and the Peroxide Ion - A Matter of Importance in Peroxide Bleaching., *Svensk Papperstidning*, **83(4)**, 106-09, (1980).

44. Hewgill, F.R. and Lee, S.L., Oxidation of Alkoxyphenols. Part XV. Autoxidation of 2- and 3- Mono- and 2,5-Di-*tert*-butyl-4-methoxyphenol and Related Compounds., *J.Chem. Soc. (C)*, 1549-56, (1968).

45. Streitwieser, A. and Heathcock, C.H., in Introduction to Organic Chemistry., 2nd edition, Chapter 27, 'Difunctional Compounds', p 858-60, Macmillan Publishing Co., New York, 1981.

46. Proudfoot, G.M. and Ritchie, I.M., A Cyclic Voltammetric Study of Some 4-Substituted Benzene-1,2-diols., *Aust. J. Chem.*, **36**, 885-94, (1983).

47. Weast, R.C. (Editor), in CRC Handbook of Chemistry and Physics., 60th Edition, p. D-156, CRC Press, Boca Raton, Florida, 1979.

48. Roberts, J.L., Morrison, M.M. and Sawyer, D.T., Base Induced Generation of Superoxide Ion and Hydroxyl Radical from Hydrogen Peroxide., *J. Amer. Chem. Soc.*, **100(1)**, 329-330, (1978).

49. Lundqvist, M., Kinetics of Hydrogen Peroxide Bleaching of Mechanical Pulp., *Svensk Papperstidning*, **82(1)**, 16-21, (1979).

50. Moldenius, S. and Sjogren, B., Kinetic Models for Hydrogen Peroxide Bleaching of Mechanical Pulps., *J. Wood Chem. Technol.*, **2(4)**, 447-71, (1982).

CHAPTER 6

DISCUSSION

The main objective of this chapter is to draw together information from the bleaching of *E. regnans* SGW and reactions of model lignin chromophores to provide an overall picture of the kinetic processes taking place under peroxide bleaching conditions. To achieve this aim, it is necessary to relate the kinetic behaviour of the lignin model chromophores studied to the bleaching kinetics of mechanical pulps. This is not a straightforward process since the reaction systems in each case are fundamentally different.

Firstly, the peroxide bleaching of mechanical pulp takes place in a heterogeneous system where the bleaching reagents must react with chromophoric structures incorporated in the lignin macromolecule. As a result of their inclusion in a polymeric system, these chromophores will most likely be stabilised to some degree, compared with the analogous monomers, due to electron delocalisation. Steric protection of the chromophores by adjacent units in the lignin polymer could also limit the ability of bleaching chemicals to reach the reaction site, providing further stability against reaction. In contrast, the kinetic study of model lignin chromophores is carried out with monomeric compounds in solution where the chromophores are more accessible towards degradation with alkaline peroxide. As a consequence, the absolute reaction rates of model chromophores in solution are probably higher than those of equivalent structures in lignin.

The kinetic study of reactions between alkaline peroxide and model chromophores are also generally performed under different experimental conditions to those used in kinetic bleaching studies on pulp. The reaction conditions used in Chapters 2 - 5 are summarised in Table 1. The Table shows that milder conditions of temperature and

reagent concentration were necessary in kinetic studies on cinnamaldehyde and 4-*tert*-butylorthoquinone, compared with the bleaching of *E. regnans* pulp. These relatively mild conditions were required to ensure that reactions for kinetic study did not proceed too quickly to be measured. For example, the reaction of 4-*tert*-butylorthoquinone with alkaline peroxide went to completion almost instantaneously at 25°C (see section 5.3.6). At 0°C, the reaction still occurred too quickly at *p*H levels above *ca.* 8.5. This led to a narrower range of practical reaction conditions for kinetic studies compared with mechanical pulp (*p*H 8.1 - 8.2, 0.006 - 0.015 M H_2O_2).

TABLE 1 : Reaction conditions used in the study of peroxide bleaching kinetics of *E. regnans* SGW and model lignin compounds in Chapters 2 - 5.

Experiment	H_2O_2 (M)	*p*H	Solvent	Temperature (°C)
Bleaching kinetics of *E. regnans* (Chapters 2 - 3)	0.03 - 0.35	9 - 12	H_2O	50
Cinnamaldehyde kinetics (Chapter 4)	0.10 - 0.29	9.2 - 10.8	1:1 H_2O / MeOH	17 - 35
	-	12.2 - 12.6	"	25
	0.007 - 0.020	9.3 - 9.4	H_2O	25
4-*tert*-butylorthoquinone kinetics (Chapter 5)	0.006 - 0.015	8.1 - 8.2	H_2O	0
	-	11.0 - 11.4	H_2O	0 - 40
Light absorption properties of 4-*tert*-butyl-orthoquinone solutions	0.01 - 0.04	8 - 12	H_2O	0

Due to the differences in reaction conditions in Table 1, it is possible that model chromophores might have displayed slightly different kinetic behaviour had they been exposed to alkaline peroxide under pulp bleaching conditions. For instance, the

limited solubility of cinnamaldehyde in aqueous solution necessitated the use of a 1:1 water / methanol solvent system in kinetic studies in Chapter 4. Methanol is known to quench hydroxyl radical reactions[1] by reacting with these species to give methoxyl radicals and water. As a consequence, the presence of methanol may have prevented the electrophilic addition of hydroxyl radicals generated by peroxide decomposition to double bonds in the chromophoric system[2]. This would result in a simplified view of the kinetics of α,β-unsaturated aldehyde elimination. Reactions due to dissolved oxygen[3] were also minimised in kinetic studies of cinnamaldehyde and 4-*tert*-butylorthoquinone bleaching to facilitate comparison with previous kinetic studies[4-6]. This was done by purging the solutions with nitrogen. The same purging was not applied during the bleaching of *E. regnans* SGW, hence molecular oxygen absorbed from the air or generated by peroxide decomposition would have been free to react with carbanions in lignin via electrophilic attack[3]. As a result, the reactions of model α,β-unsaturated aldehydes and *ortho* quinones may not represent the full range of reactions involving these chromophores in the bleaching of pulp.

Quite mild conditions of temperature were used in kinetic studies on the model *o*-quinone, 4-*tert*-butylorthoquinone, and this may also have resulted in different kinetic observations than would be expected under pulp bleaching conditions. At 0°C, 4-*tert*-butylorthoquinone was found to react with alkaline peroxide at a rapid rate to produce the coloured compound, 2-*tert*-butyl-5-hydroxy-benzoquinone, as one of a number of products (see Scheme 1, Chapter 5). This compound resisted further reaction with peroxide and caused a limit to the amount of colour which could be removed from solution (see Figure 1a). However, at the temperature used to study the bleaching kinetics of *E. regnans* (50°C), the same structure has been reported to react slowly with alkaline peroxide to produce colourless dicarboxylic acids[4]. This would eventually lead to the complete elimination of colour in a slower bleaching phase similar to that observed in mechanical pulp bleaching (Figure 1b). As a consequence, the kinetic behaviour of 4-*tert*-butylorthoquinone at 0°C probably gives an incomplete picture of the kinetic behaviour of *ortho* quinones during the bleaching of mechanical pulp at 50°C.

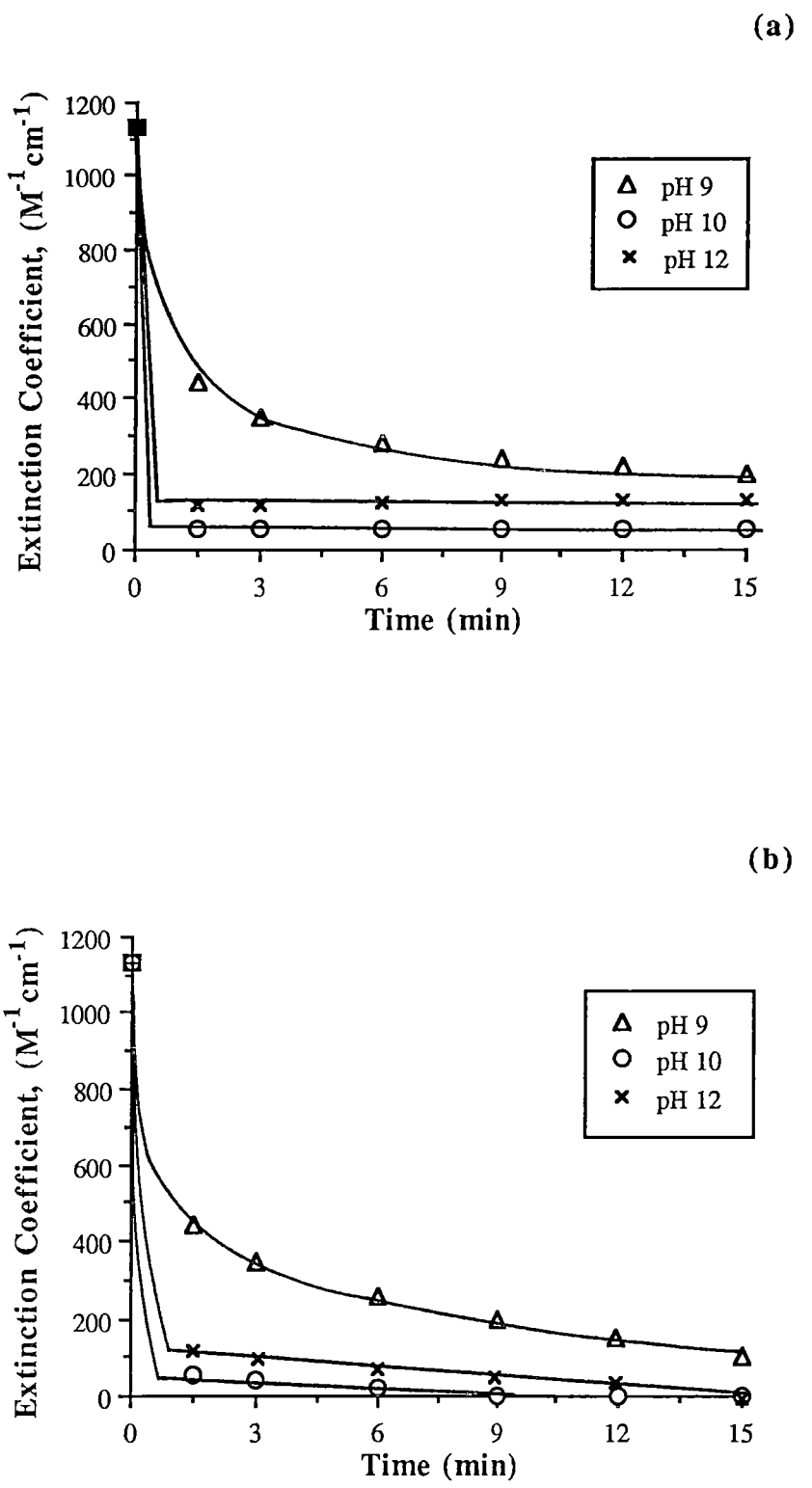

Figure 1: Kinetic profiles showing the elimination of colour from solutions of 4-*tert*-butylorthoquinone reacted with alkaline peroxide, as measured by molar extinction coefficient at 400 nm. (a) experimental behaviour from kinetic studies at 0°C, 0.01 M peroxide. (b) approximation of the predicted kinetic behaviour at 50°C, 0.01 M peroxide based on the results of Gellerstedt *et al*[4].

For the reasons mentioned above, the rate constants of the model compounds studied could not all be evaluated at a common temperature (see Table 1). However estimates of some of the rate constants for colour removal and colour creation reactions involving α,β-unsaturated aldehydes and *ortho* quinones have been made at 25°C, based on their values at other temperatures (Table 2). For example, the second order rate constant representing elimination of 4-*tert*-butylorthoquinone by perhydroxyl ion attack (see Scheme 1b) was found to have a value of 256 L $mol^{-1}s^{-1}$ at 0°C. Assuming a positive effect on reaction rate with increasing temperature, the rate constant for the same reaction at 25°C will most likely be much higher than the value at 0°C. By the same argument, the second order rate constant for the elimination of coniferaldehyde at 25°C (Scheme 3b) should have a lower value at 25°C than that reported by Gellerstedt and Agnemo at 30°C[7] (0.03 L $mol^{-1}s^{-1}$). The second order rate constant for the nucleophilic addition of hydroxide ion to 4-*tert*-butylorthoquinone (Scheme 2) was found to have a value of 0.56 L $mol^{-1}s^{-1}$ in Chapter 5, however the kinetics of the subsequent reaction with oxygen to form 2-*tert*-butyl-5-hydroxy-benzoquinone were not studied, since oxygen was excluded from the reaction system in kinetic runs. If addition of hydroxide ion is the rate determining step, then the second order rate constant for the formation of 2-*tert*-butyl-5-hydroxy-benzoquinone from 4-*tert*-butylorthoquinone will have a value close to 0.56 L $mol^{-1}s^{-1}$. However, if reaction with oxygen is the rate determining step, then the rate constant for the same process will be somewhat lower, as shown in Table 2.

TABLE 2 : Second order rate constants for major colour removal and colour creation reactions involving model α,β-unsaturated aldehydes and *ortho* quinones. T = 25°C.

Reaction	Reaction Scheme	2nd Order Rate Constant (L $mol^{-1}s^{-1}$)
4-*tert*-butylorthoquinone + HO_2^-	1(b)	> 256
Cinnamaldehyde + HO_2^-	1(a)	8.6
Coniferaldehyde Methyl Ether + HO_2^-	1(a)	1.34‡
4-*tert*-butylorthoquinone + OH^-	2	≤ 0.56
Coniferaldehyde + HO_2^-	3(b)	< 0.03*
2-*tert*-butyl-5-hydroxy-benzoquinone + HO_2^-	3(a)	~ 0†

‡ Value at 25°C obtained using the Arrhenius equation and the activation energy for the reaction over a 0 - 30°C temperature range[7].
* Value obtained at 30°C[7].
† No reaction observed at 25°C.

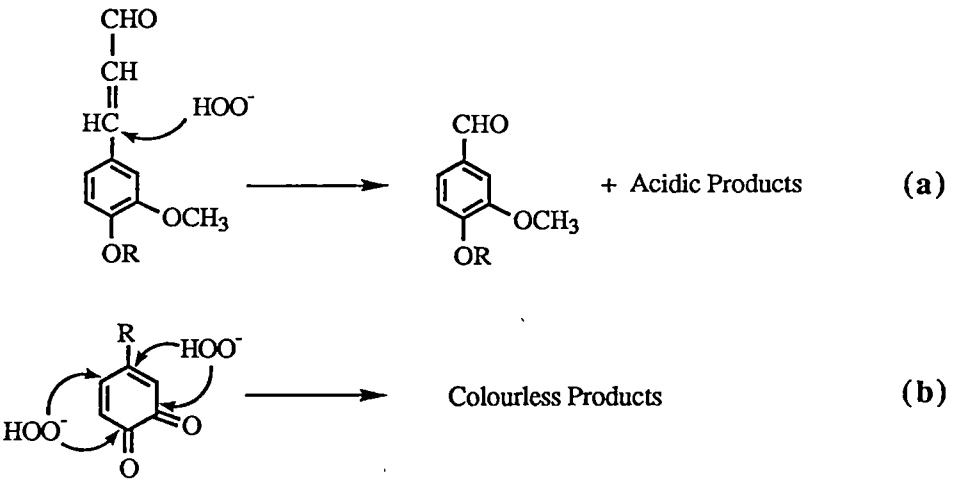

SCHEME 1: Bleaching reactions associated with the rapid elimination of chromophoric structures (a) removal of etherified α,β-unsaturated carbonyls, (b) removal of *o*-quinones. R = lignin

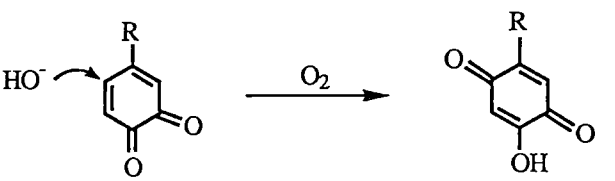

SCHEME 2: The formation of coloured 4-hydroxy *para* quinones, initiated by reaction of *o*-quinones with alkali, followed by hydrogen abstraction and radical formation in the presence of oxygen.

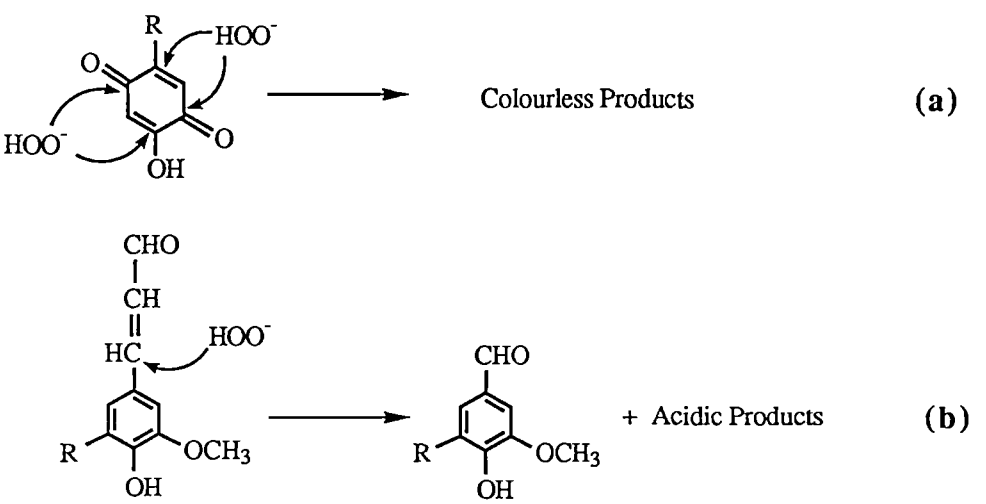

SCHEME 3: Bleaching reactions associated with the slow elimination of chromophoric structures (a) removal of 4-hydroxy *para* quinones after Gellerstedt *et al*[4], (b) removal of phenolic α,β-unsaturated carbonyls. R = lignin.

As mentioned previously, the oxidative fragmentation of 2-*tert*-butyl-5-hydroxy-benzoquinone to carboxylic acids by reaction with perhydroxyl anion (Scheme 3a) was not observed at 0°C (see Figure 1a). At 25°C, 4-*tert*-butylorthoquinone reacted rapidly with alkaline peroxide to yield the coloured *para* quinone as a reaction product, however no further reaction took place as reflected by the constant molar extinction coefficient in Figure 2. Thus, no estimate of the rate constant for this process was possible at 25°C, although 2-*tert*-butyl-5-hydroxy-benzoquinone is known to react slowly with alkaline peroxide at 50°C[4].

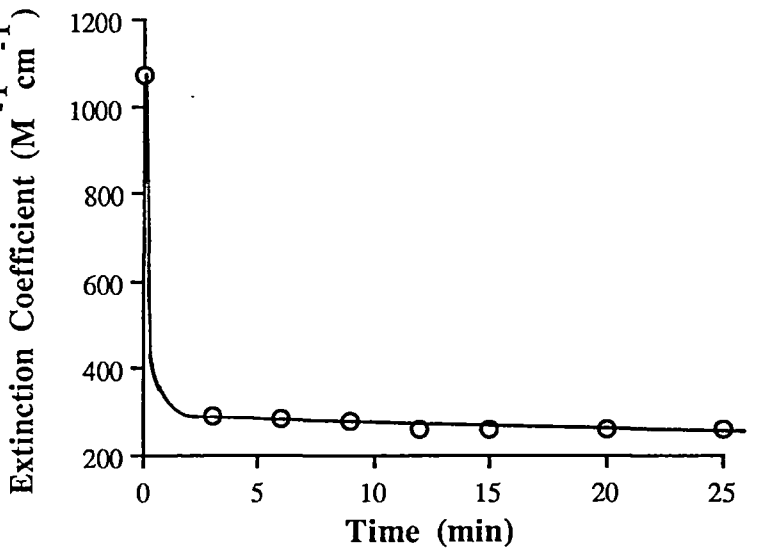

Figure 2: Extinction coefficient - time curve for the reaction of 4-*tert*-butyl-orthoquinone with alkaline peroxide at 25°C, 0.02 M H_2O_2, *p*H 9.

The preceding discussion has shown that the kinetics of reactions involving model chromophores may not accurately mirror the full range of kinetic behaviour associated with these chromophores during the bleaching of pulp. However, useful information about the kinetics of mechanical pulp bleaching can be extracted from model kinetic studies if the relative reaction rates of model α,β-unsaturated aldehydes and *ortho* quinones are assumed to be approximately the same in pulp as in solution. Based on

this assumption, the relative magnitudes of second order rate constants in Table 2 allow the reactions of α,β-unsaturated aldehydes and *ortho* quinones to be roughly divided into three categories, according to their relative rates of reaction and the nature of the products formed. These three reaction categories are shown in Schemes 1 - 3. The reactions in Schemes 1 - 3 can be further associated with different aspects of kinetic behaviour observed during the peroxide bleaching of *E. regnans* SGW under constant reagent conditions.

The first reaction category comprises rapid bleaching reactions where *o*-quinones and non-phenolic α,β-unsaturated aldehydes are irreversibly converted to colourless products (Scheme 1). The relative rates of these reactions suggest that Scheme 1 can be linked to the initial loss of colour seen in the bleaching of mechanical pulps. Colour creating reactions involving the conversion of *o*-quinones to more peroxide resistant hydroxy *p*-quinones (Scheme 2) make up the second group of reactions. In Chapter 5 it was shown that these reactions are able to at least partly explain the maximum in bleaching rate observed for mechanical pulps in the *p*H 11-12 range. The final category of reactions consists of slow bleaching reactions in which hydroxy *p*-quinones and phenolic α,β-unsaturated aldehydes are irreversibly converted to colourless products (Scheme 3). The slow relative rates of these reactions suggest that Scheme 3 can be associated with the levelling off in the bleaching response of mechanical pulps once the more easily eliminated chromophores are removed.

It was demonstrated in Chapter 2 that the kinetic bleaching response of *E. regnans* SGW could be adequately described by a two chromophore consecutive reaction model (see Figure 3). If the identification of Schemes 1 - 3 with similar aspects of kinetic behaviour observed for *E. regnans* SGW is valid, then reactions involving α,β-unsaturated aldehydes and *ortho* quinones can apparently account for the same bleaching responses described by the model in Figure 3.

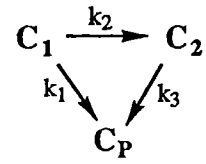

FIGURE 3: The two chromophore consecutive reaction model for the alkaline peroxide bleaching of *E. regnans* mechanical pulp under constant reagent concentrations.

The reaction scheme in Figure 3 was defined in terms of two chromophoric categories, C_1 and C_2. The C_1 category was assumed to react quickly with alkaline peroxide while the C_2 category was much more resistant to bleaching. Although the two chromophore model and the reactions in Schemes 1 - 3 were derived from separate kinetic experiments performed under slightly different conditions, the two schemes share several kinetic similarities, particularly with respect to relative rates of reaction.

The absolute values of the pseudo-first order rate constants, k_1 - k_3, in Figure 3 are not directly comparable with the second order rate constants for the model compounds in Table 2, since both sets of rate constants describe processes of different orders. Nevertheless, the relative values of k_1 - k_3 obtained by fitting the two chromophore model to the kinetic bleaching response of *E. regnans* SGW (see Table 3) are, to a broad approximation, similar in magnitude to the relative rates for Schemes 1 - 3 shown in Table 2. For instance, the reactions associated with the rapid elimination of model chromophores in Scheme 1 are parallelled by the conversion of easily removable chromophores, C_1, to colourless products, C_P, in Figure 3. The formation of more peroxide resistant chromophores from *ortho* quinones in Scheme 2 is similar in character and in relative rate to the C_1 to C_2 step in Figure 3, where harder to remove chromophores are formed from more easily removable ones. Finally, the slow elimination of chromophores in Scheme 3 to give colourless products is mirrored by the C_2 to C_P step in Figure 3, which has the slowest relative rate in Tables 2 and 3. Without more detailed information regarding the kinetics of bleaching reactions in mechanical pulp, it is difficult to say whether these similarities are merely

fortuitous, or whether Figure 3 and Schemes 1 - 3 both represent the same underlying kinetic processes which are fundamental in the peroxide bleaching of pulp.

TABLE 3: Typical values of rate constants for the two chromophore model.

Rate Constant (min^{-1})†	*p*H 9	*p*H 10	*p*H 11	*p*H 12
k_1	0.015 - 0.028	0.015 - 0.038	0.046 - 0.12	0.075 - 0.096
k_2	0.020 - 0.028	0.007 - 0.012	0.004 - 0.007	0.002 - 0.010
k_3	0.001	0.001	0.001	0.001

† Rate constants over a 0.06 - 0.18 M peroxide concentration range.

A model such as the two chromophore reaction model can reveal important aspects of underlying kinetic behaviour during peroxide bleaching, however, on a molecular level, the reaction steps probably do not represent the real chemical processes taking place during bleaching. In formulating the kinetic models in Chapters 2 and 3, chromophores possessing similar kinetic bleaching behaviour were grouped together as single 'lumped constituent' species which were assumed to react via elementary pseudo-first order processes. As a result of this simplification, pseudo-first order rate constants for each of the model steps in Figures 3 and 4 showed no simple dependence on reagent concentration.

$$C \underset{k_5}{\overset{k_4}{\rightleftharpoons}} C_L \xrightarrow{k_6} C_P$$

FIGURE 4 : Equilibrium kinetic model for the bleaching of *E. regnans* mechanical pulp under conditions of constant reagent concentration.

For example, the conversion of C_1 to C_P in Figure 3 was assumed to take place in an elementary step with a first order rate constant of k_1. It was recognised in Chapter 2 that the non-linear dependence of k_1 on perhydroxyl ion (HO_2^-) signified a more complex sequence of processes than that described by the simple reaction of C_1 to give C_P. A consecutive reaction involving an intermediate species C_1^* (Figure 5) was proposed to explain the non-linear correlation between k_1 and perhydroxyl anion concentration. A different reaction mechanism involving an intermediate species, C_I, (see Figure 6) was proposed to account for the same non-linear correlation between k_4 and HO_2^- concentration in the equilibrium model in Figure 4. Based on the kinetic behaviour of model *ortho* quinones and α,β-unsaturated aldehydes, an alternative explanation for these non-linear correlations might be to associate the C_1 to C_P step in Figure 3, or the C to C_L step in Figure 4 with at least two parallel reactions where *o*-quinones and non-phenolic α,β-unsaturated aldehydes are quickly degraded by reaction with perhydroxyl anion (Scheme 1).

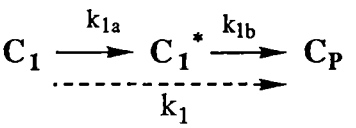

FIGURE 5: Proposed mechanism for C_1 to C_P conversion in the two chromophore consecutive reaction model (see Figure 3).

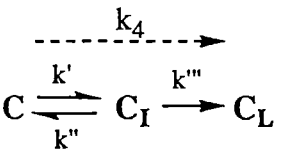

FIGURE 6: Proposed mechanism for C to C_L conversion in the equilibrium kinetic model shown in Figure 4.

It is likely that the two chromophore model reflects some of the more important kinetic aspects of peroxide bleaching chemistry, however its main drawback is that it could

not explain several kinetic observations when reagent concentrations were adjusted to different levels part way through the bleaching of *E. regnans* SGW (section 3.3.1, Chapter 3). The main kinetic features observed were:

(1) A slight darkening of the pulp following the sudden increase of *p*H from 11 to 12 at constant peroxide concentration. The bleaching profile at *p*H 11 was shifted from its original level to a higher level corresponding to the higher *p*H.

(2) An increase in the rate of brightening following the sudden increase of peroxide concentration at constant *p*H. The original bleaching profiles shifted to new, lower levels corresponding to higher peroxide concentrations.

In Chapter 3, several 'equilibrium' models were developed to explain this additional kinetic behaviour, as well as the kinetic behaviour described by the two chromophore consecutive reaction model in Figure 3. The equilibrium model was based on the reversible conversion of chromophores (C) to chromophoric precursors (C_L) and the irreversible reaction of chromophoric precursors (C_L) to give colourless products (C_P) (Figure 4). By incorporating a chromophore creation step in the reaction scheme, the equilibrium model was able to describe the full range of kinetic behaviour observed for *E. regnans* SGW in Chapters 2 and 3. The relative rates of the pseudo-first order rate constants, k_4 - k_6, (see Table 4) are similar to those in Table 3, however the reaction steps in the equilibrium model are not as readily associated with the reactions in Schemes 1 - 3, as was the case for the two chromophore model.

TABLE 4: Typical values of rate constants for the equilibrium model (see Figure 4).

Rate Constant (min^{-1})†	*p*H 9	*p*H 10	*p*H 11	*p*H 12
k_4	0.020 - 0.038	0.015 - 0.038	0.049 - 0.13	0.072 - 0.083
k_5	0.063 - 0.098	0.015 - 0.023	0.027 - 0.039	0.020 - 0.046
k_6	0.002 - 0.003	0.002 - 0.003	0.002 - 0.003	0.002 - 0.003

† Rate constants over a 0.06 - 0.18 M peroxide concentration range.

The need for some mechanism of colour formation from colourless structures suggests that chromophore creation is an important process in the peroxide bleaching of pulp. Model compound studies in this thesis concentrated exclusively on the kinetics of chromophore elimination during bleaching with alkaline peroxide, however according to the equilibrium model, kinetic processes leading to formation of chromophores from colourless compounds are just as important as chromophore removal.

Previous studies on model lignin compounds provide several possibilities for explaining chromophore formation from non-chromophoric precursors in peroxide bleaching. It has been shown that demethoxylation of model phenolic and non-phenolic structures can produce catechols and phenols respectively via hydroxyl radical attack[2] (Scheme 4). The kinetics of these processes have not been well defined, however a complex product distribution, which is dependent on *p*H, has been observed for the model lignin compound, veratrylglycol[8]. The catechols and phenols produced by radical mechanisms, or found naturally in lignin[17] can be further oxidised in alkaline peroxide to give *ortho* quinone chromophores[6,9,17]. A proportion of the *ortho* quinones may then be subsequently converted to more stable hydroxy *para* quinone chromophores by the route in Scheme 2, leading to a stable source of colour.

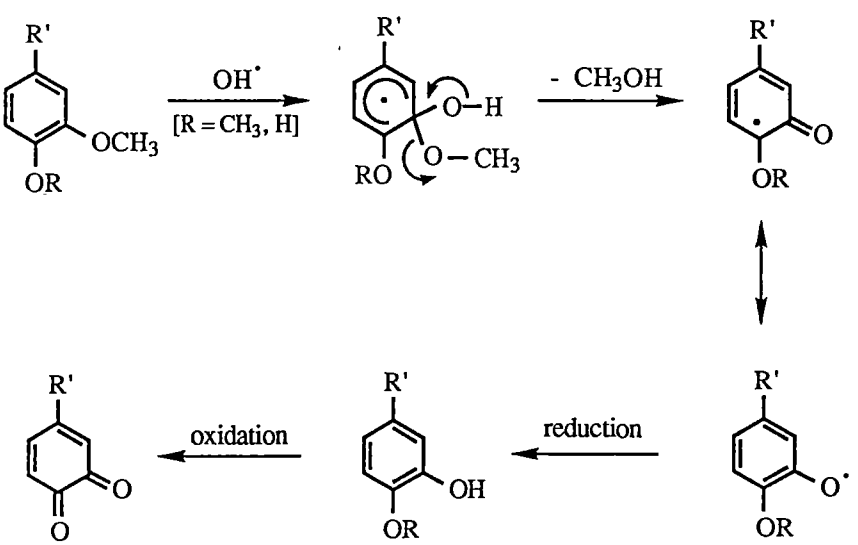

SCHEME 4: Proposed scheme for the demethoxylation of non-chromophoric structures to give *o*-quinones in the presence of alkaline peroxide (after Reitberger *et al*[2], Bailey and Dence[6] and Stone and Waters[9]).

The formation of stilbenes from 1,2-diarylpropane-1,3-diol structures has also been proposed as a colour producing reaction[10] based on the reaction of model structures (Scheme 5). These structures have been estimated to occur at a frequency of about 7 units per 100 phenylpropane units in spruce lignin[10]. The formation of stilbene structures is catalysed by ionisation of the phenolic starting material under alkaline conditions, followed by rearrangement and elimination of formaldehyde or hydrogen. As a consequence, the rate of stilbene formation depends only on the concentration of alkali and starting material. Such a mechanism of chromophore formation, involving alkali only, can explain why a slight darkening of *E. regnans* SGW was observed when *p*H was increased from 11 to 12 during bleaching, but not when peroxide concentration was decreased from 0.12 M to 0.01 M at constant *p*H (see section 3.3.1, Chapter 3).

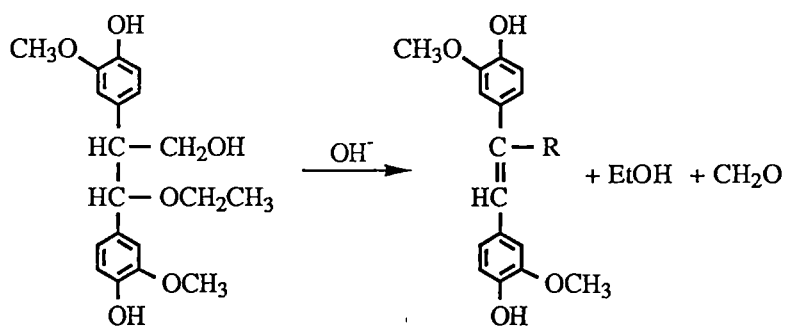

stilbene

R = H, CH_2OH

SCHEME 5: Proposed scheme for the conversion of a model 1,2-diarylpropane-1,3-diol structure to stilbenes in the presence of alkali (after Gellerstedt *et al*[10]).

Directions For Future Work

Many unanswered questions remain regarding the kinetics of reactions under alkaline peroxide bleaching conditions. This is particularly true with respect to the colour

producing reactions discussed previously. As a consequence, considerable scope exists for future work related to the characterisation of darkening reactions during peroxide bleaching. Firstly, model compound studies are required which focus on the reactions of the main non-chromophoric units in lignin with alkaline peroxide and radical species generated by peroxide decomposition. These studies are necessary in order to identify the likely reaction mechanisms responsible for chromophore formation during peroxide bleaching. Among the structural units worthy of further kinetic study are phenolic compounds, which are easily oxidised to quinones[5,6,9], and structures such as phenylcoumarans and 1,2-diarylpropane-1,3-diols, which may give rise to α,β - unsaturated structures such as stilbenes upon oxidation[10,11]. Once the principal darkening routes have been identified, techniques such as ^{13}C-nmr could be used to verify the occurrence of the same darkening reactions in pulp or in lignin preparations such as milled wood lignin, since quinones and stilbenes exhibit characteristic signals in ^{13}C-nmr spectra[11].

Further kinetic studies on the reactions of α,β-unsaturated aldehydes and *ortho* quinones in lignin are also required to confirm the results of this thesis, especially with regard to the relative reaction rates of these chromophores. Several techniques exist for studying the elimination of α,β-unsaturated aldehydes from pulp or milled wood lignin under conventional peroxide bleaching conditions. These techniques include the use of specific colour reagents, such as the phloroglucinol - HCl reagent developed by Adler and co-workers[12-14], and the method recently described by Pan and Lachenal[15] involving derivatisation by thioacidolysis followed by Raney nickel desulfuration. A kinetic analysis of α,β-unsaturated aldehyde elimination in lignin should also be possible using ^{13}C-nmr, given that the carbonyl carbon in these structures produces a readily identifiable, quantitative signal at about $\delta = 194$ ppm[11].

Nuclear magnetic resonance techniques also exist for the direct study of *ortho* quinone kinetics under alkaline peroxide bleaching conditions. Lebo *et al*[16] have described a sensitive technique involving the specific tagging of *o*-quinones in pulp with trimethyl

phosphite. The removal of *o*-quinones can be easily followed during bleaching using ^{31}P-nmr since phosphorous is a foreign element in pulp. It is also possible to study *ortho* quinone elimination *in-situ* by ^{13}C-nmr since quinone carbonyls give a characteristic signal at $\delta \sim 180$ ppm[11], however the ^{31}P-nmr method is likely to result in a more sensitive analysis.

REFERENCES

1. Kochi, J.K. and Krusic, P.J., in Essays on Free-Radical Chemistry - Special Publication 24., Chapter 7, 'ESR Studies of Free-Radicals in Non-Aqueous Solution.', p. 147-199, The Chemical Society, London, 1970.

2. Reitberger, T., Gierer, J., Jansbo, K., Yang, E. and Yoon, B-H., On the Participation of Hydroxyl Radicals in Oxygen and Hydrogen Peroxide Bleaching Processes., *6th Int. Symp. Wood and Pulp. Chem.,* Vol. 1, 93-97, (1991).

3. Gierer, J. and Imsgard, F., The Reactions of Lignins With Oxygen and Hydrogen Peroxide in Alkaline Media., *Svensk Papperstidning*, **80(16)**, 510-18, (1977).

4. Gellerstedt, G., Hardell, H-L. and Lindfors, E-L., The Reactions of Lignin with Alkaline Hydrogen Peroxide. Part IV. Products from the Oxidation of Quinone Model Compounds., *Acta Chem. Scand.*, **B34(9)**, 669-73, (1980).

5. Kempf, A.W. and Dence, C.W., The Reactions of Hardwood Lignin Model Compounds with Alkaline Hydrogen Peroxide., *Tappi*, **58(6)**, 104-08, (1975).

6. Bailey, C.W. and Dence, C.W., Reactions of Alkaline Hydrogen Peroxide with Softwood Lignin Model Compounds, Spruce Milled Wood Groundwood Lignin and Spruce Groundwood., *Tappi*, **52(4)**, 491-500, (1969).

7. Gellerstedt, G. and Agnemo, R., The Reactions of Lignin With Alkaline Hydrogen Peroxide. Part III. The Oxidation of Conjugated Carbonyl Structures., *Acta Chem. Scand.*, **B34(4)**, 275-80, (1980).

8. Jansbo, K., Reitberger, T. and Gierer, J., Mechanisms of Hydroxyl Radical Reactions with Lignin Studied with a Simple Model System., *6th Int. Symp. Wood and Pulp. Chem.*, Vol. 1, 157-60, (1991).

9. Stone, T.J. and Waters, W.A., Aryloxyl-radicals. Part IV. Electron Spin Resonance Spectra of Some *ortho*-Monobenzosemiquinones and Secondary Radicals Derived Therefrom., *J. Chem. Soc.*, 1488-94, (1965).

10. Gellerstedt, G. and Agnemo, R., The Reactions of Lignin with Alkaline Hydrogen Peroxide. Part V. The Formation of Stilbenes., *Acta Chem. Scand.*, **B34(6)**, 461-62, (1980).

11. Sjöholm, R., Holmbolm, B. and Åkerback, N., Studies of the Photo-degradation of Spruce Lignin by NMR Spectroscopy., *J. Wood Chem. Technol.*, **12(1)**, 35-52, (1992).

12. Adler, E., and Ellmer, L., Coniferyl Aldehyde Groups in Wood and in Isolated Lignin Preparations., *Acta Chem. Scand.*, **2**, 839-40, (1948).

13. Gupta, V.N., Carbonyl Chromophores in Eastern Canadian Groundwood., *Pulp and Paper Mag. Can.*, **73(6)**, 57-61, (1972).

14. Hirashima, H. and Sumimoto, M., Fundamental Properties of Mechanical Pulp Lignins II. Behaviour of Coniferyl Aldehyde Type Structures in Pulp Lignin., *Mokuzai Gakkaishi*, **33(1)**, 31-41, (1987).

15. Pan, X. and Lachenal, D., Structure and Reactivity of Spruce Mechanical Pulp Lignins. Part I. Bleaching and Photo-Yellowing of *In-Situ* Lignins., *J. Wood Chem. Technol.*, **12(2)**, 135-47, (1992).

16. Lebo, S., Lonsky, W., McDonough, T., Medvecz, P. and Dimmel, D., The Occurrence and Light Induced Formation of *ortho*-Quinonoid Lignin Structures in White Spruce Mechanical Pulp., *J. Pulp Paper Sci.*, **16(5)**, J139-43, (1990).

17. Gellerstedt, G., Pettersson, I. and Sundin, S., Chemical Aspects of Hydrogen Peroxide Bleaching, *International Symposium of Wood and Pulping Chemistry*, Volume II, p. 120-124, Stockholm, (1981).

The kinetic bleaching response of *E. regnans* stone groundwood under constant reagent conditions can be successfully described by two simple kinetic models defined in terms of first order processes. The Two Chromophore Consecutive Reaction Model gives adequate agreement between theoretical and experimental results when constant reagent concentrations are maintained, but cannot account for the observed bleaching responses when *p*H or peroxide levels are increased during bleaching. Equilibrium Models are able to describe the full range of experimental kinetic behaviour, including bleaching responses when bleached pulp is exposed to a new set of constant reagent conditions. The success of the Equilibrium Models is attributed to the inclusion of a chromophore creation step in the reaction scheme. Analysis of the behaviour of pseudo-first order rate constants for each model suggests that perhydroxyl anions are responsible for the main bleaching reactions, while alkali produces an inhibiting effect. The pseudo-first order rate constants exhibit non-linear dependence on reagent concentrations and this indicates that more complex reactions take place than are assumed in the kinetic model schemes.

Parallel kinetic studies with a model lignin α,β-unsaturated aldehyde, cinnamaldehyde, have shown that the main bleaching reactions involving α,β-unsaturated aldehydes result in epoxidation of the α,β double bond followed by ring opening and side chain cleavage to yield benzaldehyde and acidic fragments. The reactions are first order in the organic substrates and perhydroxyl ion (HO_2^-), and second order overall thus indicating a mechanism of bimolecular nucleophilic addition as the rate determining step. Methoxy and hydroxy aromatic substituents reduce the rate of α,β-unsaturated aldehyde elimination in the order: unsubstituted aldehyde > 3,4-dimethoxy substituted aldehyde >> 3-methoxy-4-hydroxy substituted aldehyde.

The reaction of a model lignin *ortho* quinone, 4-*tert*-butylorthoquinone, with alkaline peroxide and alkali results in the formation of a number of products The kinetic

behaviour of 4-*tert*-butylorthoquinone suggests that bleaching reactions occur by several different routes involving bimolecular nucleophilic attack of perhydroxyl ions as the rate determining step. A colour formation reaction, initiated by the nucleophilic attack of hydroxide ion on 4-*tert*-butylorthoquinone, competes with bleaching reactions and leads to the incomplete removal of colour in 4-*tert*-butylorthoquinone solutions.

The kinetic models developed in this study are superior to previously published empirical kinetic models for alkaline peroxide bleaching. The Two Chromophore Consecutive Reaction Model and the Equilibrium Models are able to describe a much wider range of experimental bleaching behaviour than previously reported empirical kinetic expressions. In addition, model compound studies have shown that the steps contained in the Two Chromophore Consecutive Reaction models can be associated with various reactions involving α,β-unsaturated aldehydes and *ortho* quinones. Analysis of the Equilibrium Models indicates that some mechanism of chromophore formation is also required to fully explain the bleaching response of *E. regnans* SGW. Such a process was not observed in the reactions of alkaline peroxide with model α,β-unsaturated aldehydes or *ortho* quinones, and further work is required to characterise possible colour creation mechanisms occurring under peroxide bleaching conditions.

APPENDIX 1.1

Light Absorption Coefficient - Time data for the Bleaching of E. regnans SGW with Alkaline Peroxide Under Constant Reagent Conditions

	SHEET NUMBER								
	1			2			3		
Time (min.)	R Inf.	R Zero	Mass (g)	R Inf.	R Zero	Mass (g)	R Inf.	R Zero	Mass (g)
0.00	59.50	58.69	0.2997	59.16	58.20	0.3000	59.55	58.81	0.3113
10.00	61.73	60.67	0.2934	61.78	60.45	0.2834	61.30	59.67	0.2888
15.00	62.42	61.08	0.3008	62.17	60.60	0.3001	62.09	60.60	0.2955
30.00	63.97	62.72	0.3044	62.99	60.81	0.3061	63.62	61.86	0.3031
60.00	64.12	63.17	0.3123	63.44	62.41	0.3050	63.34	61.34	0.2926
120.00	64.78	62.69	0.3025	64.35	63.06	0.3100	63.83	61.47	0.3061
240.00	67.07	65.19	0.3119	67.78	65.96	0.3250	67.25	65.10	0.3234
420.00	70.07	67.87	0.3371	69.73	68.30	0.3298	69.87	66.67	0.3202

Time (min.)	Basis-Wt. 1	s 1	k 1	Basis-Wt. 2	s 2	k 2	Basis-Wt. 3	s 3	k 3
0.00	0.045	79.008	10.890	0.045	74.600	10.516	0.047	77.965	10.711
10.00	0.044	81.243	9.638	0.043	79.002	9.340	0.043	71.696	8.758
15.00	0.045	75.963	8.593	0.045	71.967	8.283	0.044	74.053	8.570
30.00	0.046	80.928	8.212	0.046	65.327	7.103	0.046	72.373	7.528
60.00	0.047	85.591	8.592	0.046	83.685	8.816	0.044	71.218	7.556
120.00	0.046	71.449	6.841	0.047	79.821	7.882	0.046	65.486	6.711
240.00	0.047	77.938	6.300	0.049	77.576	5.941	0.049	72.356	5.770
420.00	0.051	76.432	4.886	0.050	88.641	5.824	0.048	69.619	4.523

Time (min.)	K (m2/kg)	Std.Dev
0.00	10.706	0.132
10.00	9.245	0.316
15.00	8.482	0.122
30.00	7.614	0.396
60.00	8.321	0.476
120.00	7.145	0.454
240.00	6.004	0.191
420.00	5.077	0.475

Date	=	**10-10-'90**
pH	=	**9.0**
Peroxide	=	**2.1±0.1g/L**

NOTE

	SHEET NUMBER								
	1			2			3		
Time (min.)	R Inf.	R Zero	Mass (g)	R Inf.	R Zero	Mass (g)	R Inf.	R Zero	Mass (g)
0.00	60.05	59.54	0.2941	60.30	59.28	0.2913	60.30	59.02	0.3007
10.00	61.12	59.49	0.2816	61.73	59.97	0.2757	62.22	61.02	0.2780
15.00	61.67	59.30	0.2813	61.95	60.29	0.2719	61.89	59.72	0.2744
20.00	61.05	59.03	0.2948	61.35	59.99	0.2878	61.68	59.78	0.2799
30.00	63.92	62.76	0.2916	63.63	62.03	0.2916	63.74	62.48	0.3071
60.00	64.46	63.21	0.3025	65.20	63.68	0.3114	0.00	0.00	0.0000
120.00	66.63	64.77	0.3113	66.26	63.70	0.2759	66.28	63.38	0.3007
240.00	69.02	66.57	0.3156	69.48	67.83	0.3206	69.05	66.25	0.2947
420.00	71.10	67.67	0.3268	71.11	68.31	0.3417	71.54	68.34	0.3405

Time (min.)	Basis-Wt. 1	s 1	k 1	Basis-Wt. 2	s 2	k 2	Basis-Wt. 3	s 3	k 3
0.00	0.044	91.834	12.204	0.044	78.648	10.278	0.045	71.484	9.342
10.00	0.042	73.067	9.036	0.041	74.431	8.830	0.042	84.260	9.665
15.00	0.042	65.937	7.854	0.041	77.470	9.053	0.041	70.214	8.239
20.00	0.044	64.998	8.076	0.043	76.127	9.268	0.042	71.408	8.500
30.00	0.044	86.148	8.772	0.044	77.536	8.059	0.046	79.379	8.187
60.00	0.046	82.875	8.120	0.047	78.013	7.245	0.000	0.000	0.000
120.00	0.047	77.117	6.444	0.042	76.991	6.614	0.045	67.535	5.793
240.00	0.047	75.605	5.257	0.048	86.424	5.793	0.044	77.214	5.356
420.00	0.049	69.478	4.081	0.051	71.910	4.220	0.051	69.688	3.945

Time (min.)	K (m2/kg)	Std.Dev
0.00	10.608	1.032
10.00	9.177	0.308
15.00	8.382	0.433
20.00	8.615	0.427
30.00	8.339	0.269
60.00	7.690	0.440
120.00	6.284	0.306
240.00	5.469	0.202
420.00	4.082	0.097

Date	=	**15-10-'90**
pH	=	**9.0**
Peroxide	=	**3.9±0.1g/L**

NOTE

	SHEET NUMBER								
	1			2			3		
Time (min.)	R Inf.	R Zero	Mass (g)	R Inf.	R Zero	Mass (g)	R Inf.	R Zero	Mass (g)
0.00	60.54	59.82	0.2879	61.00	60.17	0.2871	60.69	59.53	0.2806
10.00	63.12	61.76	0.2786	63.43	61.91	0.2840	63.54	61.44	0.2918
15.00	64.17	63.05	0.3039	63.49	61.82	0.2994	63.92	62.56	0.2979
20.00	63.06	60.96	0.2969	63.40	61.97	0.2880	63.22	61.48	0.2843
30.00	65.33	64.43	0.2895	65.54	63.92	0.2844	64.77	62.31	0.2846
60.00	66.81	65.37	0.2961	66.51	64.11	0.2913	66.96	64.78	0.2796
120.00	68.38	66.64	0.3021	68.93	67.59	0.2997	68.83	66.31	0.2990
240.00	71.65	69.56	0.3136	71.69	68.94	0.3170	71.70	67.73	0.2977
420.00	74.34	72.06	0.3362	73.97	70.84	0.3218	73.65	70.56	0.3413

Time (min.)	Basis-Wt. 1	s 1	k 1	Basis-Wt. 2	s 2	k 2	Basis-Wt. 3	s 3	k 3
0.00	0.043	87.871	11.300	0.043	86.375	10.769	0.042	79.872	10.168
10.00	0.042	83.707	9.019	0.043	80.302	8.465	0.044	70.761	7.402
15.00	0.046	84.229	8.425	0.045	74.148	7.784	0.045	80.541	8.201
20.00	0.045	68.375	7.398	0.043	80.573	8.512	0.043	76.349	8.169
30.00	0.044	97.841	9.001	0.043	84.790	7.681	0.043	71.772	6.877
60.00	0.045	88.406	7.288	0.044	75.287	6.348	0.042	82.424	6.719
120.00	0.045	86.563	6.328	0.045	96.515	6.758	0.045	78.451	5.537
240.00	0.047	88.786	4.980	0.048	79.771	4.459	0.045	73.442	4.102
420.00	0.051	89.283	3.954	0.048	81.668	3.740	0.051	76.429	3.603

Time (min.)	K (m2/kg)	Std.Dev
0.00	10.746	0.400
10.00	8.295	0.581
15.00	8.137	0.230
20.00	8.026	0.403
30.00	7.853	0.758
60.00	6.785	0.335
120.00	6.208	0.438
240.00	4.513	0.312
420.00	3.766	0.125

Date	=	**17-10-'90**
pH	=	**9.0**
Peroxide	=	**6.2±0.1g/L**

NOTE

	SHEET NUMBER								
	1			2			3		
Time (min.)	R Inf.	R Zero	Mass (g)	R Inf.	R Zero	Mass (g)	R Inf.	R Zero	Mass (g)
0.00	59.40	58.28	0.2908	59.99	59.16	0.2984	59.99	59.11	0.2946
10.00	66.55	64.70	0.2790	66.21	64.15	0.2755	65.89	64.18	0.2890
15.00	67.39	65.45	0.2877	67.33	65.35	0.2732	67.54	64.38	0.2739
20.00	65.53	61.78	0.2531						
30.00	69.62	65.32	0.2834	69.65	67.10	0.2828	69.23	66.36	0.2885

Time (min.)	Basis-Wt. 1	s 1	k 1	Basis-Wt. 2	s 2	k 2	Basis-Wt. 3	s 3	k 3
0.00	0.044	74.402	10.323	0.045	80.216	10.703	0.044	80.023	10.677
10.00	0.042	85.945	7.225	0.041	82.983	7.155	0.043	83.080	7.335
15.00	0.043	84.610	6.676	0.041	88.309	6.999	0.041	75.099	5.858
20.00	0.038	70.640	6.404						
30.00	0.043	69.020	4.575	0.043	85.138	5.630	0.043	78.670	5.379

Time (min.)	K (m2/kg)	Std.Dev
0.00	10.568	0.150
10.00	7.238	0.064
15.00	6.511	0.416
20.00	6.404	
30.00	5.195	0.390

Date	=	**4-11-'90**
pH	=	**9.0**
Peroxide	=	**12.4±0.4g/L**

NOTE

Difficult to maintain such high levels of peroxide.
Sheet at 20 min. damaged.

	SHEET NUMBER								
	1			2			3		
Time (min.)	R Inf.	R Zero	Mass (g)	R Inf.	R Zero	Mass (g)	R Inf.	R Zero	Mass (g)
0.00	60.30	59.44	0.3120	59.56	58.46	0.3060	59.90	58.47	0.3070
5.00	60.85	59.94	0.3110	60.71	59.79	0.3090	60.72	59.77	0.3100
10.00	60.40	59.41	0.2890	60.47	58.99	0.2940			
15.00	60.66	59.52	0.2930	60.64	59.43	0.2950	60.72	59.40	0.3050
20.00	61.49	60.41	0.2870	61.20	59.12	0.2720	61.22	59.76	0.2780
30.00	61.84	59.79	0.3100	61.97	60.85	0.3050	61.76	59.98	0.2950
60.00	63.47	62.59	0.3090	63.41	62.28	0.3110	63.07	60.61	0.2960
120.00	66.30	63.92	0.3060	66.33	63.54	0.3080	66.56	63.44	0.3180
240.00	70.94	68.15	0.3150	70.42	67.38	0.3130	69.65	65.10	0.3210
420.00	74.79	71.60	0.3420	74.39	71.07	0.3560	74.24	71.40	0.3260

Time (min.)	Basis-Wt. 1	s 1	k 1	Basis-Wt. 2	s 2	k 2	Basis-Wt. 3	s 3	k 3
0.00	0.047	76.844	10.043	0.046	71.460	9.811	0.046	66.832	8.970
5.00	0.047	77.434	9.752	0.046	77.329	9.831	0.047	76.451	9.713
10.00	0.043	80.198	10.411	0.044	70.460	9.104			
15.00	0.044	76.786	9.795	0.044	74.938	9.572	0.046	70.883	9.006
20.00	0.043	81.932	9.880	0.041	70.131	8.626	0.042	76.813	9.435
30.00	0.047	63.238	7.446	0.046	77.622	9.058	0.044	69.385	8.214
60.00	0.046	86.253	9.067	0.047	79.907	8.436	0.045	64.972	7.025
120.00	0.046	71.339	6.110	0.046	67.010	5.726	0.048	62.744	5.271
240.00	0.047	77.610	4.619	0.047	74.149	4.607	0.048	59.509	3.935
420.00	0.051	78.778	3.347	0.054	73.313	3.232	0.049	84.601	3.781

Time (min.)	K (m2/kg)	Std.Dev
0.00	9.608	0.399
5.00	9.766	0.043
10.00	9.760	1.090
15.00	9.458	0.288
20.00	9.314	0.450
30.00	8.239	0.570
60.00	8.176	0.739
120.00	5.702	0.297
240.00	4.387	0.277
420.00	3.453	0.205

Date	=	**5-9-'90**
pH	=	**10.0**
Peroxide	=	**1.2±0.1 g/L**

NOTE

	SHEET NUMBER								
	1			2			3		
Time (min.)	R Inf.	R Zero	Mass (g)	R Inf.	R Zero	Mass (g)	R Inf.	R Zero	Mass (g)
0.00	58.83	57.56	0.2983	58.59	57.63	0.2920	58.70	57.66	0.3144
5.00	63.53	61.20	0.2746	62.26	60.29	0.2751	62.46	60.57	0.2922
10.00	65.31	62.93	0.2906	64.70	61.78	0.2793	65.00	62.86	0.2840
15.00	66.57	64.06	0.2920	66.35	63.60	0.2921	66.14	63.84	0.2826
20.00	65.80	63.27	0.2903	65.59	62.00	0.2834	65.80	63.57	0.2927
30.00	69.07	65.65	0.2850	69.05	65.45	0.2658	69.54	65.54	0.2892
60.00	73.97	68.94	0.3015	74.24	68.50	0.2868	74.47	70.21	0.2886
120.00	77.74	72.07	0.2930	77.23	70.37	0.2818	76.73	70.26	0.2832
240.00	80.49	68.87	0.2830	80.67	69.38	0.2927	81.04	68.61	0.2893
420.00	81.87	70.63	0.3065	81.98	71.26	0.2994	82.08	70.94	0.2897

Time (min.)	Basis-Wt. 1	s 1	k 1	Basis-Wt. 2	s 2	k 2	Basis-Wt. 3	s 3	k 3
0.00	0.045	68.612	9.884	0.044	75.138	10.996	0.047	68.550	9.960
5.00	0.041	72.548	7.594	0.041	73.279	8.382	0.044	70.426	7.945
10.00	0.044	72.496	6.679	0.042	68.543	6.601	0.043	76.095	7.170
15.00	0.044	74.084	6.219	0.044	71.085	6.066	0.043	77.722	6.736
20.00	0.044	72.278	6.424	0.043	64.352	5.808	0.044	74.922	6.659
30.00	0.043	73.981	5.123	0.040	77.649	5.386	0.044	69.558	4.640
60.00	0.045	71.130	3.258	0.043	70.905	3.169	0.043	81.688	3.575
120.00	0.044	80.090	2.552	0.042	73.902	2.481	0.043	74.388	2.625
240.00	0.043	60.523	1.431	0.044	60.130	1.393	0.044	57.661	1.279
420.00	0.046	60.439	1.213	0.045	64.212	1.272	0.044	64.894	1.269

Time (min.)	K (m2/kg)	Std.Dev
0.00	10.280	0.439
5.00	7.974	0.279
10.00	6.817	0.218
15.00	6.340	0.249
20.00	6.297	0.311
30.00	5.050	0.267
60.00	3.334	0.151
120.00	2.553	0.051
240.00	1.367	0.056
420.00	1.251	0.023

Date	**=**	**3-9-'90**
pH	**=**	**10.0**
Peroxide	**=**	**9.5±0.2 g/L**

NOTE

	SHEET NUMBER								
	1			2			3		
Time (min.)	R Inf.	R Zero	Mass (g)	R Inf.	R Zero	Mass (g)	R Inf.	R Zero	Mass (g)
0.00	59.19	57.95	0.3087	58.91	57.98	0.2733	59.22	58.23	0.2930
5.00	62.61	61.51	0.2579	60.69	59.16	0.2729	61.68	58.98	0.2521
10.00	61.66	59.58	0.2580	60.81	57.99	0.2583	61.55	59.65	0.2663
15.00	63.26	62.05	0.2774	62.68	60.23	0.2653	63.26	61.89	0.2890
20.00	63.81	62.31	0.2791	63.34	60.66	0.2644	63.56	61.46	0.2630
30.00	64.29	62.35	0.2774	64.20	62.30	0.2732	64.15	62.16	0.2818
60.00	67.56	65.99	0.2858	67.33	63.93	0.2795	67.39	65.27	0.2795
120.00	69.80	65.95	0.2856	69.72	66.12	0.2836	69.68	65.56	0.2917
240.00	73.57	67.85	0.2912	73.01	68.37	0.2886	72.93	67.51	0.2975
420.00	76.41	72.57	0.3300	75.93	71.76	0.3145	75.43	70.80	0.3234

Time (min.)	Basis-Wt. 1	s 1	k 1	Basis-Wt. 2	s 2	k 2	Basis-Wt. 3	s 3	k 3
0.00	0.046	67.601	9.511	0.041	81.869	11.732	0.044	75.911	10.659
5.00	0.039	94.369	10.536	0.041	75.728	9.641	0.038	70.262	8.364
10.00	0.039	75.140	8.957	0.039	65.464	8.267	0.040	74.713	8.973
15.00	0.042	87.401	9.325	0.040	71.603	7.955	0.043	80.921	8.633
20.00	0.042	83.156	8.534	0.040	71.217	7.555	0.040	78.566	8.207
30.00	0.042	78.479	7.783	0.041	79.973	7.983	0.042	76.229	7.636
60.00	0.043	91.691	7.141	0.042	70.976	5.626	0.042	84.551	6.671
120.00	0.043	72.260	4.721	0.043	74.588	4.904	0.044	68.452	4.516
240.00	0.044	68.197	3.238	0.043	74.348	3.709	0.045	66.889	3.360
420.00	0.050	80.708	2.939	0.047	80.148	3.058	0.049	72.914	2.918

Time (min.)	K (m2/kg)	Std.Dev
0.00	10.634	0.786
5.00	9.513	0.772
10.00	8.732	0.285
15.00	8.638	0.484
20.00	8.099	0.352
30.00	7.801	0.123
60.00	6.479	0.549
120.00	4.714	0.138
240.00	3.436	0.173
420.00	2.971	0.053

Date	=	**29-8-'90**
pH	=	**10.0**
Peroxide	=	**2.0±0.1 g/L**

NOTE

	SHEET NUMBER								
	1			2			3		
Time (min.)	R Inf.	R Zero	Mass (g)	R Inf.	R Zero	Mass (g)	R Inf.	R Zero	Mass (g)
0.00	59.19	57.95	0.3087	58.91	57.98	0.2733	59.22	58.23	0.2930
5.00	62.61	61.51	0.2579	60.69	59.16	0.2729	61.68	58.98	0.2521
10.00	63.11	61.85	0.3037	63.83	62.19	0.2937	62.57	61.23	0.2803
15.00	66.76	64.99	0.2784	66.52	64.96	0.3011	65.12	62.63	0.2863
20.00	65.95	63.46	0.2755	65.85	63.00	0.2735	65.95	64.19	0.2844
30.00	66.17	62.53	0.2764	65.60	63.79	0.2992	66.21	64.14	0.2688
60.00	69.51	65.43	0.2830	68.88	65.53	0.2867	69.10	65.31	0.2831
120.00	73.42	68.30	0.2784	73.04	68.91	0.2804	73.22	68.38	0.2847
240.00	76.43	70.50	0.2964	75.94	69.27	0.2781	76.18	71.16	0.2770
458.00	78.38	72.29	0.3060	78.74	71.01	0.2975	78.12	71.10	0.2887

Time (min.)	Basis-Wt. 1	s 1	k 1	Basis-Wt. 2	s 2	k 2	Basis-Wt. 3	s 3	k 3
0.00	0.046	67.601	9.511	0.041	81.869	11.732	0.044	75.911	10.659
5.00	0.039	94.369	10.536	0.041	75.728	9.641	0.038	70.262	8.364
10.00	0.046	78.491	8.463	0.044	76.939	7.885	0.042	81.952	9.175
15.00	0.042	88.034	7.285	0.045	83.953	7.073	0.043	71.933	6.719
20.00	0.041	77.007	6.769	0.041	73.591	6.517	0.043	83.836	7.369
30.00	0.042	66.987	5.793	0.045	77.988	7.034	0.040	84.913	7.321
60.00	0.043	70.411	4.708	0.043	73.634	5.176	0.043	71.515	4.941
120.00	0.042	74.809	3.599	0.042	80.654	4.013	0.043	74.523	3.650
240.00	0.045	73.471	2.670	0.042	72.286	2.755	0.042	84.452	3.145
458.00	0.046	75.888	2.263	0.045	69.545	1.996	0.043	73.794	2.261

Time (min.)	K (m2/kg)	Std.Dev
0.00	10.634	0.786
5.00	9.513	0.772
10.00	8.507	0.457
15.00	7.026	0.202
20.00	6.885	0.310
30.00	6.716	0.574
60.00	4.942	0.165
120.00	3.754	0.160
240.00	2.857	0.179
458.00	2.173	0.109

Date	=	**22-8-'90**
pH	=	**10.0**
Peroxide	=	**3.9±0.1 g/L**

NOTE

	SHEET NUMBER								
	1			2			3		
Time (min.)	R Inf.	R Zero	Mass (g)	R Inf.	R Zero	Mass (g)	R Inf.	R Zero	Mass (g)
0.00	60.36	59.46	0.3010	59.79	59.03	0.2997	60.69	59.90	0.2916
5.00	62.71	61.07	0.2722	62.46	60.24	0.3016	62.65	61.32	0.2974
10.00	64.42	62.62	0.3103	64.19	62.69	0.2877	64.22	62.69	0.2957
15.00	66.30	63.68	0.2817	65.40	63.97	0.3069	65.73	63.47	0.2844
20.00	68.51	64.28	0.2708	67.64	64.04	0.2801	67.87	65.66	0.2914
30.00	68.98	66.63	0.2859	69.52	65.20	0.2773	67.78	65.03	0.2999
60.00	72.80	67.67	0.2977	72.19	67.75	0.2853	72.14	67.71	0.2974
120.00	73.42	68.54	0.2748	73.31	68.05	0.2850	72.89	67.05	0.2912
240.00	78.18	70.48	0.2815	77.50	70.49	0.2781	77.40	69.94	0.2868
458.00	76.12	66.68	0.2900	76.10	64.94	0.2847	76.83	66.49	0.2821

Time (min.)	Basis-Wt. 1	s 1	k 1	Basis-Wt. 2	s 2	k 2	Basis-Wt. 3	s 3	k 3
0.00	0.045	78.874	10.267	0.045	81.117	10.968	0.044	85.196	10.846
5.00	0.041	79.787	8.846	0.045	64.673	7.296	0.045	77.629	8.643
10.00	0.047	72.215	7.096	0.043	81.770	8.168	0.044	79.164	7.891
15.00	0.042	74.887	6.414	0.046	81.214	7.433	0.043	76.563	6.840
20.00	0.041	69.862	5.056	0.042	70.001	5.419	0.044	81.372	6.189
30.00	0.043	84.572	5.899	0.042	70.139	4.687	0.045	72.912	5.584
60.00	0.045	68.276	3.469	0.043	74.365	3.984	0.045	71.277	3.834
120.00	0.041	77.503	3.729	0.043	71.851	3.491	0.044	65.797	3.317
240.00	0.042	72.038	2.194	0.042	74.803	2.443	0.043	69.805	2.303
458.00	0.044	57.210	2.143	0.043	52.272	1.962	0.042	57.026	1.992

Time (min.)	K (m2/kg)	Std.Dev
0.00	10.694	0.265
5.00	8.262	0.596
10.00	7.718	0.394
15.00	6.896	0.362
20.00	5.554	0.409
30.00	5.390	0.445
60.00	3.762	0.187
120.00	3.512	0.146
240.00	2.313	0.088
458.00	2.032	0.069

Date	=	**13-8-'90**
pH	=	**10.0**
Peroxide	=	**5.9±0.1 g/L**

NOTE

	SHEET NUMBER								
	1			2			3		
Time (min.)	R Inf.	R Zero	Mass (g)	R Inf.	R Zero	Mass (g)	R Inf.	R Zero	Mass (g)
0.00	59.37	58.98	0.3290	59.06	58.60	0.3209	58.59	57.80	0.3197
10.00	69.01	67.37	0.3040	67.76	65.59	0.3134	69.30	67.00	0.3045
15.00	69.68	65.53	0.2993	68.88	64.07	0.2948	69.23	65.03	0.2778
20.00	70.69	64.92	0.2553	70.57	63.84	0.2573	70.85	62.71	0.2536
30.00	75.50	69.76	0.2817	74.84	69.30	0.2861	74.59	68.51	0.2927

Time (min.)	Basis-Wt. 1	s 1	k 1	Basis-Wt. 2	s 2	k 2	Basis-Wt. 3	s 3	k 3
0.00	0.049	85.115	11.833	0.048	83.236	11.811	0.048	72.215	10.568
10.00	0.046	89.726	6.243	0.047	75.828	5.816	0.046	80.960	5.505
15.00	0.045	66.507	4.387	0.044	61.457	4.320	0.042	70.123	4.795
20.00	0.038	69.589	4.228	0.039	63.606	3.903	0.038	58.780	3.525
30.00	0.042	75.774	3.012	0.043	74.009	3.130	0.044	68.412	2.961

Time (min.)	K (m2/kg)	Std.Dev
0.00	11.404	0.512
10.00	5.855	0.262
15.00	4.501	0.182
20.00	3.886	0.249
30.00	3.034	0.061

Date	=	**24-9-'90**
pH	=	**10.000**
Peroxide	=	**23 g/L**

NOTE

Test to find limiting initial slope.
Impossible to maintain constant
conditions for longer.

	SHEET NUMBER								
	1			2			3		
Time (min.)	R Inf.	R Zero	Mass (g)	R Inf.	R Zero	Mass (g)	R Inf.	R Zero	Mass (g)
0.00	58.58	58.30	0.3362	58.51	58.20	0.3368	58.22	57.88	0.3350
10.00	65.40	64.07	0.3330	65.48	64.62	0.3282	65.83	65.12	0.3333
20.00	68.54	67.72	0.3494	68.04	67.09	0.3481	68.17	67.24	0.3485
30.00	69.19	65.45	0.3211	69.44	67.98	0.3332	69.51	67.50	0.3463
60.00	72.65	69.31	0.3223	72.37	69.58	0.3387	72.05	68.66	0.3483
120.00	75.63	70.69	0.3302	76.27	71.66	0.3371	75.74	71.41	0.3488
180.00	77.23	72.56	0.3552	76.91	72.84	0.3474	77.27	73.49	0.3491
240.00	78.06	70.84	0.3548	78.29	71.93	0.3551	77.73	68.24	0.2963

Time (min.)	Basis-Wt. 1	s 1	k 1	Basis-Wt. 2	s 2	k 2	Basis-Wt. 3	s 3	k 3
0.00	0.051	86.858	12.719	0.051	84.710	12.461	0.050	82.702	12.398
10.00	0.050	76.477	7.000	0.049	87.819	7.991	0.050	91.983	8.157
20.00	0.053	93.505	6.751	0.052	88.591	6.650	0.052	89.430	6.646
30.00	0.048	63.607	4.363	0.050	86.238	5.799	0.052	75.127	5.024
60.00	0.048	75.508	3.887	0.051	76.215	4.020	0.052	67.886	3.680
120.00	0.050	69.851	2.743	0.051	72.460	2.675	0.052	70.536	2.741
180.00	0.053	71.051	2.385	0.052	76.291	2.644	0.053	79.555	2.660
240.00	0.053	58.982	1.819	0.053	63.698	1.917	0.045	59.351	1.893

Time (min.)	K (m2/kg)	Std.Dev
0.00	12.526	0.120
10.00	7.716	0.443
20.00	6.682	0.042
30.00	5.062	0.508
60.00	3.862	0.121
120.00	2.719	0.027
180.00	2.563	0.109
240.00	1.876	0.036

Date	=	**14-2-'91**
pH	=	**11.0**
Peroxide	=	**2.1±0.2g/L**

NOTE

	SHEET NUMBER								
	1			2			3		
Time (min.)	R Inf.	R Zero	Mass (g)	R Inf.	R Zero	Mass (g)	R Inf.	R Zero	Mass (g)
0.00	60.11	59.69	0.2955	60.38	60.00	0.3001	60.78	60.51	0.3006
10.00	70.20	67.61	0.2973	69.91	68.39	0.3024	70.19	68.13	0.3101
20.00	72.89	68.81	0.2926	72.69	69.61	0.2923	72.25	68.71	0.3078
30.00	74.93	71.29	0.3021	74.99	70.82	0.3053	74.55	70.94	0.3226
54.00	77.31	71.96	0.3073	76.65	69.42	0.2935	77.08	72.13	0.3167
120.00	79.75	69.58	0.3106	79.84	70.27	0.2980	79.51	69.87	0.3055
180.00	81.37	71.58	0.3131	81.32	73.11	0.3043	81.14	72.32	0.3050
235.00	81.83	71.61	0.3016	82.33	70.69	0.3044	81.78	68.97	0.3115

Time (min.)	Basis-Wt. 1	s 1	k 1	Basis-Wt. 2	s 2	k 2	Basis-Wt. 3	s 3	k 3
0.00	0.044	95.684	12.665	0.045	97.212	12.636	0.045	105.684	13.373
10.00	0.045	82.199	5.199	0.045	95.535	6.186	0.047	85.357	5.403
20.00	0.044	77.255	3.895	0.044	86.092	4.417	0.046	76.061	4.053
30.00	0.045	84.992	3.565	0.046	79.547	3.318	0.049	78.678	3.418
54.00	0.046	77.238	2.572	0.044	67.406	2.397	0.048	77.079	2.627
120.00	0.047	58.615	1.507	0.045	63.766	1.623	0.046	61.105	1.613
180.00	0.047	63.620	1.357	0.046	72.922	1.565	0.046	69.124	1.515
235.00	0.045	65.425	1.320	0.046	60.496	1.147	0.047	53.938	1.095

Time (min.)	K (m2/kg)	Std.Dev
0.00	12.891	0.295
10.00	5.596	0.369
20.00	4.122	0.189
30.00	3.433	0.088
54.00	2.532	0.085
120.00	1.581	0.046
180.00	1.479	0.077
235.00	1.187	0.083

Date	=	**11-2-'91**
pH	=	**11.0**
Peroxide	=	**4.0±0.3g/L**

NOTE

	SHEET NUMBER								
	1			2			3		
Time (min.)	R Inf.	R Zero	Mass (g)	R Inf.	R Zero	Mass (g)	R Inf.	R Zero	Mass (g)
0.00	60.56	60.39	0.3366	59.88	59.65	0.3431	60.09	59.85	0.3344
10.00	72.64	70.36	0.3167	72.22	69.97	0.3209	71.40	67.90	0.3187
20.00	75.65	72.86	0.3061	75.18	71.73	0.3090	75.16	70.94	0.3056
30.00	76.86	70.60	0.3051	76.66	72.08	0.3006	76.98	71.89	0.3064
60.00	78.86	69.68	0.3062	78.85	70.19	0.3017	78.92	69.59	0.2890
120.00	81.53	71.83	0.2995	81.67	71.60	0.2965	81.81	73.70	0.3048
180.00	82.79	72.56	0.2838	83.03	72.18	0.2696	82.67	71.77	0.2761
240.00	82.89	69.74	0.2686	82.86	64.78	0.2356	82.60	70.85	0.3015

Time (min.)	Basis-Wt. 1	s 1	k 1	Basis-Wt. 2	s 2	k 2	Basis-Wt. 3	s 3	k 3
0.00	0.051	102.374	13.148	0.052	92.609	12.447	0.050	94.926	12.581
10.00	0.048	88.633	4.567	0.048	86.461	4.620	0.048	71.466	4.094
20.00	0.046	95.988	3.762	0.046	85.801	3.515	0.046	79.585	3.267
30.00	0.046	70.608	2.460	0.045	82.784	2.941	0.046	78.306	2.695
60.00	0.046	61.274	1.736	0.045	64.422	1.827	0.043	64.421	1.814
120.00	0.045	67.349	1.409	0.045	66.767	1.373	0.046	74.865	1.514
180.00	0.043	72.302	1.293	0.041	73.854	1.281	0.042	70.820	1.286
240.00	0.040	64.126	1.132	0.035	56.156	0.996	0.045	61.341	1.124

Time (min.)	K (m2/kg)	Std.Dev
0.00	12.725	0.263
10.00	4.427	0.205
20.00	3.515	0.175
30.00	2.699	0.170
60.00	1.792	0.035
120.00	1.432	0.052
180.00	1.287	0.004
240.00	1.084	0.054

Date	=	**12-2-'91**
pH	=	**11.0**
Peroxide	=	**6.0±0.9g/L**

NOTE

	SHEET NUMBER								
	1			2			3		
Time (min.)	R Inf.	R Zero	Mass (g)	R Inf.	R Zero	Mass (g)	R Inf.	R Zero	Mass (g)
0.00	60.04	59.42	0.3263	59.62	59.02	0.3202	59.35	58.49	0.3184
10.00	66.93	64.60	0.3027	67.06	64.36	0.3099	67.12	64.60	0.3077
15.00	68.42	65.13	0.3024	68.19	64.56	0.3079	67.71	64.76	0.3167
20.00	68.86	65.39	0.3165	69.07	66.66	0.3175	68.88	66.37	0.3234
30.00	69.53	63.54	0.3005	70.07	66.18	0.3119	71.00	67.31	0.3002
60.00	71.48	65.60	0.2876	71.67	65.18	0.2777	72.63	68.95	0.3079
120.00	73.80	67.48	0.2937	73.97	68.80	0.3010	73.42	66.99	0.2781
170.00	74.14	67.17	0.2818	74.64	68.60	0.3133	74.07	67.50	0.3032
240.00	75.15	68.68	0.2980	75.24	67.07	0.2972	75.51	66.68	0.2872
360.00	76.92	70.01	0.3137	76.88	69.37	0.3207	77.76	71.23	0.3063

Time (min.)	Basis-Wt. 1	s 1	k 1	Basis-Wt. 2	s 2	k 2	Basis-Wt. 3	s 3	k 3
0.00	0.049	79.027	10.509	0.048	79.986	10.938	0.048	72.842	10.140
10.00	0.046	74.326	6.072	0.047	69.204	5.599	0.046	71.615	5.767
15.00	0.045	69.138	5.039	0.046	64.744	4.804	0.048	67.090	5.165
20.00	0.048	65.726	4.628	0.048	75.732	5.245	0.049	72.769	5.116
30.00	0.045	55.642	3.715	0.047	66.541	4.253	0.045	73.147	4.332
60.00	0.043	63.007	3.585	0.042	62.521	3.501	0.046	75.926	3.916
120.00	0.044	64.873	3.017	0.045	70.334	3.221	0.042	66.943	3.221
170.00	0.042	65.060	2.934	0.047	64.250	2.768	0.046	62.223	2.824
240.00	0.045	66.493	2.732	0.045	58.869	2.398	0.043	58.796	2.335
360.00	0.047	65.327	2.262	0.048	60.943	2.119	0.046	71.291	2.267

Time (min.)	K (m2/kg)	Std.Dev
0.00	10.529	0.282
10.00	5.813	0.170
15.00	5.003	0.130
20.00	4.996	0.230
30.00	4.100	0.238
60.00	3.667	0.155
120.00	3.153	0.083
170.00	2.842	0.060
240.00	2.488	0.151
360.00	2.216	0.060

Date	**=**	**29-1-91**
pH	**=**	**12.000**
Peroxide	**=**	**2.4±0.1 g/L**

NOTE

	SHEET NUMBER								
	1			2			3		
Time (min.)	R Inf.	R Zero	Mass (g)	R Inf.	R Zero	Mass (g)	R Inf.	R Zero	Mass (g)
0.00	58.87	58.30	0.3299	58.76	58.16	0.3371	58.54	57.99	0.3349
10.00	66.88	64.20	0.2945	66.78	63.56	0.3135	66.92	64.01	0.3177
20.00	70.36	66.11	0.3011	70.81	66.46	0.2994	70.69	65.71	0.3070
30.00	71.49	66.42	0.2978	71.57	66.68	0.3010	72.12	69.07	0.3076
45.00	74.19	66.61	0.2703	73.94	66.54	0.2678	73.34	65.93	0.2672
60.00	74.74	66.78	0.2916	74.79	67.02	0.2987	74.87	65.70	0.2811
120.00	76.39	63.92	0.2332	76.54	63.43	0.2319	76.52	65.18	0.2359
180.00	78.67	66.28	0.2833	78.55	67.02	0.2452	78.62	68.59	0.2627
240.00	79.08	63.25	0.2559	79.18	66.58	0.2405	79.13	62.58	0.2449
360.00	0.00	0.00	0.0000	0.00	0.00	0.0000	0.00	0.00	0.0000

Time (min.)	Basis-Wt. 1	s 1	k 1	Basis-Wt. 2	s 2	k 2	Basis-Wt. 3	s 3	k 3
0.00	0.050	76.557	11.000	0.051	73.733	10.671	0.050	75.182	11.038
10.00	0.044	72.547	5.949	0.047	63.374	5.236	0.048	65.327	5.341
20.00	0.045	67.093	4.189	0.045	67.915	4.086	0.046	62.058	3.771
30.00	0.045	65.351	3.715	0.045	65.940	3.723	0.046	80.347	4.330
45.00	0.041	64.916	2.914	0.040	65.778	3.021	0.040	64.418	3.121
60.00	0.044	59.763	2.551	0.045	59.258	2.518	0.042	57.323	2.418
120.00	0.035	59.741	2.180	0.035	58.268	2.095	0.035	63.396	2.284
180.00	0.043	53.835	1.557	0.037	65.129	1.907	0.040	66.898	1.945
240.00	0.038	50.176	1.388	0.036	63.888	1.749	0.037	50.625	1.393
360.00	0.000	0.000	0.000	0.000	0.000	0.000	0.000	0.000	0.000

Time (min.)	K (m2/kg)	Std.Dev
0.00	10.903	0.143
10.00	5.509	0.272
20.00	4.015	0.154
30.00	3.923	0.249
45.00	3.019	0.073
60.00	2.495	0.049
120.00	2.186	0.067
180.00	1.803	0.151
240.00	1.510	0.146
360.00	0.000	0.000

Date	=	**23-1-91**
pH	=	**12.000**
Peroxide	=	**4.3±0.2 g/L**

NOTE

	SHEET NUMBER								
	1			2			3		
Time (min.)	R Inf.	R Zero	Mass (g)	R Inf.	R Zero	Mass (g)	R Inf.	R Zero	Mass (g)
0.00	61.42	60.40	0.3137	61.14	60.61	0.3141	61.06	60.28	0.3017
12.00	70.38	66.19	0.3031	70.36	65.80	0.3066	70.60	65.70	0.3081
15.00	71.91	67.55	0.3166	71.38	67.57	0.3080	71.21	67.83	0.3155
20.00	73.33	68.00	0.3075	73.23	69.96	0.3041	72.93	68.70	0.3075
30.00	75.47	68.99	0.2952	75.63	71.26	0.2966	76.13	71.23	0.3041
60.00	78.49	71.36	0.2948	78.75	71.36	0.2908	78.46	70.86	0.2945
120.00	80.41	71.03	0.2852	80.73	72.96	0.2997	80.83	70.30	0.2840
170.00	81.34	71.30	0.2793	81.09	71.60	0.2798	80.97	71.23	0.2816
240.00	82.19	69.40	0.2647	81.92	70.30	0.2542	81.75	68.68	0.2673
360.00	83.12	72.83	0.2703	82.81	70.93	0.2724	82.60	68.89	0.2616

Time (min.)	Basis-Wt. 1	s 1	k 1	Basis-Wt. 2	s 2	k 2	Basis-Wt. 3	s 3	k 3
0.00	0.047	75.957	9.203	0.047	88.548	10.935	0.045	83.691	10.392
12.00	0.046	67.110	4.183	0.046	63.885	3.988	0.046	62.092	3.801
15.00	0.048	66.846	3.667	0.046	71.363	4.095	0.047	72.690	4.230
20.00	0.046	66.226	3.212	0.046	82.527	4.038	0.046	72.482	3.641
30.00	0.044	67.899	2.707	0.045	82.251	3.229	0.046	77.653	2.906
60.00	0.044	72.720	2.143	0.044	73.019	2.094	0.044	70.149	2.074
120.00	0.043	69.042	1.648	0.045	74.639	1.717	0.043	65.399	1.487
170.00	0.042	70.067	1.500	0.042	71.809	1.583	0.042	69.825	1.561
240.00	0.040	64.597	1.246	0.038	71.336	1.423	0.040	61.848	1.260
360.00	0.041	76.669	1.314	0.041	67.941	1.212	0.039	63.035	1.155

Time (min.)	K (m2/kg)	Std.Dev
0.00	10.177	0.626
12.00	3.991	0.135
15.00	3.997	0.208
20.00	3.630	0.292
30.00	2.947	0.187
60.00	2.104	0.025
120.00	1.617	0.083
170.00	1.548	0.031
240.00	1.310	0.070
360.00	1.227	0.057

Date	=	**29-1-91**
pH	=	**12.000**
Peroxide	=	**6.0±0.4 g/L**

NOTE

TUTSIM Input and Output for Modelling Bleaching Kinetics Using the Two Chromophore Model.

For the Two Chromophore Model

$C_1 \rightarrow C_P$, rate constant k_1
$C_2 \rightarrow C_P$, rate constant k_2

and $C = C_1 + C_2$

Rate of loss of chromophores (C)

$$-\frac{dC}{dt} = k_1C_1 + k_2C_2 \qquad (1)$$

Equation 1 can be integrated using TUTSIM by linking the basic TUTSIM block operations (INTegrate, GAIn, SUM) in following way. The integrated data can then be compared to experimental data through a least squares fit, and the parameters adjusted to minimise the fit.

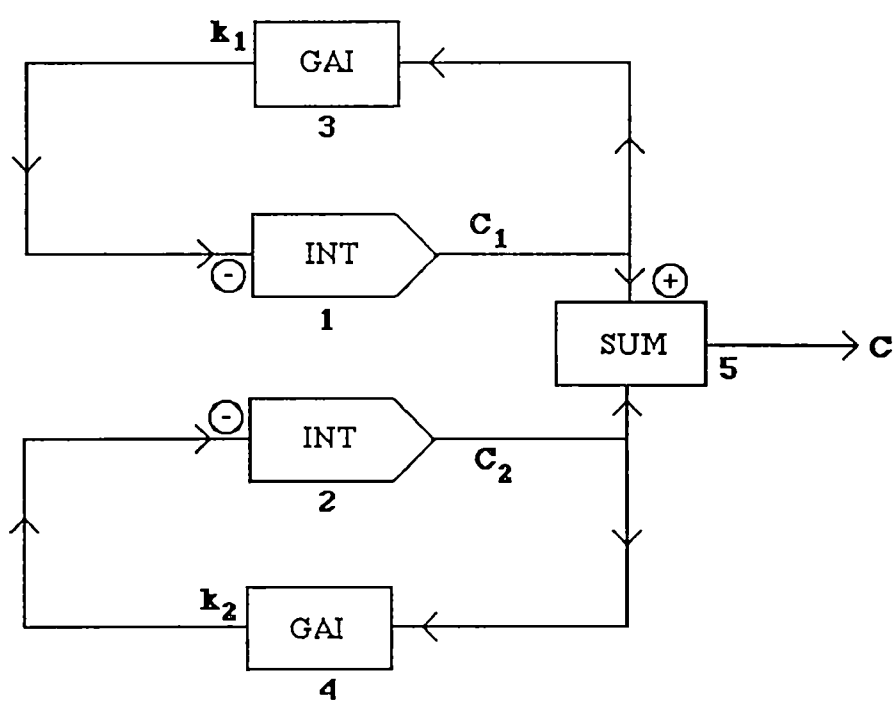

```
Model File:       TCM
Date:       14/   9/    1991
Time:       11:   21
Timing:     1.000, DELTA      1.000e+03, RANGE

PlotBlocks and Scales:
Format:
         BlockNo,    Plot-Minimum, Plot-Maximum;       Comment
Horz:       0,           0.0000,     1.000E+03;       Time Axis
Y1:
Y2:
Y3:
Y4:         5,           0.0000,     12.0000;         K (m2/kg)

4.86        1   INT   -3
5.93        2   INT   -4
0.0280000   3   GAI    3
0.0010900   4   GAI    2
            5   SUM    1      2
```

Explanation

Line 1
Model File Name = TCM

Line 2
Date

Line 3
Time

Line 4

1.0000	=	time increments for integration (delta for integration slices)
1.000E+03	=	maximum time (range 0 - 1.000E+03 minutes)

Lines 5 - 7
PlotBlocks and Scale formatting information

Line 8

0	=	default block number for horizontal co-ordinate (time)
0.0000	=	minimum value on horizontal axis
1.000E+03	=	maximum value on horizontal axis

Lines 9 - 11
Empty Y co-ordinates ie. Y co-ordinates not assigned to a TUTSIM block

Line 12

5	=	TUTSIM block corresponding to co-ordinate Y4
0.0000	=	minimum value on Y axis
12.0000	=	maximum value on Y axis

Line 13

6.6200	=	initial value assigned to integration block 1
1 INT	=	assigns block 1 to an integration function
-3	=	instructs block 1 to receive the -ve value of data produced by block 3 as input

Line 14

```
        3.8700  =  initial value for integration block 2
        2  INT  =  assigns block 2 to an integration function
            -4  =  instructs block 2 to receive the -ve value of
                       data produced by block 4 as input
```

Line 15

```
     0.0280000  =  amount of gain to be applied to block 3
        3  GAI  =  assigns block 3 to a gain function
             1  =  instructs block 3 to receive the data produced by
                   block 1 as input
```

Line 16

```
     0.0010900  =  amount of gain to be applied to block 4
        4  GAI  =  assigns block 4 to a gain function
             2  =  instructs block 4 to receive the data
                   produced by block 2 as input
```

Line 17

```
        5  SUM  =  assigns block 5 to sum data
          1, 2  =  block numbers to be added together
```

Output File for Simulating Bleaching Kinetics Using the Two Chromophore Model.

```
0.11 M peroxide, pH 10, k1=0.0280, k2=0.00109

Experimental Data

Time (min) C (Model)   C(Exp.)     Residual
    0        10.53       10.53       +0.00
    5         9.48        9.27       +0.20
   10         8.61        8.51       +0.06
   15         7.90        7.03       +0.87
   20         7.31        6.89       +0.42
   30         6.41        6.72       -0.31
   60         5.03        4.94       +0.09
  120         4.13        3.75       +0.38
  240         3.26        2.86       +0.40
  458         2.16        2.17       -0.01

Standard Error = +0.3920
```

Explanation

Line 1

```
0.11 M peroxide =  peroxide concentration in bleaching run
         pH 10  =  pH during bleaching run
         0.0280 =  rate constant k1 used to generate model points
        0.00109 =  rate constant k2 used to generate model points
```

Lines 2 - 14

Self explanatory from output file

Sample Input File Showing Format of Kinetic Data for Fitting to Two Chromophore Consecutive Reaction Model Using Simplex Optimisation Program.

Input File "2gLpH10"

```
9.08    1.55    0
1000
0.05    0.01    0.001
0.01    0.005   0.0
1e-05   1e-05   1e-06    1e-04
0     10.63
5     9.51
10    8.73
15    8.64
20    8.10
30    7.80
60    6.48
120   4.71
240   3.44
420   2.97
```

Explanation of Input File

Line 1

```
   9.08  =  initial value for chromophore C1
   1.55  =  initial value for chromophore C2
      0  =  initial value for chromophore CP
```

Line 2

```
   1000  =  maximum number of iterations allowed
```

Line 3

```
   0.05  =  initial guess for k1
   0.01  =  initial guess for k2
  0.001  =  initial guess for k3
```

Line 4

```
   0.01  =  step increment for k1
  0.005  =  step increment for k2
      0  =  step increment for k3
```

Line 5

```
  1e-05  =  maximum error allowed in k1
  1e-05  =  maximum error allowed in k2
  1e-06  =  maximum error allowed in k3
  1e-04  =  maximum total error allowed
```

Lines 6-15
contains the raw data (time in minutes, light absorption coefficient) to be fitted.

```
0     10.63
5     9.51
10    8.73
15    8.64
20    8.10
30    7.80
60    6.48
```

```
240    3.44
420    2.97
```

Sample Output File from the Fitting of E. regnans Bleaching Kinetics to the Two Chromophore Consecutive Reaction Model Using Simplex Optimisation.

Output File "2gLpH10.opt"

```
NON EQUILIBRIUM MODEL  C1 -> C2;   C2 -> CP;   C1 -> CP
SIMPLEX Optimisation for "2gLpH10"
Starting values:  9.0800      1.5500      0.0000


Program exited after 114 iterations.

The mean is:      1.526456e-02      7.491963e-03      1.000000e-03

The estimated fractional error is: 9.864793e-08      4.646166e-07
                                   5.053962e-07      2.755510e-07


#          X                Y              Y''              DY
0     0.000000e+00     1.063000e+01     1.063000e+01    -1.144409e-07
1     5.000000e+00     9.510000e+00     9.888348e+00    -3.783476e-01
2     1.000000e+01     8.730000e+00     9.249465e+00    -5.194650e-01
3     1.500000e+01     8.640000e+00     8.698060e+00    -5.806004e-02
4     2.000000e+01     8.100000e+00     8.221127e+00    -1.211266e-01
5     3.000000e+01     7.800000e+00     7.448082e+00    +3.519176e-01
6     6.000000e+01     6.480000e+00     6.051359e+00    +4.286413e-01
7     1.200000e+02     4.710000e+00     4.900240e+00    -1.902404e-01
8     2.400000e+02     3.440000e+00     3.813954e+00    -3.739539e-01
9     4.200000e+02     2.970000e+00     2.692344e+00    +2.776556e-01

The standard deviation is 1.128606e+00

The estimated error of the function is 4.233999e-01
```

Explanation of Output

Line 1

Model Scheme = C1 -> C2; C2 -> CP; C1 -> CP

Line 2

"2gLpH10" = input file

Line 3

```
9.0800  =  initial Value of C1
1.5500  =  initial Value of C2
0.0000  =  initial Value of CP
```

Line 4

```
114  =  no. of iterations before optimisation of fit
```

Line 5

1.526456e-02 = fitted value of k_1
7.491963e-03 = fitted value of k_2
1.000000e-03 = fitted value of k_3

Line 6

9.864793e-08 = fractional error in k_1
4.646166e-07 = fractional error in k_2
5.053962e-07 = fractional error in k_3
2.755510e-07 = fractional error in the function

Lines 7 - 17

contains the raw data and fitted data points

# = data set number
X = x - co-ordinate (time in minutes)
Y = y - co-ordinate (light absorption coefficient)
Y'' = model values of Y calculated using k_1, k_2, k_3
DY = delta y (Y-Y'')

Line 18

1.128606e+00 = standard deviation in the fit

Line 19

4.233999e-01 = standard error in the function

APPENDIX 2.1

Light Absorption Coefficient - Time Data for the Bleaching of E. regnans SGW with Alkaline Peroxide Under Constant Reagent Concentrations

	SHEET NUMBER								
	1			2			3		
Time (min.)	R Inf.	R Zero	Mass (g)	R Inf.	R Zero	Mass (g)	R Inf.	R Zero	Mass (g)
0.00	60.20	59.82	0.3331	59.82	59.52	0.3425	60.02	59.66	0.3384
30.00	74.86	70.80	0.3166	75.22	69.88	0.3131	74.95	72.02	0.3251
60.00	77.05	71.20	0.3170	77.20	70.23	0.3053	76.97	71.61	0.3255
120.00	79.54	70.61	0.3073	79.38	69.70	0.2996	79.51	71.08	0.2993
180.00	81.00	71.22	0.3094	81.31	73.35	0.3023	81.34	73.70	0.3094
195.00	81.43	70.01	0.2443	81.25	70.63	0.2610	81.04	68.31	0.2616
210.00	80.80	68.82	0.3143	80.85	71.49	0.2926	80.72	71.84	0.3099
240.00	82.20	70.00	0.3202	81.91	68.17	0.2880	82.14	71.04	0.2991

Time (min.)	Basis-Wt. 1	s 1	k 1	Basis-Wt. 2	s 2	k 2	Basis-Wt. 3	s 3	k 3
0.00	0.050	87.030	11.450	0.052	87.784	11.846	0.051	86.122	11.468
30.00	0.048	77.211	3.259	0.047	69.863	2.852	0.049	86.228	3.610
60.00	0.048	70.886	2.423	0.046	67.548	2.274	0.049	71.867	2.476
120.00	0.046	63.804	1.679	0.045	61.826	1.656	0.045	67.760	1.789
180.00	0.047	63.460	1.414	0.045	74.740	1.605	0.047	74.901	1.603
195.00	0.037	73.671	1.560	0.039	71.963	1.557	0.039	62.663	1.390
210.00	0.047	53.989	1.232	0.044	68.599	1.556	0.047	66.588	1.533
240.00	0.048	55.309	1.066	0.043	55.615	1.111	0.045	63.166	1.226

Time (min.)	K (m2/kg)	Std.Dev
0.00	11.588	0.158
30.00	3.240	0.268
60.00	2.391	0.074
120.00	1.708	0.050
180.00	1.541	0.078
195.00	1.502	0.069
210.00	1.440	0.128
240.00	1.134	0.059

Date	=	**4-2-91**
pH	=	**11**
Peroxide	=	**see note**

NOTE

Bleached at 3.9±0.2 g/L for 180 min., then at 2.0±0.1 g/L for remainder.

	SHEET NUMBER								
	1			2			3		
Time (min.)	R Inf.	R Zero	Mass (g)	R Inf.	R Zero	Mass (g)	R Inf.	R Zero	Mass (g)
0.00	61.28	61.00	0.3180	60.93	60.14	0.3384	61.58	61.30	0.3343
30.00	75.48	70.90	0.2898	75.33	71.86	0.3200	75.35	71.71	0.3059
60.00	77.20	70.43	0.3067	77.24	71.33	0.2935	76.99	69.85	0.3087
120.00	78.23	64.83	0.3105	78.26	64.46	0.2982	78.73	66.65	0.3000
180.00	81.99	71.68	0.3059	81.71	71.34	0.3003	81.55	73.22	0.3018
200.00	79.29	65.71	0.2130	78.98	64.89	0.2250	78.91	63.46	0.2492
215.00	80.61	63.70	0.1994	79.92	64.40	0.1914	80.36	67.79	0.2244
245.00	81.00	65.33	0.2107	81.33	64.07	0.2163	81.28	69.45	0.2635

Time (min.)	Basis-Wt. 1	s 1	k 1	Basis-Wt. 2	s 2	k 2	Basis-Wt. 3	s 3	k 3
0.00	0.048	100.933	12.347	0.051	74.034	9.274	0.050	97.035	11.630
30.00	0.044	81.932	3.263	0.048	83.151	3.359	0.046	85.347	3.441
60.00	0.046	68.306	2.300	0.044	76.745	2.573	0.046	65.390	2.248
120.00	0.047	45.618	1.382	0.045	46.515	1.405	0.045	51.883	1.491
180.00	0.046	64.552	1.277	0.045	64.753	1.326	0.045	73.589	1.536
200.00	0.032	68.540	1.854	0.034	62.351	1.744	0.037	52.219	1.472
215.00	0.030	64.554	1.505	0.029	70.372	1.775	0.034	71.793	1.723
245.00	0.032	66.095	1.473	0.033	60.092	1.288	0.040	66.227	1.428

Time (min.)	K (m2/kg)	Std.Dev
0.00	11.083	1.137
30.00	3.354	0.063
60.00	2.374	0.124
120.00	1.426	0.041
180.00	1.379	0.097
200.00	1.690	0.139
215.00	1.668	0.101
245.00	1.396	0.068

Date	=	**5-2-91**
pH	=	**see note**
Peroxide	=	**3.8±0.5 g/L**

NOTE

Bleached at pH 11 for 180 min.
then at pH 12 for remainder.

	SHEET NUMBER								
	1			2			3		
Time (min.)	R Inf.	R Zero	Mass (g)	R Inf.	R Zero	Mass (g)	R Inf.	R Zero	Mass (g)
0.00	60.20	59.82	0.3331	59.82	59.52	0.3425	60.02	59.66	0.3384
30.00	74.86	70.80	0.3166	75.22	69.88	0.3131	74.95	72.02	0.3251
60.00	77.05	71.20	0.3170	77.20	70.23	0.3053	76.97	71.61	0.3255
120.00	79.54	70.61	0.3073	79.38	69.70	0.2996	79.51	71.08	0.2993
180.00	81.00	71.22	0.3094	81.31	73.35	0.3023	81.34	73.70	0.3094
195.00	81.35	66.93	0.2613	81.15	67.58	0.2587	0.00	0.00	0.0000
210.00	81.05	68.02	0.2755	81.30	68.77	0.2660	81.15	69.42	0.2746
240.00	81.42	66.58	0.2722	81.40	67.21	0.2757	81.27	65.84	0.2752

Time (min.)	Basis-Wt. 1	s 1	k 1	Basis-Wt. 2	s 2	k 2	Basis-Wt. 3	s 3	k 3
0.00	0.050	87.030	11.450	0.052	87.784	11.846	0.051	86.122	11.468
30.00	0.048	77.211	3.259	0.047	69.863	2.852	0.049	86.228	3.610
60.00	0.048	70.886	2.423	0.046	67.548	2.274	0.049	71.867	2.476
120.00	0.046	63.804	1.679	0.045	61.826	1.656	0.045	67.760	1.789
180.00	0.047	63.460	1.414	0.045	74.740	1.605	0.047	74.901	1.603
195.00	0.039	57.754	1.235	0.039	60.667	1.328	0.000	0.000	0.000
210.00	0.041	58.507	1.296	0.040	62.990	1.355	0.041	63.603	1.392
240.00	0.041	54.342	1.152	0.041	55.540	1.180	0.041	51.783	1.118

Time (min.)	K (m2/kg)	Std.Dev
0.00	11.588	0.158
30.00	3.240	0.268
60.00	2.391	0.074
120.00	1.708	0.050
180.00	1.541	0.078
195.00	1.290	0.050
210.00	1.348	0.034
240.00	1.150	0.022

Date	=	**6-2-91**
pH	=	**11**
Peroxide	=	**see note**

NOTE

Bleached at 3.9±0.2 g/L for 180 min., then at 2.0±0.1 g/L for remainder.

	SHEET NUMBER								
	1			2			3		
Time (min.)	R Inf.	R Zero	Mass (g)	R Inf.	R Zero	Mass (g)	R Inf.	R Zero	Mass (g)
0.00	58.56	57.82	0.3558	58.34	57.91	0.3521	57.93	56.50	0.3637
15.00	72.16	69.69	0.3365	71.63	66.76	0.3127	71.58	67.54	0.3053
30.00	76.12	70.01	0.3301	75.35	69.41	0.3149	75.32	68.92	0.3137
60.00	79.31	73.01	0.3467	79.05	71.48	0.3205	79.50	71.41	0.3008
90.00	79.24	69.31	0.3076	78.93	64.86	0.2412	79.57	72.79	0.3726
105.00	81.97	73.96	0.3477	82.35	73.22	0.3140	82.00	74.48	0.3335
120.00	81.89	73.32	0.3549	81.69	73.16	0.3485	81.33	71.82	0.3448
135.00	81.93	71.99	0.3317	82.35	74.50	0.3560	82.03	73.68	0.3638
150.00	81.90	73.23	0.3555	81.67	73.05	0.3509	81.89	72.73	0.3524
180.00	82.26	76.20	0.3706	81.92	72.52	0.3440	82.18	74.10	0.3651

Time (min.)	Basis-Wt. 1	s 1	k 1	Basis-Wt. 2	s 2	k 2	Basis-Wt. 3	s 3	k 3
0.00	0.054	65.902	9.663	0.053	75.106	11.172	0.055	52.671	8.046
15.00	0.051	79.583	4.274	0.047	63.734	3.581	0.046	70.764	3.992
30.00	0.050	64.190	2.404	0.047	66.248	2.671	0.047	63.939	2.585
60.00	0.052	68.354	1.845	0.048	66.149	1.836	0.045	69.063	1.825
90.00	0.046	58.915	1.602	0.036	58.116	1.634	0.056	61.801	1.621
105.00	0.052	66.568	1.320	0.047	69.102	1.307	0.050	72.128	1.425
120.00	0.053	62.387	1.249	0.052	63.183	1.297	0.052	58.768	1.259
135.00	0.050	60.842	1.212	0.054	66.881	1.265	0.055	62.204	1.224
150.00	0.053	61.864	1.237	0.053	62.295	1.281	0.053	60.271	1.207
180.00	0.056	74.043	1.416	0.052	60.809	1.213	0.055	63.632	1.229

Time (min.)	K (m2/kg)	Std.Dev
0.00	9.627	1.105
15.00	3.949	0.247
30.00	2.554	0.096
60.00	1.835	0.007
90.00	1.619	0.011
105.00	1.351	0.046
120.00	1.268	0.018
135.00	1.234	0.020
150.00	1.242	0.026
180.00	1.286	0.080

Date	=	**22-1-'92**
pH	=	**11**
Peroxide	=	**see notes**

NOTE

5.5 g/L for 90 min.
then 0.75 g/L for 90 min.

Listing of Main Procedures Required to Execute Simplex Optimisation of Peroxide Bleaching Kinetic Data. All Programs are Written in the C Programming Language.

Program 'Main .C' (the main simplex routine)

```
#include <stdio.h>
#include "simplex.h"

double **matrix(nr,nc)
{
int i;
double **m;
m = (double **) malloc((unsigned) (nr+1)*sizeof(double *));
for(i = 0; i <= nr; i++){
  m[i] = (double *)malloc((unsigned)(nc+1)*sizeof(double));
  if (!m[i]){
    printf("out of memory\n"); exit(0);
  }
}
return m;
}

int M, NVPP, N, *h, *l;
double *next, *mean, *error, *maxerr, *step, **data, **simp;
double CL0, C0;

main(argc,argv)
int argc; char *argv[];
{
extern int sfit();

M = 3; NVPP = 2; N = M+1;
h = (int *) malloc(N*sizeof(int));
l = (int *) malloc(N*sizeof(int));
next = (double *)malloc(N*sizeof(double));
mean  = (double *)malloc(N*sizeof(double));
error = (double *)malloc(N*sizeof(double));
maxerr = (double *)malloc(N*sizeof(double));
step = (double *)malloc(N*sizeof(double));
simp = matrix(N,N);
data = matrix(200,NVPP);

sfit(argv[1]);

free(h); free(l); free(next); free(mean);
free(error); free(maxerr); free(step);

}
```

Program 'Simplex.h'

```
#include <math.h>
#include <stdio.h>


#define MNP     200
#define ALPHA   1.0
#define BETA    0.5
#define GAMMA   2.0
#define LW      5
#define ROOT2   1.414214


extern int M,NVPP,N;
extern int          *h, *l;
extern int          np, maxiter, niter;
extern double       *next, *mean, *error, *maxerr, *step, **simp;
extern double       **data;
extern double       C0, CL0;
extern FILE         *fpdata;

extern double       f();
```

Program 'Enter.c'

```
#include "simplex.h"

enter(fname)
char *fname;
{
     register int   i, j;

     printf("EQUILIBRIUM MODEL 1 C=CL ; CL -> CP\n");
     printf("SIMPLEX Optimization for \"\%s\"\n",fname);
     fscanf(fpdata,"%F %F", &C0, &CL0);
     printf("starting values: %10.4f %10.4f\n", C0,CL0);
     fscanf(fpdata, "%d", &maxiter);
     for (i=0 ; i<M ; i++)  fscanf(fpdata, "%F", &simp[0][i]);


     for (i=0 ; i<M ; i++)  fscanf(fpdata, "%F", &step[i]);

     printf("\n\n");

     for (i=0 ; i<N ; i++)  fscanf(fpdata, "%F", &maxerr[i]);

     np = 0;
     while (!feof(fpdata)) {
          for (j=0 ; j<NVPP ; j++) {
               if (fscanf(fpdata, "%F", &data[np][j]) == EOF)
                    break;
          }
          np++;
     }
     np--;

}
```

Program 'First.c'

```
#include "simplex.h"

first()
{
     register int   i, j;

     printf("Starting Simplex\n");
     for (j=0 ; j<N ; j++) {
          printf(" simp[%d]", j+1);
          for (i=0 ; i<N ; i++) {
               if ((i+1) % LW == 0)
                    printf("\n");
               printf("  %e", simp[j][i]);
          }
          printf("\n");
     }
     printf("\n");
}
```

Program 'MakeFile'

```
CFLAGS= -g
SRC= sfit.c enter.c    new_vert.c report.c f.c  main.c \
      order.c  sum_resi.c

FILES= sfit.o enter.o    new_vert.o report.o f.o  main.o \
      order.o  sum_resi.o

simplex: $(FILES)
      cc -o simplex $(FILES) -lm

hc: $(SRC)
      vgrind -lc -Plw268 $(SRC)
```

Program 'Order.c'

```
#include "simplex.h"

order()
{
     register int   i, j;

     for (j=0 ; j<N ; j++)
          for (i=0 ; i<N ; i++) {
               if (simp[i][j] < simp[l[j]][j])
                    l[j] = i;
               if (simp[i][j] > simp[h[j]][j])
                    h[j] = i;
          }
}
```

Program 'New_Vert.c'

```
#include "simplex.h"

new_vertex()
{
     register int   i;

     for (i=0 ; i<N ; i++) {
          simp[h[N-1]][i] = next[i];
     }
}
```

Program 'Report.c' (executes output report)

```
#include "simplex.h"

report()
{
     register int   i, j;
     double         y, dy, sigma;

     printf("\nProgram exited after %d iterations.\n\n", niter);

     printf("The mean is:");
     for (i=0 ; i<N ; i++) {
          if ((i+1) % LW == 0)
               printf("\n");
          printf("  %e", mean[i]);
     }
     printf("\n\n");

     printf("The estimated fractional error is:");
     for (i=0 ; i<N ; i++) {
          if ((i+1) % LW == 0)
               printf("\n");
          printf("  %e", error[i]);
     }
     printf("\n\n");

     printf("\n\n");

     printf("   #         X              Y              Y''
DY\n");
     sigma = 0.0;
     for (i=0 ; i<np ; i++) {
          y = f(mean, data[i][0]);
          dy = data[i][1] - y;
          sigma += (dy*dy);
          printf("%4d  ", i);
          printf("%13e  %13e  ", data[i][0], data[i][1]);
          printf("%13e  %13e\n", y, dy);
     }
     printf("\n");
     sigma = sqrt(sigma);
     printf("The standard deviation is %e\n\n", sigma);
     sigma /= sqrt((double) (np-M));
     printf("The estimated error of the function is %e\n\n", sigma);
}
```

Program 'Sfit.c'

```
#include "simplex.h"

#define until(x) while (!(x))

int       np, maxiter, niter;

FILE      *fpdata;

sfit(name)
char  *name[];
{
   register int   i, j, done;
   double *center, *p, *q;

   center = (double *)malloc((unsigned)N*sizeof(double));
   p = (double *)malloc((unsigned)N*sizeof(double));
   q = (double *)malloc((unsigned)N*sizeof(double));

   if ((fpdata = fopen(name, "r")) == NULL) {
      fprintf(stderr, "simplex: can't open %s\n", name);
      exit(1);
   }

   enter(name);

   /* First Vertex */
   sum_residual(simp[0]);

   /* Compute offset of Vertices */
   for (i=0 ; i<M ; i++) {
      p[i] = step[i] * (sqrt((double) N) + M - 1) / (M * ROOT2);
      q[i] = step[i] * (sqrt((double) N) - 1) / (M * ROOT2);
   }

   /* All Vertices of the Starting Simplex */
   for (i=1 ; i<N ; i++) {
      for (j=0 ; j<M ; j++)
         simp[i][j] = simp[0][j] + q[j];
      simp[i][i-1] = simp[0][i-1] + p[i-1];
      sum_residual(simp[i]);
   }

   /* Preset */
   for (i=0 ; i<N ; i++) {
      l[i] = 1;
      h[i] = 1;
   }
   order();

   niter = 0;

   /* Iterate */
   do {
      /* Wish it were True */
      done = 1;
      niter++;

      /* Compute Centroid...Excluding the Worst */
      for (i=0 ; i<N ; i++)
         center[i] = 0.0;
      for (i=0 ; i<N ; i++)
         if (i != h[N-1])
            for (j=0 ; j<M ; j++)
```

```
                center[j] += simp[i][j];

        /* First Attempt to Reflect */
        for (i=0 ; i<N ; i++) {
           center[i] /= M;
           next[i] = (1.0+ALPHA) * center[i] - ALPHA * simp[h[N-
1]][i];
        }
        /* changed from plural to singular 9-28-89
        sum_residuals(next);
        */
        sum_residual(next);

        if (next[N-1] <= simp[l[N-1]][N-1]) {
           new_vertex();
           for (i=0 ; i<M ; i++)
              next[i] = GAMMA * simp[h[N-1]][i] + (1.0-GAMMA) *
center[i];
           sum_residual(next);
           if (next[N-1] <= simp[l[N-1]][N-1])
              new_vertex();
        }
        else {
           if (next[N-1] <= simp[h[N-1]][N-1])
              new_vertex();
           else {
              for (i=0 ; i<M ; i++)
                 next[i] = BETA * simp[h[N-1]][i] + (1.0-BETA) *
center[i];
              sum_residual(next);
              if (next[N-1] <= simp[h[N-1]][N-1])
                 new_vertex();
              else {
                 for (i=0 ; i<N ; i++) {
                    for (j=0 ; j<M ; j++)
                       simp[i][j] = BETA * (simp[i][j] + simp[l[N-
1]][j]);
                    sum_residual(simp[i]);
                 }
              }
           }
        }

        order();

        /* Check For Convergence */
        for (j=0 ; j<N ; j++) {
           error[j] = (simp[h[j]][j] - simp[l[j]][j]) / simp[h[j]][j];
           if (done)
              if (error[j] > maxerr[j])
                 done = 0;
        }

     } until(done || (niter == maxiter));

     /* Average Each Parameter */
     for (i=0 ; i<N ; i++) {
        mean[i] = 0.0;
        for (j=0 ; j<N ; j++)
           mean[i] += simp[j][i];
        mean[i] /= N;
     }

     report();
free(center);free(p);free(q);
}
```

Program 'Sum_Resid.c'

```
#include "simplex.h"

#define sqr(x) ((x) * (x))

sum_residual(x)
double    *x;
{
     register int   i;

     x[N-1] = 0.0;

     for (i=0 ; i<np ; i++)
          x[N-1] += sqr(f(x, data[i][0]) - data[i][1]);
/* mod to force all params to be > 0 */
     for (i=0 ; i< M ; i++)
      {
      if (x[i] < 0.0) x[N-1]= 9.999e99;
      }
}
```

Program 'M1f.c' (contains the explicit equations for equilibrium model #1 to be solved by the simplex algorithm).

```
#include "simplex.h"

double f(x, d)
double    *x;
double   d;
{

/* C = CL; CL -> CP  model */

float p,prod,h,q,a,b,result;
float k1,k2,k3,t;

t =  d;
k1 = x[0];
k2 = x[1];
k3 = x[2];

p    = k1+k2+k3;
prod = k1*k3;
h    = (k2+k3) + (k2 *CL0/C0);
q    = sqrt(p*p-4.0*prod);
a    = -(p-q)/2.0;
b    = -(p+q)/2.0;

result= C0/(b-a) *  (exp(b*t)*(b+h)-exp(a*t)*(a+h));

return (result);
}
```

Program 'M2f.c' (contains the explicit equations for equilibrium model #2 to be solved by the simplex algorithm).

```
#include "simplex.h"

double f(x, d)
double    *x;
double   d;
{

/* C = CL; C -> CP  model */

float p,prod,h,q,a,b,result;
float k1,k2,k3,t;

t =  d;
k1 = x[0];
k2 = x[1];
k3 = x[2];

p    = k1+k2+k3;
prod = k2*k3;
h    = (C0+CL0)*k2;
q    = sqrt(p*p-4.0*prod);
a    = -(p-q)/2.0;
b    = -(p+q)/2.0;

result= (exp(b*t)*(C0*b+h)-exp(a*t)*(C0*a+h))/(b-a);

return (result);
}
```

Program 'M3f.c' (contains the explicit equations for the two chromophore consecutive reaction model to be solved by the simplex algorithm).

```
#include "simplex.h"

double f(x, d)
double    *x;
double   d;
{

/* C1 -> C2;  C2 -> CP;  C1 -> CP  model */

float a, b,h,result;
float k1,k2,k3,t;

t =  d;
k1 = x[0];
k2 = x[1];
k3 = x[2];

a = -(k1 + k2);
b = - k3;
h = (C20 * -a) + (C10 * k2);

result=( C10 * exp(a*t) ) + (exp(b*t)/(b-a))*(C20*b+h)-(exp(a*t)/(b-
a))*(C20*a+h);

return (result);
}
```

Sample Input File Showing Format of Kinetic Data for Fitting to Equilibrium Model Using Simplex Optimisation Program.

Input File "2gLpH10"

```
10.63    0         0
1000
0.01     0.01      0.001
0.001    0.001     0.0005
1e-05    1e-05     1e-06     1e-04
0      10.63
5      9.51
10     8.73
15     8.64
20     8.10
30     7.80
60     6.48
120    4.71
240    3.44
420    2.97
```

Explanation of Input File

Line 1

```
  10.63   =  initial value for chromophoric group C
      0   =  initial value for leuco-chromophoric group CL
      0   =  initial value for chromophoric products CP
```

Line 2

```
   1000   =  maximum number of iterations allowed
```

Line 3

```
   0.01   =  initial guess for k1
   0.01   =  initial guess for k2
  0.001   =  initial guess for k3
```

Line 4

```
  0.001   =  step increment for k1
  0.001   =  step increment for k2
 0.0005   =  step increment for k3
```

Line 5

```
  1e-05   =  maximum error allowed in k1
  1e-05   =  maximum error allowed in k2
  1e-06   =  maximum error allowed in k3
  1e-04   =  maximum total error allowed
```

Lines 6-15

contains the raw data (time in minutes, light absorption coefficient) to be fitted.

```
0      10.63
5      9.51
10     8.73
15     8.64
20     8.10
30     7.80
60     6.48
120    4.71
240    3.44
420    2.97
```

Sample Output File from the Fitting of E. regnans Bleaching Kinetics to the Equilibrium Model Using Simplex Optimisation.

Output File "2gLpH10.opt"

```
EQUILIBRIUM MODEL 2  C <-> CL;   C -> CP
SIMPLEX Optimisation for "2gLpH10"
Starting values:10.63   0.0000      0.0000


Program exited after 122 iterations.

The mean is: 1.187054e-02     1.963894e-02      3.261121e-03

The estimated fractional error is: 4.468377e-07   4.504017e-07
                                   6.331946e-07   1.052956e-05
```

#	X	Y	Y''	DY
0	0.000000e+00	1.063000e+01	1.063000e+01	-1.144409e-07
1	5.000000e+00	9.510000e+00	9.888348e+00	-3.783476e-01
2	1.000000e+01	8.730000e+00	9.249465e+00	-5.194650e-01
3	1.500000e+01	8.640000e+00	8.698060e+00	-5.806004e-02
4	2.000000e+01	8.100000e+00	8.221127e+00	-1.211266e-01
5	3.000000e+01	7.800000e+00	7.448082e+00	+3.519176e-01
6	6.000000e+01	6.480000e+00	6.051359e+00	+4.286413e-01
7	1.200000e+02	4.710000e+00	4.900240e+00	-1.902404e-01
8	2.400000e+02	3.440000e+00	3.813954e+00	-3.739539e-01
9	4.200000e+02	2.970000e+00	2.692344e+00	+2.776556e-01

```
The standard deviation is 9.997949e-01

The estimated error of the function is 3.778870e-01
```

Explanation of Output

Line 1

Model Scheme = C <-> CL; C -> CP

Line 2

"2gLpH10" = input file

Line 3

10.63 = initial Value of C
0.0000 = initial Value of CL
0.0000 = initial Value of CP

Line 4

122 = no. of iterations required for optimisation of fit

Line 5

1.187054e-02 = fitted value of k_1
1.963894e-02 = fitted value of k_2
3.261121e-03 = fitted value of k_3

Line 6

4.468377e-07 = fractional error in k_1
4.504017e-07 = fractional error in k_2
6.331946e-07 = fractional error in k_3
1.052956e-05 = fractional error in the function

Lines 7 - 17

contains the raw data and fitted data points

\# = data set number
X = x - co-ordinate (time in minutes)
Y = y - co-ordinate (light absorption coefficient)
Y'' = model values of Y calculated using k_1, k_2, k_3
DY = delta y (Y-Y'')

Line 18

9.997949e-01 = standard deviation in the fit

Line 19

3.778870e-01 = standard error in the function

(A) Mass Spectrum of Cinnamaldehyde Epoxide

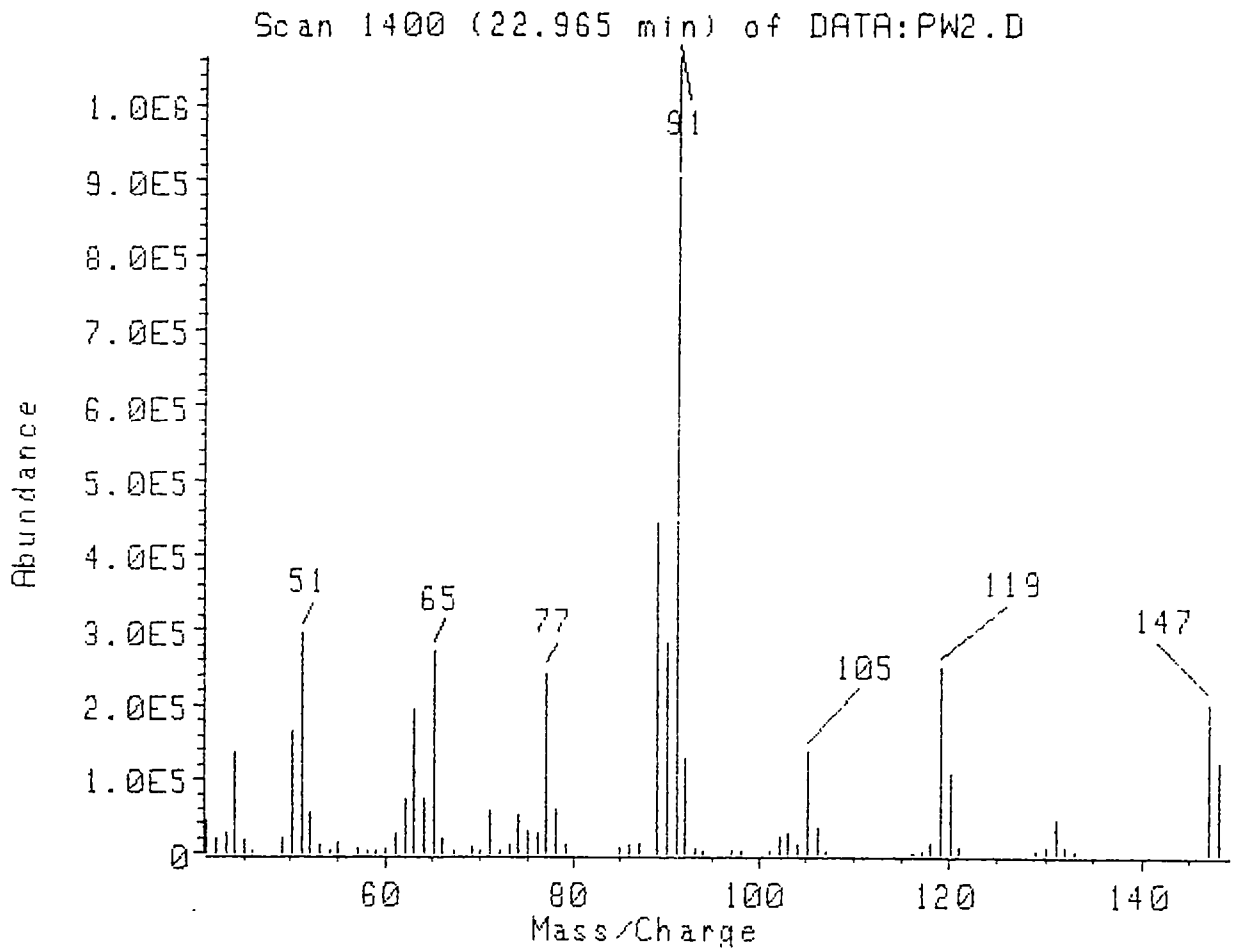

(B) ^{1}H-nmr of Cinnamaldehyde Epoxide Isomers

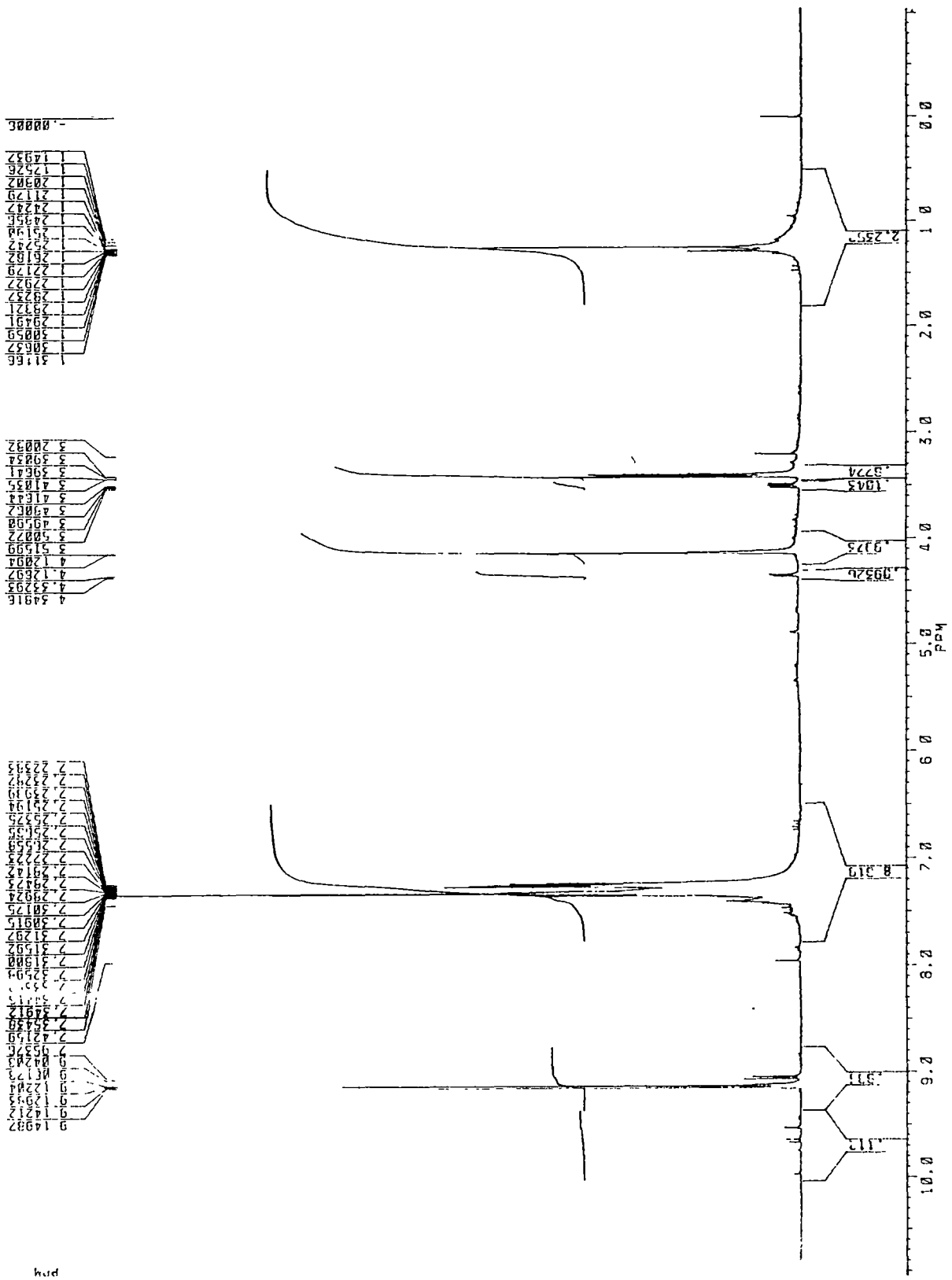

Molar Ratio / Peak Area Ratio Standard Curves for Quantitative GC Analysis

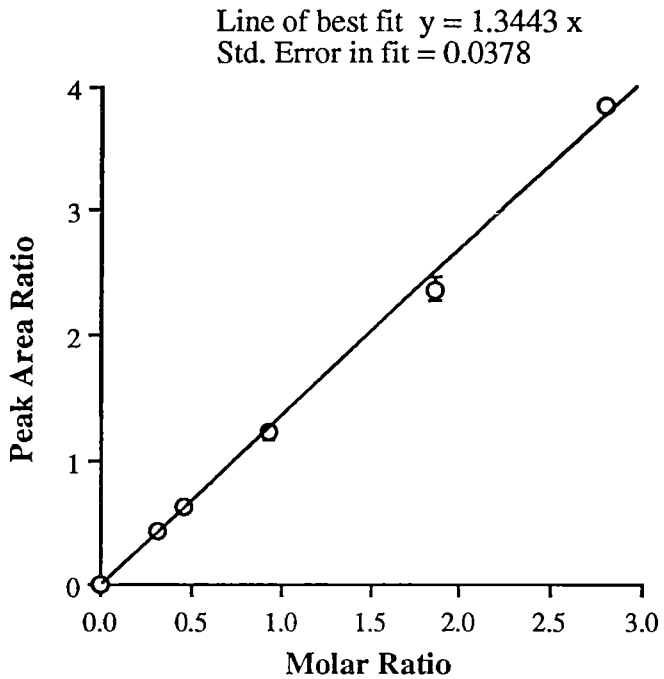

FIGURE A: Molar ratio vs. GC peak area ratio for 3,4-dimethoxy-acetophenone (internal standard) : p-dichlorobenzene (external standard). Correlation coefficient, $r^2 = 0.998$.

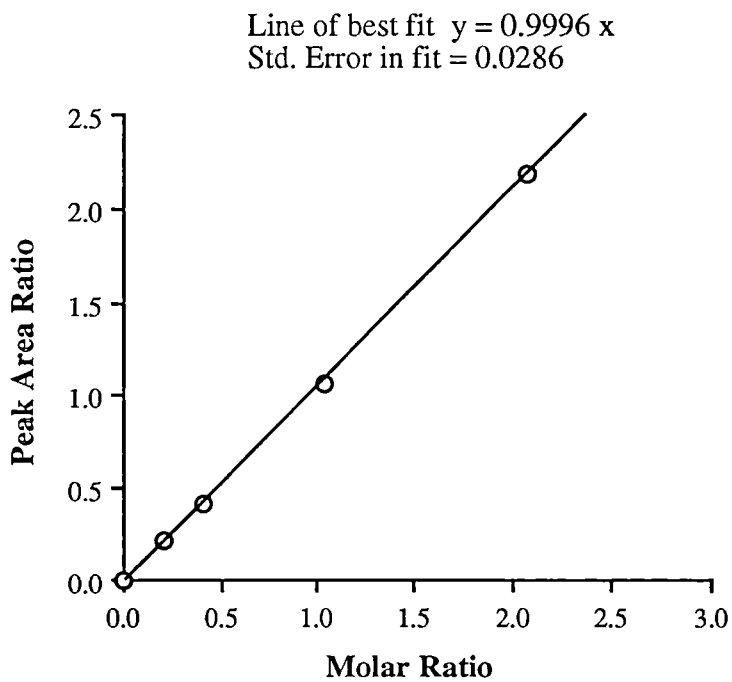

FIGURE B: Molar ratio vs. GC peak area ratio for cinnamaldehyde : 3,4-dimethoxy-acetophenone (internal standard). Correlation coefficient, $r^2 = 1.000$.

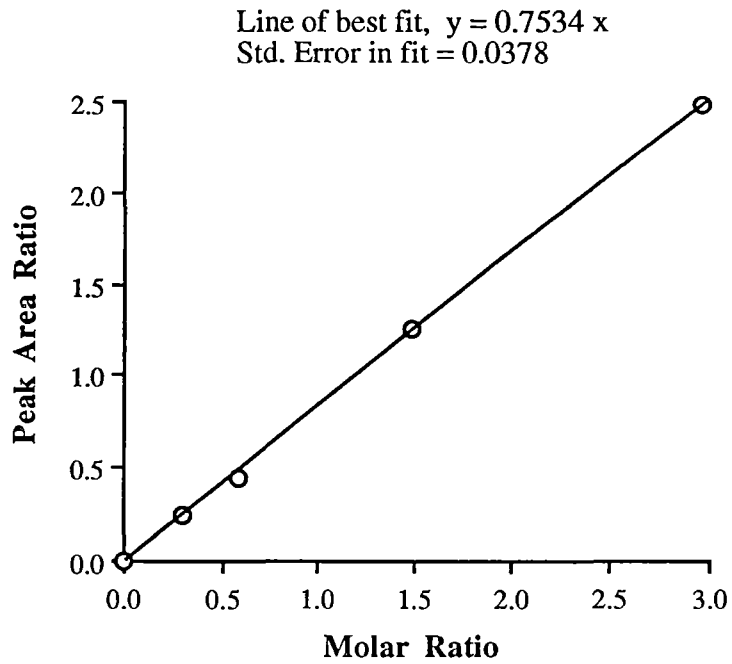

FIGURE C: Molar Ratio vs. GC peak area ratio for benzaldehyde : 3,4-dimethoxy-acetophenone (internal standard). Correlation coefficient, $r^2 = 0.999$.

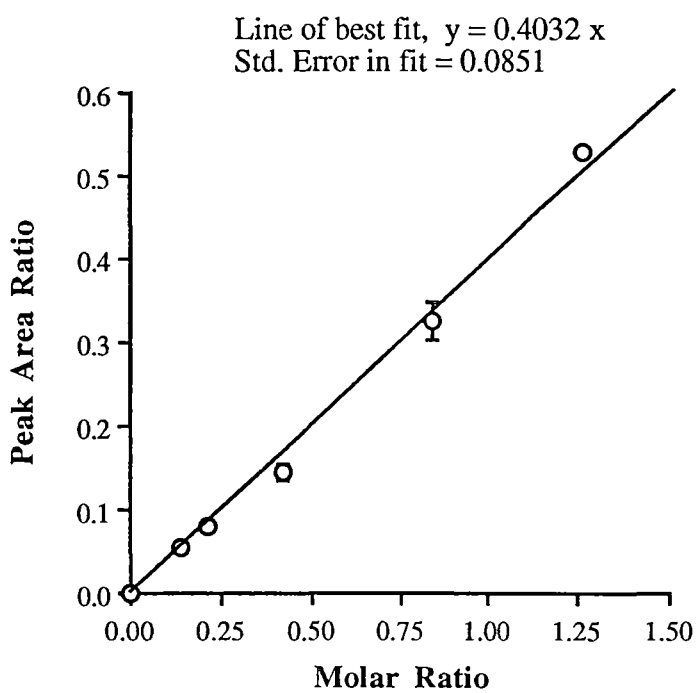

FIGURE D: Molar Ratio vs. GC peak area ratio for cinnamaldehyde epoxide : 3,4-dimethoxy-acetophenone (internal standard). Correlation coefficient, $r^2 = 0.995$.

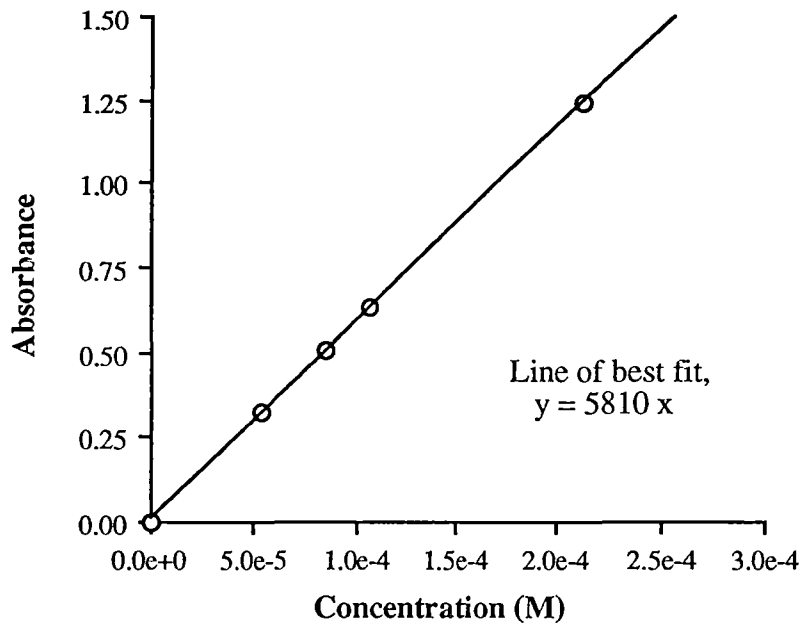

FIGURE A: UV-visible calibration curve for aqueous solutions of cinnamaldehyde measured at 315 nm. (Correlation coefficient, $r^2 = 1.000$).

Input Files for Modelling Cinnamaldehyde to Epoxide and Epoxide to Benzaldehyde Conversion Using Program REACT

Input File "6gLpH10.e"

```
C       E       B

Explanation
       C, E, B  =  reactive species
```

Input File "6gLpH10.f"

```
100
2       3
1       2
C       E       B
0.01    0.001
0.05    0.05    0.1
0       1.324e-2        0               0
1       9.658e-3        3.582e-3        0
6       2.860e-3        1.013e-2        2.530e-4
11      6.640e-4        1.219e-2        3.851e-4
16      2.488e-4        1.244e-2        5.492e-4
21      0               1.243e-2        6.749e-4
31      0               1.222e-2        8.943e-4
46      0               1.199e-2        1.253e-3
61      0               1.148e-2        1.666e-3
76      0               1.110e-2        2.059e-3
91      0               1.062e-2        2.515e-3
```

Explanation

Line 1

100 = maximum number of iterations

Line 2

2 = number of rate constants to be solved
3 = number of species in reaction

Line 3

1 = subscript for rate constant (ie k_1')
2 = subscript for rate constant (ie k_2')

Line 4

C, E, B = reactive species (cinnamaldehyde, epoxide, benzaldehyde).

Line 5

0.01 = increment step size for C -> E pseudo 1st order rate constant (k_1').
0.001 = increment step size for E -> B pseudo 1st order rate constant (k_2').

Line 6

0.05 = maximum fractional error in k_1'
0.05 = maximum fractional error in k_2'
0.1 = maximum total error in function

Lines 7-17
Raw data for modelling (time in minutes, concentration of C, E and B).

```
0       1.324e-2        0               0
1       9.658e-3        3.582e-3        0
6       2.860e-3        1.013e-2        2.530e-4
11      6.640e-4        1.219e-2        3.851e-4
16      2.488e-4        1.244e-2        5.492e-4
21      0               1.243e-2        6.749e-4
31      0               1.222e-2        8.943e-4
46      0               1.199e-2        1.253e-3
61      0               1.148e-2        1.666e-3
76      0               1.110e-2        2.059e-3
91      0               1.062e-2        2.515e-3
```

Input File "6gLpH10.m"

```
2.647394e-01    C  -> E
2.442314e-03    E  -> B
```

Explanation

Line 1
2.647394e-01 = estimate of rate constant k_1' for C -> E.

Line 2
2.442314e-03 =estimate of rate constant k_2' for E -> B.

Input File "6gLpH10.p"

```
0       90      10      1e-09
C       1.324e-2        1E-9    1E-9
E       0       1E-9    1E-9
B       0       1E-9    1E-9
```

Explanation

Line 1
```
             0  =  initial time (min).
            90  =  final time (min).
            10  =  increment step size (min).
         1e-09  =  slice size in integration steps
```

Line 2
```
       1.324e-2  =  initial concentration of C (M).
           1E-9  =  integration increment
           1E-9  =  maximum error in integrated slice
```

Line 3
```
             0  =  initial concentration of E (M).
           1E-9  =  integration increment
           1E-9  =  maximum error in integrated slice
```

Line 4
```
             0  =  initial concentration of B (M).
           1E-9  =  integration increment
           1E-9  =  maximum error in integrated slice
```

Example Output File from the Kinetic Modelling of Cinnamaldehyde to Epoxide and Epoxide to Benzaldehyde Conversion Using Program REACT.

```
Output File "6gLpH10.out"

1)    2.647394e-01      C  -> E
2)    2.442314e-03      E  -> B
SIMPLEX Optimization


Program exited after 5 iterations.

The mean is:  2.682115e-01  2.474644e-03  8.899718e-07

The estimated fractional error is: 2.280084e-02
                  4.779754e-02     3.073245e-02


The standard deviation is 9.329702e-04

The estimated error of the function is 1.675664e-04


2 reactions involving 3 species
C  E  B

    time                C                   E                   B
0.0000e+00      1.3240e-02      0.0000e+00      0.0000e+00
1.0000e+01      9.3786e-04      1.2094e-02      2.0787e-04
2.0000e+01      6.6434e-05      1.2659e-02      5.1440e-04
3.0000e+01      4.7059e-06      1.2414e-02      8.2087e-04
4.0000e+01      3.3335e-07      1.2119e-02      1.1205e-03
5.0000e+01      2.3597e-08      1.1827e-02      1.4129e-03
6.0000e+01      1.6473e-09      1.1542e-02      1.6982e-03
7.0000e+01      1.5086e-10      1.1263e-02      1.9767e-03
8.0000e+01     -1.5146e-11      1.0992e-02      2.2485e-03
9.0000e+01      3.5652e-12      1.0726e-02      2.5137e-03
```

Explanation of Output File

Line 1

name of output file = 6gLpH10.out

Line 2

2.647394e-01 = estimated pseudo 1st order rate constant for cinnamaldehyde to epoxide conversion (min^{-1}).

Line 3

2.442314e-03 = estimated pseudo 1st order rate constant for epoxide to benzaldehyde conversion (min^{-1}).

Line 4

Simplex Optimisation

Line 5

5 = number of iterations for optimisation of fit.

Line 6

2.682115e-01 = pseudo first order rate constant for cinnamaldehyde to epoxide conversion k_1' (min^{-1}).

2.474644e-03 = pseudo first order rate constant for epoxide to benzaldehyde conversion k_2' (min^{-1}).

8.899718e-07 = total error in rate constants.

Line 7

2.280084e-02 = fractional error in k_1'

4.779754e-02 = fractional error in k_2'

3.073245e-02 = total fractional error in function

Line 8

9.329702e-04 = standard deviation in fit

Line 9

1.675664e-04 = standard error in the function

Line 10

Model generated points (time in minutes, cinnamaldehyde concentration, epoxide concentration, benzaldehyde concentration).

time	C	E	B
0.0000e+00	1.3240e-02	0.0000e+00	0.0000e+00
1.0000e+01	9.3786e-04	1.2094e-02	2.0787e-04
2.0000e+01	6.6434e-05	1.2659e-02	5.1440e-04
3.0000e+01	4.7059e-06	1.2414e-02	8.2087e-04
4.0000e+01	3.3335e-07	1.2119e-02	1.1205e-03
5.0000e+01	2.3597e-08	1.1827e-02	1.4129e-03
6.0000e+01	1.6473e-09	1.1542e-02	1.6982e-03
7.0000e+01	1.5086e-10	1.1263e-02	1.9767e-03
8.0000e+01	-1.5146e-11	1.0992e-02	2.2485e-03
9.0000e+01	3.5652e-12	1.0726e-02	2.5137e-03

(A) Mass Spectrum of 4-*tert*-butylorthoquinone

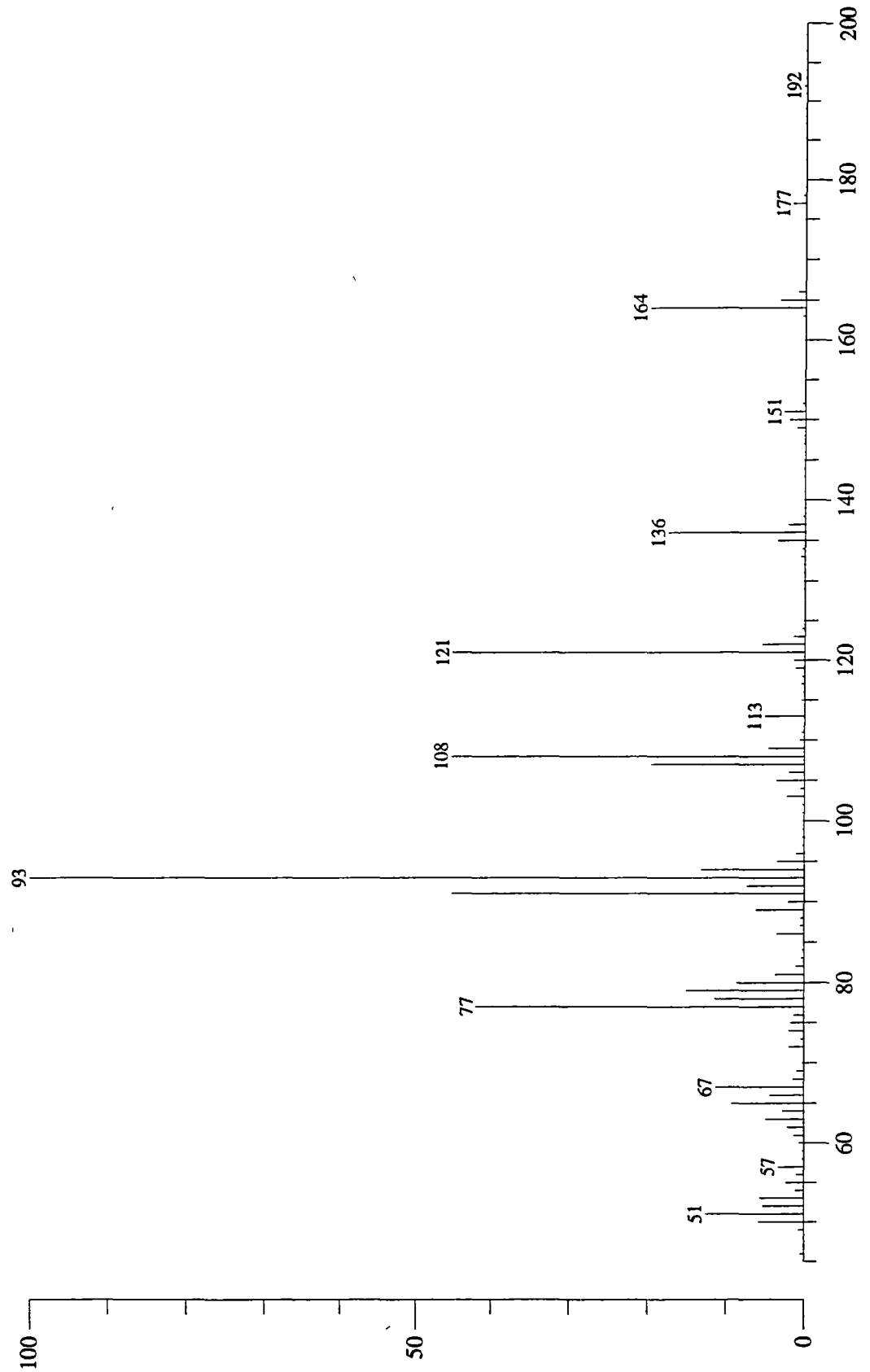

(B) ^{1}H-nmr of 4-*tert*-butylorthoquinone

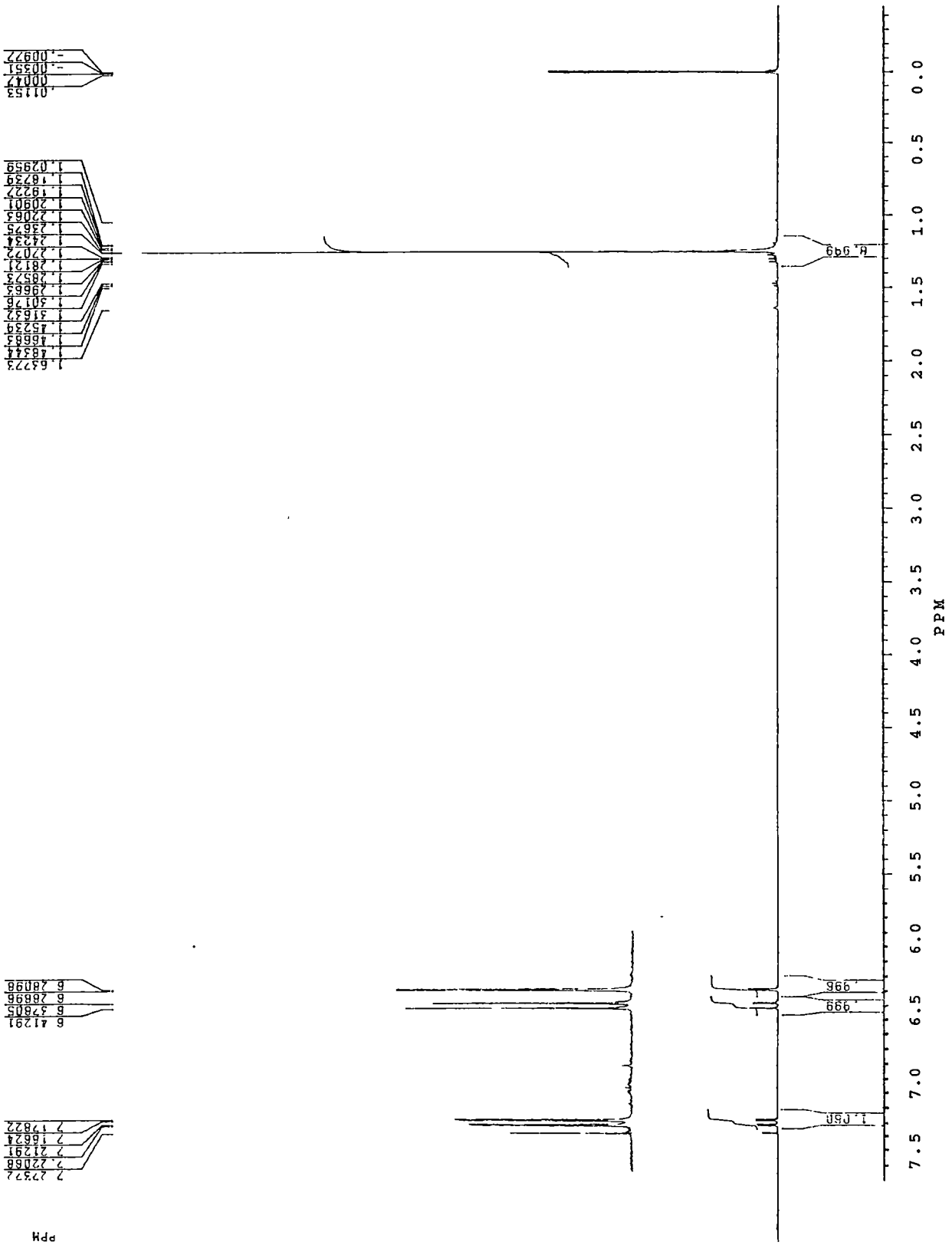

(C) ^{13}C-nmr of 4-*tert*-butylorthoquinone

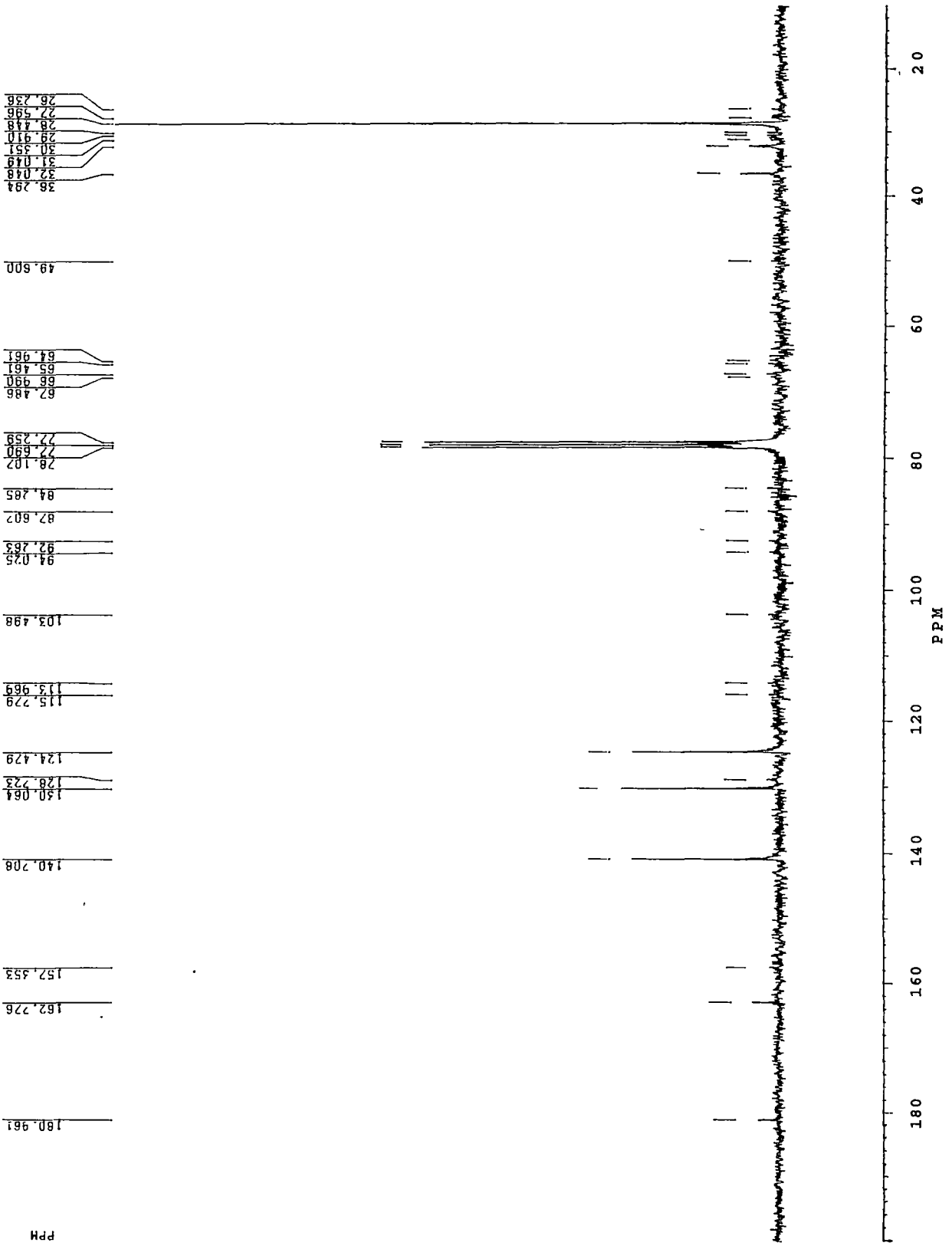

(D) Mass Spectrum of 4-*tert*-butylcatechol

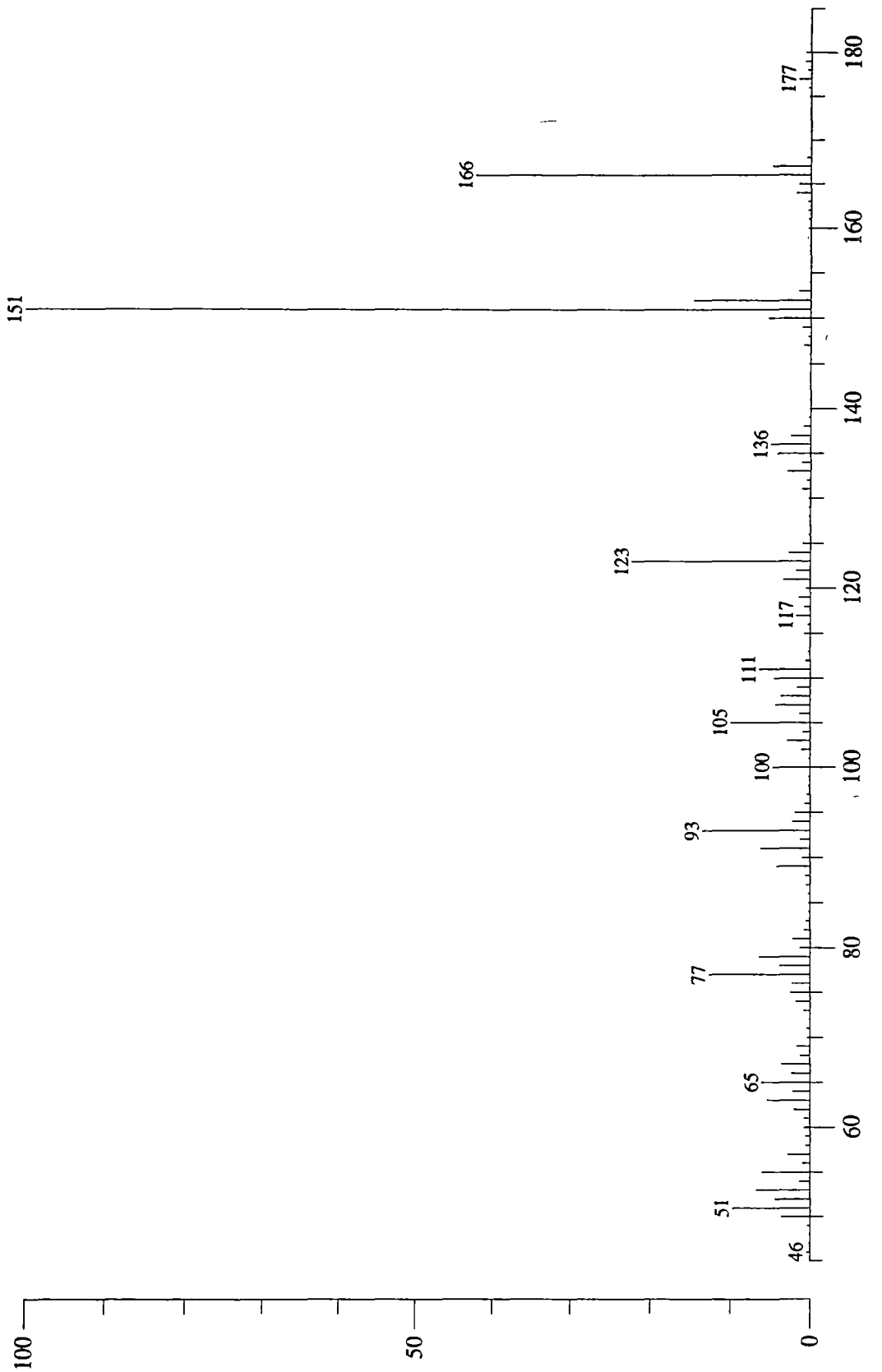

(E) ^{1}H-nmr of 4-*tert*-butylcatechol

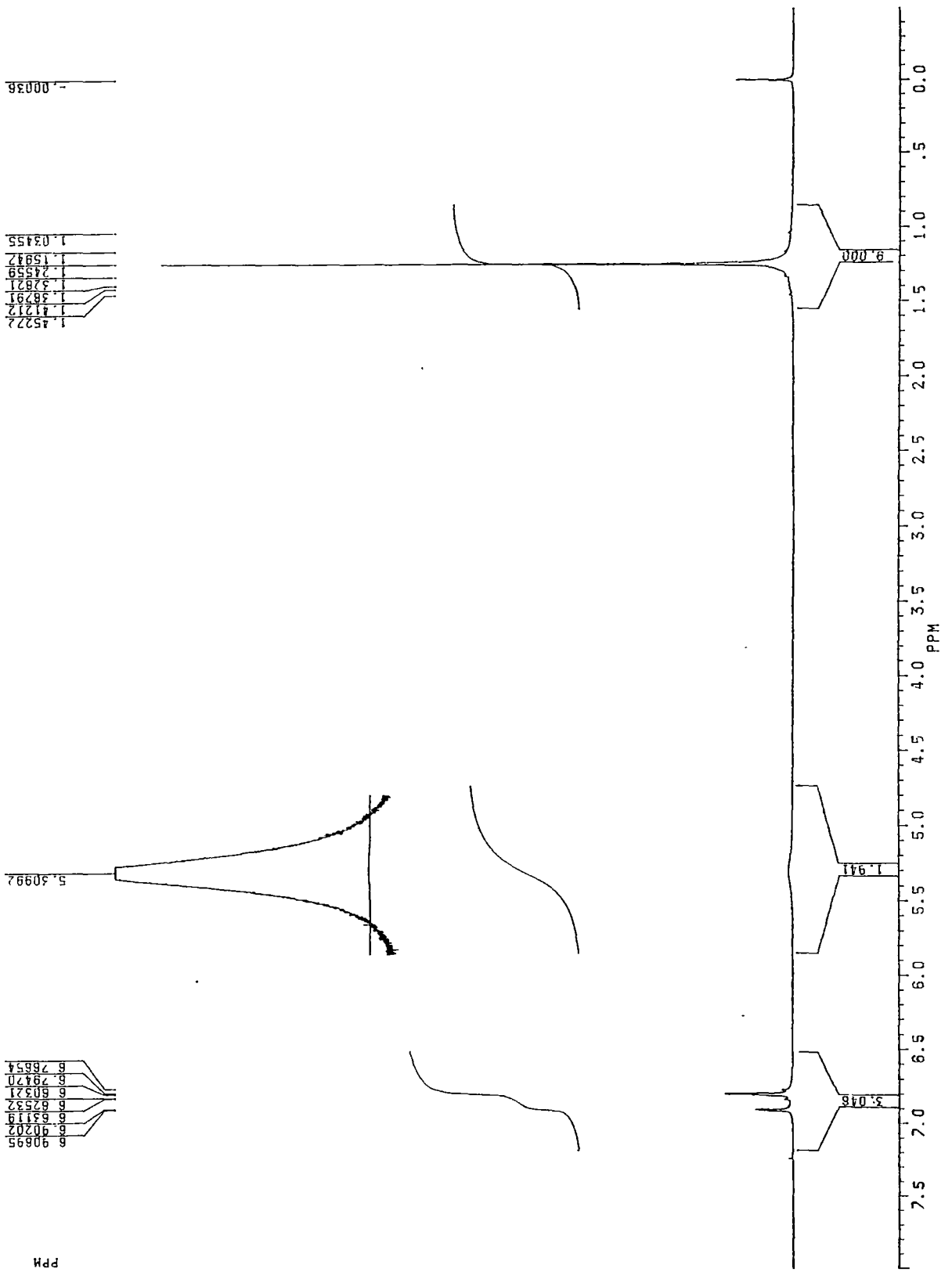

(F) ^{13}C-nmr of 4-*tert*-butylcatechol

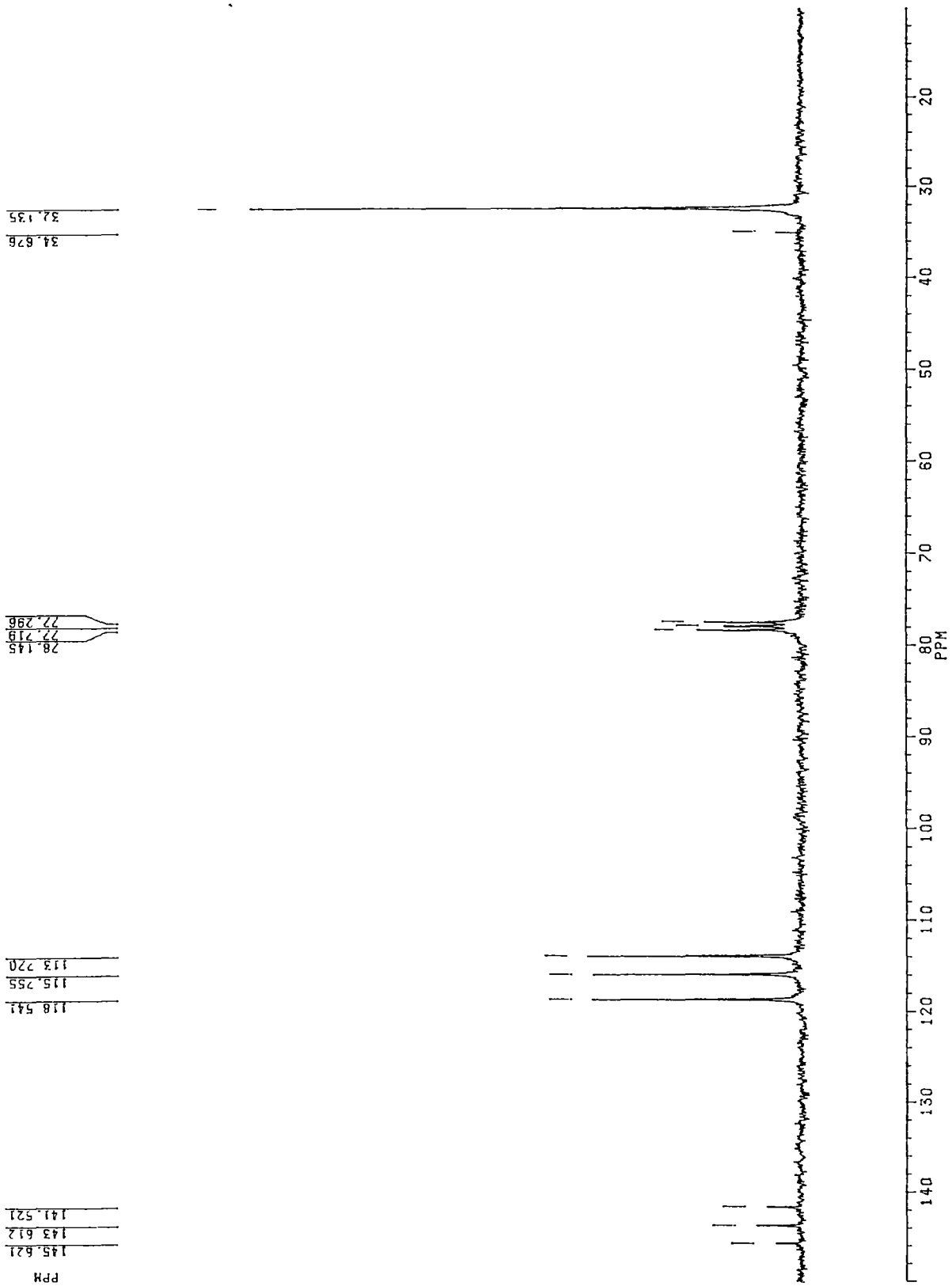

(G) Mass Spectrum of 2-*tert*-butyl-5-hydroxy-benzoquinone

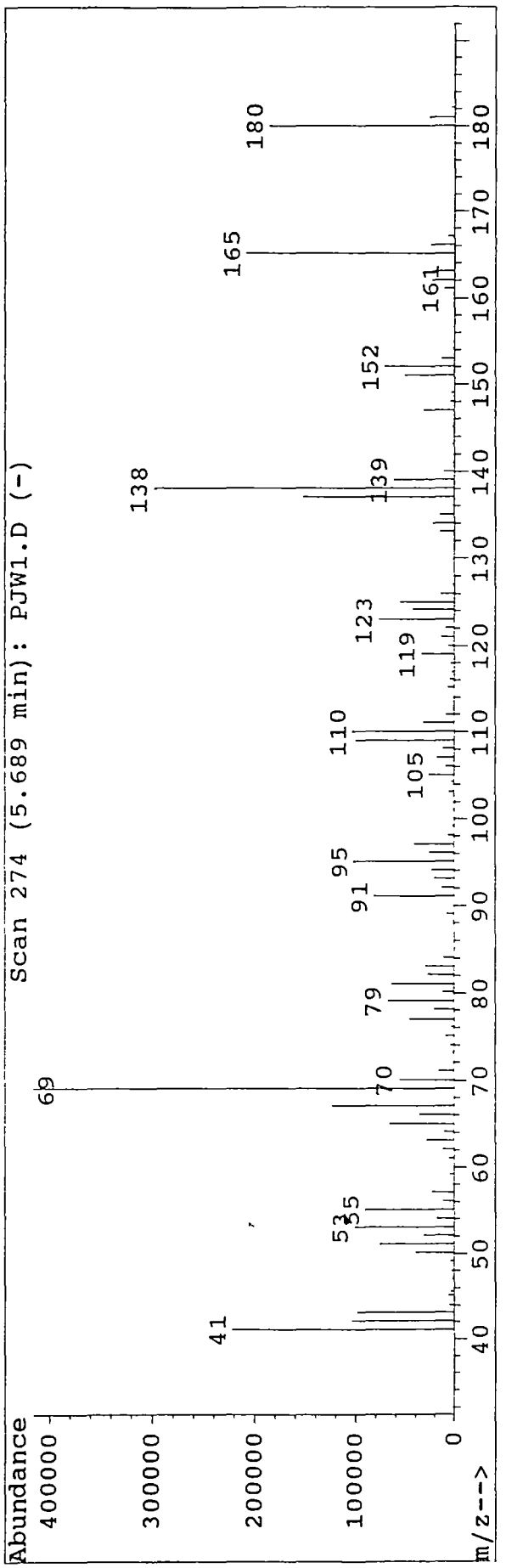

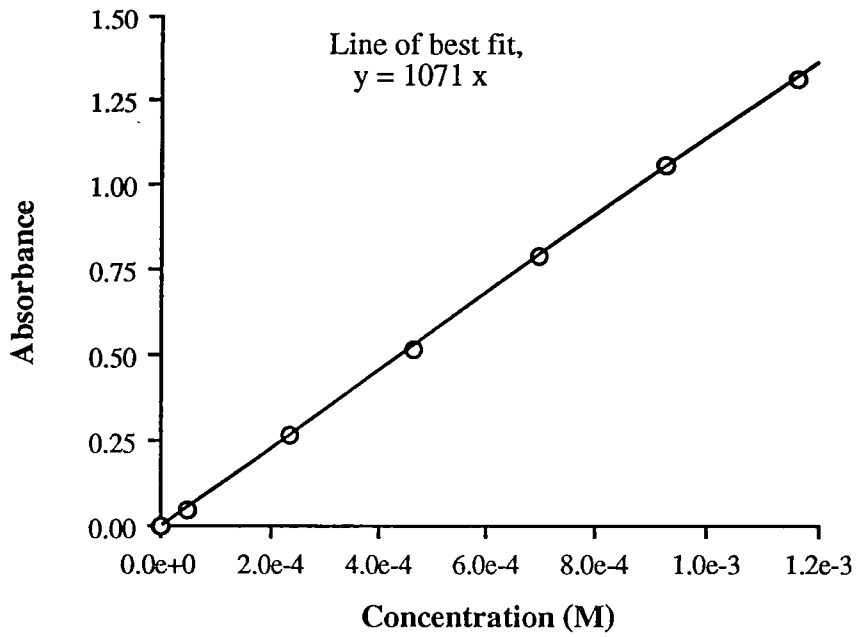

FIGURE A: UV-visible calibration curve for aqueous solutions of 4-tert-butyl-orthoquinone measured at 400 nm. (Correlation coefficient, $r^2 = 1.000$).